

**Liquisolid tablets – A rationale for formulation and process design**

**Michael John Frodsham**

**A thesis submitted in partial fulfilment of the requirements of Liverpool John  
Moore's University for the degree of PhD**

**May 2020**

## **DECLARATION**

No portion of the work referred to in the thesis has been submitted in support of an application for another degree or qualification of this or any other university or other institute of learning.

## Abstract

A significant proportion of new API's in development are poorly soluble and require alternative formulation approaches to achieve adequate oral bioavailability. One option is to develop lipid-based formulations. Lipid formulations are typically liquids but can be converted into solid dosage forms via adsorption onto solid porous carriers. The term liquisolid describes a formulation which has been modified from a liquid to a solid for delivery as either a capsule or tablet dosage form.

The aim of these studies was to investigate the compression properties of lipid-based liquisolid tablet formulations. The purpose was to establish a rationale and framework that could be used by a formulator when embarking on the development of a liquisolid formulation. The studies aimed to evaluate a range of lipid-based formulations loaded onto a selected adsorbent.

The optimal sorbent on to which lipid formulations were loaded was selected through screening studies. A Type I lipid formulation (Labrafac Lipophile WL1349®) was loaded onto selected sorbents, physical and compression characteristics were determined. The magnesium aluminometasilicates (Neusilin® grades) were the only sorbents to exhibit suitable compression properties with relatively low strain rate sensitivity values (< 3 %). The sorbent of choice (selected on compression characteristics) was determined to be Neusilin® US2.

Further studies evaluated a model Type III (lipid formulation) SMEDDS preconcentrate (SPc) formulation, containing Labrafac Lipophile WL1349®. Neusilin® US2 was loaded at 50 %, 70 % and 90 % relative to the dry adsorbent. The compressibility of the Neusilin® US2 was reduced with increased SPc loading. The tablets produced from the SPc loaded Neusilin® US2 granules (without additional compression aids), were not suitably robust (relatively low tensile strength, low friability and extended disintegration). The compression range over which viable tablets were formed was limited for all granules at each loading level. For all granules, a critical force was reached at which the liquid phase appeared to dominate, and tablet tensile strength was reduced with increased force. This finding does not comply with general rules for powder compression. Rather than a 'yield point' at which certain materials permanently deform; the granules appeared to reach a 'liquid point' at which the liquid dominated the tablet characteristics with increasing force/pressure applied. The addition of the 'extra-granular' excipients improved tablet robustness (tensile strength and disintegration), however friability was not improved at higher SPc loading levels as many tablets were found to cap/laminate during testing.

To investigate the cause of variable tablet friability, Raman spectroscopy was used to analyse loaded granules and tablets. Dipyridamole was included as a model API in the SPc formulation (DSPc), at a relatively low concentration, which allowed a qualitative assessment of dipyridamole distribution within the loaded granules and tablets. Characterisation of both the granules and tablets showed poor dipyridamole homogeneity, with 'pockets' of high concentration. The size distribution of the pockets was similar irrespective of loading level. However, the quantity of pockets increased proportionally with DSPc loading. These observations suggest that the loaded granules prior to compression were inhomogeneous and of variable density and that the loading process required refinement. This inhomogeneity may be a contributory factor to tablet friability.

Alternative Type IV lipid formulations consisting of semi-solid excipients, Gelucire®44/14 and Vitamin E TPGS with the inclusion of dipyridamole were evaluated to determine if such excipients could infer improved tablet characteristics compared to Type I and III liquid formulations.

The studies showed that the semi-solid materials Gelucire®44/14 and vitamin E TPGS when loaded on Neusilin®US2 at loading levels of up to 90 % (relative to adsorbent weight) produced tablets > 1 MPa tensile with low friability (< 0.4 %) and rapidly disintegrated (< 10 min). The tablet formulations did not require the addition of extra granular compression aids, only 5 % w/w super-disintegrant (croscarmellose Na) and 1 % w/w lubricant (sodium stearyl fumarate) were necessary. *In vitro* dissolution testing was performed upon the various D-GEL and D-TPGS tablet formulations. The data showed that the D-GEL formulations achieved complete release of the API irrespective of loading level with 30 min. However, for the D-TPGS formulations exhibited a retarded release in comparison, 90 % loaded tablets compressed at 10 kN failed to release the full extent of API under the test conditions.

As a result of these studies a novel investigational plan has been proposed for the development of liquisolid tablet formulations, to aid a formulator when embarking on such a development exercise, highlighting considerations against which formulations could be designed and characterised.

A number of characteristics are advised to be determined, which have been detailed as the 'liquid points'. The understanding of these 'liquid points' is critical as it is these values for compression force/pressure and solid fraction that indicate the point at which the 'liquid phase' predominates the compression process and is likely to limit tablet robustness. These values therefore drive compression parameters and guide product scale-up.

# Contents

Abstract .....	3
List of abbreviations .....	9
Chapter 1.....	12
1.0 Introduction.....	13
1.1 Fundamental Considerations for Oral Drug Delivery .....	14
1.1.1 Biopharmaceutical Classification System (BCS) .....	15
1.1.2 Lipid Delivery Systems .....	17
1.1.3 In-vitro and in-vivo considerations for lipidic delivery .....	22
1.1.4 Semi solid solutions and suspensions .....	25
1.1.5 Efflux Mechanisms .....	26
1.2 Tablets as a dosage form .....	28
1.2.1 Powder properties. ....	28
1.2.2 The compression process .....	29
1.2.3 Tableting Properties.....	32
1.2.4 Tablet Characteristics.....	34
1.3 Mechanics of Tablet Compression .....	36
1.4 State of the art – Solid SMEDDS formulations .....	37
1.5 Adsorbent Selection .....	39
1.6 Structure of Thesis .....	39
1.6.1 Aims and Objectives .....	39
1.7 Thesis Overview .....	40
Chapter 2.....	42
“Evaluation of sorbent characteristics pre and post loading with a Type I lipid formulation/substrate” .....	42
2.1 Introduction and aims .....	42
2.2 Materials.....	44
2.3 Methods .....	45
2.3.1 Carrier loading .....	45
2.3.2 Scanning Electron Microscopy .....	45
2.3.2 Tapped and bulk density determination .....	45
2.3.3 True density determination .....	46
2.3.4 Flow through an orifice .....	46
2.3.5 Compaction .....	46

2.3.6 Tablet Characterisation .....	47
2.4 Results .....	47
2.4.1 Characterisation of Sorbents .....	47
2.4.2 Sorbent Compression .....	48
2.4.3 Heckel analysis and Strain Rate Sensitivity Determination.....	49
2.4.4 Physical characterisation of sorbents post loading of labrafac lipophile W1349 .....	50
2.4.5 Density and flow data for Neusilin® US2 loaded with Labrafac Lipophile W1349 ®.....	52
2.4.6 Compression data.....	54
2.4.7 SEM Images .....	60
2.5 Conclusions.....	61
Chapter 3 .....	63
<b>Evaluation of sorbent compression properties pre- and post-loading with SMEDDS formulation and the addition of selected excipients to improve tablet characteristics</b> .....	63
3.1 Introduction and aims .....	63
3.2 Materials.....	64
3.3 Methods .....	64
3.3.1 SMEDDS preconcentrate preparation.....	64
3.3.2 Carrier loading .....	65
3.3.3 Tapped and bulk density determination .....	65
3.3.4 True density determination .....	65
3.3.5 Flow through an orifice .....	65
3.3.6 Blend preparation .....	65
3.3.7 Compaction .....	66
3.3.8 Tablet Characterisation .....	66
3.3.9 Statistical Analysis .....	66
3.4 Results .....	67
3.4.1 Characterisation of Neusilin®US2 loaded with SPc.....	67
3.4.2 Compression results for tablets containing Neusilin® US2 loaded with SMEDDS preconcentrate. ....	68
3.5 Excipient addition to enhance tablet characteristics .....	79
3.5.1 Formulation details.....	80
3.5.2 Compression data.....	81
3.6 Further Discussion and Conclusions .....	100

Chapter 4.....	104
<b>An investigation into the distribution of SMEDDS preconcentrate in Liquisolid tablets using Raman Spectroscopy.....</b>	<b>104</b>
4.1 Introduction and aims .....	104
4.1.1 Applications of Raman spectroscopy for tablet characterisation .....	105
4.2 Materials.....	106
4.3 Methods .....	106
4.3.1 SMEDDS preconcentrate preparation.....	106
4.3.2 Carrier loading (SPc).....	107
4.3.3 Dipyridamole SMEDDS preconcentrate (DSPc) preparation .....	107
4.3.4 Carrier loading of DSPc.....	107
4.3.5 Compaction .....	107
4.3.6 Raman Analysis of Samples .....	107
4.4 Results and Discussion.....	108
4.4.1 Raman Analysis of Neusilin®US2 loaded with SPc.....	108
4.4.2 Raman Analysis of the surface(s) of tablets consisting of Neusilin®US2 loaded with SPc.....	111
4.4.3 Raman Analysis of ‘granules’ consisting of Neusilin®US2 loaded with DSPc. ....	115
4.4.4 Raman Analysis of the surface(s) of tablets consisting of Neusilin®US2 loaded with DSPc.....	116
4.5 Further Discussion and Conclusions .....	122
 Chapter 5.....	 124
<b>“Evaluation of sorbent properties post-loading with Gelucire®44/14 and Vitamin E TPGS” .....</b>	<b>124</b>
5.1 Introduction and aims .....	124
5.2 Materials.....	125
5.3 Methods .....	126
5.3.1 Dipyridamole/Molten carrier preparation.....	126
5.3.2 Carrier loading of Neusilin®US2.....	126
5.3.3 Tapped and bulk density determination .....	126
5.3.4 True density determination .....	126
5.3.5 Flow through an orifice .....	126
5.3.6. Blend preparation .....	126
5.3.7 Compaction .....	127

5.3.8 Tablet Characterisation .....	127
5.3.9 In-vitro dissolution – Sample analysis .....	127
5.3.10 <i>In vitro</i> dissolution parameters .....	128
5.4 Results and Discussion .....	129
5.4.1 Characteristics of Neusilin®US2 loaded with D. GEL and D. TPGS.....	129
5.4.4 Compression of Neusilin® US2 loaded with D-TPGS.....	137
5.4.4 Compression of loaded granule blends.....	143
5.4.5 Tablet Characteristics.....	143
5.4.5 In-vitro dissolution assessment.....	150
5.5 Further Discussion and Conclusions .....	154
 Chapter 6.....	 157
General Discussion and Conclusions .....	157
6.1 Background and Summary of the Research Project .....	157
6.1.1 Sorbent Evaluation Studies.....	159
6.1.2 Type III Lipid Loading Studies .....	160
6.1.3 Raman characterisation studies .....	162
6.1.5 Semi-solid loading studies .....	163
6.2 Conclusion .....	165
6.3 Potential Future Work .....	167
 References:.....	 168

## List of abbreviations

ABC - adenosine tri-phosphate (ATP) binding cassette

ATP - adenosine tri-phosphate

API - active pharmaceutical ingredient

BCS - biopharmaceutical classification system

CTAB - cetyltrimethylammonium bromide

DCS - developability classification system

D-GEL - Dipyridamole GEL

D-TPGS - Dipyridamole TPGS

DDI - drug-drug interaction

DOE - design of experiments

DSC - differential scanning calorimetry

EMCA - empty modelling component analysis

EPR - electron paramagnetic resonance

FaSSIF - fasted simulated intestinal fluid

GEL - Gelucire®44/14

GL- gastric lipase

GI/GIT – gastrointestinal/gastrointestinal tract

HLB – hydrophilic lipophilic balance

HPLC - high-performance liquid chromatography

HPMC - hydroxypropylmethyl cellulose

ICH – International committee on harmonisation

LLW - Labrafac Lipophile WL1349®

MCC - microcrystalline cellulose

MDCK- Madin Darby canine kidney

MDR - multidrug resistance

NaCMC - sodium carboxymethylcellulose

P - partition coefficient

PEG - poly(ethylene glycol)

Ph Eur - European Pharmacopoeia

PK - pharmacokinetics

PSI – Pounds per inch<sup>2</sup>

QTTP - quality target product profile  
SAXS - small angle X-ray scattering  
SEM - scanning electron microscopy  
SLAD - solubility limited absorbable dose  
SMEDDS- self-micro emulsifying drug delivery systems  
SPc – SMEDDS preconcentrate.  
SRS - strain rate sensitivity  
SSA - specific surface area(s)  
TEM - transmission electron microscopy  
TPGS - D- $\alpha$ -tocopheryl polyethylene glycol succinate  
US – United States  
USP - United States pharmacopeia  
XRPD - X-ray powder diffraction

## Acknowledgements

I wish to thank Dr Matthew Roberts and Professor James Ford, for their advice, assistance, and patience during this study. I also wish to thank Professor John Collett for his encouragement and Ms Maireadh Pedersen and Professor Mike Rubinstein for their support in allowing me to pursue these studies part time.

There are several other people who have helped and advised me on various aspects of the work who I offer my gratitude to:

Mr Paul Gibbons, for his help during SEM analysis of samples.

Mr David Reece and Mrs Hazel Garvie-Cook for their help with Raman analysis.

Mr Nicholas Weeks, Mr Matt Moran, Ms Netanya Cooper, Mrs Georgina Sullivan and Ms Sidonia Onisa for their help with *in vitro* dissolution assessment.

Mr Robert Anderson for advice and guidance with data modelling.

And last but not least, I wish to thank my wife, Jane, for her encouragement, support and patience.

## Dedication

Dedicated to Mr Thomas Hodgett, who taught me to approach activities in a methodical, measured manner.

So on, so forth and all the rest of it.....

# Chapter 1.

## 1.0 Introduction

For most active pharmaceutical ingredients (API's) to be delivered by the oral route, the extent of bioavailability (of the API) which can be achieved following administration, is of significant concern during formulation development activities and the clinical study design process.

Bioavailability may be defined as the extent to which, and sometimes rate at which, the active pharmaceutical ingredient (API) enters the systemic circulation, thereby gaining access to the site of action (Beers and Berkow, 1999). When a medication is administered intravenously, its bioavailability is 100% (Ponikvar, 2008). However, when an API is administered orally, bioavailability is driven by physiological, physicochemical, and biopharmaceutical factors (El-Katten and Varma, 2012). The physiological factors that must be considered include gastro-intestinal anatomy and physiology, the unstirred water layer adjacent to the intestinal membrane, gastrointestinal (GI) transit times, gastrointestinal tract (GIT) pH, bile fluid composition, bacterial microflora throughout the GIT, lymphatic absorption and intestinal drug transporters (El-Katten and Varma 2012). The physicochemical factors which drive bioavailability include ionisation state, molecular weight (MW), lipophilicity, polar descriptors and free rotatable bonds. The biopharmaceutical factors include particle size, salt form, polymorphism and drug complexation (El-Katten and Varma, 2012).

Following oral dosing, drug molecules can cross the luminal membrane through various mechanisms that involve passive diffusion or active transport. Passive diffusion is comprised of two pathways: the paracellular pathway, in which drug diffuses through the aqueous pores at the tight junctions between the intestinal enterocytes; and the transcellular (lipophilic) pathway, which requires drug diffusion across the lipid cell membrane of the enterocyte. The active transport pathway is mediated by transporters and is divided into active drug influx and efflux (El-Katten and Varma, 2012). Figure 1.1 shows the influx and efflux mechanisms diagrammatically (Chan et al., 2004).

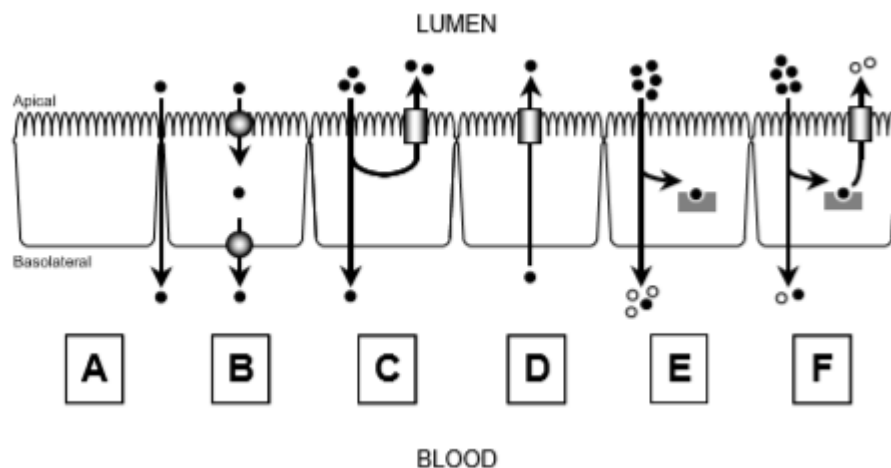


Figure 1.1 The intestinal epithelium as a barrier of entry to compounds entering the blood. Where (A) is absorption via the paracellular route, restricted by tight junctions. (B) Carrier mediated mechanism – transcellular absorption. (C) Efflux transporters in apical membranes driving API back into the lumen. (D) Apical efflux transporters in the blood. (E) Intracellular metabolising enzymes modifying compounds prior to entering the blood stream. (F) Apical efflux transporters and intracellular metabolising enzymes may co-ordinately metabolise and excrete compounds Taken from Chan, 2004

In more general terms, it is the solubility and permeability of the API which drive bioavailability. A formulator must therefore exploit these parameters, by the most appropriate means when developing formulations to enhance and maximise oral bioavailability; whilst aiming to achieve the requirements of a quality target product profile (QTPP). A QTPP as defined in accordance with International committee on harmonisation (ICH) Q8 (2009) considers:

- Intended use in clinical setting, route of administration, dosage form, delivery systems
- Dosage strength(s)
- Container closure system
- Therapeutic moiety release or delivery and attributes affecting pharmacokinetic characteristics (e.g., dissolution, aerodynamic performance) appropriate to the drug product dosage form being developed.
- Drug product quality criteria (e.g., sterility, purity, stability, and drug release) appropriate for the intended marketed product

### 1.1 Fundamental Considerations for Oral Drug Delivery

It is essential for a formulator to understand the basic principles behind dosage selection and to understand the physicochemical and biopharmaceutical properties of the API to be formulated; prior to the commencement of any pre-formulation or formulation development activities. For lipid-based delivery systems; a wide variety of

options for delivery are available to the formulator to address the limitations for bioavailability as posed by the characteristics of the API for delivery.

### 1.1.1 Biopharmaceutical Classification System (BCS)

Amidon et al (1995) proposed the theoretical basis for biopharmaceutical classification of API's, through correlation of both in-vitro dissolution rate and in-vivo bioavailability (of API's). The theory categorises API's in to four distinct classes as detailed in Table 1.1.

*Table 1.1 Basic principles of biopharmaceutical classification system (BCS) Amidon, 2005.*

<b>BCS Classification</b>	<b>Solubility</b>	<b>Permeability</b>
I	High	High
II	Low	High
III	High	Low
IV	Low	Low

The biopharmaceutical classification theory was subsequently expanded and refined by Butler and Dressman (2010) into the develop-ability classification system (DCS) as detailed in Figure 1.2. Butler and Dressman (2010) proposed that the use of in-vivo solubility values as determined in fasted simulated intestinal fluid (FaSSIF) was a more reliable means of prediction of the extent of likely absorption, than solubility determined in simple buffer or buffer surfactant systems. Two further modifications were made to the system; that for class II compounds with solubility limited absorbable dose (SLAD) permeability and solubility are compensatory, and finally, that dissolution rate when expressed as a target drug particle size rather than dose/solubility ratio, provided a better means of assessing the development risks for API's with dissolution rate limited extent of absorption.

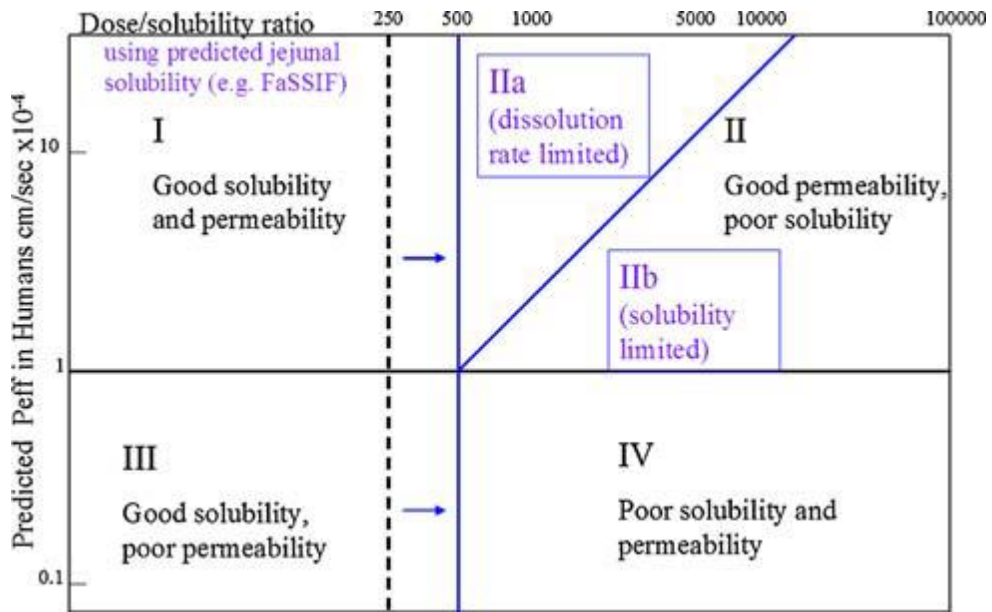


Figure 1.2 The developability classification system (DCS) Taken from Butler and Dressman, (2010)

Both the BCS and the DCS have assisted formulators significantly in the selection of design approach for formulations. The rationale for formulation selection can be narrowed and focussed as detailed in Fig 1.3 by Kawabata et al (2011).

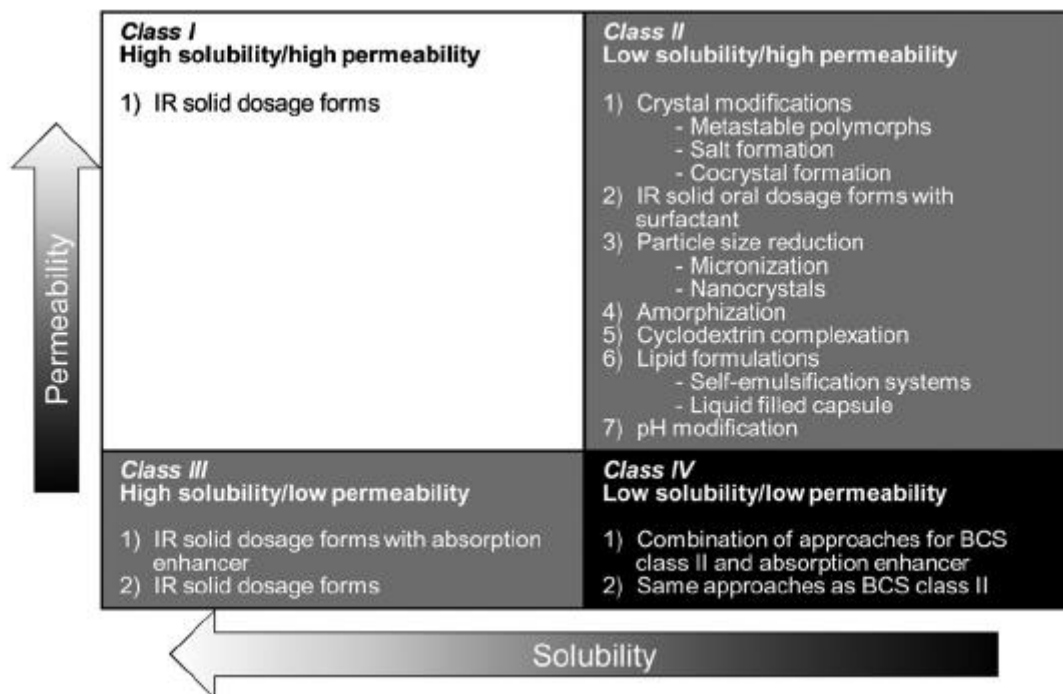


Figure 1.3. The rationale for formulation approach in accordance with BCS classification Taken from Kawabata et al (2011)

A high proportion of lead candidate molecules for clinical evaluation exhibit poor aqueous solubility which is a critical factor influencing dissolution rate (Kohli et al., 2010). A high proportion of molecules are categorised as BCS class II. Where, formulation enabling strategies are key to enabling absorption and thus increasing the resultant bioavailability.

### **1.1.2 Lipid Delivery Systems**

A number of marketed products have employed lipid systems successfully to overcome solubility and dissolution rate limited challenges associated with specific API's (Kawabata et al., 2010). A significant amount of research has been published into the development and optimisation of lipid delivery systems over the past three decades.

For an API to be considered as a candidate whereby lipid delivery would be a suitable solution for absorption enhancement, some general rules may be applied as suggested by Pouton and Porter (2007), such as good lipophilicity and  $\text{Log } P > 5$ , whereas molecules with high melting points and  $\text{Log } P$  values  $\sim 2$ , maybe more akin to alternative formulation approaches such as the use of solid dispersions. Typically described as the partition coefficient ( $P$ ), the relative hydrophilic / lipophilic nature of a molecule as evidenced by its distribution between an aqueous environment and a lipidic environment is often expressed as a  $\text{Log } P$  value.

Later work reported by Jannin et al (2015) suggests however, that BSC class II molecules with  $\text{Log } P$  values between 2 and 3 which are less lipophilic, may also be suitable candidates for lipidic delivery by utilising self-micro emulsifying drug delivery systems (SMEDDS) see 1.1.2.1.

#### **1.1.2.1 Lipid formulation classification system.**

In 2000 the concept of the lipid formulation classification system (LFCS) was introduced by Porter, which was later refined in 2006 (Porter). The purpose of the system was to aid in the understanding of formulation selection upon *in-vivo* exposure and to guide the selection of formulation approach considering the physicochemical properties of the API to be delivered. The classification of formulations stems from the polarity of the 'blend of excipients' used for delivery.

Four types of formulations are classified as detailed in Table 1.2 reported by Kohli et al (2010).

Table 1.2 Lipid formulation classification system: characteristic features of the four essential types of lipid formulations (Kohli et al 2010)

Formulation	Excipients	Properties	Pros	Cons
Type I	Oils without surfactants	Non dispersing, are digested	Simple, excellent capsule compatibility	Poor solvent capacity unless drug is lipophilic
Type II	Oils with water insoluble surfactants	Form self-emulsifying systems, without water soluble components.	Unlikely to lose solvent capacity on dilution	Turbid o/w emulsion
Type III	Oils, surfactants (soluble and insoluble), cosolvents	Form self-emulsifying/self-micro emulsifying systems with water soluble components	Clear to almost clear dispersion; absorption achieved without digestion	Loss of solvent capacity on dilution; less easily digested.
Type IV	Water soluble surfactants and cosolvents (no oils)	Typically form micellar solutions	Good solvent capacity	Likely loss of solvent capacity on dispersion might not be digested.

Porter et al (2007) describe lipid formulations as those formulations which can enhance drug solubilization in the intestinal milieu, recruit intestinal lymphatic drug transport and can alter enterocyte lipid trafficking. These characteristics can lead to an indirect effect on poorly water-soluble drug absorption and cellular disposition and has the potential to avoid first pass metabolism.

A lipid in the context of a lipid formulation could be considered to fit into five classes of excipients; ranging from pure triglyceride oils, through mixed glycerides, lipophilic surfactants, hydrophilic surfactants and water-soluble cosolvents.

#### 1.2.2.2 Excipient selection for lipid formulations

Porter and Pouton 2008 and Jannin et al 2008 provided detailed rationales for the selection criteria of excipients for lipid-based formulations. Whilst the studies performed as part of this thesis were not aimed at developing

a formulation for delivery of a specific API it is important to understand the potential limitations of excipient selection. A major consideration for excipient selection in lipid-based dosage forms is that of toxicity. The suitability of most excipients can be assessed using the FDA's inactive ingredients database which details those excipients previously registered in marketed products:

<https://www.accessdata.fda.gov/scripts/cder/iig/index.cfm>.

In addition to toxicity, other factors for excipient selection include; solvent capacity, miscibility (with both aqueous systems and other selected excipients), melting point, dispersibility, digestibility, compatibility with capsule shells (gelatin and HPMC where capsule delivery is appropriate), chemical stability and purity.

Vegetable oils and their derivatives are the primary source for manufacture of lipid-based excipients intended for oral bioavailability enhancement (Jannin et al., 2008). Vegetable oils are predominately composed > 90 % of triglycerides. The chemical structure composition of a 'triglyceride' is detailed in Figure 1.4.

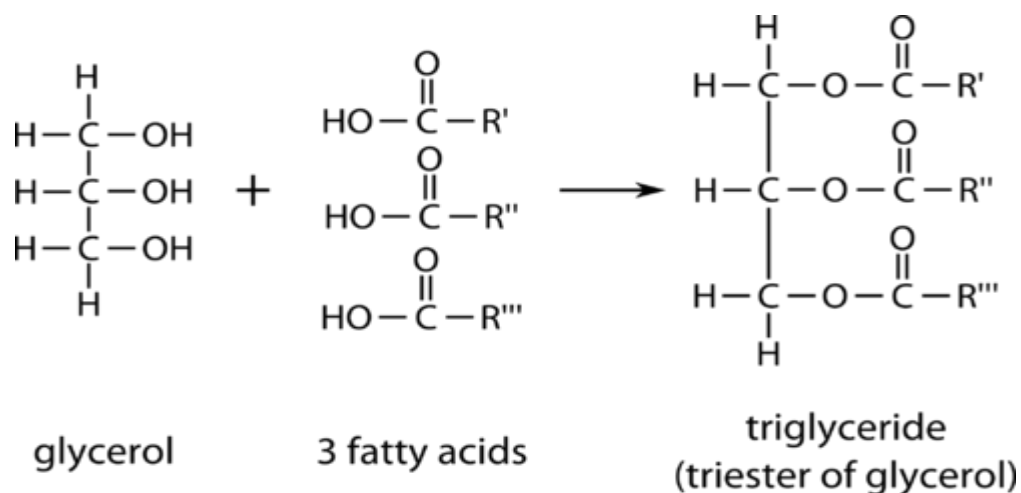
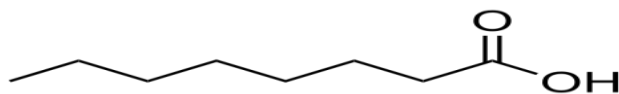


Figure 1.4 Chemical structure of a 'triglyceride'

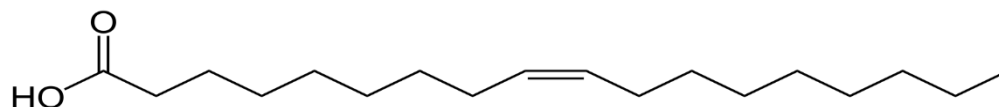
[https://chem.libretexts.org/Bookshelves/Introductory\\_Chemistry/Book%3A\\_Introductory\\_Chemistry\\_\(CK-12\)/26%3A\\_Biochemistry/26.8%3A\\_Triglycerides](https://chem.libretexts.org/Bookshelves/Introductory_Chemistry/Book%3A_Introductory_Chemistry_(CK-12)/26%3A_Biochemistry/26.8%3A_Triglycerides)

Significant other components include fatty acids, phospholipids and water-soluble vitamins. Table 1.3 details characteristics of common fatty acids found in lipid-based excipients (Jannin et al., 2008).

Typically, the fatty acids found in triglycerides are carboxylic acids (even numbered) with varying degrees of unsaturation. The structures of caprylic acid and oleic acid are detailed in Figure 1.5.



a. [https://upload.wikimedia.org/wikipedia/commons/thumb/d/d2/Caprylic\\_acid.svg/500px-Caprylic\\_acid.svg.png](https://upload.wikimedia.org/wikipedia/commons/thumb/d/d2/Caprylic_acid.svg/500px-Caprylic_acid.svg.png)



b. <https://www.eptes.com/wp-content/uploads/2018/07/Oleic-acid-d2.png>

Figure 1.5a Caprylic acid and 5b. Oleic acid.

Table 1.3 Characteristics of fatty acids found in lipid-based excipients (Jannin, 2008)

Fatty acid chain length	Number and position of unsaturated bonds	Common Name	Melting temperature (°C)
8	0	Caprylic acid	16.5
10	0	Capric acid	31.6
12	0	Lauric acid	44.8
14	0	Myristic acid	54.4
16	0	Palmitic acid	62.9
18	0	Stearic acid	70.1
18	1 Δ 9	Oleic acid	16.0
18	2 Δ 9, 12	Linoleic acid	-5.0
18	3 Δ 6, 9, 12	γ-linoleic acid	-11.0
18	1 Δ 9,(OH:12)	Ricinoleic acid	6.0
20	0	Arachidic acid	76.1
22	0	Behenic acid	80.0

Companies such as Gattefosse (France) and Abitec (US) specialise in the synthesis of vegetable oil derivatives to support the development of lipid-based formulations. Examples of 'oil phase' excipients are detailed in

Table 1.4 (Saxena et al., 2013); such excipients could be considered for range of lipid formulations (Type I, II and III).

*Table 1.4 Excipients commonly used as 'oil' phases in lipid formulations*

<b>Chemical Name</b>	<b>Trade Name</b>	<b>HLB</b>	<b>Supplier</b>
Glyceryl mono-oleate	Peceol™	1	Gattefosse
Glyceryl monolinoleate	Maisine™ 35-1	4	Gattefosse
Glyceryl caprylate/capratae	CAPMUL® MCM	3-4	Abitec
Medium chain triglycerides	Labrafac lipophile WL 1349	1	Gattefosse

Partial glycerides may be synthesised to increase the hydrophilicity (increase the HLB value) or modify the melt characteristics of vegetable oils. Hydrophilic–lipophilic balance (HLB) is the balance of the size and strength of the hydrophilic and lipophilic moieties of a surfactant molecule. The HLB scale ranges from 0 to 20. Common methods used to modify glycerides include glycerolysis, polyglycolysis, and ethoxylation (Jannin et al., 2008).

Glycerolysis is a common mechanism of partial glyceride production, which is a transesterification reaction of triglycerides with glycerol under heating with alkaline catalyst. Macroglycerides can be formed by polyglycolysis of vegetable oils with polyoxyethylene glycols (PEGs) of selected molecular weights. Polyoxylglycerides are composed of selected mixtures of mono, di and triglycerides with mono and diesters of PEG.

Specific ethoxylated lipids can be obtained from castor oil due to the presence of a hydroxyl group on ricinoleic acid which is a major component of castor oil. Cremophor EL (ethoxylated castor oil and Cremophor RH 40 (ethoxylated hydrogenated castor oil) are specific examples (Jannin et al., 2008). Polyalcohol esters may also be used to form amphiphilic compounds with relatively high HLB values using polyglycerol, propylene glycol, sorbitan, sorbitol or sucrose.

Type II lipid formulations generally consist of oil and non-water soluble surfactants with HLB values < 12. Examples of such excipients are detailed in Table 1.5.

Table 1.5 Excipients commonly used in type II lipid formulations

Chemical Name	Trade Name	HLB	Supplier
Oleyl polyoxyglycerides	Labrafil M1944CS	4	Gattefosse
Propylene glycol monocaprylate	Capryol™90	5	Gattefosse
Polyglyceryl-3 diisostearate	Plurol oleique CC 497	6-7	Gattefosse

Type III lipid formulations typically considered as 'self-microemulsifying systems as described by Porter (2000), due to clarity of emulsion formed on dilution; these systems containing more hydrophilic water-soluble surfactants compared to Type II formulations. Examples of such are detailed in Table 1.6. The HLB values for these systems  $\geq 12$ .

Table 1.6 Excipients commonly used in type III lipid formulations

Chemical Name	Trade Name	HLB	Supplier
Polyethylene-20 sorbitan oleate	Tween 80	14	VWR
Polyethylene-40 hydrogenated castor oil	Kolliphor RH40	12	BASF
Caprylo caproyl polyoxyl-8 glycerides	Labrasol ALF	12	Gattefosse

### 1.1.3 In-vitro and in-vivo considerations for lipidic delivery

Porter et al produced a comprehensive review of lipids and lipid-based formulations in Nature 2007. It was reported that the mechanisms by which lipid-based formulations affect drug adsorption and bioavailability are, alteration of the composition and character of intestinal milieu, recruitment of intestinal lymphatic drug transport and interaction with enterocyte-based transport processes.

As lipidic formulations present the API to the GI tract in a solubilised form they avoid the activation energy limitations typically associated with the API in a solid-state that must be overcome during *in-vivo* dissolution.

The presence of lipids in the GI tract can stimulate physiological processes such as increased bile salt and phospholipid secretion, which can thus increase the solubilisation capacity of the GI environment. Figure 1.6 taken from Porter's review article 2007, details a high-level overview of the process of lipid digestion following administration and subsequent drug solubilisation in the small intestine.

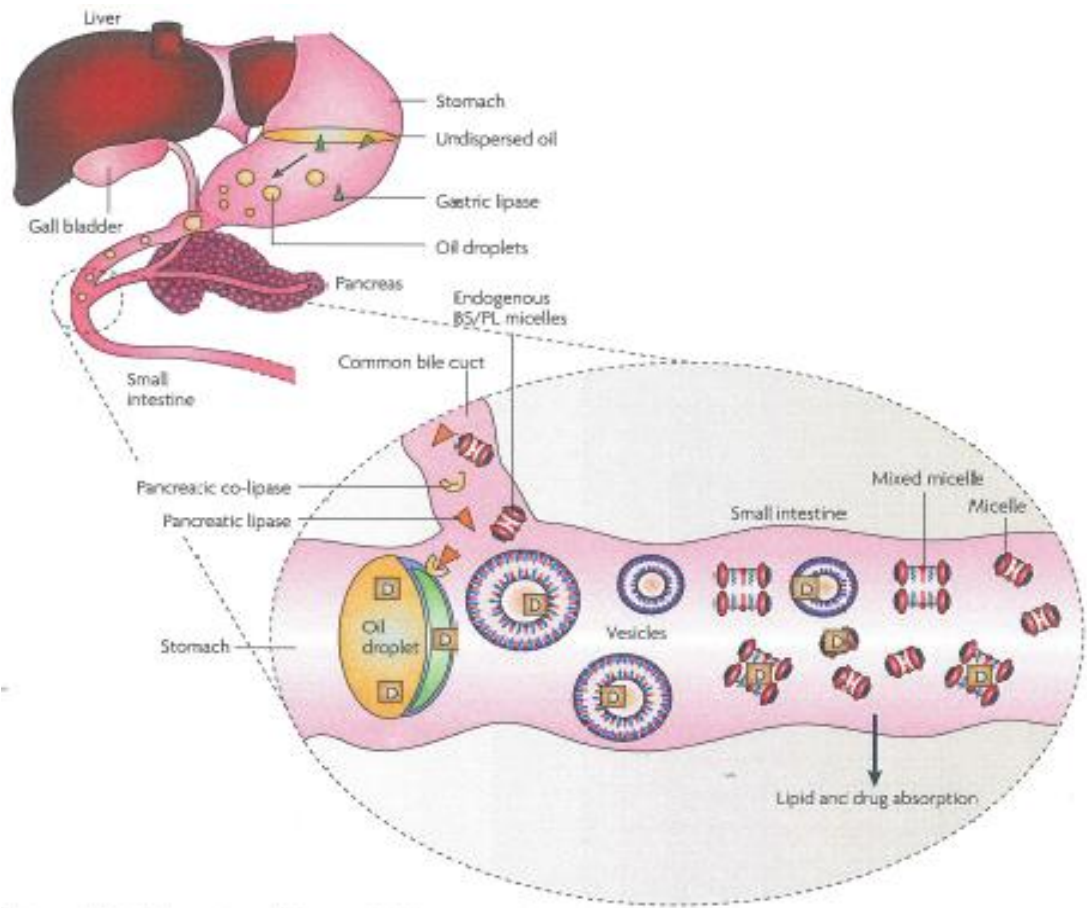


Figure 1.6 Lipid digestion and drug solubilisation in the small intestine (Taken from Porter, 2007)

Figure 1.6 shows that, post administration, the lipid-based formulation is initially digested in the stomach by gastric lipase (GL), producing diglycerides and fatty acids. The natural mixing process in the gut generates a crude emulsion which passes through to the small intestine. Thomas et al (2012) report that up to 25 % of the total digestion process (lipolysis) is performed by gastric lipase. In the small intestine pancreatic lipase in combination with its cofactor co-lipase complete the digestion process resulting in the generation of diglyceride, monoglyceride and fatty acids. The presence of these lipid components in the small intestine stimulates the secretion of bile salts, phospholipid and cholesterol from the gall bladder. Colloidal structures are formed from the gall bladder secretions in combination with the digestion products (monoglycerides and fatty acids). The structures formed may be vesicles (multi or unilamellar), mixed micelles and micelles. It is the formation of the colloidal structures that improves the solubilising capacity of the GIT and thus driving the absorption process.

Several publications (Porter 2007, Jannin et al., 2015; Thomas et al., 2012) report investigations into the influence of triglyceride selection and the digestion process (lipolysis) using *in-vitro* test methods, to determine formulation robustness and to screen formulations for likely *in-vivo* success, which is defined as enhancement in bioavailability compared to administration of the API in a solid state. Whilst it is not the intention of this thesis to develop a specific formulation for API delivery, it is important to understand the screening methods employed during both excipient and formulation selection; particularly where subsequent excipient addition to a formulation (in order to produce tablets) may impact upon the colloidal structures formed both when dispersed *in-vitro* and *in-vivo*.

The principle of *in-vitro* lipolysis methodology is the titration of fatty acids produced by the enzymatic breakdown of triglycerides (2:1 stoichiometric ratio) during digestion against NaOH. From a formulator's perspective the aim of test is two-fold; firstly, it can be used evaluate the influence of formulation composition upon the resultant colloidal species formed following digestion. Secondly it can be used to establish the concentration of drug present in the colloidal phase and thus would be expected to be in the most favourable form for absorption. Thomas et al (2012) reviewed a number of investigations in their lipolysis review article which described a typical *in-vitro* system as a thermo-controlled reaction vessel containing digestion medium representative of either the fed or fasted state. The medium is likely to contain aqueous buffer solution containing, bile salts, phospholipids and NaCl. The titration approach is controlled by a pH-device which linked to a pH probe titrates the NaOH in accordance with decreases in pH due to fatty acid formation. A number of techniques were reported (Thomas et al., 2012) to have been used to characterise the colloidal species formed including cryogenic scanning/transmission electron microscopy (SEM/TEM), small angle X-ray scattering (SAXS) and electron paramagnetic resonance (EPR).

To determine the fate of the API during lipolysis, samples tend to be withdrawn then centrifuged to form a sample containing either 2 or 3 phases. The top layer (if present) will consist of undigested (insoluble) lipid (subject to the initial formulation composition), the aqueous phase may contain the API dispersed within the colloidal systems formed and the solid pellet layer formed will contain any API which has precipitated along with any fatty acid precipitates formed. Although earlier it was assumed that the API present in the colloidal species in

the aqueous phase was optimal for absorption, it may be possible (*in-vitro*) for API to still be readily absorbed if the API precipitates out in an amorphous state.

#### **1.1.4 Semi solid solutions and suspensions**

The formulation types detailed in Table 1.2 and discussed in section 1.1.2 generally refer to liquid lipid-based formulations. There are, however, several lipid-based excipients that can be used to produce semi-solid solutions or suspensions of API which fall under the 'lipid delivery' banner (Type IV formulations). These excipients may play a constituent part in a 'classical' lipid emulsion pre-concentrate formulation; however, they may also be utilised alone or as the major carrier in a semi solid oral formulation. Excipients which fall into this category tend to be non-ionic surfactants with amphiphilic character having melting points above body temperature and have been used to not only enhance bioavailability, but also to modify release rate. Examples of such excipients includes the Gelucire™ (Gattefosse) range which as Panigrahi and coworkers (2018) report is derived from mixtures of mono, di and triglycerides with PEG esters of fatty acids. Multiple grades of Gelucire® are available with varying HLB values and melting points ranging from 33 to 65 °C (Panigrahi et al., 2018). Examples of API's delivered as solid solutions/suspensions in Gelucire® include Astra Zeneca's Lynparza™ (Olaparib) which is delivered with Gelucire® 44/14™ in a hard hypromellose capsule as confirmed in the summary of product characteristics (2015).

Another example of a semi-solid carrier for bioavailability enhancement is Vitamin E TPGS (D- $\alpha$ -tocopheryl polyethylene glycol succinate). Yang et al 2018, in their review, describe the molecule as synthesized by esterification of vitamin E succinate with poly(ethylene glycol) (PEG) 1000. The reaction forms a water-soluble derivative of natural vitamin E. It has an amphiphilic structure comprising hydrophilic polar head portion and lipophilic alkyl tail. The molecule is reported in Yang's review (2018) to inhibit P-glycoprotein. Sun et al (2014) showed that incorporation of Vitamin E TPGS as a nano emulsion stabiliser enhanced intestinal lymphatic transport.

The semi-solid based formulations confer certain processing advantages compared to liquid formulations. These semi-solid formulations can be filled directly into hard capsules in a molten state, which then solidify on cooling, making

these formulations more compatible than liquid formulations with (hard) capsule shells.

Li et al 2008, investigated PEG 3350 as a semi-solid carrier in conjunction with additional excipients to form a micro-emulsion preconcentrate which was filled into capsules.

Solvent selection can limit the compatibility of liquid formulations with (hard capsule shells) many solvents such as PEG's (< 1,000 Mw) and alcohols can react with capsule shells causing either deformation or embrittlement (Fulper and Wang 2009). The production of a stable tablet formulation would therefore be advantageous to overcome capsule instability (where required).

#### **1.1.5 Efflux Mechanisms**

As mentioned in Section 1.1.4, p-glycoprotein (P-gp) inhibition may be a strategy employed to enhance bioavailability particularly for BCS class IV molecules where permeation enhancement is necessary.

Chan et al (2004) explained in their review, the role that efflux mechanisms play in limiting accumulation of potentially toxic substances in the plasma membrane; they describe P-gp as a human adenosine tri-phosphate (ATP) binding cassette (ABC) protein, which is one of family of protective proteins forming the first line of defence in the intestinal epithelial cells. In the context of API absorption in the small intestine, P-gp may actively drive compounds which have entered cells, back into the intestinal lumen (Chan et al., 2004). P-glycoprotein may also alter the activity of metabolising enzymes such as CYP450 in the cell and is over-expressed in cancer cells which leads to tumour multidrug resistance (MDR); in addition, inhibition or induction of P-gp can cause changes in disposition and pharmacokinetics of substrate drugs which are the basis of drug-drug interaction (DDIs) as reported by Gurjar et al (2018).

If an API is a substrate for efflux; then administration of an efflux inhibitor may be advantageous. A study by Gurjar et al (2018) identified the potential for P-gp inhibition of a number of commonly used excipients. These studies utilised a MDCK MDR1 (Madin Darby canine kidney transfected with multidrug resistance 1 gene) cell line (which over expresses P-gp) to determine which excipients enhanced the accumulation of Digoxin in the cells; digoxin being a recognised

substrate for efflux. The study (Gurjar et al., 2018) showed that in a concentration dependant manner, cell accumulation of digoxin increased with selected excipients as follows: Cremophor EL™ (poly(ethylene oxide)<sub>35</sub> modified castor oil) > Vit-E PEG (D-α-tocopherol poly-(ethylene glycol) succinate) > Brij 58™ (poly(ethylene glycol) hexadecyl ether) > Tween 80 (poly(ethylene oxide)<sub>20</sub> sorbitan Monooleate) > NaCMC (sodium carboxymethylcellulose) > Tween 20 (poly(ethylene oxide)<sub>20</sub> sorbitan monolaurate) > CTAB (cetyltrimethylammonium Bromide) > Solutol HS 15™ (polyethylene glycol<sub>15</sub> hydroxystearate) > AOT (sodium 1,4-bis (2-ethylhexoxy)-1,4- dioxobutane-2-sulfonate).

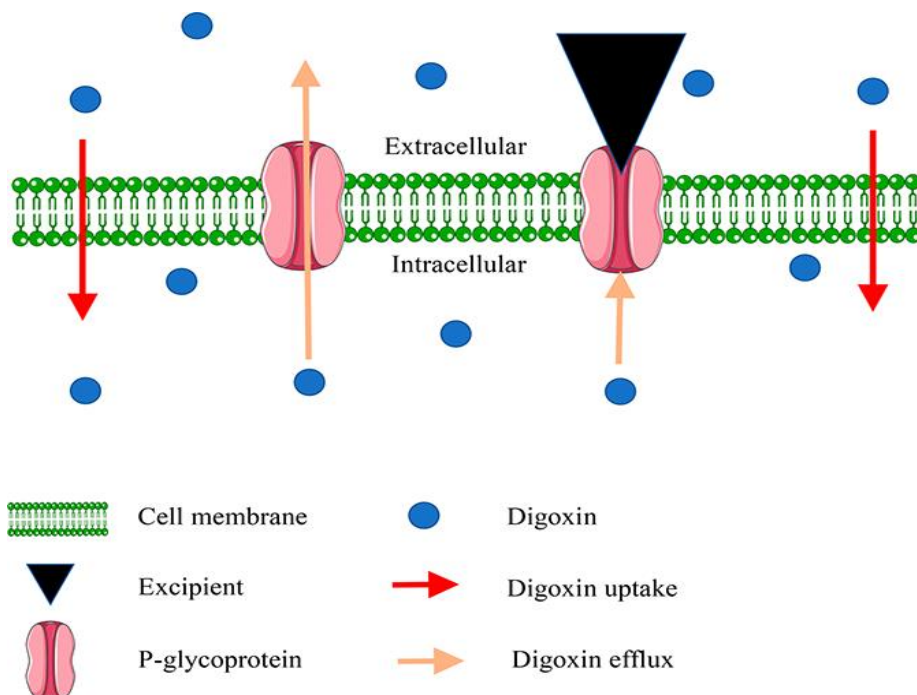


Figure 1.7. Diagrammatic representation of excipient interaction with P-glycoprotein to inhibit digoxin efflux. (Taken from Gurjar, 2018)

Whilst the mechanism(s) of efflux inhibition are not well understood, the selection of specific excipients can be investigated to increase potential for absorption of known efflux substrates. Consideration must however be given to the influence of such excipients upon the pharmacokinetics (PK) of co-administered API's, which may be dosed concurrently due to the disease state in question. During clinical evaluation of new drug products containing excipients known to inhibit efflux, additional drug-drug interaction studies may be requested by the registration authorities to understand the likely PK effects.

## **1.2 Tablets as a dosage form**

On December 8<sup>th</sup>, 1843, William Brockendon was granted English patent no 9977 for 'Shaping pills, lozenges and black lead by pressure in dies'. So significant was the invention that the Druggist and Chemist magazine dedicated a section in their August addition in 1954 to commemorate 100 years of his passing. Fast forward approximately 170 years and the review performed by Shulka et al (2016) reported that tablet formulations are the most prominent and patient compliant formulation since its evolution, two thirds of total prescriptions written by medical practitioners has tablets as the preferred dosage form.

The European Pharmacopoeia (Ph Eur) 9.0 describes tablets as solid preparations each containing a single dose of one or more active substances. They are obtained by compressing uniform volumes of particles or by another suitable manufacturing technique, such as extrusion, moulding or freeze-drying.

Subject to the intended disease state for which the tablet has been designed to treat or the demographic of the patient base; then the tablet may be formulated as one of the following sub-groups of tablet 'classes':

- Immediate release (uncoated).
- Coated
- Gastro resistant
- Modified release
- Effervescent
- Soluble/dispersible
- Oro-dispersible
- Chewable
- Sublingual/buccal.

It was only intended to investigate immediate release tablet formulations as part this thesis, therefore all subsequent subject matter is focussed accordingly.

### **1.2.1 Powder properties.**

For a powder to be compressed successfully in accordance with the stages detailed in 1.2.2, it first must be formulated to be amenable to allow to it flow into a die. Powder flow is intimated by a number of physical particle characteristics

including, particle size, shape and density, and also blend characteristics such as overall charge, moisture content (hygroscopicity of the blend and environmental conditions), particle size distribution of the blend and (as reported by Patel et al (2006)) a high proportion of fines and excessive lubricant levels.

Powder flow can be characterised by a number of physical tests including, flow through an orifice, angle of repose and by measurements of consolidation (density) to produce Carr's Index and Hausner ratio values (Aulton, 2018).

### **1.2.2 The compression process**

The process of powder compression has been well documented and studied; in 2016 the United States Pharmacopeia (USP) introduced a new general chapter <1062> Tablet compression characterisation. In this chapter compression behaviour is described as governed by the physical and mechanical properties of the material as well as aspects of the compression process such as pressure (i.e., stress), degree of deformation (i.e., strain), and rate of deformation (i.e., strain rate). It explains that the knowledge of stress, strain, and strain rate is important for understanding powder behaviour during the compression process and goes to state that the majority of pharmaceutical tablets are manufactured by "uniaxial powder compression". Thus, each tablet is formed by the densification of a loosely packed powder sample confined within a rigid die using two rigid punches that approach from above and below (in a vertical plane).

The compression process is typically described in four stages:

1. Particle rearrangement
2. Compression
3. Decompression
4. Ejection

During particle rearrangement pore volume is reduced and the density of the powder is increased as a result of particle consolidation. Patel et al (2006) state that finer particles enter the voids between the larger ones and give a closer packing arrangement during this phase.

United States Pharmacopeia (USP 40, <1062>, 2020) describes compression as when; particles are deformed at points of contact with other particles, the die wall, or the punch surfaces. During this stage, compression pressure often increases rapidly, causing volume reduction as the powder density increases. Under

pressure, particles initially undergo elastic deformation. Depending on mechanical properties and stress at points of contact, particles can subsequently undergo varying degrees of fragmentation and/or plastic deformation. Relative particle movement is limited when the powder is highly consolidated. For most pharmaceutical materials, plastic deformation is an important part of the compression process that leads to an increase in the area of contact between particles, contributing to higher compact strength. Clean particle surfaces generated from fragmentation also contribute to higher compact strength. The deformation behaviour and resultant tablet mechanical properties of many pharmaceutical powders are also sensitive to the compression speed (punch velocity) and the length of time at which the powder is held under pressure at a constant volume (dwell time). The end of the second stage is usually the time of highest compression pressure.

Patel et al (2006) explained that based on their mechanical properties, powders can be classified as plastic, elastic, and viscoelastic. However, under the influence of an applied pressure, the particles not only deform plastically or elastically, but also fragment to form smaller particles (brittle fracture) the type of deformation can be attributed to the rate and magnitude of the applied force and the duration of locally induced stress. Figure 1.8 was taken from Patel et al (2006) and explains the Stress strain relationship in powders with different mechanisms of compression.

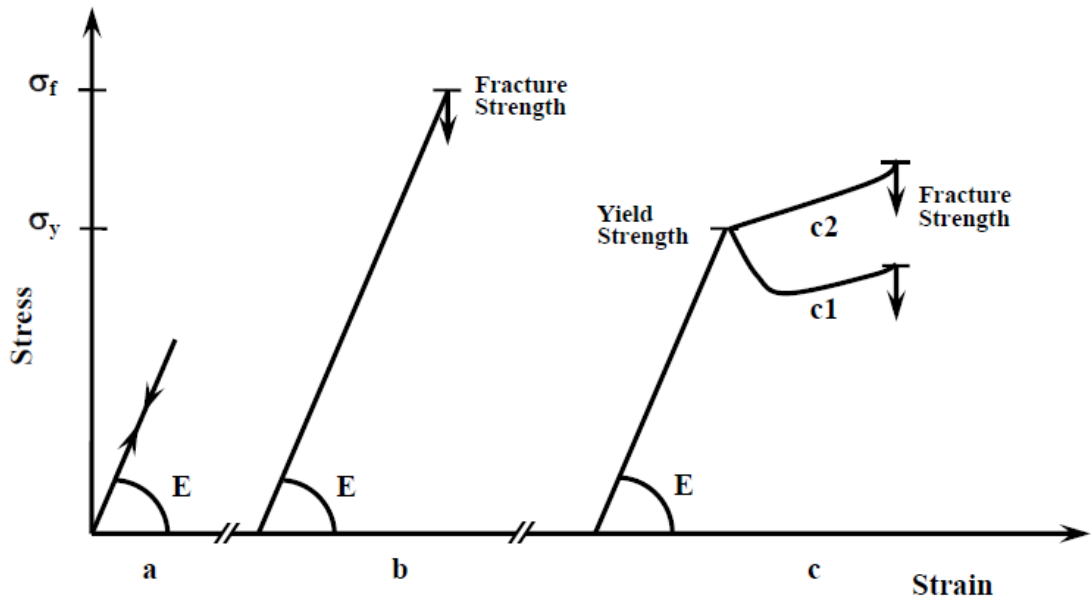


Figure 1.8 Stress strain relationship in powders with different mechanisms of compression (Patel et al 2006)

As a result of the resistance of a material against deformation (strain), the stress inside the particles increases. If the applied stress is released before the deformation reaches a specific critical value, the particles deform elastically, i.e., the deformation is reversible and the particles inside the powder bed regain their original shapes. Until this critical value, the stress is linearly proportional to the deformation and is characterized by elastic or Young's modulus ( $E$ ). (Figure 1.8a). For the brittle materials, particles fragment into smaller units at a certain stress value ( $\sigma_f$ ). This stress is the fracture strength (Figure 1.8b). For ductile/plastic materials, after a critical stress ( $\sigma_y$ ), the particles yield and start to deform plastically. This critical stress is the yield strength of a material (Figure 1.8c). Material fracture eventually occurs at higher deformations. Elastic deformation is a reversible process, whereas plastic deformation results in a permanent change in the particle shape.

Decompression was described (USP 40, <1062>, 2020) as when the punches retract, resulting in a decreasing axial punch pressure. As axial pressure is reduced to zero during decompression, residual die wall pressure typically exists in the radial direction. During this phase, particles primarily undergo elastic recovery, depending both the pressure and the mechanical properties of the particles. Elastic recovery may provide insight into the elastic deformation that

the powder experienced during compression. Excessive elastic recovery may reduce the inter-particle bonding and can result in a significant decrease in tablet mechanical strength.

The ejection phase was described (USP 40, <1062>, 2020) as when the tablet is pushed out of the die by the lower punch. As the tablet emerges from the die, the ejected portion of the tablet is free to expand radially due to elastic recovery (i.e., release of residual die wall pressure). Significant shear stress may develop within the tablet and at the edges of the tablet–die interface because the lower portion of the tablet remains constrained by the die wall. In severe cases, this shear stress can result in tablet lamination or capping.

### 1.2.3 Tableting Properties

Osumura et al (2016) described the tableting properties of powders in terms of ‘compressibility’, ‘compactability’ and ‘manufacturability’. USP 40, <1062>, (2020) defines these terms as:

Compressibility – the dependence of tablet solid fraction (see Section 1.3.4) on compression pressure. Equation 1.1 can be used to determine compressibility over a range of solid fractions, where  $a$  and  $b$  are empirical constants.

$$\text{Log}(\text{compression pressure}) = a \times (\text{solid fraction}) + b \quad \text{Equation 1.1}$$

Formulations or materials can be screened for compressibility by comparison of the compression pressure required to form tablets with a specific solid fraction. Historically, compressibility of powders was evaluated using either Heckel Plots (Heckel 1961) or Kawakita Plots. The Heckel equation is detailed in (Equation 1.2)

$$\text{Ln} (1/1-D) = KP + A \quad \text{Equation 1.2}$$

where  $D$  is the relative density of the compact in die at pressure  $P$ ,  $K$  and  $A$  are regression coefficients of the linear portion of the curve, and the reciprocal of  $K$  is the mean yield pressure ( $P_y$ ), which is generally considered to reflect the effective deformability of the particles during compression (Heckel 1961). The mean yield pressure when established at different compression speeds can be used to determine the strain rate sensitivity of a material (Heckel, 1961).

$$\%SRS = ((Py_2 - Py_1) / Py_2) \times 100 \quad \text{Equation 1.3}$$

Compactability as defined by USP 40, <1062>, 2020 is the relationship between tensile strength (see Section 1.3.4) and solid fraction, which is formed on the general principle that tablet tensile strength increases exponentially with increasing solid fraction and is described by the Ryshkewitch-Duckworth equation, (Equation 1.4)

$$\text{Log (tensile strength)} = k \times (\text{solid fraction}) + A \quad \text{Equation 1.4}$$

Where k and A are empirical constants. Where solid fraction is calculated as per Equation 1.4 a (taken from USP 40, <1062>, 2020).

$$\text{Solid Fraction} = \frac{(\text{density of the tablet})}{(\text{true density of material})} = \frac{(\text{mass of tablet})}{(\text{volume of tablet})} \times \frac{1}{(\text{true density of material})}$$

$$\text{Equation 1.4 a}$$

Tabletability is an additional term described by USP 40, <1062> 2020 and is defined as the relationship between tablet tensile strength and compression pressure (see Equation 1.5).

$$\text{Log (tensile strength)} = k \log (\text{compression pressure}) + B \quad \text{Equation 1.5}$$

Where k and B are empirical constants.

By utilising tablet tensile strength (which accounts for tablet size) and compaction pressure (force per unit area across the punch tip) the variables of tablet size, thickness and weight can be minimised upon compression data interpretation; thus giving confidence that a formulation would be sufficiently robust to such changes. In addition, when screening formulations this approach can be used to compare the tensile strength of tablets (mechanical strength) when compressed at a set pressure.

Figure 1.9 shows a three-dimensional compression profile which details the relationships between compression parameters and tablet properties.

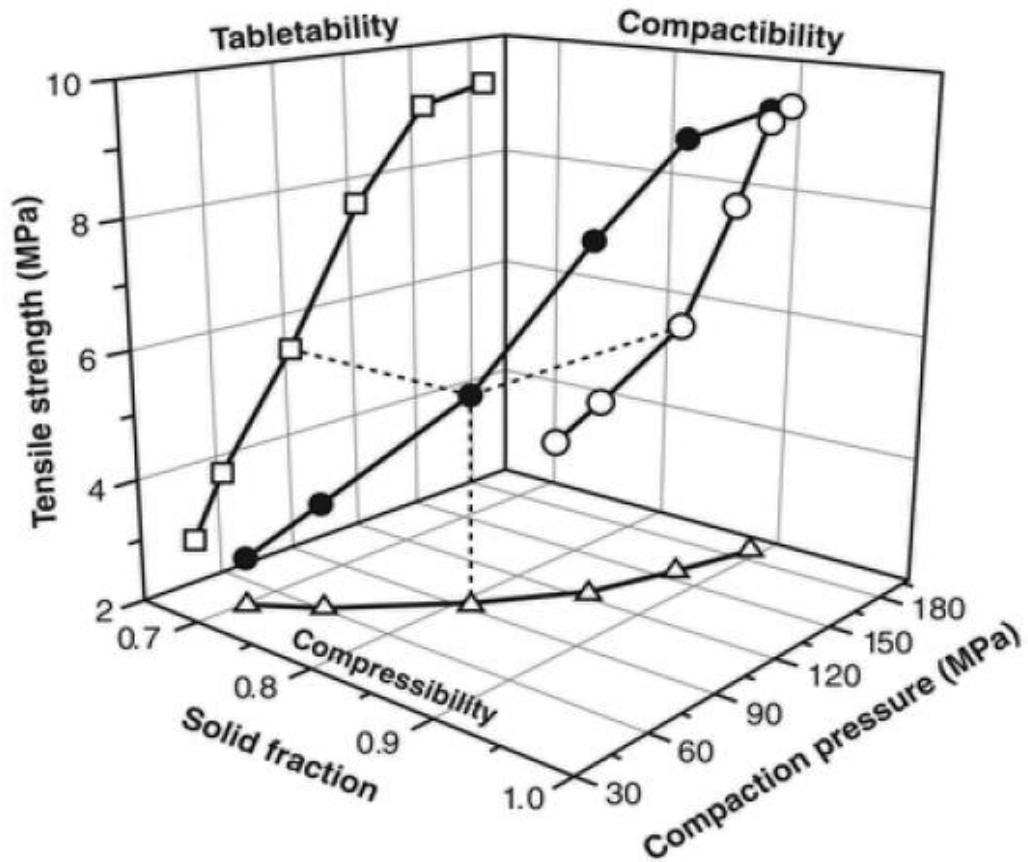


Figure 1.9 Three-dimensional compression profile (Taken from USP<1062>).

#### 1.2.4 Tablet Characteristics

The physical characteristics of tablets are governed by multiple factors, including the formulation composition, the moisture composition of functional components (diluents, compression aids and lubricants), the compression force applied (stress) and the duration of application (of applied stress); the shape and size of the punches used to form the tablets.

The mechanical strength of tablets is typically characterised by breaking force (commonly described as ‘hardness’) in accordance with USP 40, <1217>, 2020. Fell and Newton (1970) described a method to determine tablet hardness, expressed as tensile strength using a diametral-compression test which has subsequently formed the basis for mechanical strength determination across the industry. The equation for tensile strength is detailed in Equation 1.6.

$$\sigma_0 = \frac{2P}{\pi Dt} \quad \text{Equation 1.6}$$

where P= applied load (N), D = tablet diameter (mm) and t = tablet thickness (mm)

In accordance with USP 40, <1217>, (2020) Equation 1.6 only applies to cylindrical tablets (with flat faces). Pitt et al (2013, 2015) proposed two further equations may be used to determine the tensile strength of convex face tablets (Equation 1.7) and caplet shape tablets (Equation 1.8).

$$\sigma_t = \frac{10P}{\pi D^2 \left( 2.84 \frac{t}{D} - 0.126 \frac{t}{W} + 3.15 \frac{W}{D} + 0.01 \right)}$$

Equation 1.7

$$\sigma_t = \frac{2}{3} \left( \frac{10P}{\pi D^2 \left( 2.84 \frac{t}{D} - 0.126 \frac{t}{W} + 3.15 \frac{W}{D} + 0.01 \right)} \right)$$

Equation 1.8

$\sigma_t$  is the tensile strength, P is the fracture load, D is the length of the short axis or diameter of the tablet, t is the overall thickness and W is the wall height of the tablet.

Pitt et al (2013, 2015) explained that generally, a tensile strength greater than 1.7 MPa will usually suffice in ensuring that a tablet is mechanically strong enough to withstand commercial manufacture and subsequent distribution. Ideally, tensile strengths greater than 2 MPa should be targeted to ensure a satisfactory robust product. Tensile strengths as low as 1 MPa may suffice for small batches where the tablets are not subjected to large mechanical stresses.

The mechanical strength of the tablets will be influenced by the punch velocity (see Equation 1.4), Roberts and Rowe (1985) reported that for materials known to deform plastically there was an increase in yield pressure (determined using Heckel analysis) attributable to the time-dependant nature of plastic flow. Thus, the period (dwell time) under which a tablet is under the maximum applied force (strain) will influence the tensile strength of the tablet. The influence of tablet press speed must therefore be a consideration during formulation development activities to assess formulation robustness and potential for product scale up.

The ejection force for a tablet is the force required to eject the tablet from a die after compaction. If the ejection force for a tablet is too high, then capping and

lamination will occur. Wang et al (2004) determined that the ejection force is dependent on the compaction pressure applied to the tablet, typically the higher the compaction pressure, the higher the ejection force. Pitt et al (2015), explained that consideration must be given to the size of tablets being compressed and that the effect of the ejection force depends on the size of the tablet; a larger tablet will be able to withstand a higher ejection force. Therefore, to compare across the scales they determined ejection shear stress by dividing the peak ejection force by the area of the tablet in contact with the die wall. The lower the ejection shear stress, the less likely that tablet defects will occur. Generally, an ejection shear stress of less than 3 MPa from a commercial tablet press will suffice in producing a tablet which does not cap or laminate. Ejection shear stresses up to 5 MPa may be acceptable where the tablets are not subjected to large mechanical stresses on subsequent processing such as film-coating. Ejection shear stresses above 5 MPa would be expected to cause failure as determined by Lixia et al (2013) and Soh et al (2013).

### **1.3 Mechanics of Tablet Compression**

Tablets can be produced by several means subject to the aims of the production process. Single punch eccentric systems are often used during early phase clinical batch production where API availability may be scarce (small batch sizes), only the upper punch is active during the compression cycle (Sovany et al., 2009). Rotary machines are used for commercial manufacture due to their high product outputs. On such machines, the die table along with many punches rotates and pushes each set of upper and lower punch between compression rollers. This causes the punches to move inside the die and compress the powder (Natoli et al., 2017). Figure 1.10, details the compression cycle on a rotary press

The compression cycle on a rotary machine is double-sided with a pre-compression stage followed by a main compression stage. On an eccentric press the compression cycle is single sided without pre-compression. The relative speed (high punch velocity and reduced dwell time) of a rotary press is higher than that of an eccentric press. For materials/formulations which exhibit strain rate sensitivity it is important to understand the limitations of press speed (punch velocity and dwell time) upon tablet characteristics.

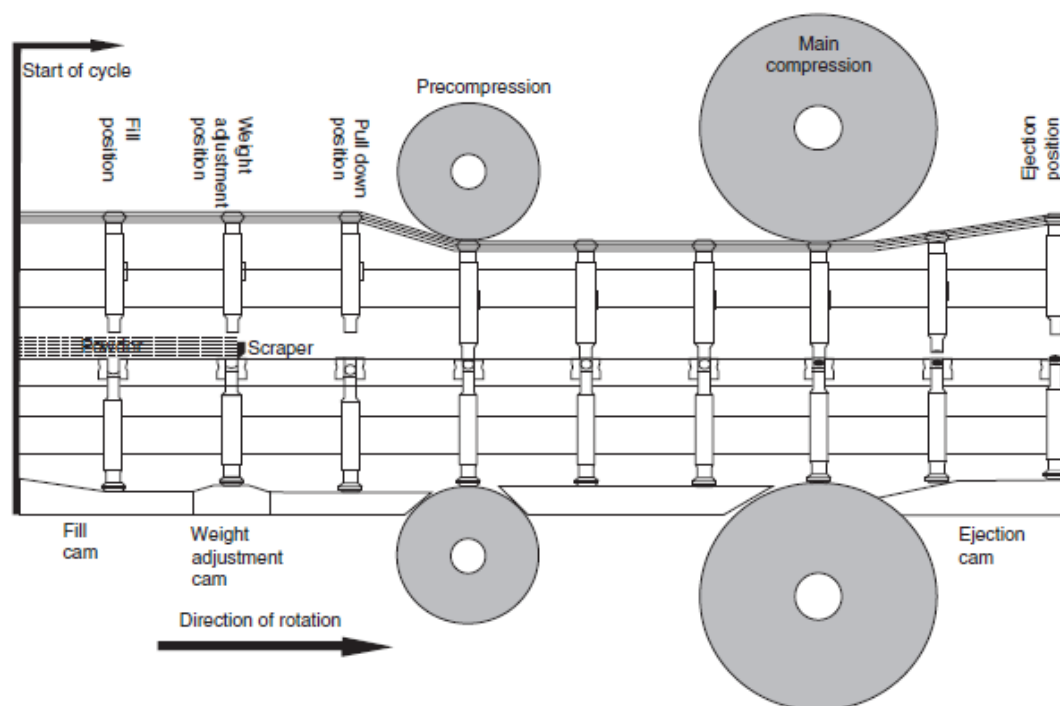


Figure 1.10 Rotary Press cycle (taken from Natoli, 2017)

A compaction simulator can reproduce upper and lower punches displacement profiles of any rotary tablet press with variable speed and require a low quantity of powder. Rotary tablet press simulators are very useful in investigating the effect of punch velocity on the compaction properties of powders. These studies are essential for the scale-up from an eccentric press to a rotary machine in industrial production. (Michaut et al., 2010). The studies reported in this thesis will utilise a Stylcam 100 R (MedelPharm, Lyon, France). The Stylcam 100R, is rotary press simulator, designed to simulate speed profiles of rotary tablet presses (Michaut et al., 2010).

#### 1.4 State of the art – Solid SMEDDS formulations

Investigations into the potential for solid lipid or semi-solid carrier formulations is not new. Larhrib et al (1997) investigated the compressibility of a range of PEG grades and the influence of process parameters upon tablet characteristics. Whilst their study evaluated a single carrier, more recently studies have focussed upon the use of adsorbent based carrier systems onto which the 'lipid' based formulations are loaded. Table 1.7 details several investigations into the establishment of solid lipid-based formulations.

Table 1.7 Examples of investigations into the establishment of solid lipid-based formulations.

Author(s)	Year	API	Formulation Type	Adsorbent	Loading method	Compression Parameters, Tablet characteristics evaluated
Spireas and Srinivas	1998	Prednisolone	Single liquids	Microcrystalline cellulose	Not specified	Not specified
Ito et al.	2005	Gentamicin	SMEDDS (liquid)	Florite™, Neusilin® (US2), Sylsia™	Kneading	None (powder filled into capsule)
Sander and Holm	2009	Cyclosporine	SMEDDS (liquid)	Neusilin® (US2)	Adsorption onto pre-formed tablet (wicking)	Tablet porosity, hardness, compression force
Hentzschel et al.	2012	Griseofulvin	PEG300 (liquid)	Neusilin® (US2), Aerosil 200™, Avicel PH200™	Mixing (mortar and pestle)	Tablet hardness, compression force and tensile strength
Gumaste et al.	2013	N/A	Single lipids (liquid)	Various*	Alcoholic slurry and drying	Tabletability (tensile strength versus compaction pressure)
Gumaste et al.	2013	Probucol	SEDDS (liquid)	Neusilin®(US2)	Adsorbent added to liquid SEDDs by overhead mixing.	Tabletability (tensile strength versus compaction pressure), friability
Reddy et al.	2014	Efavirenz	SMEDDS (liquid)	Neusilin	Drop wise with stirring	None (powder characterisation only)
Cirri et al.	2016	Glyburide	SMEDDS (liquid)	Neusilin® (US2)	Mixing (mortar and pestle)	Tablets characterised for hardness and friability and disintegration.
Vranikova	2016	Rosuvastatin	PEG400 (liquid)	Neusilin® (US2)	Fluid bed spray onto adsorbent	Hardness, friability and disintegration
Seljak	2018	Resveratrol	SMEDDS (liquid)	Neusilin® (US2)	Mixing (mortar and pestle)	Compression force, hardness (Ts), elastic relaxation, friability and disintegration

Whilst tablet formulations have been studied, and certain tablet characteristics determined, little consideration appears to have applied to understanding the influence of compression parameters, the compaction mechanism of adsorbents loaded with lipid formulations or the limitations of process parameters upon tablet characteristics. The focus of most studies is upon the bioavailability enhancement of selected API's and the

characteristics of the micro-emulsion formed (*in-vitro*) post de-sorption of the pre-concentrate from the carrier.

The loading methods of the liquids on to the adsorbent carriers varies significantly between investigations; from complex and difficult to scale such as the loading through capillary action (wicking) employed by Sander and Holm (2009) or the alcoholic slurry formation used by Gumaste et al (2013).

The studies documented in this thesis, will aim to address some of these unknown considerations (influence of process parameters) upon tablet characteristics, and will employ methods for loading that are anticipated to be amenable to scale up.

## **1.5 Adsorbent Selection**

The studies detailed in Table 1.7, show that a range of adsorbents have been investigated as carriers for solid lipid-based formulations (SLBF's). Chaven et al (2015) reported that differential drug release behaviour from solid SEDDS was attributed to the different physico-chemical properties of solid carriers; therefore careful selection of adsorbents based upon properties such as surface area, porosity and hydrophobicity-hydrophilicity is critical to ensure that a successful formulation can be established.

The most reported adsorbent is Neusilin US2 which is an magnesium aluminometasilicate manufactured by Fuji. Gumaste et al (2013) established the compaction properties of a range of silicate based adsorbents and the influence of drug release properties from such formulations containing lipid.

Considerations for selection of adsorbent for the studies documented in this thesis included; surface area, porosity, pore size, compressibility, ease of handling (processing of liquid onto the solid substrate) which is a function of material density, particle size distribution and flowability. Flowability is likely to be influenced by surface morphology, particle charge, moisture content and crystalline form.

## **1.6 Structure of Thesis**

### **1.6.1 Aims and Objectives**

The aim of these studies was to investigate the compression properties of lipid-based tablet formulations. The purpose was to provide an in depth understanding of the potential, or conversely; limitations of liquid-solid dosage forms. To support a formulator during dosage form design of new formulations,

as to the viability of selecting a lipid-based tablet formulation as a realistic option to progress for clinical evaluation, with confidence that the formulation could be scaled.

The primary objectives of these studies were as follows:

- I. To screen a range of adsorbent materials to understand their potential as lipid carriers and suitably compressible materials post sorption.
- II. To establish the boundaries/design space for optimum lipid loading versus acceptable compression characteristics.
- III. To understand and justify the requirement for additional excipient addition to produce tablet formulations which produce suitably robust tablets in compliance with pharmacopoeial specifications.
- IV. To understand the influence of selected lipid carriers on the established 'design space' for loading and tablet characteristics.
- V. To evaluate the influence of compression parameters and lipid selection upon the in-vitro release characteristics of a selected active pharmaceutical ingredient (API) from model lipid formulations

### **1.7 Thesis Overview**

The aim of the studies detailed in Chapter 2 was to evaluate the compression properties of a range of sorbents before and after the sorption of a Type I lipid formulation substrate. The most promising adsorbent identified (Neusilin®US2), was selected for further studies. The purpose was to establish the potential limitations for robust tablet production (including the influence of lipid loading level and dwell time during compression upon tablet tensile strength). The findings of this study would form the basis upon which further studies would be performed, to evaluate the influence of loading alternative formulations and strategies to be employed to optimise tablet characteristics.

The studies detailed in Chapter 3, aimed to evaluate the compression properties of Neusilin® US2 loaded with a Type 3 lipid formulation (SMEDDS pre-concentrate (SPc) formulation). A Type III lipid formulation was selected due to the potential for SMEDDS based formulations to improve API bioavailability. Following the characterisation of SPc 'loaded' Neusilin® granules and their compression properties; excipients were selected to be added to the granules, to produce formulation blends, to improve tablet characteristics. Tablet characterisation data was

analysed using design of experiments software to derive a predictive model for the purposes of identifying those critical factors which drive tablet characteristics.

Due to the characterisation data generated in Chapter 3 which showed poor and variable tablet friability; Raman spectroscopy was used in Chapter 4, to determine the distribution of the SMEDDS pre-concentrate throughout loaded granules and tablets produced from these loaded granules. The aim was to understand if pressure applied during compression produced concentration gradients (variable density) throughout a tablet; and did this variability give rise to unfavourable tablet characteristics.

In Chapter 5 two semi solid excipients considered representative of Type IV lipid formulations, were selected for evaluation and loaded on to Neusilin®US2. The influence of Gelucire®44/14 and vitamin E TPGS upon the compression characteristics of Neusilin®US2 and physical properties of the tablets produced, were determined. The data was compared against the previously loaded liquid formulations. Dipyridamole (a model BCS class II API) was added to the Type IV excipients prior to loading, the influence of compression force upon *in-vitro* release rate was determined.

## Chapter 2.

### **“Evaluation of sorbent characteristics pre and post loading with a Type I lipid formulation/substrate”**

#### **2.1 Introduction and aims**

The aim of these studies was to evaluate the physical characteristics and compression properties of a range of sorbents before and after the sorption of a lipid substrate, in this case Labrafac Lipophile WL1349® (LLW). The purpose was to establish the potential limitations for robust tablet production (including the influence of lipid loading level and dwell time during compression upon tablet tensile strength) and to select the most favourable adsorbent for further investigation.

Sorbents were selected (as detailed in Table 2.1) based upon previously reported studies (Spireas and Srinivas, 1998; Gumaste et al, 2013; Veranikova et al, 2015), those excipients listed as adsorbents in the Handbook of Pharmaceutical Excipients 8<sup>th</sup> (Sheskey et al., 2017), or excipients that were thought to worthy of investigation based upon previous use as diluents for tablets and likely tableting properties. The materials selected (Table 2.1) possessed a wide range of individual specific surface areas (SSA). The specific surface area of a powder is determined by physical adsorption of a gas on the surface of the solid and by calculating the amount of adsorbate gas corresponding to a monomolecular layer on the surface (USP general Chapter <846> (2017). The potential for high lipid loading to be achieved was likely to be influenced by the surface area of adsorbents where high surface area values are attributable to the porous structure of the adsorbent.

Table 2.1 Sorbents selected for evaluation

Material	Grade(s)	Typical Application/Use	Specific Surface Area m <sup>2</sup> /g
Hydrophobic fumed silica (Evonik, 2019)	Aerosil® R972 Pharma	Glidant.	90 - 130
Silicon dioxide (Evonik, 2019)	Aeroperl® 300 Pharma	Glidant, anticaking agent, viscosity modifier.	270 - 330
	Aerosil® 200 VV Pharma	Glidant, anticaking agent.	175 - 225
Silicon dioxide (Grace, Apr 2009)	Syloid® 244 FP	glidant, tableting-aid and liquid carrier.	Not determined according to product specification
Silicon dioxide (Grace, Apr 2017, Monsuur, 2015)	Syloid® AL-1 FP	Glidants, and anti-caking agent	700
Magnesium aluminometasilicate (Fuji, 2009)	Neusilin® UFL2	Tablet formulation diluent, binder, flow aid. Liquid solidification.	300
	Neusilin® NFL2N	Tablet formulation diluent, binder flow aid. Liquid solidification	250
	Neusilin® US2	Tablet formulation diluent and binder. Liquid solidification	300
Magnesium carbonate (Sheskey, 2017)	USP	Adsorbent; antacid; tablet and capsule diluent	14.64–14.78
Tricalcium phosphate (Sheskey, 2017)	TRI-CAFOS 500	Anticaking agent; buffering agent; dietary supplement; glidant; tablet and capsule diluent.	70–80
Hydrated magnesium aluminium silicate (Sheskey, 2017)	Veegum HS	Adsorbent; stabilizing agent; suspending agent; viscosity increasing agent	Not determined according to product specification
Magnesium Trisilicate (Sheskey, 2017)	Fine powder	Anticaking agent; glidant; therapeutic agent	Not determined according to product specification

As discussed in Chapter 1, the powder properties (flow, density and compaction mechanism) of a material are essential to understand, when embarking on the development of tablet dosage form. The ideal properties for sorbents pre-loading, would be high surface high area/porosity (for absorption), a relatively high density to allow ease of handling, be free flowing and compress well with little strain rate sensitivity. The same characteristics would be necessary post loading and those sorbents which were able to adsorb relatively high loads of LLW whilst maintaining such properties would be selected for further evaluation.

It should be noted that chemical compatibility and binding potential between the sorbent and the formulated API; should be evaluated as early as possible during a development programme; to mitigate later stage stability and product performance risks. Where

product performance risks may include poor API recovery during *in-vitro* dissolution assessment (Speybroeck et al., 2012, Williams et al., 2014). The studies in this Chapter deliberately did not include an API, instead the focus was upon the physical characteristics of the sorbents pre and post loading with LLW.

Previous studies have investigated the potential for lipid matrix-based tablets termed liquisolids (Spireas and Srinivas, 1998; Gumaste et al., 2013a; Veranikova et al., 2015), which are preferred by patients both in terms of familiarity and ease of administration. Gumaste et al (2013b) established the compaction properties of a range of silicate-based adsorbents and the influence of drug release properties from such formulations containing lipid.

However, none of the previous studies reviewed have investigated the influence of punch velocity/dwell time on tablet characteristics. The author believes such understanding to be a pre-requisite for the potential scale up of such a formulation.

## **2.2 Materials**

Table 2.2 details the sorbents and supplier details evaluated in these studies. The substrate for this study was medium chain triglycerides - Labrafac Lipophile WL 1349 (LLW) batch number, 313JVI-162219, received from Gattefosse, Bracknell, UK. LLW was selected as the lipid substrate for loading; with a HLB value of 1 the lipid is classed as an 'oil carrier' and could therefore be used as a single lipid system in a type I lipid based formulation (as detailed in Section 1.1.2 in Chapter 1). It was deemed appropriate during these studies to evaluate a single substrate rather than a more complex mixture at this sorbent screening stage. In addition to Type I lipid systems, LLW has previously been used in the development of SMEDDS formulations (Guo et al., 2011; Raval et al., 2012).

Table 2.2 List of sorbents investigated

Material	Grade(s)/Batch No.	Supplier details
Hydrophobic fumed silica	Aerosil® R972 Pharma/ 103010051	Evonik Degussa GmbH, Hanau, Germany
Silicon dioxide	Aeroperl® 300 Pharma/ 3151011119 Aerosil® 200 VV Pharma/ 315041414	
Silicon dioxide	Syloid® 244 FP/ 271064. Syloid® AL-1 FP/ 220727	Grace GmbH & Co. KG, Worms, Germany
Magnesium aluminometasilicate	Neusilin® UFL2/ 110034, Neusilin® NFL2N/ 101001, Neusilin® US2/ 103010	Fuji Chemical Industry Co.; Ltd, Toyama, Japan
Magnesium carbonate	USP/ 1209601918	J.T. Baker Center Valley, Pennsylvania, USA
Tricalcium phosphate	TRI-CAFOS 500/ B45030A	Budenheim, Frankfurt, Germany
Hydrated magnesium aluminium silicate	Veegum HS/ 2011043450	R.T. Vanderbilt Company, Inc. Norwalk, USA
Magnesium Trisilicate	Fine powder / 1015674-1	Dr. Paul Lohmann, Emmerthal, Germany

## 2.3 Methods

### 2.3.1 Carrier loading

Sorbents were 'loaded' with LLW (lipid) using a simple mixing process. The adsorbent (25 g) was added to a glass beaker and mixed using an overhead stirrer at 400 rpm (Heidolph RZR2051, Germany). The lipid was added drop-wise via a syringe. Following complete addition of the lipid the mass was mixed for a further 1 min prior to sieving via a 2 mm screen followed by a 1 mm screen (Endecotts, UK). A weight of 50 % relative to the dry adsorbent weight was used as the starting point for loading of LLW to each of the adsorbents. Thereafter additions were made at 20 % relative to the dry adsorbent weight.

### 2.3.2 Scanning Electron Microscopy

Samples were coated with palladium in an argon fed vacuum Emitech K550X, (Quorum, UK). Images were captured using an Inca x-act machine, (Oxford Instruments, UK).

### 2.3.2 Tapped and bulk density determination

The bulk and tapped densities of sorbents and sorbents following loading were measured using a TAP-2 density tester, Logan Instruments (Somerset, New Jersey, USA). For each determination, a known weight of powder was added to the measuring cylinder, the volume occupied (V) was determined and following

10, 500 and 1250 "taps". Measurements were made in triplicate. Bulk ( $\rho_{Bmin}$ ) and tapped ( $\rho_{Bmax}$ ) density ( $gmL^{-1}$ ) were calculated using Equations 2.1 and 2.2 respectively.

Hausner ratios were calculated for the sorbents and sorbents post loading using Equation 2.3.

$$\rho_{Bmin} = W / V_0 \quad \text{Equation 2.1}$$

$$\rho_{Bmax} = W / V_{1250} \quad \text{Equation 2.2}$$

Where  $V_0$  is the bulk volume and  $V_{1250}$  is the tapped volume

$$\text{Hausner ratio} = \rho_{Bmin} / \rho_{Bmax} \quad \text{Equation 2.3}$$

### 2.3.3 True density determination

The true density of the sorbents (without lipid only) was determined using a Helium Pycnometer (Multipycnometer, Quantachrome, Florida, USA). The machine was calibrated prior to use. The powder was filled into the microcell of the chamber, to occupy approximately 50 – 70 % of the cell volume. The pressure in the cell was increased to approximately 17 PSI, prior to taking readings. Measurements were made in triplicate.

### 2.3.4 Flow through an orifice

Flow through an orifice was performed using a BEP apparatus (Copley Scientific Nottingham, UK) with aperture sizes of 10, 15 and 25 mm. The powder was loaded into the apparatus and the time taken for a known amount of material (approximately 50 (g)) to pass through the orifice was measured using a stopwatch. The test was performed in triplicate.

### 2.3.5 Compaction

Tablets were produced using the Stylcam<sup>®</sup> 100R simulator (Medelpharm, France) fitted with 7.0 mm flat-faced tooling and using the 'direct cam' rotary press profile. The die was filled manually prior to compression. A range of compaction forces starting from approximately 1 kN increasing to up to 20 kN in approximately 1 kN intervals were targeted to be applied. Press speeds of 5 tablets per minute (TPM) and 20 TPM (respective dwell times of 60 ms and 15 ms) were used to determine the influence of press speed upon tablet

characteristics. Prior to each compression run the force sensors on the Stylcam® were calibrated using a 3 mm gauge block.

Heckel analysis was performed, where possible upon the sorbents. The reduction in volume of the compact upon application of force was calculated using the Heckel Equation (See Equation 1.2). Mean yield pressures MPa were determined at low ( $P_{y1}$ ) and high ( $P_{y2}$ ) simulated press speeds (60 ms and 15 ms respectively), over the applied force range of 100 to 200 MPa; using the Analis® software associated with the Stylcam® to enable the calculation of strain rate sensitivity (%SRS) using Equation 1.3.

### 2.3.6 Tablet Characterisation

Tablets were characterised for weight, using an analytical balance (Sartorius, Germany) thickness using a digital micrometer (Mitutoyo, UK); and crushing strength (C50 tablet tester, I.Hollands, UK). The tensile strength of the tablets was determined in accordance with Equation 1.6.

## 2.4 Results

### 2.4.1 Characterisation of Sorbents

Table 2.3 details the density characteristics of the sorbents evaluated prior to loading. The tapped density of the materials varied significantly from 0.05 g/cm<sup>3</sup> (Aerosil R792) to 0.91 g/cm<sup>3</sup> for Vegum HS.

Table 2.3 Density characteristics of sorbents evaluated (mean  $\pm$  SD, n=3)

Material	True Density (g cm <sup>-3</sup> )	Bulk Density (g cm <sup>-3</sup> )	Tapped Density (g cm <sup>-3</sup> )
Syloid® 244 FP	1.77 $\pm$ 0.15	0.07 $\pm$ 0.00	0.09 $\pm$ 0.00
Magnesium Carbonate	2.01 $\pm$ 0.05	0.12 $\pm$ 0.01	0.15 $\pm$ 0.00
Syloid® ALAL1FP	2.08 $\pm$ 0.02	0.33 $\pm$ 0.01	0.47 $\pm$ 0.01
Tricafos	0.72 $\pm$ 0.01	0.47 $\pm$ 0.00	0.53 $\pm$ 0.01
Neusilin® NFL2N	1.98 $\pm$ 0.00	0.23 $\pm$ 0.00	0.26 $\pm$ 0.00
Neusilin® UFL2	1.91 $\pm$ 0.01	0.10 $\pm$ 0.00	0.12 $\pm$ 0.00
Magnesium Trisilicate	1.87 $\pm$ 0.04	0.38 $\pm$ 0.00	0.54 $\pm$ 0.04
Aeropearl® 300	2.05 $\pm$ 0.09	0.22 $\pm$ 0.00	0.27 $\pm$ 0.00
Neusilin® US2	2.15 $\pm$ 1.47	0.17 $\pm$ 0.00	0.20 $\pm$ 0.00
Aerosil® R792	1.90 $\pm$ 0.11	0.04 $\pm$ 0.00	0.05 $\pm$ 0.00
Aerosil® 200VV	1.95 $\pm$ 0.05	0.14 $\pm$ 0.05	0.13 $\pm$ 0.01
Vegum® HS	2.18 $\pm$ 0.38	0.79 $\pm$ 0.01	0.91 $\pm$ 0.03

Only eight of the 12 materials characterised were found to flow through the 25 mm orifice and only 5 of the 12 materials characterised (Tricafos, Neusilin® NFL2N, Aeropearl 300, Neusilin® US2 and Veegum HS) (see Table 2.4) were found to flow through both the 15 mm and 10 mm orifice. Veegum HS possessed far superior flow properties to that of the other materials evaluated achieving a flow rate greater than 4 times that (approximately 8g/s) of the next best material; Tri-cafos 500 (approximately 2 g/s).

Table 2.4 Flow characteristics of sorbents (mean  $\pm$  SD, n=3)

Material	15 mm (g/s)		10 mm (g/s)	
	Mean	SD	Mean	SD
Tricafos	6.690	0.116	2.101	0.014
Neusilin® NFL2N	3.061	0.010	0.860	0.036
Aeropearl® 300	18.204	2.418	0.642	0.012
Neusilin® US2	3.294	0.157	0.925	0.021
Vegum® HS	22.622	0.136	8.462	0.021

#### 2.4.2 Sorbent Compression

In the present study, the term “compress” is used to define a material that produced a robust compact, which could be ejected from the die intact and be tested for crushing strength. The magnesium aluminometasilicates (Neusilin®, US2, NFL2N and UFL2) were the only sorbents found to compress satisfactorily. This was achieved at applied forces (3.5 to 12.0 kN) with a dwell time of 32 – 38 milliseconds. Lubricants were not added to aid tablet ejection from the die and to prevent adherence to punch surfaces so as not to compromise inter-particulate bonding during compression.

Tablets of magnesium aluminometasilicates possessed acceptable tensile strength in excess of 6 MPa. Although several tablets were characterised, it should be noted that others adhered strongly to the lower punch or laminated/cracked during ejection; indicating the requirement for suitable lubrication of the material. A significant amount of powder was expelled from the die through the clearance space between the upper punch and the die wall during the compression of Neusilin® UFL2 and NFL2N grades. This expulsion was probably due to the low density and relatively small particle size of these grades

compared to the granular Neusilin® US2 grade (mean particle size UFL2, 2 – 8 µm. US2, 60 -120 µm; Fujichemical, 2007).

### 2.4.3 Heckel analysis and Strain Rate Sensitivity Determination

Strain rate sensitivity values (Table 2.5) were generated for the Neusilin® grades; the data suggested that consolidation was by fragmentation, as minimal change in yield pressure with decreasing dwell time (increased punch velocity) was reported which was supported by the relatively low SRS values produced (< 3 %). Materials that undergo deformation independently of compression rate have low SRS values (2%) whereas materials that deform plastically (i.e., time-dependent deformation) have higher SRS values (Roberts and Rowe, 1985): Neusilin® US2 and NFL2N produced lower SRS values (0.6 % and 0.1 % respectively) than that of the UFL2 grade (3.0 %), as a result of the relatively lower yield pressures which resulted during compression (Table 2.5). Figure 2.1 shows a Heckel plot generated during the compression of Neusilin® US2 at a simulated press speed of 20 tablets per minute which is equivalent to a dwell time of 15 ms. Note: a small precompression curve is present on Figure 2.1, subject to the level of powder within the die when manually filling, the sensitivity of the Stylcam sometimes results in a small amount of pre compression detected. Experience shows this is insignificant and doesn't influence the yield pressure calculated from the slope of the main curve

Table 2.5 SRS values determined for Neusilin® grades (mean ± SD, n=3)

	<b>Neusilin® US2</b>	<b>Neusilin® NFL2N</b>	<b>Neusilin® UFL2</b>
Py <sub>1</sub> (MPa)	1187 ± 17	1049 ± 3	1909 ± 6
Py <sub>2</sub> (MPa)	1194 ± 19	1051 ± 8	1967 ± 11
%SRS	0.6	0.1	3.0

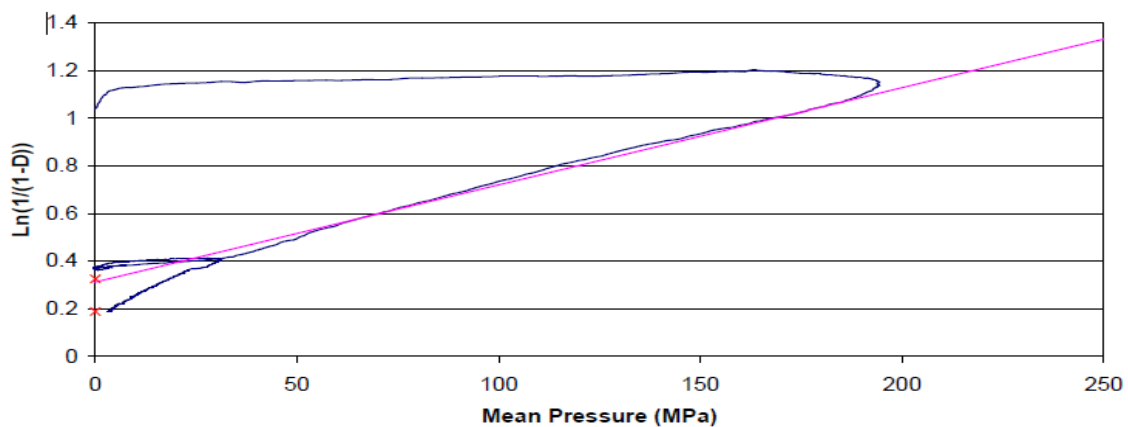


Figure 2.1 Heckel plot of Neusilin® US2, dwell time 15 ms

The major difference between the Neusilin® grades is that of particle size distribution, Neusilin® US2 is supplied as granules whereas Neusilin® NFL2N and UFL2 are supplied as powders, the bulk density of Neusilin® NFL2N is greater than UFL2 (0.08 – 0.13 and 0.06 – 0.11 g/mL respectively; Fuji, 2009). The yield values or calculated SRS values do not correspond with a decreasing trend in particle size. However, Neusilin® UFL2 produced higher yield pressure values than both Neusilin® US2 and Neusilin® NFL2N, which suggests that Neusilin® UFL2 is more brittle in nature and consolidates by a higher degree of fragmentation. It is likely that the number of particle surfaces which undergo shear during compression is increased with the Neusilin® UFL2 grade compared to that of Neusilin® US2 or Neusilin® NFL2N grades due to the higher porosity (lower density) of the UFL2 grade and hence gave the high resultant yield pressure.

#### **2.4.4 Physical characterisation of sorbents post loading of labrafac lipophile W1349**

The data in Tables 2.6 and Figure 2.2 detail the density and flow characteristics of the sorbents post loading expressed as % weight relative to the dry sorbent, (50%, 70%, 90%). The data showed that the density (bulk and tapped) of the majority of samples increased relative to the amount of LLW loaded due to the reduction in interstitial space between particles and pores present within individual particles allowing the adsorption of the liquid lipid.

Magnesium trisilicate and Vegum HS were observed to be saturated following the addition of 50% LLW, where saturated is defined as the adsorbent no longer remaining a loosely bound powder, instead appearing as an aggregated mass which does not flow. Neusilin® NFL2N and tricalcium phosphate exhibited a reduction in density at 90% loading compared to 70% loading (Table 2.6) which suggested that the samples had become saturated. The appearance of the tricalcium phosphate supported this finding. However, the Neusilin® NFL2N did not appear to be saturated when compared to the 50% loaded sample. Table 2.7 details the flow rate for those sorbents which flowed through a 10 mm orifice post loading.

Table 2.6 The effect of loading with LLW on the density characteristics of sorbents (mean  $\pm$  SD, n=3), determined using a TAP-2 density tester.

Material	% Loading relative to dry sorbent	Tapped Density (g/cm <sup>3</sup> )	Bulk Density (g/cm <sup>3</sup> )
Syloid 244 FP	50	0.14 $\pm$ 0.00	0.12 $\pm$ 0.00
	70	0.17 $\pm$ 0.00	0.15 $\pm$ 0.01
	90	0.20 $\pm$ 0.00	0.18 $\pm$ 0.00
Magnesium Carbonate	50	0.21 $\pm$ 0.01	0.17 $\pm$ 0.01
	70	0.25 $\pm$ 0.02	0.20 $\pm$ 0.01
	90	0.28 $\pm$ 0.03	0.22 $\pm$ 0.02
Syloid ALAL1FP	50	0.48 $\pm$ 0.01	0.39 $\pm$ 0.01
	70*	0.55 $\pm$ 0.01	0.44 $\pm$ 0.01
Tricafos	50	0.78 $\pm$ 0.01	0.68 $\pm$ 0.02
	70	0.77 $\pm$ 0.01	0.68 $\pm$ 0.01
	90	0.62 $\pm$ 0.02	0.53 $\pm$ 0.08
Neusilin® NFL2N	50	0.40 $\pm$ 0.00	0.36 $\pm$ 0.00
	70	0.45 $\pm$ 0.00	0.40 $\pm$ 0.00
	90	0.48 $\pm$ 0.03	0.44 $\pm$ 0.00
Neusilin® UFL2	50	0.17 $\pm$ 0.01	0.21 $\pm$ 0.00
	70	0.24 $\pm$ 0.00	0.19 $\pm$ 0.01
	90	0.26 $\pm$ 0.00	0.16 $\pm$ 0.00
Magnesium Trisilicate	50*	0.43 $\pm$ 0.00	0.33 $\pm$ 0.04
Aeropearl 300	50	0.41 $\pm$ 0.00	0.36 $\pm$ 0.01
	70	0.47 $\pm$ 0.01	0.40 $\pm$ 0.01
	90	0.53 $\pm$ 0.01	0.45 $\pm$ 0.01
Neusilin® US2	50	0.31 $\pm$ 0.00	0.23 $\pm$ 0.00
	70	0.31 $\pm$ 0.00	0.34 $\pm$ 0.00
	90	0.34 $\pm$ 0.00	0.38 $\pm$ 0.00
Aerosil 200VV	90**	0.30 $\pm$ 0.00	0.28 $\pm$ 0.01
Vegum HS	50*	0.70 $\pm$ 0.02	0.58 $\pm$ 0.04
Aerosil R792	90**	0.11 $\pm$ 0.06	0.09 $\pm$ 0.01

KEY

\* saturated above this loading level

\*\* loading started at 90 % due to poor handling properties of the excipient

Table 1.7 The effect of loading with LLW on flow rate of sorbents determined by flow through an orifice using BEP apparatus. (mean  $\pm$  SD, n=3)

Material	% Loading	Flow (gs <sup>-1</sup> )
Tricafos	50	4.54 $\pm$ 0.19
Neusilin® NFL2N	50	2.68 $\pm$ 0.12
	70	2.47 $\pm$ 0.05
	90	2.46 $\pm$ 0.05
Aeroperl® 300	50	1.37 $\pm$ 0.14
	70	1.87 $\pm$ 0.09
	90	2.27 $\pm$ 0.19
Neusilin® US2	50	2.56 $\pm$ 0.03
	70	2.92 $\pm$ 0.03
	90	3.51 $\pm$ 0.06
Aerosil® 200VV	90*	2.60 $\pm$ 0.11

Key: \* Not loaded below this percentage due to handling problems

The addition of LLW to Aerosil® 200 vv, Aeroperl® 300, Tricafos®, Neusilin® NFL2N and Neusilin® US2, increased their flow properties compared to the unmodified sorbents. The increase in flow was probably due to the increased density of the loaded materials and a reduction in inter-particulate bonding due to coating of the surface of the particles with the lipid.

#### 2.4.5 Density and flow data for Neusilin® US2 loaded with Labrafac Lipophile W1349®

Neusilin® US2 was selected to assess the influence of increasing the amount of lipid added (> 90% relative to the dry material) upon the density and flow properties of the sorbent when loaded with LLW. Figure 2.2 shows that the density of the loaded Neusilin® US2 increased in a straight-line fashion up to the adsorption of 250% LLW.

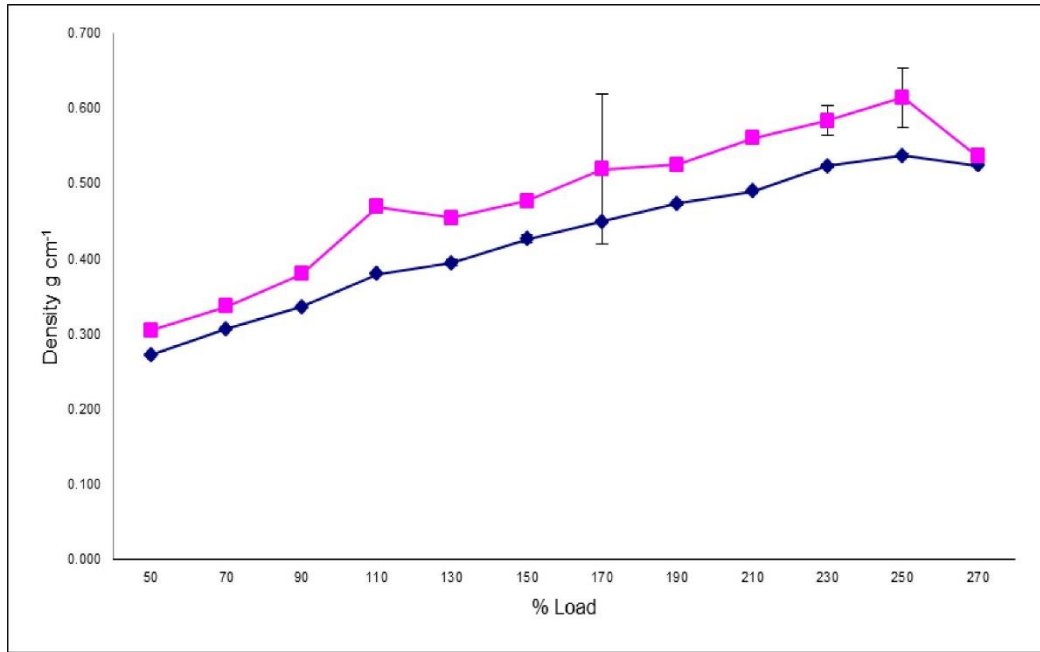


Figure 2.2 The effect of Labrafac Lipophile WL1349 loading on the mean tapped density (■) and mean bulk density (◆) of Neusilin® US2 (n=3, ± SD).

Figure 2.3 shows that the loaded material generally flowed well through a 10 mm orifice up to the loading of 170 % LLW, above which Neusilin® US2 did not flow.

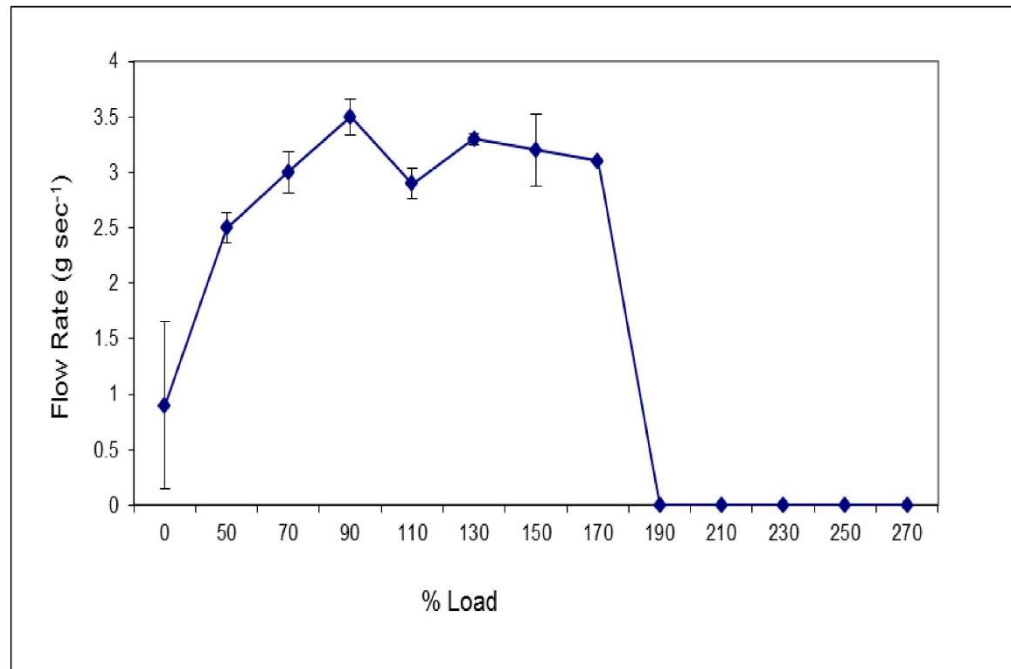


Figure 2.3 Mean flow rate through a 10 mm orifice for Neusilin® US2 loaded with Labrafac Lipophile WL1349 (n=3, ± SD)

Hausner ratio values (Equation 2.3) suggested that the modified material flowed well as all values were  $< 1.2$ , irrespective of the amount of lipid added.

Correlation between the Hausner ratio values and the flow through an orifice test ( $\text{gs}^{-1}$ ) cannot be made across the loading range. The Hausner ratio is related to inter-particulate friction (Aulton, 2013), it is likely that following 50% loading the inter-particulate friction is reduced and continues to reduce as the LLW concentration increases. However, flow will not necessarily increase proportionally with additional loading due to a reduction in inter-particulate friction between Neusilin® US2 particles. As the lipid concentration increased the modified material probably changed to become more liquid in nature resulting in increased cohesive tendency (effective viscosity), as the liquid becomes the predominant phase in which the Neusilin® US2 is dispersed. These findings suggest that the calculation of Hausner ratio and Carr's Index values which also indicate good flow properties across the range of US2/lipid modifications are not applicable to indicate the flow properties of US2 following lipid loading.

Vranikova et al (2015) studied the flowable liquid retention potential of Neusilin® US2 following the adsorption of PEG200, PEG 400 and propylene glycol. They found that a loading of almost 150 % could be achieved with PEG200 whilst retaining suitable flow properties of the loaded carrier. Suitable flow properties were achieved only at the lower loadings of 100% and 120% for propylene glycol and PEG 400 respectively. The data generated from Vranikova et al (2015) and findings presented here using LLW as the substrate suggest that flowability of US2 post loading is specific to the amount of substrate applied and its properties. The viscoelastic characteristics of the substrate are likely to play an important role in wetting during application of the substrate onto the sorbent (Neusilin® US2).

#### **2.4.6 Compression data**

Only 5 of the sorbents used in this study produced viable tablets following loading of LLW (Equivalent to 50% of the dry sorbent weight). The magnesium aluminometasilicates (Neusilin® grades) each produced robust tablets  $> 1$  MPa (tensile strength) and magnesium carbonate and tricalcium phosphate were also found to compress (which prior to sorption had not been possible). However, the tensile strength of the tablets containing the modified magnesium carbonate and tricalcium phosphate was  $< 1$  MPa and therefore these excipients once loaded

would require additional compression aids to produce intact tablets. The inherent compressibility of the excipient and ability to form inter-particulate bonds appeared to be key to tablet formation, irrespective of the specific surface area or porosity of the excipient, when comparing the values presented in Table 2.1.

Figures 2.4 and 2.5 detail the tensile strength values for the modified sorbents, containing 50% and 70% relative lipid respectively, compressed with increasing compression force at a low press speed (dwell time:  $60 \pm 2$  ms).

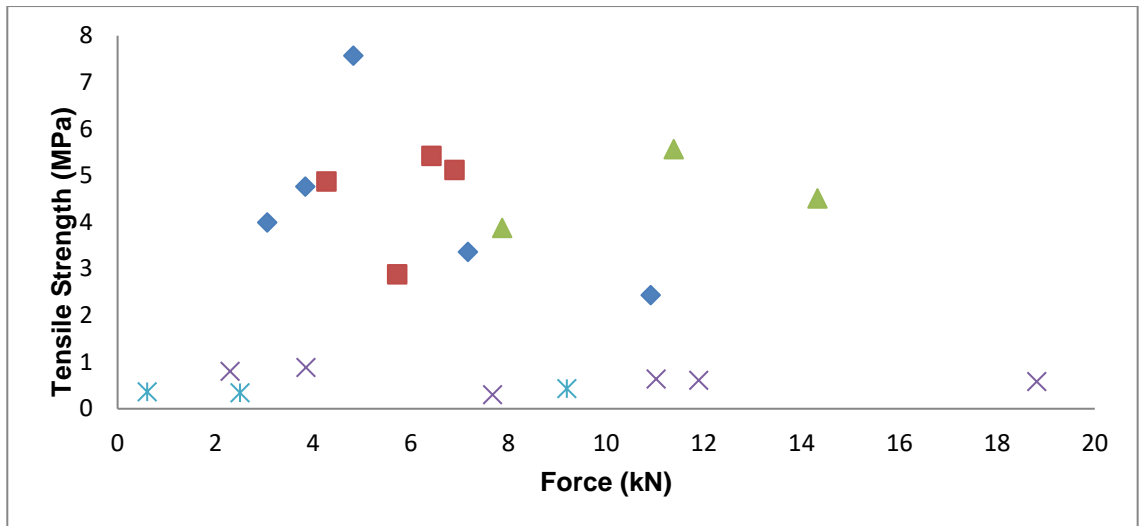


Figure 2.4 The effect of compaction force on the tensile strength of tablets of various sorbents loaded 50 % LLW, compressed with a dwell time  $60 \text{ ms} \pm 2 \text{ ms}$ . (◆) Neusilin US2, (■) Neusilin UFL2, (▲) Neusilin NFL2N, (×) Tricafos, (✱) Magnesium Carbonate, (n=1)

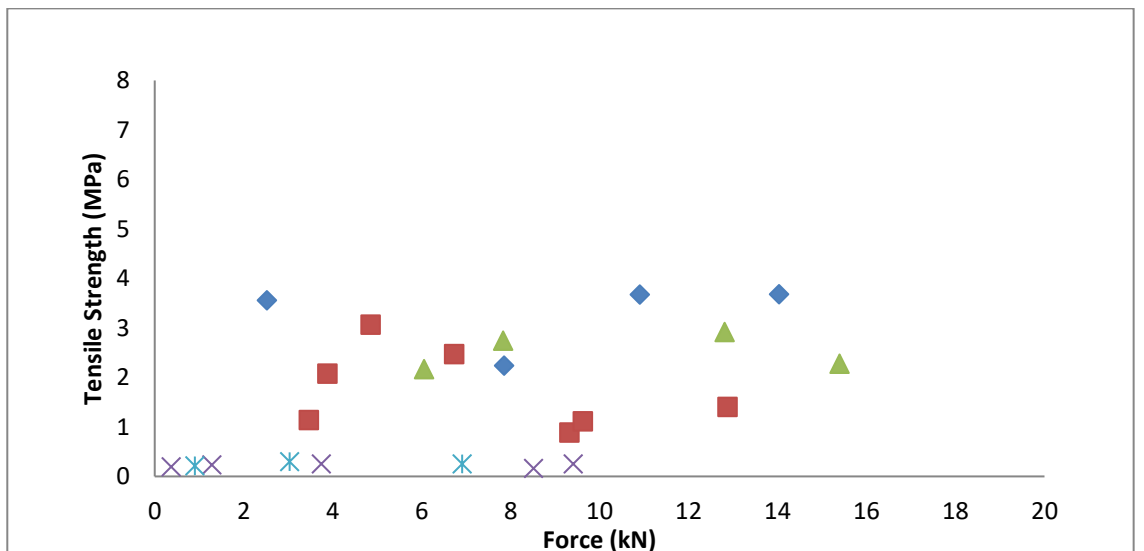


Figure 2.5 The effect of compaction force on the tensile strength of tablets of various sorbents loaded 70 % LLW, compressed with a dwell time  $60 \text{ ms} \pm 2 \text{ ms}$ . (◆) Neusilin US2, (■) Neusilin UFL2, (▲) Neusilin NFL2N, (×) Tricafos, (✱) Magnesium Carbonate, (n=1)

The data show that the tensile strength of the produced tablets typically decreased as the percentage lipid loaded increased from 50% to 70%. Only Neusilin®US2 and Neusilin® NFL2N produced robust tablets (> 2MPa) over a range of applied forces. It is apparent that when loaded with the same concentration of LLW, Neusilin® US2 and Neusilin® NFL2N produced tablets of similar tensile strengths (produced at similar applied force) despite the difference in particle size distribution (granule versus powder) of the unloaded materials. This finding suggests that the distribution of LLW in the loaded granules influences/reduces the potential for bond formation between solid particles which becomes the predominant factor for tablet strength. For standard powders it would be expected that tensile strength increases with increasing applied force USP 40, <1062>, (2020); as tablet density increases (porosity decreases/solid fraction increases) the difference in tensile strength between the two grades would be reduced, as the granule structure of the US2 grade would be compromised due to the increased applied force. These findings concur with those of Sander and Holm (2009) who found that tablet hardness decreased with relatively high liquid loads due to the “squeezing out” of liquid from pores.

Figures 2.6 and 2.7 show the tensile strength values for the loaded sorbents (50% and 70% relative loading) compressed at a faster speed (reduced dwell time  $15 \pm 2$  ms).

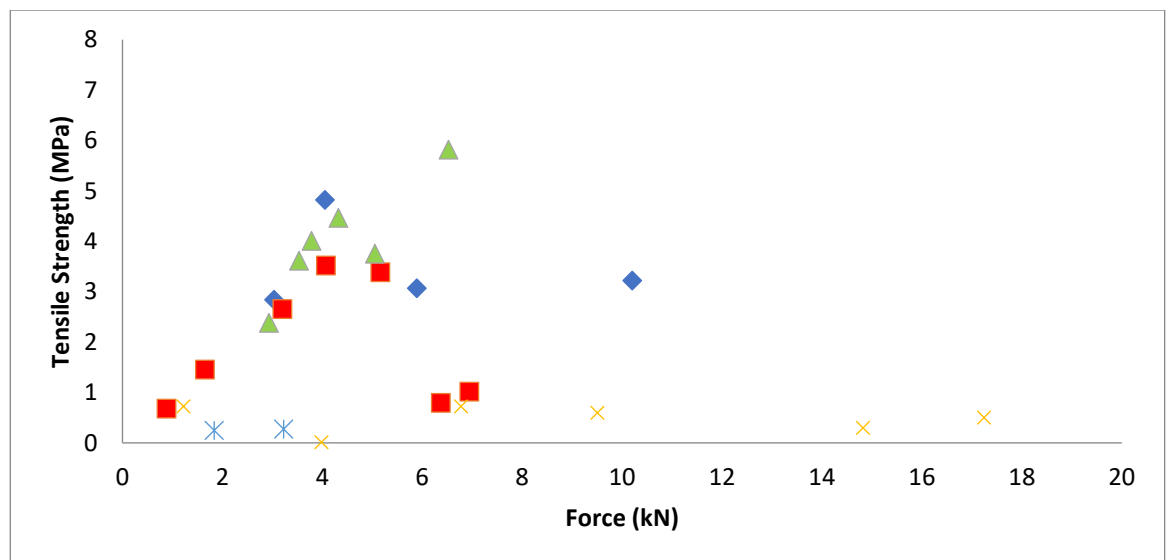


Figure 2.6 The effect of compaction force on the tensile strength of tablets of various sorbents loaded 50 % LLW, compressed with a dwell time  $15 \text{ ms} \pm 2 \text{ ms}$ . (◆) Neusilin US2, (■) Neusilin UFL2, (▲) Neusilin NFL2N, (×) Tricafos, (✱) Magnesium Carbonate, (n=1)

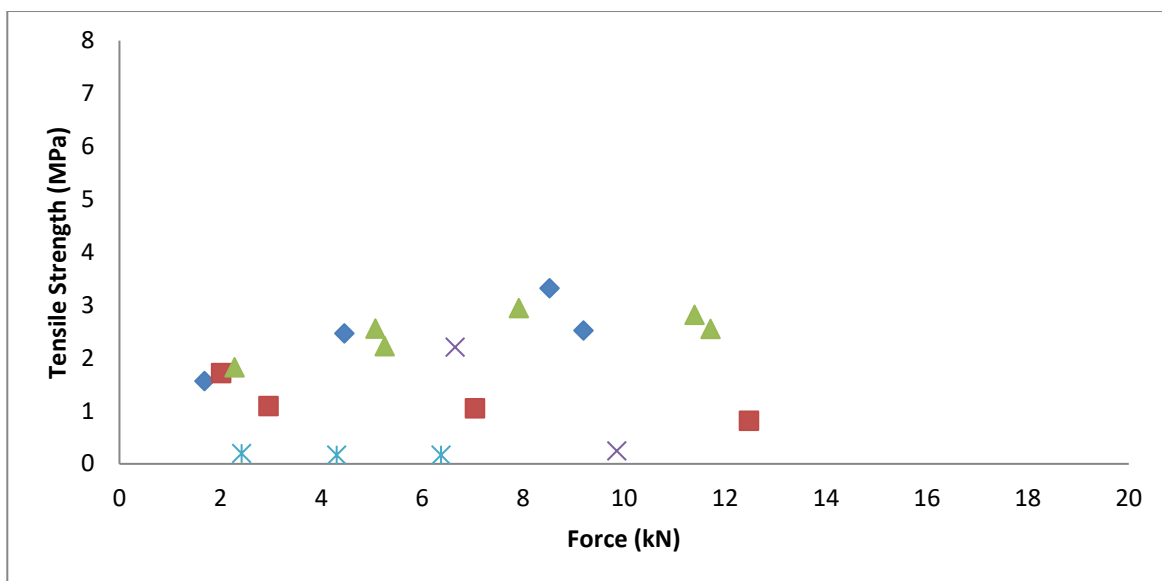


Figure 2.7 The effect of compaction force on the tensile strength of tablets of various sorbents loaded 70 % LLW, compressed with a dwell time 15 ms  $\pm$  2 ms. (◆) Neusilin US2, (■) Neusilin UFL2, (▲) Neusilin NFL2N, (×) Tricafos, (✱) Magnesium Carbonate, (n=1)

When compared to those modified sorbents compressed with a dwell time of 60 ms (Figures 2.4 and 2.5), a reduction in tensile strength of all tablets was apparent. The data suggest that all modified adsorbents deformed plastically during compression as evidenced by the reduction in tensile strength with decreased dwell time. No apparent trends suggest that any of the samples fragmented under the compression conditions although Neusilin® NF2LN exhibited a relatively linear increase in tensile strength between 0 – 7 kN (applied force) at 50% loading. However, this trend was not apparent following the sorption of 70% LLW.

Neusilin® US2 was selected for further evaluation following the loading of increased weights of lipid. Figures 2.8 and 2.9 show the tensile strengths for Neusilin® US2 (with 50% to 130% loading) compressed over a range of compaction forces at two press speeds with dwell times of 60 ms (Figure 2.8) or 15 ms (Figure 2.9).

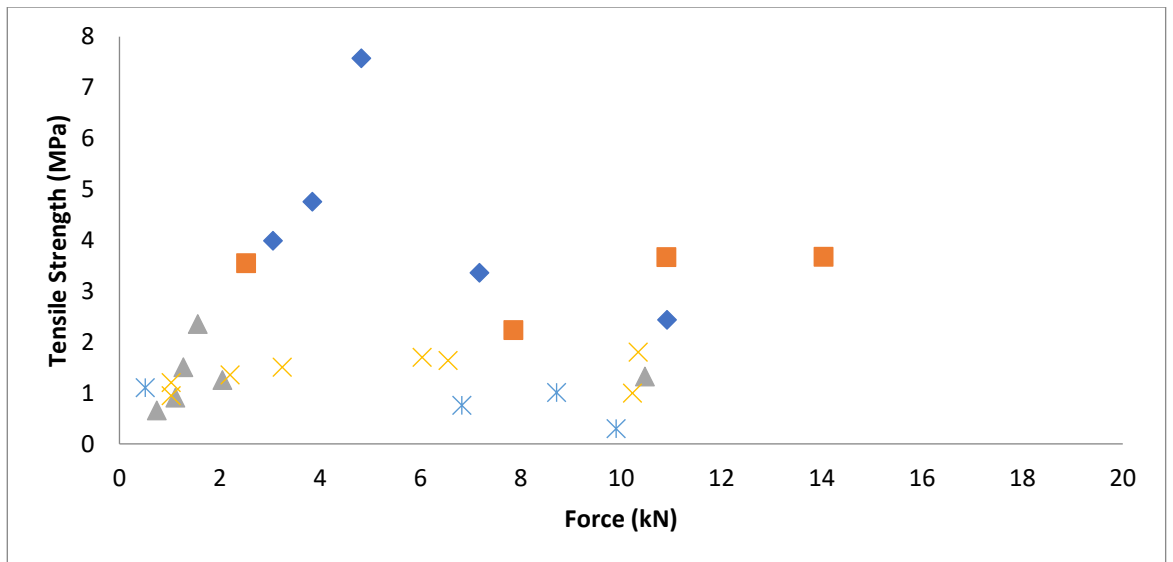


Figure 2.8 The effect of compaction force on the tensile strength of tablets of Neusilin US2 loaded with LLW, compressed with a dwell time 60 ms  $\pm$  2 ms. (◆) 50 % loaded, (■) 70 % loaded, (▲) 90 % loaded, (×) 110 % loaded, (✱) 130 % loaded (n=1)

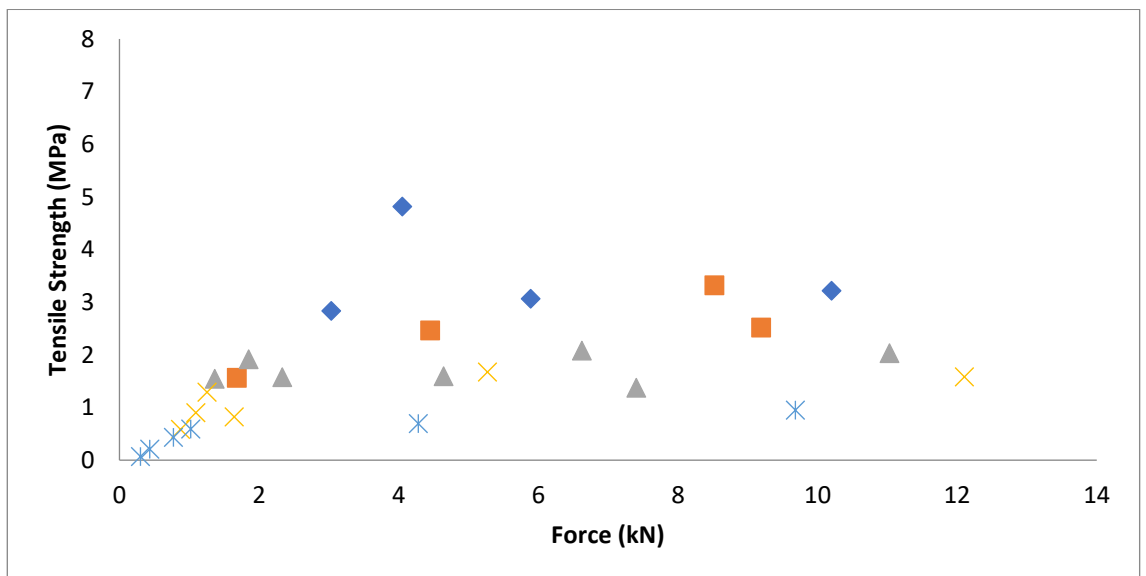


Figure 2.9 The effect of compaction force on the tensile strength of tablets of Neusilin US2 loaded with LLW, compressed with a dwell time 15 ms  $\pm$  2 ms. (◆) 50 % loaded, (■) 70 % loaded, (▲) 90 % loaded, (×) 110 % loaded, (✱) 130 % loaded (n=1)

Figures 2.8 and 2.9 show that, as the % lipid loaded increased, the tensile strengths of the tablets decreased. Irrespective of dwell time, suitably robust tablets (> 1 MPa) could not be produced with 130 % (relative) lipid sorbed. The maximum amount of LLW that can be loaded onto Neusilin® US2 which still results in the production of robust tablets was between 110 % and 130 % (relative to dry adsorbent). The % w/w of LLW in a simple tablet formulation consisting of

Neusilin® US2 and LLW alone therefore lies between 52 % and 57 % for the production of viable tablets. Tan et al (2013) suggested that a lipid load of 40 % w/w was typical for liquisolid compacts and is therefore likely to vary subject to the substrate and the addition of other excipients required to optimize the formulation, such as disintegration and lubrication aids.

An alternative approach to substrate loading was demonstrated by Sander and Holm (2009). Tablets of Neusilin® US2 were produced with various porosities by using a range of applied compression forces. Tablets, following compression, were placed in an excess of substrate, which entered the tablet by capillary action until constant tablet weights were achieved. Loadings of between 0.92 and 2.21 mL/g were achieved, which would suggest that this alternative method allowed a much higher substrate loading, than was possible to produce viable tablets in the current study. However, subsequent characterisation of the loaded tablets was not reported. Studies performed by Spireas and Srinivas (1998) and Hentzchel et al (2012) established and evaluated the use of a model, Equation 2.4, to evaluate the “liquid load factor” ( $L_f$ ) to establish the maximum liquid load that produces “acceptable flow characteristics and acceptable compressibility characteristics” of a loaded material,

$$L_f = W/Q \qquad \text{Equation 2.4.}$$

where  $W$  is the weight ratio of the liquisolid medication (liquid phase) and  $Q$  is weight the carrier powder.

Their studies supported the rationale for Equation 2.4 and that through characterisation of tablets produced,  $L_f$  values can be calculated.

The studies documented here suggest that an important factor for consideration during the determination of liquid load factors, in order for a formulator to be confident in the identification of a formulation which is suitable for scale up and commercialisation, is that of press speed during compression (dwell time). When loaded with LLW, Neusilin® US2 underwent plastic deformation, resulting in tablets whose hardness differed according to dwell time, as would be expected by plastically deforming materials (Roberts and Rowe, 1985). Although the current study only reports the behaviour of Neusilin® US2 loaded with LLW, it is likely that other ‘liquid lipids’ loaded onto US2 may increase the tendency for plastic deformation during compression.

### 2.4.7 SEM Images

Figure 2.10, 2.11 and 2.12 show SEM images of Neusilin® US2, loaded with 50 % LLW and a cross section of a tablet produced from the 50 % loaded material (respectively).

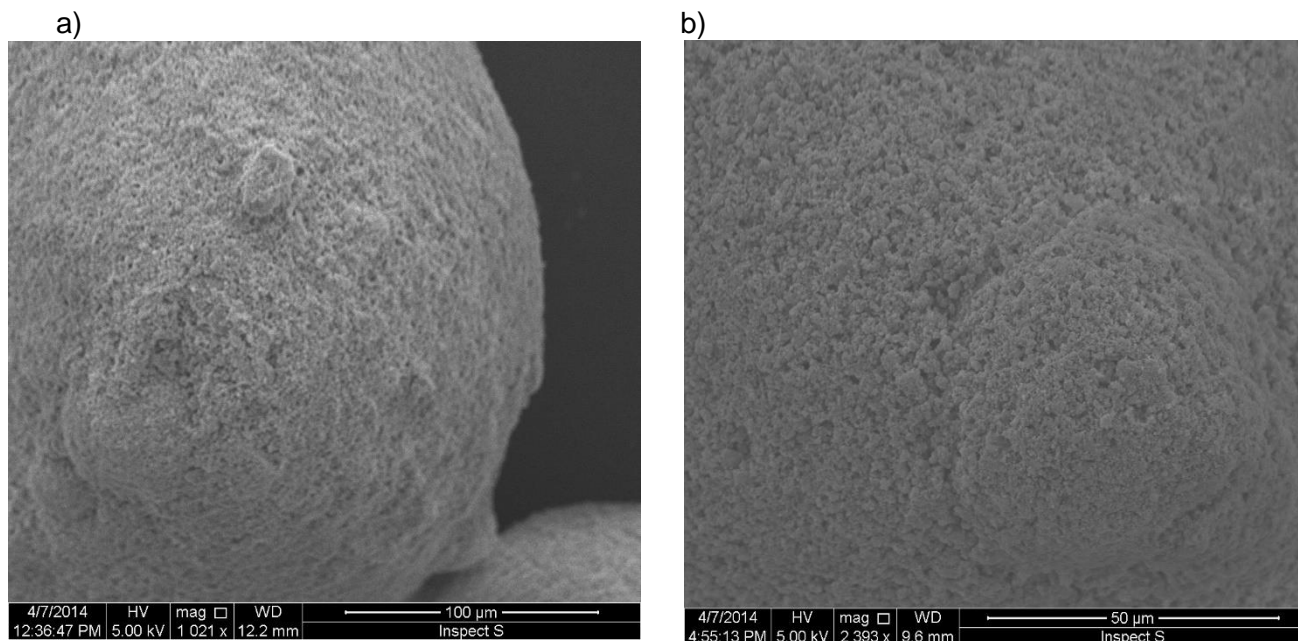


Figure 2.10 SEM images of Neusilin US2 at (a) 1,021 x and (b) 2,393x magnification.

The Neusilin® US2 particles appear to be granular from image a) with a porous surface (a and b). Gumaste et al (2013) reported that only micropores (> 50 nm) would be visible by SEM imaging and that the mesoporous structure reported (Qian, 2012) for the material (pores 2 – 50 nm) would not be visible by the technique.

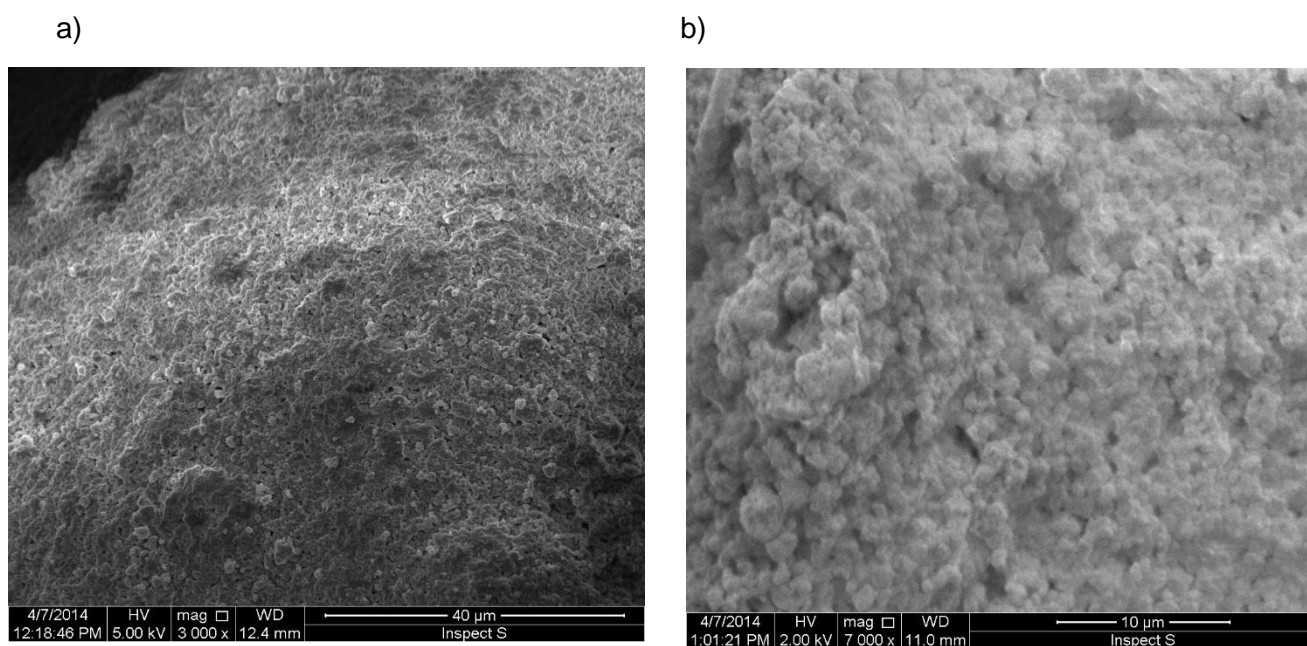


Figure 2.11 SEM images of Neusilin US2 loaded with 50 % LLW at (a) 3,000 x and (b) 7,000 x magnification.

Figure 2.11 shows the surface of US2 particles loaded with 50 % LLW. Compared to the Neusilin® US2 granules (Figure 2.10); it is difficult to determine the presence and influence of LLW on the surface structure of the Neusilin® US2 granules. The size and quantity of pores apparent in Figure 2.10 b does appear to be reduced in Figures 2.11 a) and b) which suggests that either the pores have been filled with the liquid LLW or that a surface layer of LLW is present which distorts the ability to visual the pores present at the granule surface. It is likely that both events take place during lipid loading, namely capillary movement of the liquid lipid into the pores present at the surface of the granules and surface adsorption of LLW at the outer layer of Neusilin® US2 granule.

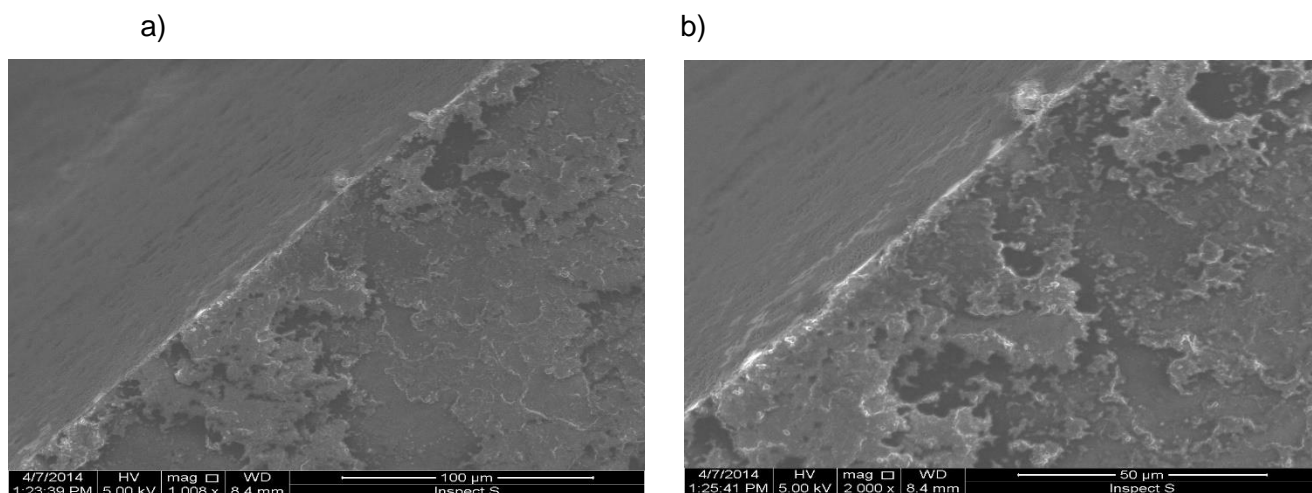


Figure 2.12 SEM images of a tablet cross section (Neusilin US2 loaded with 50 % LLW compressed at 60 ms) at (a) 1,000 x and (b) 2,000 x magnification.

Figures 2.12 a and b show SEM images of a tablet (Neusilin® US2, 50 % loaded with LLW) cross section. The tablet surface can be seen in the upper left corner of each figure and indicates a relatively continuous phase with few pores present. The lower right section of each figure shows the cross section of the tablet following breaking. The cross section again appears relatively uniform with few pores. It is not possible to distinguish between areas of either Neusilin® US2 or LLW.

## 2.5 Conclusions

The purpose of the study presented in this chapter was to evaluate the compression properties of a wide range of sorbents and sorbents loaded with LLW. The aim was to guide the formulator in the selection of sorbent, lipid loading level and compression parameters when developing tablet formulations containing liquid components.

Only 5 of the loaded sorbents exhibit suitable flow characteristics following loading of LLW > 50 % relative to the sorbent (see Table 2.6). Despite similar SSA values to the colloidal silicon dioxide grades (see Table 2.1) and flow properties (see Table 2.6) the magnesium aluminometasilicates (Neusilin® grades) were the only sorbents to exhibit suitable compression properties with relatively low strain rate sensitivity values (< 3 %). The improved compressibility of the magnesium aluminosilicates is likely due to increased intra particulate bonding potential compared to silicon dioxide.

The sorbent of choice (selected on compression characteristics) was Neusilin® US2; which was evaluated further due to possessing a larger modal particle size which conferred easier handling properties. Loadings up to 170 % LLW produced free flowing powders. Tablets were successfully produced at up to 110 % loading (of LLW) without the addition of other excipients. Tablet press speed (dwell time) was found to influence the tensile strengths of the tablets. Compression speed should therefore be a major factor for investigation during the development of liquisolid tablet formulations, especially when scaling up formulations from the laboratory to pilot scale. Dwell time (press speed) is likely to be a limiting factor when assessing acceptable compression characteristics of loaded materials when trying to establish the liquid load factor.

## Chapter 3

### “Evaluation of sorbent compression properties pre- and post-loading with SMEDDS formulation, and the addition of selected excipients to improve tablet characteristics”.

#### 3.1 Introduction and aims

The aim of these studies was to expand upon the findings reported in Chapter 2; to evaluate the compression properties of Neusilin® US2 loaded with a type III lipid formulation (SMEDDS preconcentrate formulation). In Chapter 2 a type I system was evaluated; however, Table 6 (Chapter 1) shows that SMEDDS based formulations (type III systems) are very common and therefore may be a more representative guide for formulators considering liquisolid development activities.

A model SMEDDS formulation was selected for evaluation containing Labrafac Lipophile WL1349 (as previously used as the ‘Type I’ lipid model in Chapter 2) as detailed in Table 3.1; and reported by Guo et al (2011).

*Table 3.1 SMEDDS Preconcentrate formulation*

Material	% w/w
Labrafac Lipophile WL1349	12
Solutol (Kolliphor) HS	42
Oleic Acid	18
Isopropyl Alcohol	28

Neusilin® US2 was loaded with SMEDDS Preconcentrate (SPc) at 50 %, 70 % and 90 % loading levels. The Neusilin® US2 loaded with SPc was characterised, prior to compression, at two different press speeds (dwell times) over a range of forces, to characterise the loaded material in accordance with USP 40, <1062> (2020) for manufacturability, tableability, compressibility and compactability. The tablets produced were characterised and evaluated against Ph Eur monograph (2017) for immediate release tablet dosage forms.

Following a review of the data, excipients were selected to produce formulation blends, with the aim of evaluating the influence of excipient selection upon tablet characteristics.

Several studies have reported the inclusion of compression aids (Gumaste et al., 2013; Vranikova et al., 2017; Seljak et al., 2018) during the establishment of liquisolid tablet formulations. However, limited rationale has been presented for selection of the type and

concentration of compression aids used. The purpose of this study was to understand the influence of diluent inclusion and to justify such inclusion in a tablet formulation. Due to the potential for diluent inclusion to limit API concentration in a tablet formulation where high API loading is required. The maximum quantity of API that can be loaded into a tablet is a critical factor to be understood during liquisolid formulation development studies.

Tablet characterisation data was analysed using statistical analysis software to derive a predictive model to understand the critical parameters which drive tablet characteristics from both formulation and compression parameter perspectives.

### **3.2 Materials**

The sorbent magnesium aluminometasilicate Neusilin® US2 was supplied by Fuji Chemical Industry Co.; Ltd, Toyama, Japan. The components of the SMEDDS preconcentrate were medium chain triglycerides - Labrafac Lipophile WL 1349 (LLW) received from Gattefosse, Bracknell, UK. Oleic acid, batch number MKBX4864V, was purchased from Aldrich, St Louis, USA. Kolliphor HS15 (macrogol 15 hydroxystearate), batch number 30494788Q0, was received from BASF, Ludwigshafen, Germany. Isopropyl alcohol, batch number 14G040507, was purchased from VWR, France.

Compression aids selected for inclusion in tablet formulations included microcrystalline cellulose (Avicel® 200 LM) batch number 1704-1007 from FMC, Ireland, mannitol spray dried (Mannogem EZ), batch number 121707505, SPI Pharma; USA and calcium carbonate spray dried, batch number TP500DG-BER, from Omya, Spain. Two further excipients were included in the tablet formulations, croscarmellose sodium (Ac-Di-Sol®), batch number T1602C, from IMCD, UK which was added as a super-disintegrant and sodium stearyl fumarate, batch number 149, from JRS, Patterson, U.S.A, as a lubricant, these materials were received free of charge as laboratory samples for evaluation.

### **3.3 Methods**

#### **3.3.1 SMEDDS preconcentrate preparation**

The SMEDDS preconcentrate as detailed in Table 3.1 was prepared as a 300 g batch. LLW and Solutol HS15 were dispensed into a 1,000 mL glass beaker and heated at 65 °C on a hotplate (Stuart US, Cole Palmer, U.K.) for 15 mins with occasional stirring, until a homogenous liquid formed. Oleic acid was added to the mixture, the liquid stirred using an overhead stirrer (IKA Eurostar 20, Germany) with a 3 blade stainless steel propeller stirrer and mixed until visibly homogenous. Isopropyl alcohol was then added, the liquid then mixed for 10

mins at 700 rpm. Once cooled to ambient temperature the liquid was stored in an amber glass bottle (1,000 mL Schott, Duran) until used for loading studies.

The viscosity of the SMEDDS pre-concentrate was not determined. However, for future studies it is recommended that viscosity measurements be taken to understand the influence of pre-concentrate viscosity upon sorbent surface morphology and loaded granule and tablet characteristics.

### **3.3.2 Carrier loading**

Neusilin® US2 was 'loaded' with SMEDDS pre-concentrate using a simple mixing process. The Neusilin® US2 (100 g) was added to a 500 mL glass beaker and mixed using an overhead stirrer (IKA Eurostar 20, Germany) with a 3-blade paddle at 400 rpm. The SMEDDS formulation was added dropwise via a syringe over a two minute period. An SPc weight of 50 % relative to the dry adsorbent weight was used as the starting point for loading of the SMEDDS pre-concentrate to each of the adsorbents. Thereafter additions were made at 20 % increments relative to the dry adsorbent weight to 90 %. Following complete addition of the SPc the mass was mixed for a further 1 min prior to sieving via both 2 mm and 1 mm screens (Endecotts, UK).

### **3.3.3 Tapped and bulk density determination**

As detailed in Section 2.3.1. Samples were tested in triplicate.

### **3.3.4 True density determination**

As detailed in Section 2.3.3. Samples were tested in triplicate.

### **3.3.5 Flow through an orifice**

As detailed in Section 2.3.4. Samples were tested in triplicate.

### **3.3.6 Blend preparation**

Where additional excipients were added to the loaded sorbent; the loaded sorbent was added to a 100 mL HDPE container with the compression aid and super disintegrant. The container was sealed and inverted end over end 100 times. The lubricant was then added, the container sealed and inverted end over end a further 50 times.

### **3.3.7 Compaction**

Tablets were produced using the Stylcam<sup>®</sup> 100R simulator (Medelpharm, France) fitted with 11.0 mm flat-faced tooling and using the 'direct cam' rotary press profile. The die was filled manually prior to compression, target fill weight 250 mg. A range of compaction forces starting from approximately 1 kN increasing to up to 20 kN in approximately 1 kN intervals were targeted to be applied. Tablets were produced to generate manufacturability, tableability, compressability and compactability profiles. Press speeds of 5 tablets per minute (TPM) and 20 TPM (respective dwell times of 60 ms and 15 ms) were used to determine the influence of press speed upon tablet characteristics.

To produce samples for physical characterisation testing tablets were compressed at selected forces (5, 7 and 9 kN) at two speeds (dwell times 60 ms and 15 ms).

### **3.3.8 Tablet Characterisation**

For the generation of manufacturability, tableability, compressability and compactability profiles tablets were characterised for weight (mg), using an analytical balance (Sartorius, Germany), thickness (mm) using a digital micrometer (Mitutoyo, UK); and crushing strength (N) (C53 tablet tester, I.Hollands, UK). Tablet tensile strength was determined as per Equation 1.6 and solid fraction values were determined as per Equation 1.4a.

For the physical characterisation of tablets compressed at target compression forces, (in addition to those tests detailed above) disintegration times (mm:ss) were determined in 800 mL of deionised water using USP disintegration apparatus (Copley, UK). Where disintegration time was determined as the last tablet to disintegrate (n = 6). Friability was determined using 10 tablets, the friabulator (Copley, UK) was set at 400 revolutions. The % weight loss following dedusting of tablets was calculated to determine friability (%).

### **3.3.9 Statistical Analysis**

Tablet characterisation data were analysed using JMP 14.0.01 software (SAS). Variability charts were produced to display the data easily allowing comparison of multiple X variables (% loading, extra granular excipient selection and target force applied) to see differences in means and variability across the responses for tensile strength, disintegration and friability.

Models were generated (using the JMP software) to predict average tensile strength, friability and disintegration times following the addition of selected excipients to the loaded Neusilin US2™. To generate a model, the Analyze option was selected and ‘fit model’ function utilised. The input factors used were ‘% loaded’, ‘excipient selected’ and ‘target force’. An automatic stepwise linear regression was selected to process the data using both single and two factor interactions. The software generates a predictive plot from the calculated model, which is used to show figuratively how well the model fits the actual data generated. The model automatically selects those input factors which are significant at a 95 % confidence level ( $P < 0.05$ ), these factors are displayed in the form of ‘effect summaries’.

### 3.4 Results

#### 3.4.1 Characterisation of Neusilin®US2 loaded with SPc.

The characteristics of Neusilin® US2 loaded with SMEDDS preconcentrate are detailed in Table 3.2. The values reported for density and flow concur in trend with those values reported in Section 2.4.5, where Neusilin® US2 was loaded with LLW. Differences in absolute values are attributable to the viscosity of the loading liquid which is likely to influence pore penetration and surface characteristics of the loaded particles. Studies were not performed to evaluate the influence of viscosity upon these characteristics.

Table 3.2 The effect of loading with SMEDDS preconcentrate on the characteristics of Neusilin®US2 (mean  $\pm$  SD, n=3)

Material	% Loading relative to dry sorbent	Tapped Density (g/cm <sup>3</sup> )	Bulk Density (g/cm <sup>3</sup> )	Carr’s Index <sup>1</sup> (%)	Hausner Ratio <sup>1</sup>	Flow (g/s <sup>-1</sup> )	True Density (g/cm <sup>3</sup> )
Neusilin®US2	50	0.28 $\pm$ 0.00	0.25 $\pm$ 0.00	10.7	1.12	2.41 $\pm$ 0.06	1.77 $\pm$ 0.16
	70	0.32 $\pm$ 0.00	0.28 $\pm$ 0.00	12.03	1.14	2.76 $\pm$ 0.05	1.67 $\pm$ 0.06
	90	0.39 $\pm$ 0.00	0.34 $\pm$ 0.00	11.96	1.14	2.79 $\pm$ 0.08	1.55 $\pm$ 0.05

The true density of the loaded Neusilin® US2 batches was reported to decrease with increasing loading, which does not correlate with increasing bulk and tapped density respectively. The method to determine true density by which helium penetrates the smallest pores and crevices and permits to approach the real volume (Vianna et al., 2002); shows that pore volume (intra-particulate rather inter-particulate) is reduced with increased loading. This finding would be expected, due to adsorption of the liquid substrate reducing the volume of the intra particulate pores. The decrease in true density may be apparent due

to the density difference between the solid and liquid phases (when porosity is normalised as per true density determination). The relative influence of the liquid phase is to reduce the true density of the loaded Neusilin® US2 with increasing SPc concentration.

The increase in flow rate reported with increased loading suggests that the adsorbate (SPc) penetrates the pores of the Neusilin® US2 particles, rather than remaining in the inter-particulate space. It may be expected that if excessive liquid was deposited on the surface of particles that flow would be reduced, due to cohesive forces reducing the potential for particle consolidation within a bed. Reduced particle flow would also likely influence consolidation of the powder bed, if this were case it would be expected that this phenomenon be confirmed with Carr's Index or Hausner ratio values above 16 % or 1.2 respectively, which is not the case.

### **3.4.2 Compression results for tablets containing Neusilin® US2 loaded with SMEDDS preconcentrate.**

#### **3.4.2.1 Manufacturability profiling at 2 compression speeds.**

Figures 3.1 and 3.2 show manufacturing profiles (USP 40, <1062>, 2020) for Neusilin® US2 loaded with SMEDDS pre-concentrate compressed at two different speeds (dwell times of 60 ms and 15 ms respectively). Manufacturability is defined as the relationship between compression force and tablet breaking force and is typically used as the criterion in a production setting to monitor tablet compression (USP 40, <1062>, 2020).

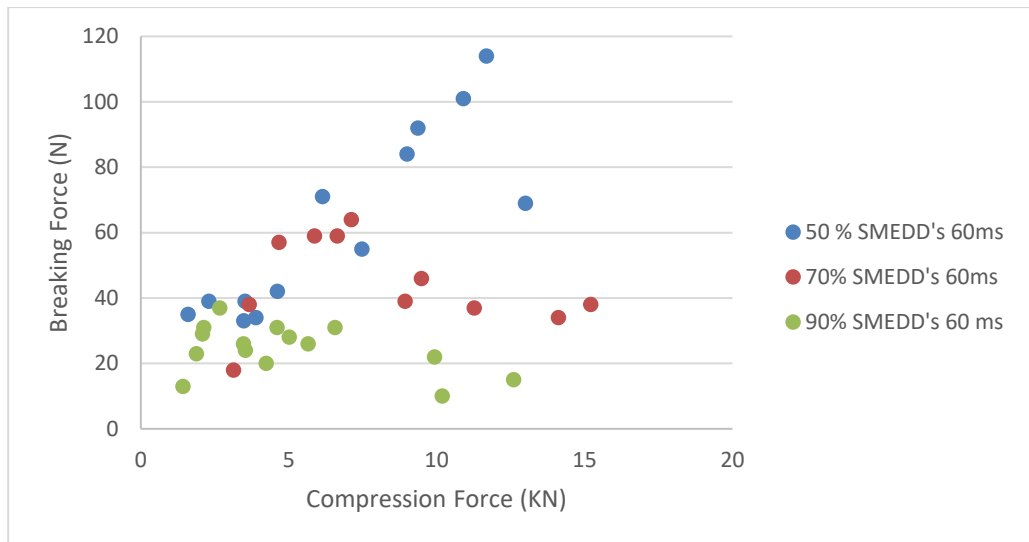


Figure 3.1. Manufacturability profile of Neusilin® US2 loaded with 50, 70, 90% SMEDDS preconcentrate (dwell time 60 ms)

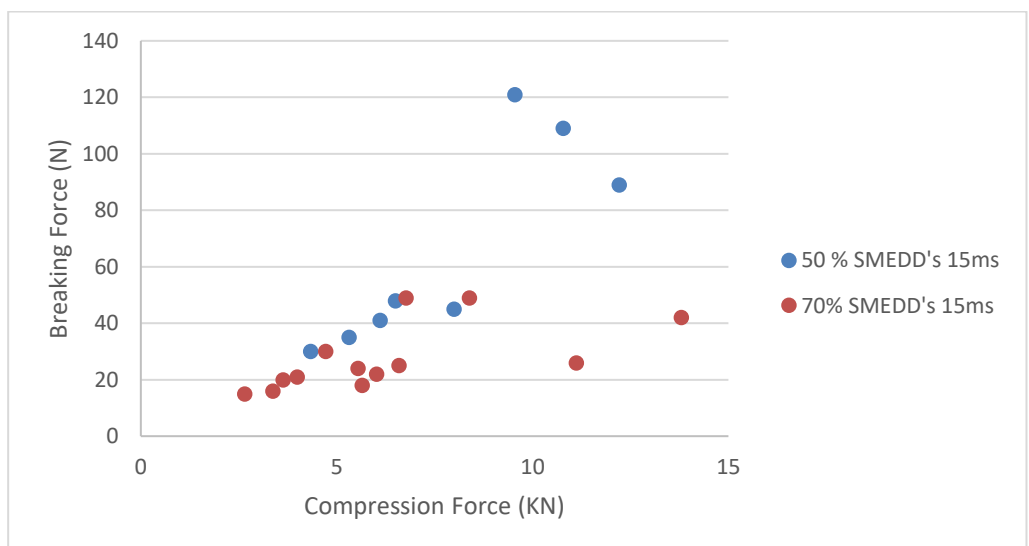


Figure 3.2 Manufacturability profiles of Neusilin® US2 loaded with 50, 70 SMEDDS preconcentrate (dwell time 15 ms)

The data show similar trends to that of Neusilin®US2 loaded with LLW reported in Section 2.4.6 Chapter 2, with the major factors identified influencing tablet properties being SPc loading and compression speed. The data in Figure 3.1 shows that tablets loaded with 50 % SPc exhibited a linear increase in breaking force with increased compression force (up to 10 kN). However, for those tablets containing 70 % (SPc), at approximately 7 kN applied force, a maximum breaking force was determined and for those tablets containing 90 % SPc a

plateau in breaking force was reached following the application of 2 kN applied force.

Figure 3.2 only shows data for tablets produced containing 50 % and 70 % SPc. It was not possible to produce robust tablets containing 90 % SPc when the dwell time was reduced to 15 ms. This finding was not consistent with the data reported in Chapter 2 (Figure 2.9) where viable tablets containing 130 % LLW could be produced. This finding suggests that the specific type of substrate loaded onto Neusilin® US2 influences the compression characteristics and must be considered during formulation development studies.

Figure 3.3 shows the comparison of Neusilin® US2 loaded with 50 % SPc compressed with dwell times of 60 ms and 15 ms. The data show that a similar profile is obtained with increasing compression force up to 10 kN, irrespective of dwell time (press speed). As the compression force increases > 10 kN, tablet breaking force decreases. This data suggests that at 50 % loading the material does not show significant strain rate dependency.

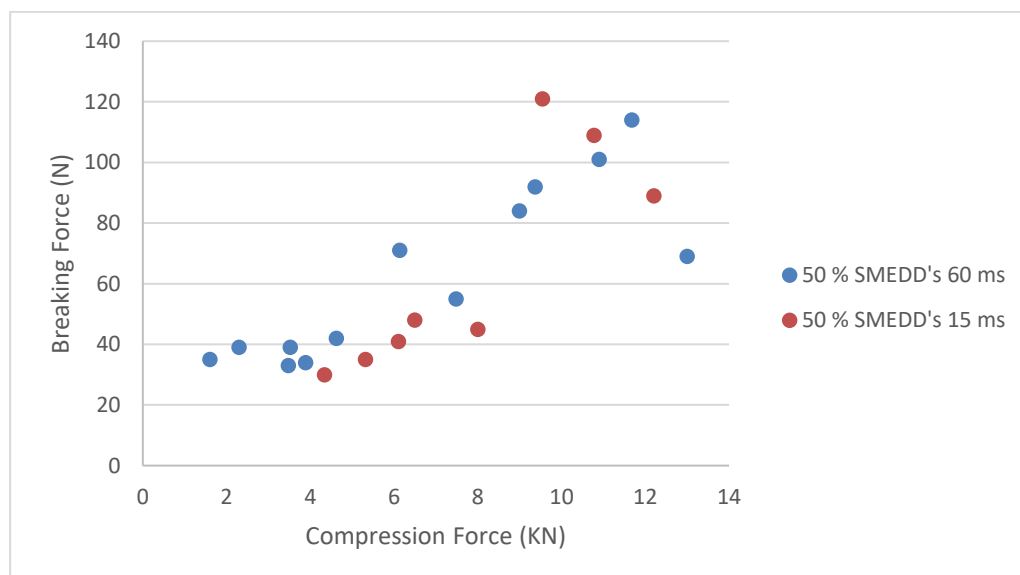


Figure 3.3 Manufacturability profiles of Neusilin® US2 loaded with 50 % SMEDDS preconcentrate (dwell time 60 ms and 15 ms).

Figure 3.4 shows a manufacturability profile of Neusilin® US2 loaded with 70 % SPc compressed at dwell times of 60 ms and 15 ms. The data shows that with increased SPc loading the material exhibits greater strain rate sensitivity,

compared to the 50 % loaded material (Figure 3.3). Over the range of applied force from 4 to 8 kN, the tablets compressed with the longer dwell time (60 ms) exhibit a higher breaking force than those compressed at 15 ms. However, above 8 kN applied force, irrespective of dwell time, tablet breaking force appears to be reduced with increased force applied. It was not possible to quantify the strain rate sensitivity of the 90 % loaded samples, as tablets could not be produced when a dwell time of 15 ms was applied (due to lamination on ejection). The failure to produce tablets though, confirms the strain rate sensitivity of the 90 % loaded material.

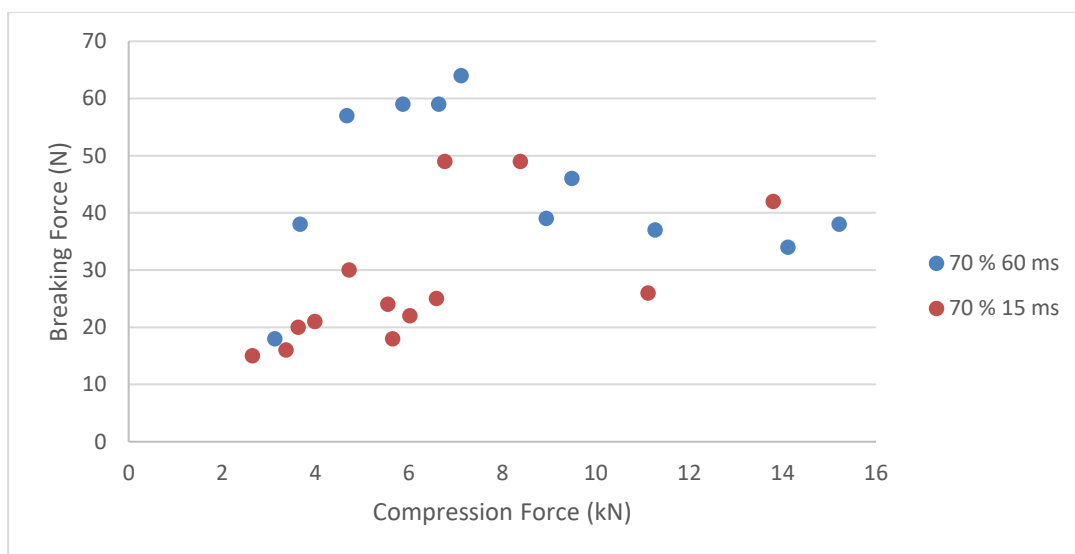


Figure 3.4 Manufacturability profiles of Neusilin® US2 loaded with 70 % SMEDDS preconcentrate (dwell time 60 ms and 15 ms).

### 3.4.2.2 Tableability

Figure 3.5 shows tableability profiles for Neusilin®US2 loaded with 50, 70 and 90 % SPc. The profiles show that only the 50 % and 70 % loaded materials formed tablets with tensile strength values > 1 MPa, which are typically desired for tablets to withstand stress (Amidon et al., 2009). Whilst manufacturability profiles (Figure 3.1) suggests that the 90 % loaded material can be used for the production of viable tablets, the tableability profile shows that this is not the case.

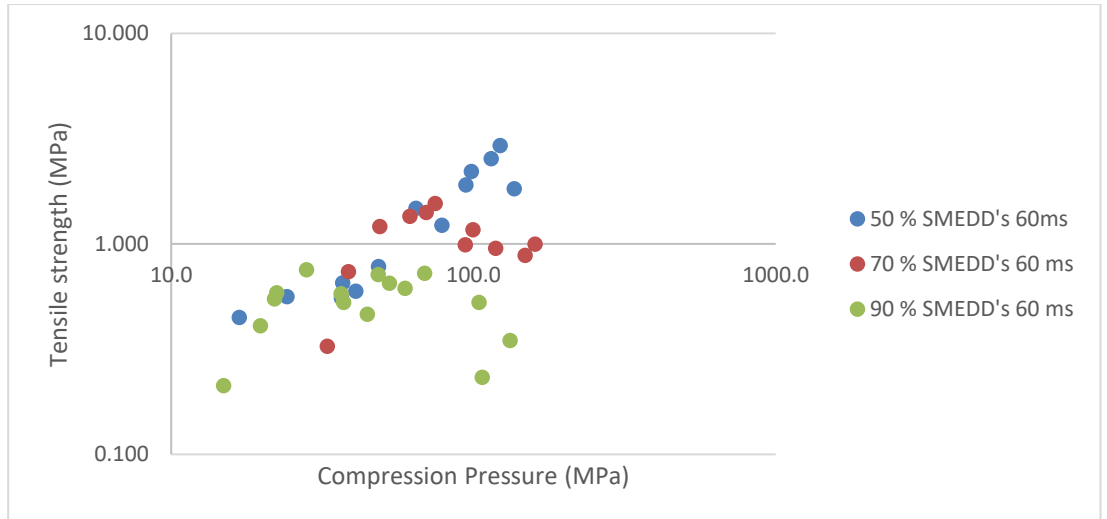


Figure 3.5 Tableability profiles of Neusilin® US2 loaded with 50, 70, 90% SMEDDS preconcentrate (dwell time 60 ms) Line at 1MPa used to differentiate between viable and non-viable tablets

Figure 3.6 compares the tableability profiles of the 50 % loaded material; it shows that a compression pressure above 65 MPa would be the minimum target pressure required to form robust tablets with > 1 MPa tensile strength for dwell times between 15 and 60 ms.

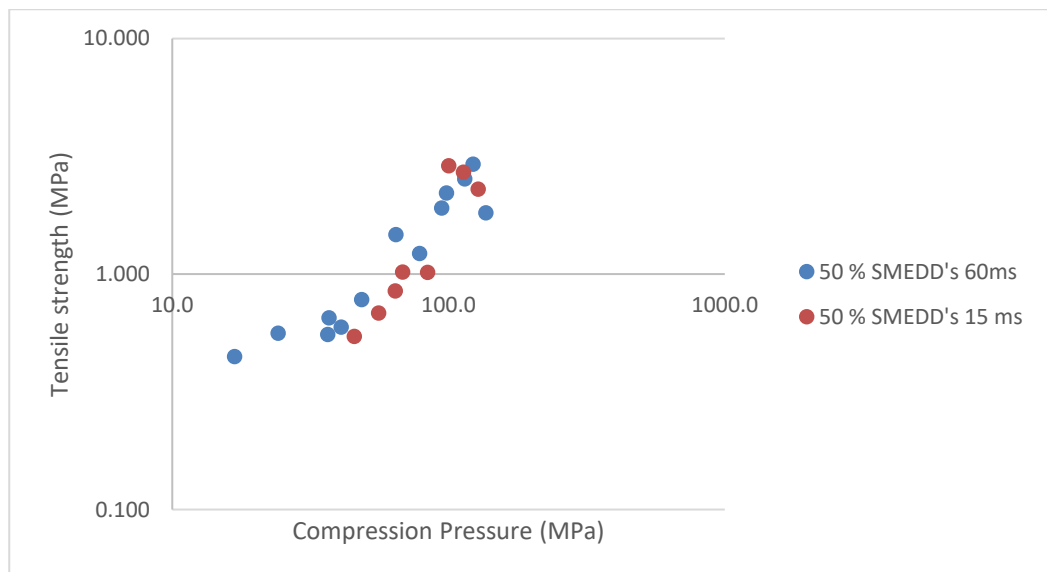


Figure 3.6 Tableability profiles of Neusilin® US2 loaded with 50 % SMEDDS preconcentrate (dwell time 60 ms and 15 ms).

Gumaste et al (2013) investigated the production of tablets following lipid based adsorption onto Neusilin® US2; their studies loaded Neusilin US2 with 100 % liquid (1:1 ratio) and they were able to produce tablets with > 1 MPa tensile strength. The lipid formulations differ to the SPc selected in Table 3.1, therefore

direct comparison was not possible. The tablets produced by Gumaste et al (2013) were formed using a Carver hydraulic press and it is hypothesised that the dwell time applied will be longer than 60 ms due to the compression profile of that Carver press.

### **3.4.2.3 Compressibility**

Compressibility is the dependence of tablet porosity on compression pressure (USP 40, <1062>, 2020). Figure 3.7 shows compressibility profiles for Neusilin® US2 loaded with 50, 70 and 90 % SPc (dwell time 60 ms). The figures show that as lipid loading increases, a rapid reduction in porosity is reported with increasing compression pressure. This phenomenon is likely due to the liquid (SPc) being forced out from the pores of the Neusilin® US2 particles which causes a rapid reduction in inter-particulate porosity (as the liquid fills spaces between particles). As the pressure increases the volume of intra-particulate pores is reduced (due to deformation of individual particulate structure or filling of the pore completely). The available volume for the liquid phase to occupy is subsequently reduced.

The profiles show that the solid fraction of the 90 % loaded tablets begins to plateau at around 0.68 at a compression pressure of approximately 50 MPa. For 70 % loaded samples a higher solid fraction (0.72), is achieved at a higher compression pressure (approximately 140 MPa). The reduction in compressibility (with SPc loading) would be expected due to the reduced intra-particulate pore volume associated with increased SPc concentration (effectively increased material density). Following the application of pressure to the powder bed; the transfer of the liquid to the inter-particulate pore space, from the intra-particulate pore space will be more rapid with increasing liquid concentration until an equilibrium is achieved (maximum solid fraction).

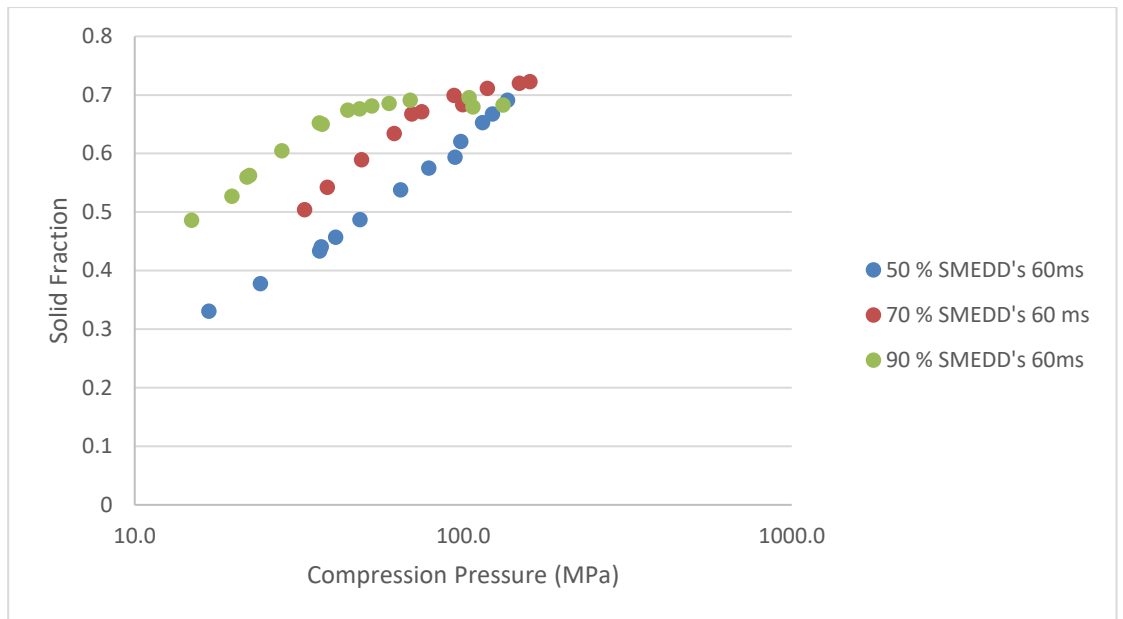


Figure 3.7 Compressibility profiles of Neusilin® US2 loaded with 50, 70, 90% SMEDDS preconcentrate (dwell time 60 ms)

Figure 3.8 shows compressibility profiles comparing the influence of SPc loading level and compression speed (dwell time). The data suggest that press speed does not influence solid fraction values as similar profiles are obtained for each loading level of SPc irrespective of dwell time.

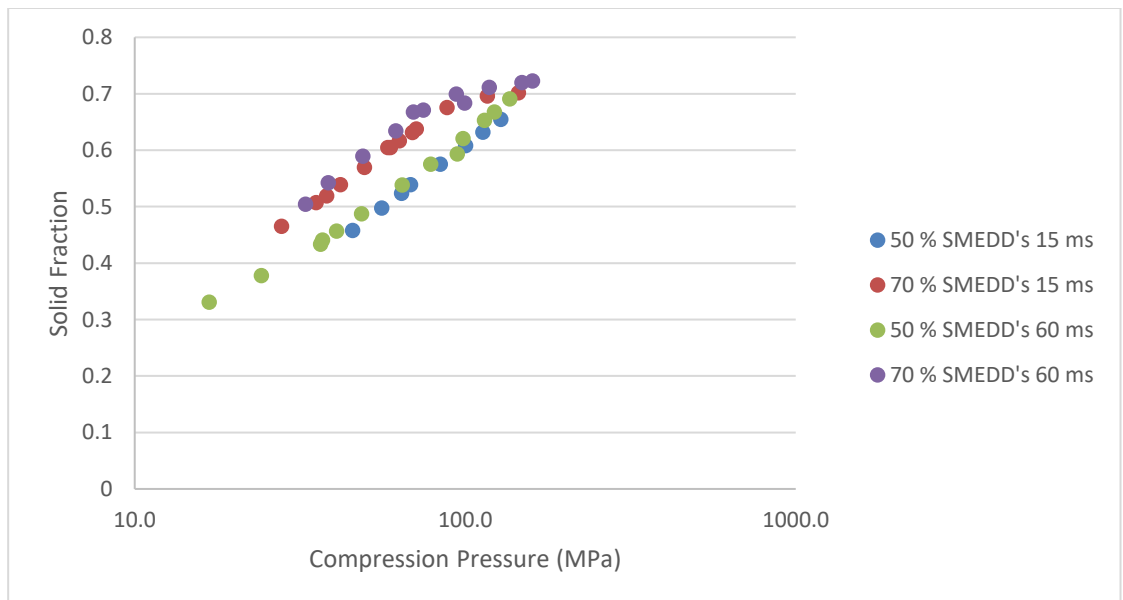


Figure 3.8 Compressibility profiles of Neusilin® US2 loaded with 50, 70% SMEDDS preconcentrate (dwell time 60 ms and 15 ms)

It has been reported that a solid fraction of 0.85 is optimal for tablet formulations (Pitt, 2015); however, this data suggest that liquisolid formulations may not be able to achieve such values and that an alternative target may need to be considered.

### 3.4.2.1 Compactability

As a general rule, tablet strength increases exponentially with increasing solid fraction (USP 40, <1062>, 2020). However, Figure 3.9 shows that for each of the SPc loaded materials this general rule does not apply. The data show that for each of the materials a critical solid fraction is reached, following which tensile strength begins to decrease; for 50 % and 70 % SPc loaded this value is approximately 0.67 and for 90 % SPc loaded this is likely to be between 0.60 and 0.68. When considering the compressibility profile in conjunction with the compactability profile, it is likely that the reduction in tensile strength is linked to liquid present between particles preventing the formation of inter-particulate bonds or bond formation between new surfaces formed due to particle shear during compression. Gumaste et al (2013) described this phenomenon as inter-particulate spreading of liquid in the tablet bed.

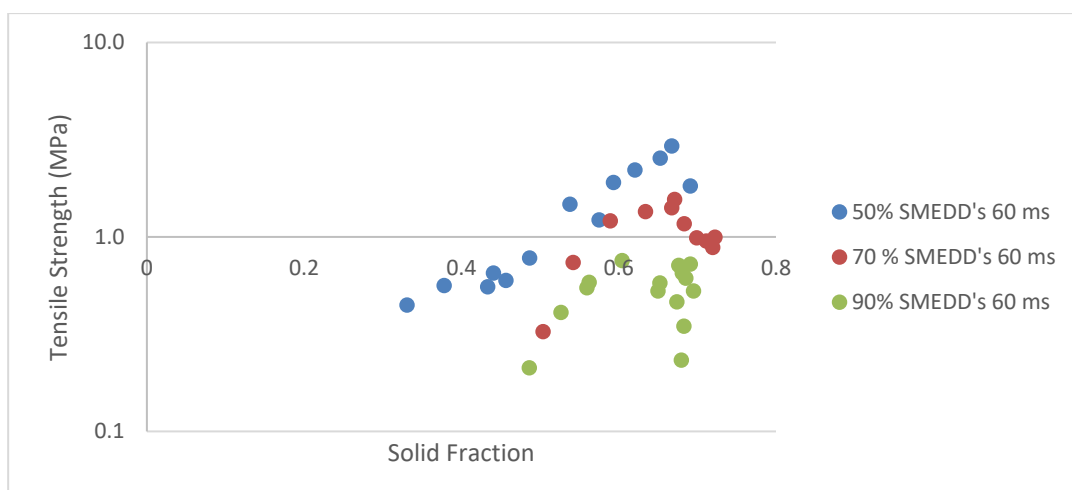


Figure 3.9 Compactability profiles of Neusilin® US2 loaded with 50, 70, 90% SMEDDS preconcentrate (dwell time 60 ms)

Figures 3.10 and 3.11 show compactability profiles comparing the influence of SPc loading level and compression speed (dwell time). The data indicate that press speed may influence tensile strength values as although similar profiles are obtained for each loading level, Figure 3.11 suggests that a

difference is apparent between 70 % loaded tablets compressed at different speeds (between solid fraction values from 0.58 to 0.65). A decrease in tensile strength in accordance with increasing press speed (decrease in dwell time) may be expected if the rate of liquid spreading is faster than that required for bond formation. Alternative considerations could be given to tablet ejection force/speed which may also influence tablet strength, but were not evaluated as part of this study.

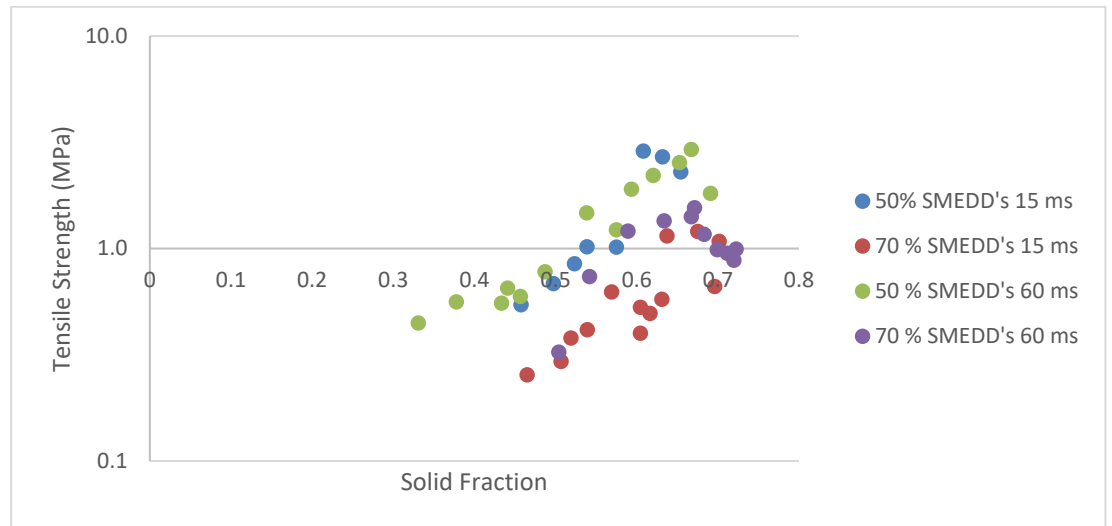


Figure 3.10 Compactability profiles of Neusilin® US2 loaded with 50 and 70 % SMEDDS preconcentrate (dwell time 60 ms and 15 ms)

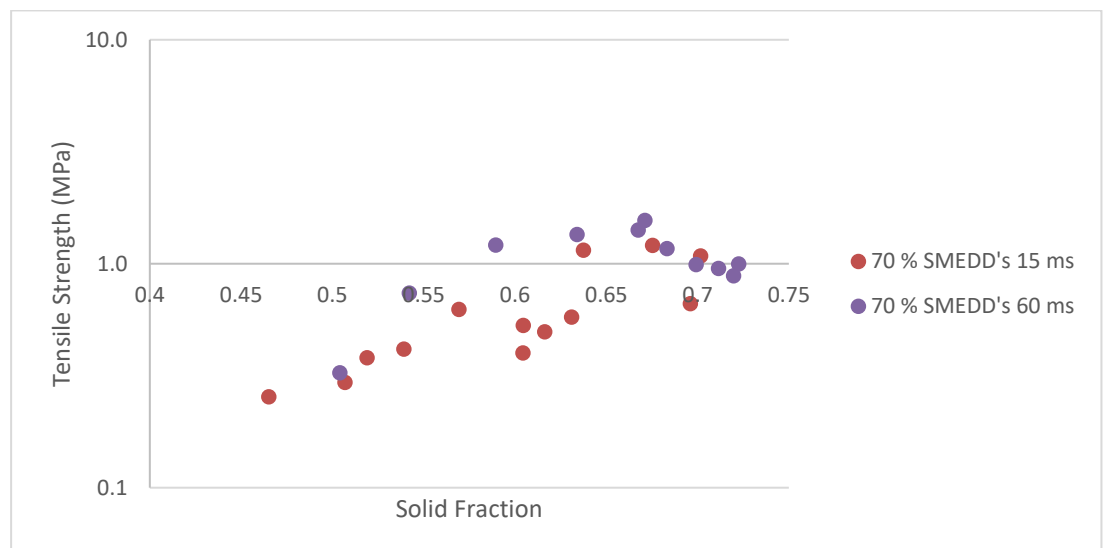


Figure 3.11 Compactability profiles of Neusilin® US2 loaded with 70 % SMEDDS preconcentrate (dwell time 60 ms and 15 ms)

### 3.4.2.5 Tablet Characteristics

Tablets were compressed at selected forces (5, 7 and 9 kN) at two speeds (dwell times 60 ms and 15 ms); the force selected for each loading concentration was based upon achieving a relatively high tablet tensile strength based upon the data presented in Figures 3.1 – 3.4. The aim of this study was to determine if the ‘native’ loaded US2 powder, could produce tablets with favourable characteristics, or highlight those characteristics which needed optimisation through further excipient inclusion in the formulation. Characterisation data are presented in Table 3.3. It was not possible to produce tablets containing 90 % SPc above 5 kN applied force or at higher press speed (dwell time 15 ms).

*Table 3.3 Characteristics of tablets containing Neusilin®US2 loaded with SMEDDS pre-concentrate compressed at selected forces (dwell time 60 ms and 15 ms). Where mean (n=5) (range) values are quoted for breaking force, thickness and tensile strength.*

Description	Dwell Time (ms)	Target Force applied (kN)	Friability (%)	Breaking Force (N)	Thickness (mm)	Tensile Strength (MPa)	Disintegration (mm:ss)
50 % Loaded	60	9	2.778%	60.6 (46.3 – 60.6)	2.47 (2.46 – 2.48)	1.43 (1.09 – 1.67)	> 60:00
50 % loaded	15	9	5.265%	64.1 (49.7 – 85.2)	2.49 (2.48 – 2.49)	1.49 (1.18 – 1.98)	> 60:00
70 % Loaded	60	7	4.609%	58.9 (37.0 – 83.0)	2.44 (2.43 – 2.44)	1.40 (0.88 – 1.97)	> 60:00
70 % loaded	15	7	4.525%	32.5 (6.1 – 50.6)	2.46 (2.46 – 2.46)	0.76 (0.14 – 1.19)	> 60:00
90 % Loaded	60	5	6.087%	25.2 (22.1 – 29.2)	2.50 (2.50 – 2.15)	0.58 (0.51 – 0.67)	> 60:00

The results show that irrespective of loading level, dwell time or applied force; all tablets were friable (> 1 %); only tablets containing either 50 % loaded SPc or 70 % SPc with longer dwell time (60 ms), possessed a tensile strength > 1 MPa, and all tablets failed to disintegrate in under 60 min which is not suitable for immediate release tablet formulations, where the limit for disintegration is 15 min. (Ph. Eur. 2017).

### 3.4.2.6 Discussion and conclusions

The data have shown that the compression characteristics of Neusilin®US2 loaded with SPc varies according to loading level.

The 50 % loaded material does not appear to be strain rate sensitive and produces linear manufacturability and compressibility profiles up to approximately 12 kN and 150 MPa applied force/pressure respectively. However, both the 70 % and 90 % materials exhibit strain rate sensitivity and the linear range over which tablet strength increases with increasing force/pressure is reduced compared to the 50 % loaded material.

The maximum tensile strength achieved across all samples appears to be limited by the loading level of the Neusilin® US2. The lower the loading, the higher the tensile strength possible, which is independent of press speed. The compressibility limitations may be due to a two-phase process, which can be described as the 'double pore theory' whereby, the initial stage of the compression process involves particle rearrangement and consolidation of the powder bed due to air entrapment within the bed (as described in Section 1.2.2). Effectively this stage removes a significant volume of inter-particulate pores from within the powder. The second phase is likely to involve movement of the adsorbed liquid to the areas of least pressure (radial axis) within or surrounding a particle (both inter and intra porous areas), with almost simultaneous failure of the internal porous structure of the particle under pressure. The potential for a compact to form relies on the ability of inter and intra particle rearrangement and particle fracture to form new bonds (USP 40, <1062>, 2020; Patel et al., 2006). The area of surfaces (both inter-granular and intra-granular surfaces) free from liquid (which is likely to interfere with bond formation) is likely to be limited as the liquid concentration/loading is increased and hence why tablet strength is reduced with increased loading.

The low friability reported for the tablets is likely due to the relatively low tensile strength values reported (< 1.5 MPa) for all batches, which is probably attributable to weak particle bonding as discussed earlier.

The long disintegration times for the tablets (across all formulations) may not however be expected due to the low tensile strength of the tablets and the addition of an SPc formulation which produces a micro-emulsion on dispersion in water. One explanation for the slow disintegration time of the tablets may be the gelation of SPc on contact with water. Gumaste et al (2013) found that some liquid-surfactant mixtures containing API could not be fully

recovered during dissolution studies as it was shown that these mixtures would form gels on exposure to water, and thus they postulated that gel formulation in the pores of a particle as per Figure 3.12 would reduce the rate and extent of API release.

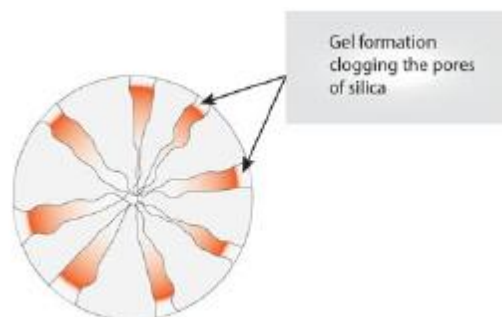


Figure 3.12. Depiction of a cross section of Neusilin®US2 with its pores filled with lipid surfactant mixture (taken from Gumaste et al 2013). The red colour portrays clogging of the pores due to gel formation on contact with the dispersion medium.

It is postulated that gelation at the surface of the tablet would reduce the rate at which the disintegration medium would wick into the tablet core, thus significantly reducing the disintegration rate of the tablets.

To enhance the robustness and characteristics of tablets, strength (improved tensile strength and friability) and disintegration rate needed to be improved.

### 3.5 Excipient addition to enhance tablet characteristics

Three compression aids with different compression mechanisms/properties were selected for evaluation to be added to the SPc loaded Neusilin®US2. Firstly, microcrystalline cellulose (MCC) (Avicel 200 LCM) was selected. MCC is generally considered to deform plastically, is a diluent with exceptional binding properties and is recognized as one of the preferred DC binders. In addition, MCC and super-disintegrants may be complementary to promote fast disintegration (Thoorens et al., 2014). Mannitol (spray dried) was selected as an alternative compression aid as compression studies performed by Tarlier et al (2018) on mannitol crystals confirmed a more brittle behaviour than MCC. Finally, a spray dried grade of calcium carbonate was also selected, due to the brittle nature of compression exhibited by calcium carbonate (Grote and Kleinebudde 2018). Spray dried grades of mannitol and calcium carbonate were selected for their improved flow properties and their porous structure; which was hypothesised to improve the distribution of liquid during compression and thereby improve tablet properties.

To improve disintegration rate, croscarmellose sodium (Ac-Di-Sol®) was selected for evaluation as a super-disintegrant at a concentration of 5 % w/w. Previous studies performed by Veranikova et al (2017) demonstrated that croscarmellose sodium inclusion in liquisolid tablets at > 2.5 % had been effective in achieving fast disintegration and complete drug release.

Sodium stearyl fumarate (Pruv®) was selected as lubricant rather than the traditionally used magnesium stearate. Pruv® is reported to be more hydrophilic than magnesium stearate whilst conferring similar lubrication properties; therefore, is less likely to impact upon disintegration rate of tablets (JRS literature).

### 3.5.1 Formulation details

Table 3.4 details the composition of blends produced containing extra-granular excipients to improve tablet characteristics compared to those tablets produced in section 3.4.2.

The concentration of compression aid selected was 10 % w/w in the formulation. A number of investigations included extra-granular excipients (Cirri et al., 2016; Gumaste et al., 2013; Vranikova et al., 2017; Seljak et al., 2018) but the concentration of excipients ranged from 15 % w/w to 40 % w/w. There was concern about too great a dilution effect upon the potential for API loading within a tablet; hence the concentration of the diluent was limited to 10 % w/w.

Table 3.4 Formulation composition details. Note: where granule is referred to, granule is defined at Neusilin® US2 loaded with SPc.

Formulation	% w/w								
	A	B	C	D	E	F	G	H	J
50 % Granule	84	84	84						
70 % Granule				84	84	84			
90 % Granule							84	84	84
Ac-di-sol	5	5	5	5	5	5	5	5	5
Mannitol (Spray Dried)	10			10			10		
Avicel PH 200		10			10			10	
Calcium Carbonate (Spray Dried)			10			10			10
Sodium Stearyl fumarate	1	1	1	1	1	1	1	1	1

### 3.5.2 Compression data

The focus of this investigation was to assess the influence of excipient addition on tablet characteristics. The influence of press speed was not investigated during this study and all tablets were compressed with a dwell time of 60 ms.

#### 3.5.2.1 Tableability of formulations loaded with SPc and extra-granular excipients

Figure 3.13 details tableability profiles for formulation containing Neusilin® US2 loaded with SPc and selected compression aids (MCC, spray dried mannitol and spray dried calcium carbonate). For comparison purposes, the equivalent SPc loaded Neusilin® US2 formulation without extra-granular excipient addition are included in the Figures.

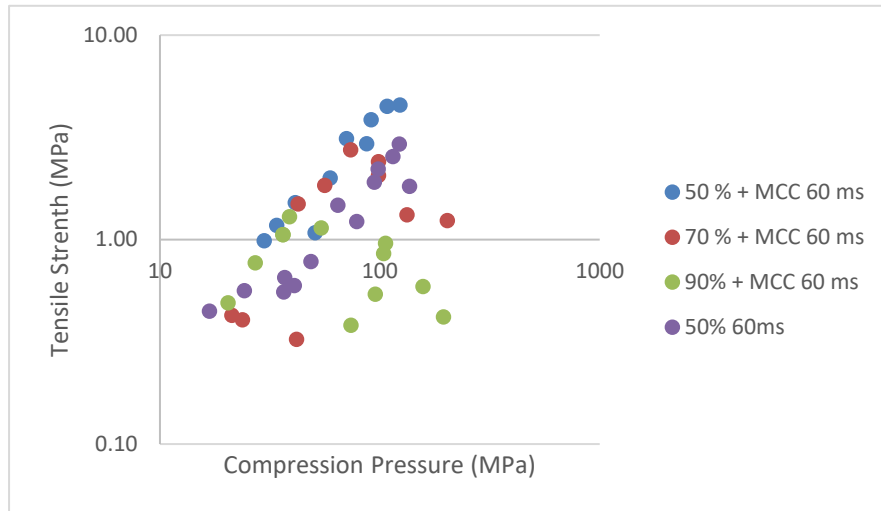
Figure 3.13a shows the influence of 10 % w/w MCC addition to Neusilin®US2/SPc mixture. It was possible to produce viable tablets (tensile strength > 1MPa) for all formulations, although, for 90 % SPc loaded Neusilin® US2, the compression range over which viable tablets were produced was narrow (from approximately 30 – 55 MPa). Direct comparison of formulations containing 50 % loaded Neusilin®US2 showed that the addition of MCC improved tablet robustness across the full compression range with viable tablets produced at lower compression forces (approximately 30 MPa compared to approximately 50 MPa).

Figure 3.13b and c show the influence of 10 % w/w mannitol and calcium carbonate addition to the Neusilin®US2/SPc mixtures, respectively. Similarly to MCC, when added to 50 % and 70 % loaded mixtures, mannitol improved tablet viability over the range of applied pressure. However, when added to 90 % SPc loaded mixture, the mannitol failed to produce viable tablets (> 1 MPa tensile strength). For formulations containing calcium carbonate an improvement in robustness was seen at the 50 % SPc loading level. However, results for 70 % and 90 % loaded mixtures were variable and, similarly to the mannitol formulation containing 90 % SPC loaded mixture, viable tablets could not be produced.

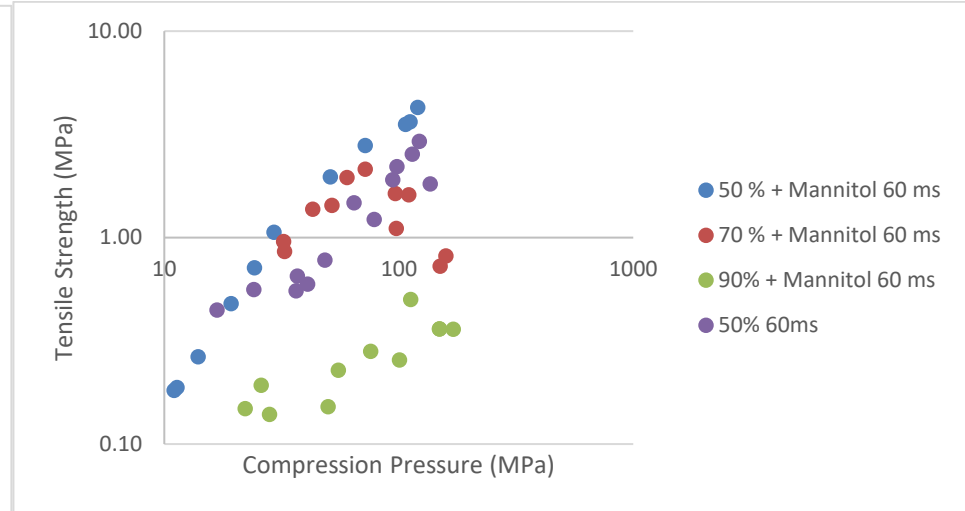
Figures 3.13d to f show the influence of the excipients compared to each other at incremental loading levels. At the 50 % and 70 % loading levels the addition of each of the excipients shows an improvement in tablet robustness compared to the formulations without extra-granular excipients. However, at the 90 % loading level only the MCC can be seen to produce viable tablets (> 1 MPa tensile strength) although this is over a reduced range of applied forces.

These data show a decline in tablet robustness with increased SPc loading with the extra-granular excipients as previously reported during compression of the loaded mixtures alone. MCC appeared to be preferential for tablet robustness at the highest loading level.

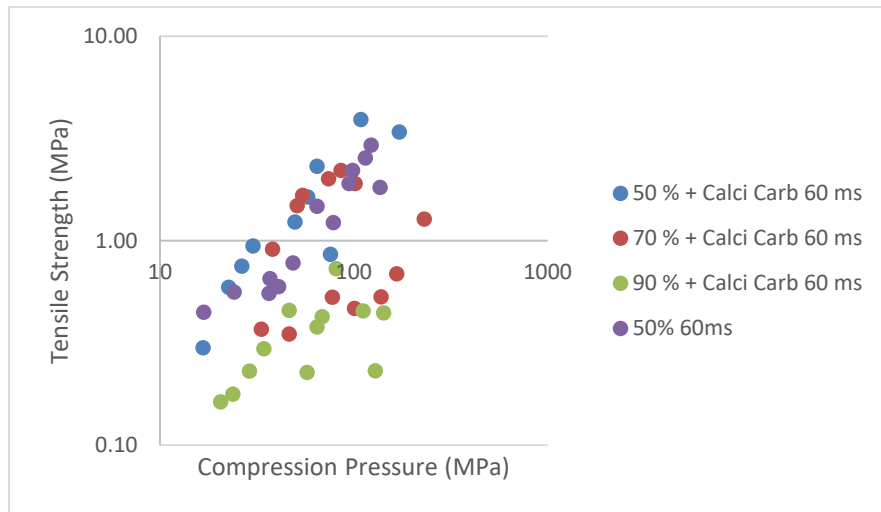
a)



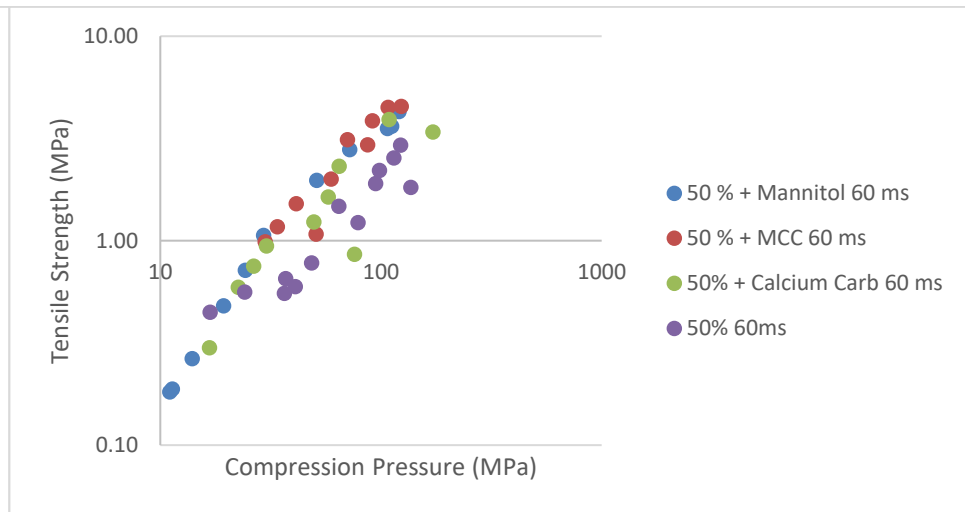
b)



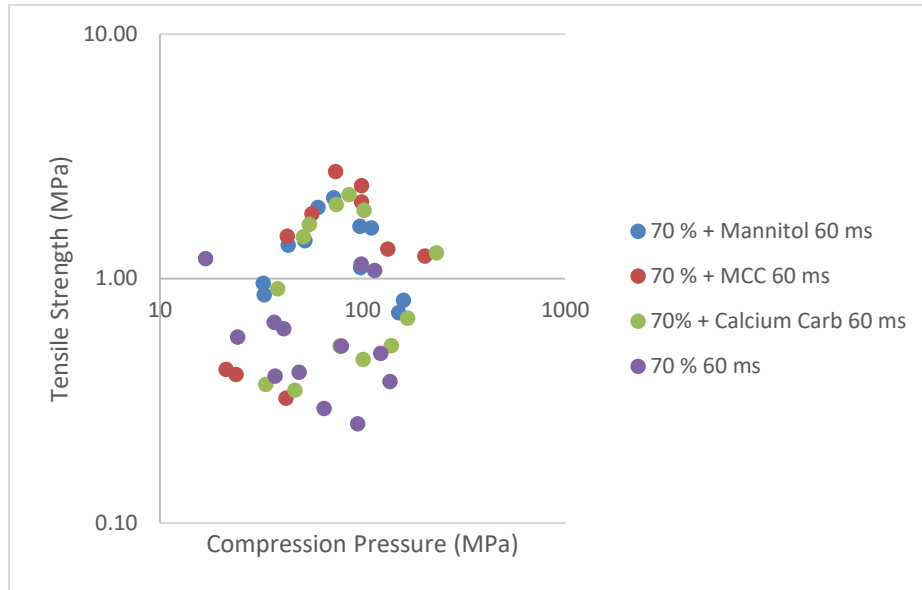
c)



d)



e)



f)

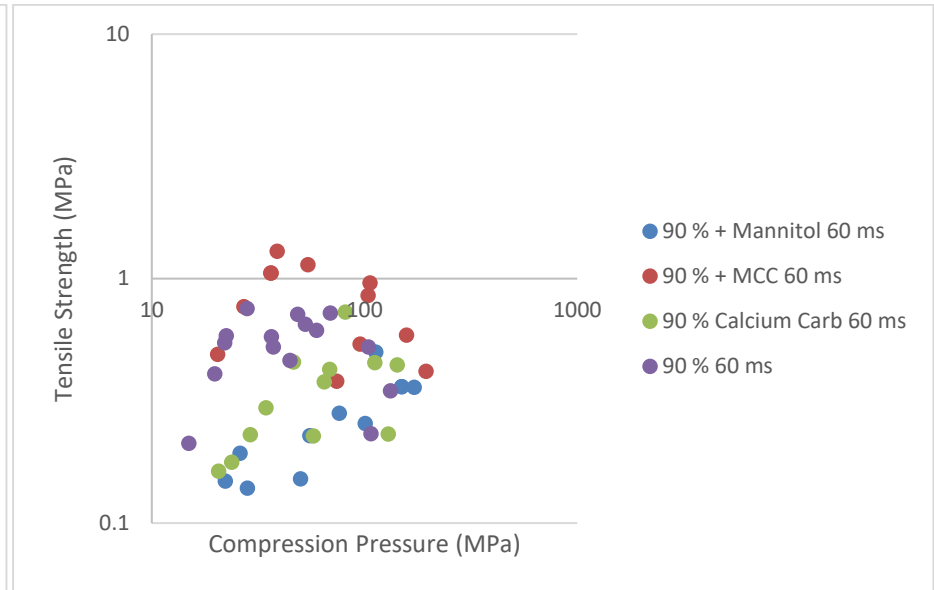


Figure 3.13 Tableability profiles of tablets containing Neusilin® US2 loaded with 50, 70 and 90 % SPC and selected compression aids; a – f from left to right in descending order.

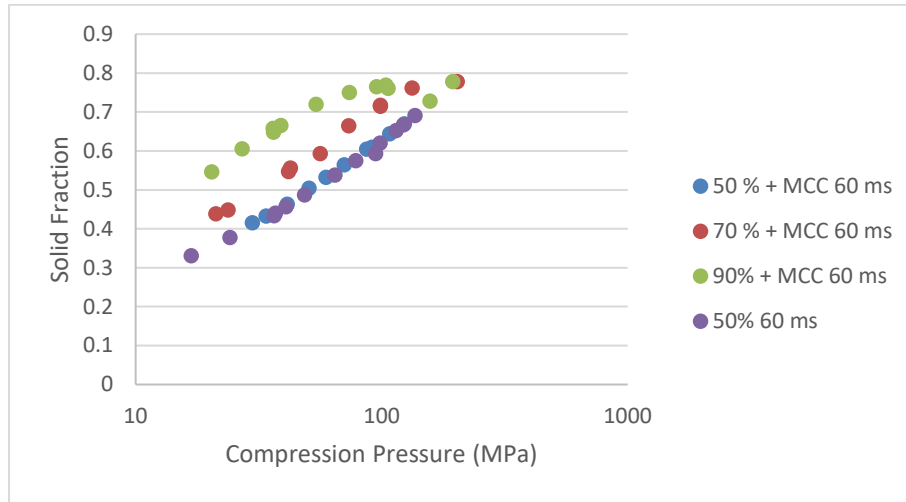
### **3.5.2.2 Compressibility of formulations loaded with SPc and extra-granular excipients**

Figure 3.14 details compressibility profiles for formulations containing Neusilin® US2 loaded with SPc and selected compression aids (MCC, spray dried mannitol and spray dried calcium carbonate). For comparison purposes, the equivalent SPc loaded Neusilin US2 formulation without extra-granular excipient addition are included in the Figures.

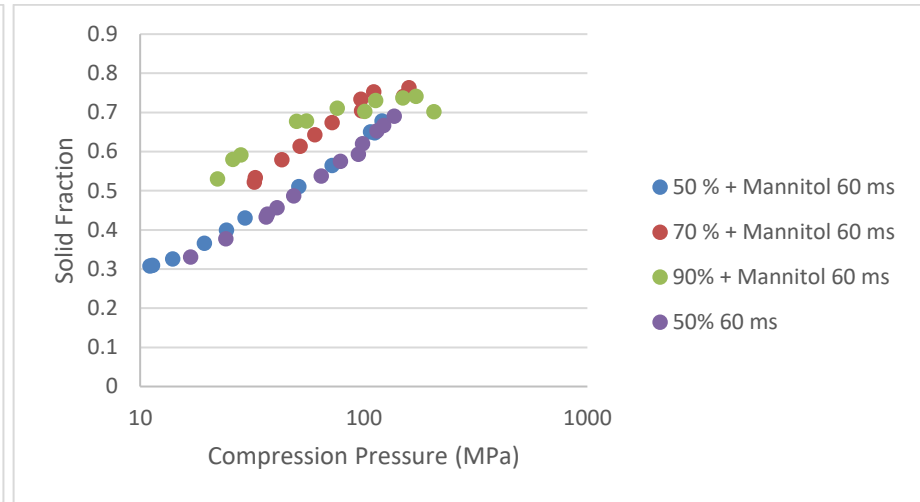
Figures 3.14 a to c show that with increased loading, formulations exhibit an earlier plateau (lower applied force) in solid fraction value; irrespective of the extra-granular excipient selected. As discussed earlier in the chapter this is likely due to the predominance of the liquid phase with increased applied force (at higher loading levels) and saturation of inter and intra particulate pores prevented further compression. No obvious difference was reported between grades, although greater variability in data was reported for tablets containing calcium carbonate.

Figures 3.14 d to f show the influence of the excipients compared to each other at incremental loading levels. Figure 3.14 d (50 % loaded levels) suggests that there are no notable differences are apparent in solid fraction values irrespective of the presence of extra-granular excipient(s). However, as SPc loading level increased (Figures 3.14 e and f) mannitol addition appears to result in a lower solid fraction value at higher applied force compared to that of tablets containing MCC or calcium carbonate. These data suggest that in the presence of mannitol the liquid phase predominates to a greater extent than when MCC or calcium carbonate are present. An obvious consideration could be the solubility of mannitol (1 in 5.5, Sheskey et al., 2017) in the liquid phase compared to other excipients (Avicel, and calcium carbonate are practically insoluble, Sheskey et al., 2017) which may explain this phenomenon; but was not investigated as part of this study.

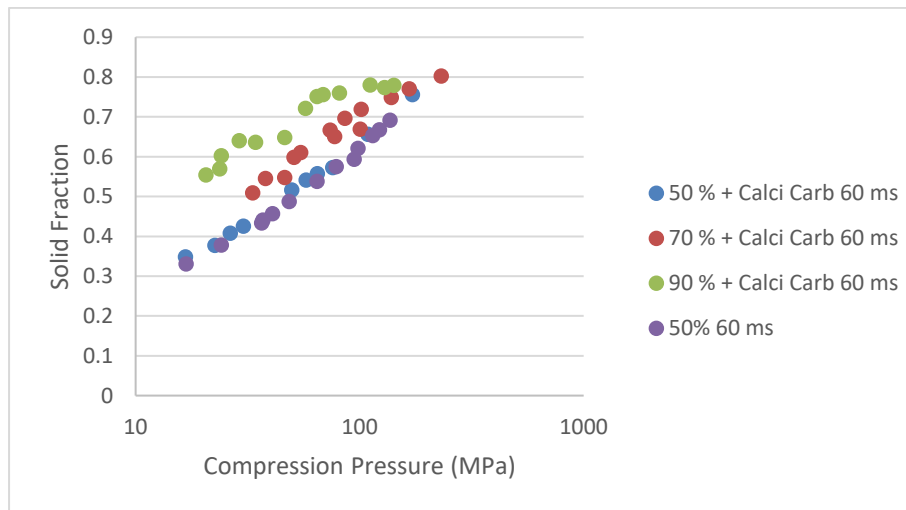
a)



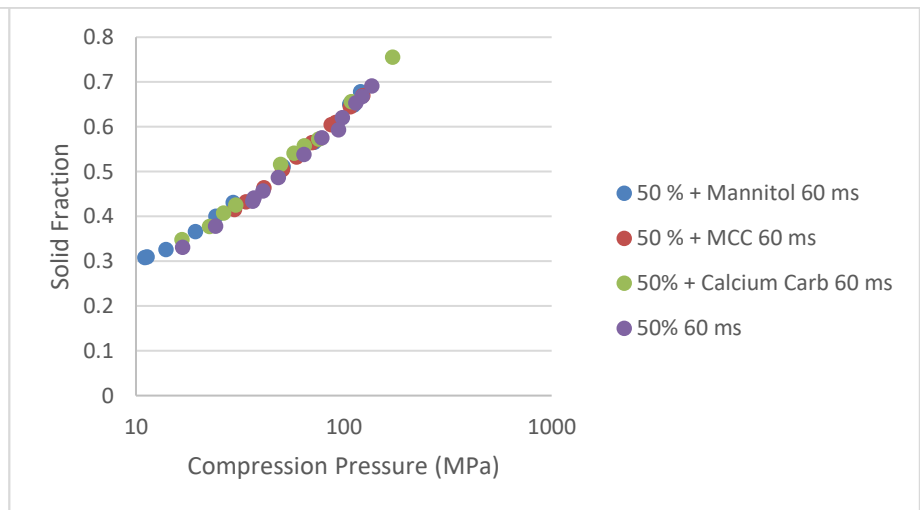
b)



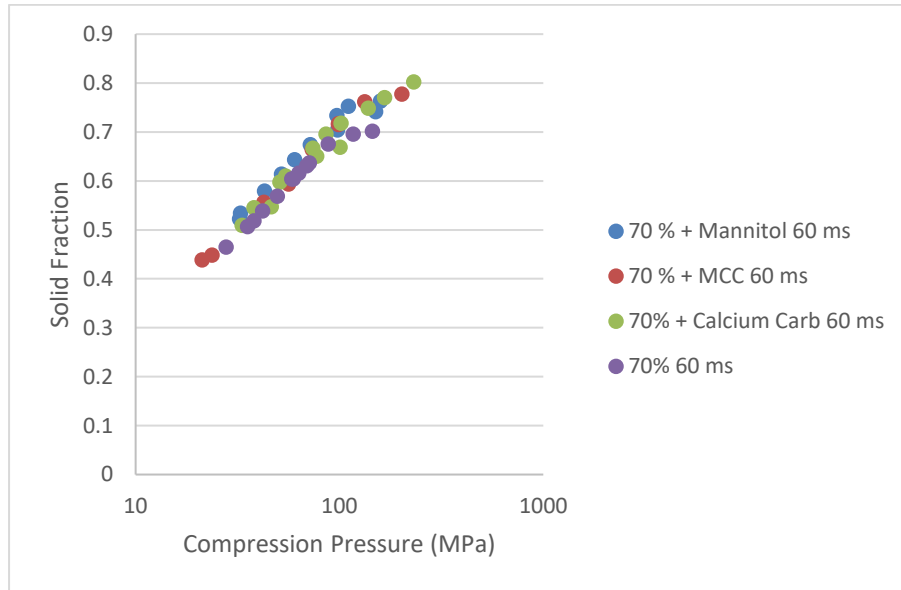
c)



d)



e)



f)

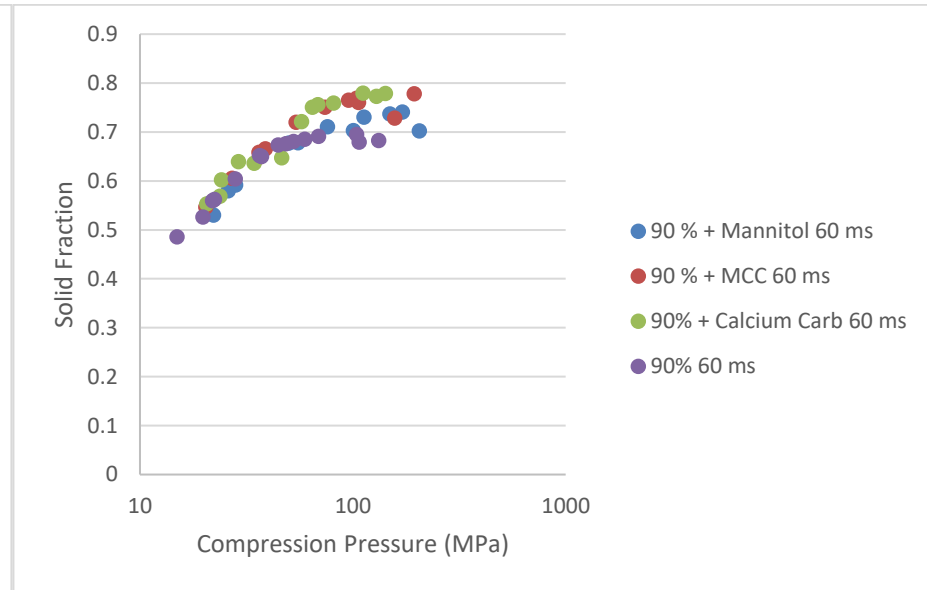


Figure 3.14 Compressibility profiles of tablets containing Neusilin® US2 loaded with 50, 70 and 90 % SPC and selected compression aids; a – f from left to right in descending order.

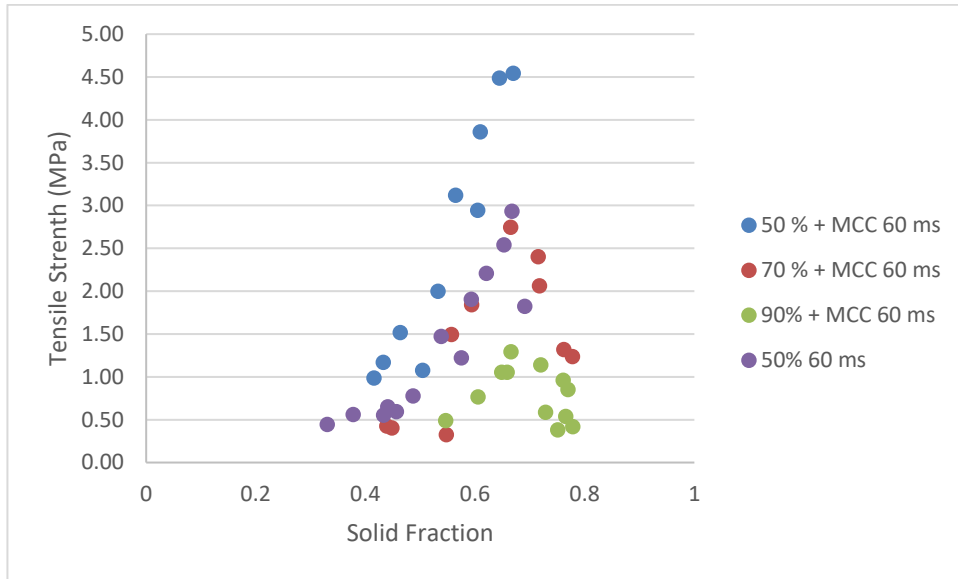
### 3.5.2.2 Compactability of formulations loaded with SPc and extra-granular excipients

Figure 3.15 details compactability profiles for formulations containing Neusilin® US2 loaded with SPc and selected compression aids (MCC, spray dried mannitol and spray dried calcium carbonate). For comparison purposes, data for the equivalent SPc loaded Neusilin US2 formulation without extra-granular excipient addition are included in 3.15a to f.

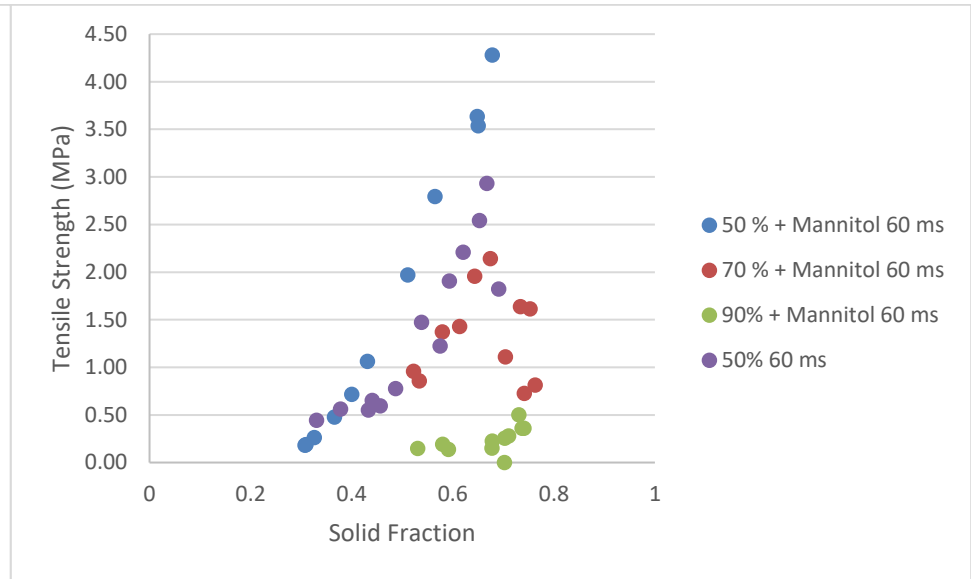
Figures 3.15 a to f show that the general theory for compactability does not hold true for liquisolid tablets above 50 % loading; whereby in accordance with the Ryshkewitch-Duckworth equation (Equation 1.3), it would be expected that tablet tensile strength increases exponentially with increasing solid fraction. Figures 3.15 a to c, show similar compactability profiles irrespective of the extra-granular excipient selected.

Figure 3.15 d shows that at 50 % SPC loading a relatively linear correlation between increased tensile strength and increased solid fraction. However, as SPC loading increased the linear increase in tensile strength with increased solid fraction peaked at approximately 0.68 – 0.71 (solid fraction) following which, further increases in solid fraction (increased compression pressure applied) resulted in a decreased tensile strength. Not exceeding such a solid fraction is therefore key to maintaining tablet robustness. Figures 3.15 e and f, show that higher tensile strength values were produced for those tablets containing MCC. However, the inflection point (solid fraction value) at which tensile strength began to decrease was similar, irrespective of the extra-granular excipient selected.

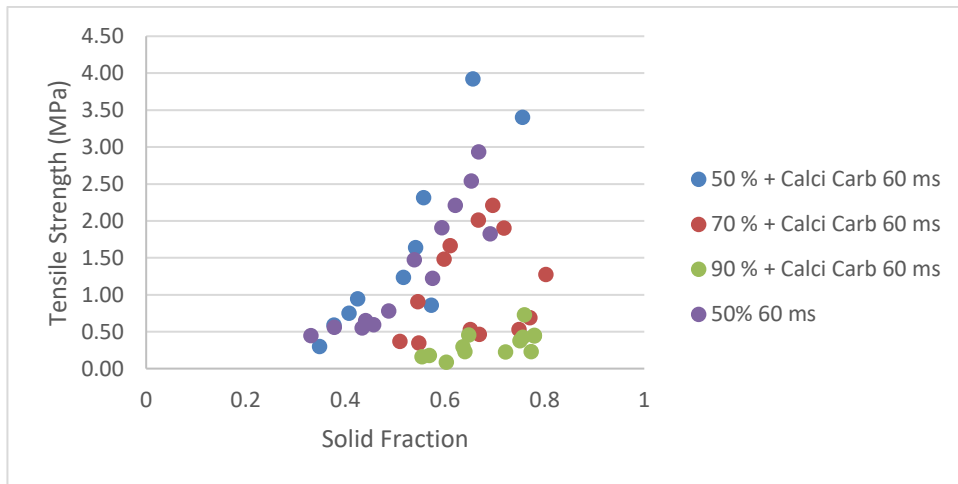
a)



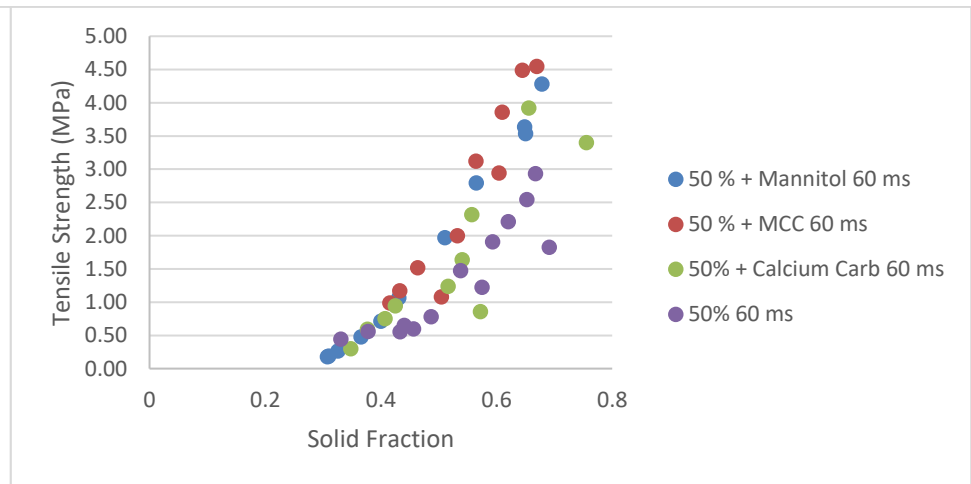
b)



c)



d)



e)

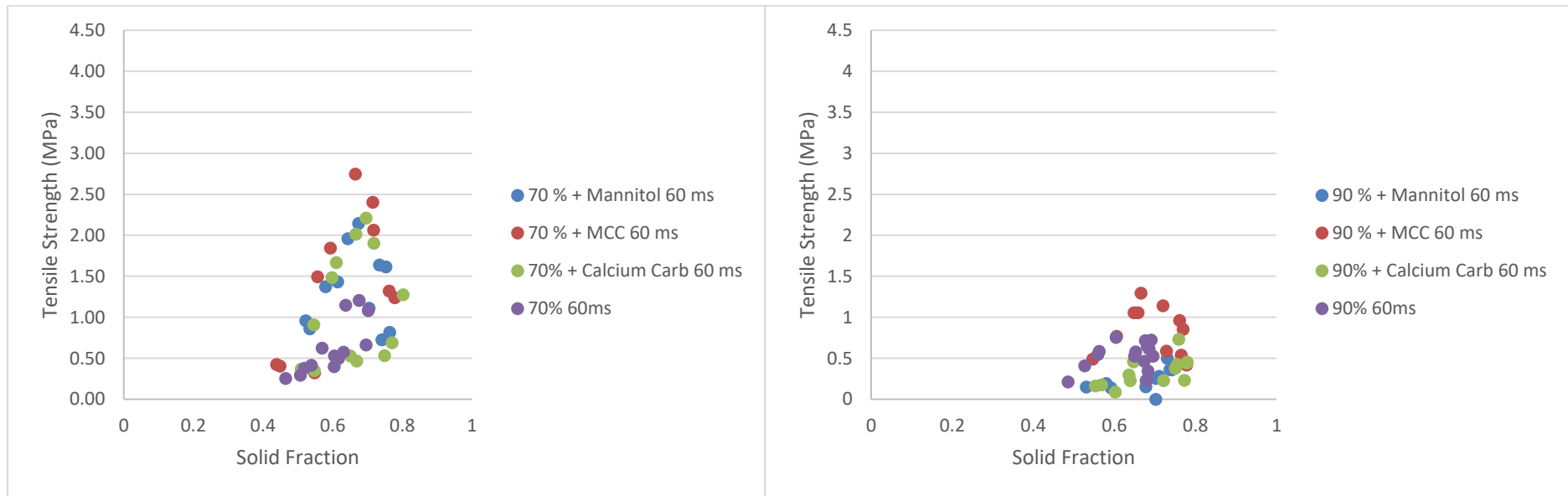


Figure 3.15 Compactability profiles of tablets containing Neusilin® US2 loaded with 50, 70 and 90 % SPC and selected compression aids; a – f from left to right in descending order.

### 3.5.2.6 Tablet Characteristics

Tablets were compressed at selected forces, (dwell time 60 ms). The aim of this study was to evaluate the influence of extra-granular excipients upon tablet characteristics following the need to improve tensile strength and disintegration rate, when the SPc loaded mixtures were compressed alone (Section 3.4.2.5). Characterisation data are presented in Table 3.6.

It is difficult to determine the influence of the selected variables (SPc loading, target force and extra granular excipient) upon the tablet characteristics, from the data in Table 3.6 alone. Therefore, a modelling programme (JMP 14.0) was used for further data analysis and interpretation. See Figures 3.16 to 3.18.

From the data in Table 3.6, it was clear that the inclusion of super-disintegrant and compression aid drastically increased the disintegration rate of the tablets. Table 3.3 shows that the tablets characterised containing the SPc loaded Neusilin® US2 alone did not disintegrate with 60 min. However, all tablets tested in this investigation disintegrated within 10 min. The friability of the tablets within increasing SPc concentration was reduced as was tensile strength which would be expected. However, a number of tablets laminated during friability testing, resulting in the failure of some batches to pass the test. The general appearance of the tablets was good and without edge chipping which would be expected with weak friable tablets. In addition, a number of batches (across all formulations) failed the friability test despite tablets having relatively high tensile strength values (> 1 MPa) which would suggest sufficient tablet robustness. Further investigation is required to understand this phenomenon. The concentration and distribution of the lubricant within the formulation may be a contributory factor or concentrated liquid areas within the tablet may result in 'weak' spots which gives rise to tablet lamination during friability testing.

Table 3.6 Characteristics of tablets containing Neusilin®US2 loaded with 50, 70 and 90 % SMEDDS preconcentrate compressed at selected forces (dwell time 60 ms). Friability (n=10). Av. Breaking force (n=5). Av. Tensile strength (n=5). Disintegration (n=6).

Description	Target Force	Friability	Av. Breaking Force	Range (N)		Thickness	Av. Tensile Strength	Range (MPa)		Disintegration	
	kN			(%)	(N)			Low	High	(mm)	(MPa)
50 % SPc 10 % Mannitol	5	0	84.9	80.4	88.1	2.86 - 2.84	1.72	1.63	1.78	00:50	01:02
50 % SPc 10 % Mannitol	7.5	Fail	97.1	71.8	124.5	2.50 - 2.53	1.97	1.66	2.83	01:03	01:47
50 % SPc 10 % Mannitol	10	0.00	90.1	31.6	133.8	2.29 - 2.35	2.25	0.80	3.27	02:28	03:01
50 % SPc 10 % Avicel	5	0.00	105.6	85.1	113.6	2.81 - 2.90	2.14	1.75	2.25	00:47	00:53
50 % SPc 10 % Avicel	7.5	0.00	114.2	45.9	142.9	2.49 - 2.53	2.63	1.07	3.24	01:31	01:55
50 % SPc 10 % Avicel	10	0.00	139.7	61.6	172.6	2.20 - 2.36	3.55	1.62	4.20	02:21	02:55
50 % SPc 10 % Calci. Carb.	5	0.06	94.2	77.5	106.3	2.71 - 2.74	2.00	1.65	2.23	00:15	00:25
50 % SPc 10 % Calci. Carb.	7.5	0.00	107.5	82.2	134.6	2.49 - 2.53	2.48	1.91	3.05	00:51	01:24
50 % SPc 10 % Calci. Carb.	10	0.00	121.4	98.6	131.9	2.26 - 2.35	3.05	2.52	3.22	01:41	02:56
70 % SPc 10 % Mannitol	5	0.11	74.2	68.8	74.2	2.70 - 2.77	1.57	1.47	1.54	01:28	02:02
70 % SPc 10 % Mannitol	7.5	Fail	84.4	79	87.9	2.51 - 2.55	1.93	1.82	1.98	01:30	01:45
70 % SPc 10 % Mannitol	10	Fail	63	17.8	86.7	2.34 - 2.40	1.54	0.44	2.07	04:40	08:13
70 % SPc 10 % Avicel	5	Fail	71.9	41.1	89.5	2.52 - 2.66	1.76	0.94	1.93	00:55	01:15
70 % SPc 10 % Avicel	7.5	0.34	88.1	74	103.7	2.32 - 2.38	2.15	1.85	2.50	02:30	03:10
70 % SPc 10 % Avicel	10	Fail	73.8	63.8	87.5	2.13 - 2.19	1.80	1.73	2.29	03:31	04:48
70 % SPc 10 % Calci. Carb.	5	0.33	39.2	14.9	76.1	2.64 - 2.75	0.96	0.33	1.59	01:17	01:47
70 % SPc 10 % Calci. Carb.	7.5	Fail	70.5	33.3	94.2	2.10 - 2.22	1.72	0.92	2.43	02:20	04:10
70 % SPc 10 % Calci. Carb.	10	Fail	47.3	8.6	73.4	1.99 - 2.06	1.16	0.25	2.04	04:59	06:48
90 % SPc 10 % Mannitol	5	Fail	14.8	11.2	23.8	2.25 - 2.50	0.36	0.29	0.55	01:09	02:10
90 % SPc 10 % Mannitol	7.5	Fail	12.2	3.6	20.7	2.23 - 2.37	0.30	0.09	0.50	01:59	03:02
90 % SPc 10 % Mannitol	10	Fail	8.5	5.8	14.7	2.33 - 2.37	0.21	0.14	0.36	01:24	02:32
90 % SPc 10 % Avicel	5	Fail	47.7	23.7	60.1	2.43 - 2.48	1.17	0.56	1.39	02:29	04:04
90 % SPc 10 % Avicel	7.5	Fail	25.5	17.3	30.9	2.31 - 2.43	0.62	0.43	0.73	02:11	03:25

Description	Target Force	Friability	Av. Breaking Force	Range (N)		Thickness	Av. Tensile Strength	Range (MPa)		Disintegration	
90 % SPc 10 % Avicel	10	1.63	27.4	19.1	31.6	2.36 - 2.42	0.67	0.47	0.75	01:51	04:18
90 % SPc 10 % Calci. Carb.	5	N/A	N/A	N/A	N/A	N/A	N/A	N/A	N/A	N/A	N/A
90 % SPc 10 % Calci. Carb.	7.5	N/A	N/A	N/A	N/A	N/A	N/A	N/A	N/A	N/A	N/A
90 % SPc 10 % Calci. Carb.	10	N/A	N/A	N/A	N/A	N/A	N/A	N/A	N/A	N/A	N/A

### 3.4.2.6 Data Modelling and further analysis

To establish a correlation between the influence of loading level, excipient selection and applied force upon disintegration rate (mm:ss), friability (%) and tensile strength (MPa), JMP 14.0 data analysis software was used to display and analyse the data.

Variability charts are used to specify multiple X variables and see differences in means and variability across all these variables at once (JMP, SAS 2020). Variability charts were produced using the characterisation data as Y responses (disintegration rate, friability (%) and tensile strength) and % loading, excipient and target force were used as the X groupings.

Figure 3.16 shows that formulations containing 50 % SPc loaded Neusilin®US2 exhibit the trend of increasing tensile strength with increasing force applied (relatively linear increase irrespective of excipient selected), as shown by the tableability profiles (Figure 3.13). Those formulations containing 70 % SPc loaded Neusilin®US2 resulted in maxima peaks for tensile strength reached at approximately 7.5 kN for each excipient. For formulations containing 90 % SPc loaded Neusilin®US2 a general decrease in tensile strength was reported with increased compression force.

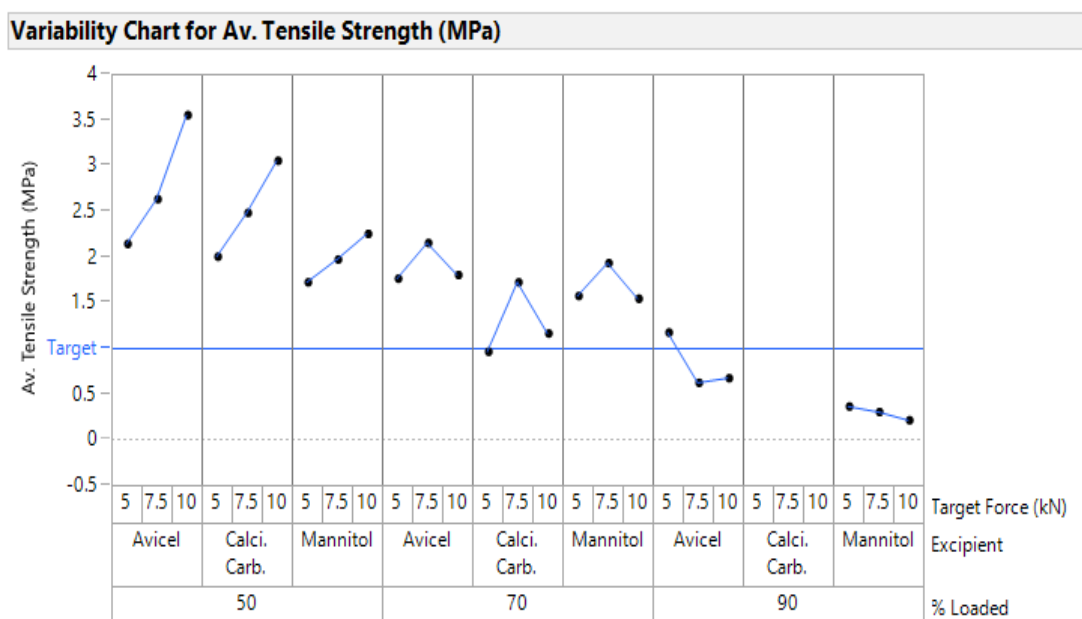


Figure 3.16 Variability chart for Av. Tensile strength (MPa)

Figure 3.17 shows a trend in disintegration rate across the formulations containing 50 to 70 % SPc loaded Neusilin® US2, disintegration time increased with increased compression force as would be expected. Formulations containing 70 % SPc loaded Neusilin®US2, appear to show an excipient-related difference in disintegration rate (MCC > calcium carbonate > mannitol) which does not correlate with increased tensile strength (Figure 3.16). This phenomenon was not necessarily expected. Formulations containing 90 % SPC loaded Neusilin®US2 did not show a trend in disintegration rate with increased force. This phenomenon is likely due to the liquid/SPc component in the formulation becoming a predominant phase in the tablet and driving disintegration rate. The disintegration rate is then likely to be driven by the wettability/miscibility and dispersibility of the liquid phase. These characteristics of the SPc were not evaluated as part of this study.

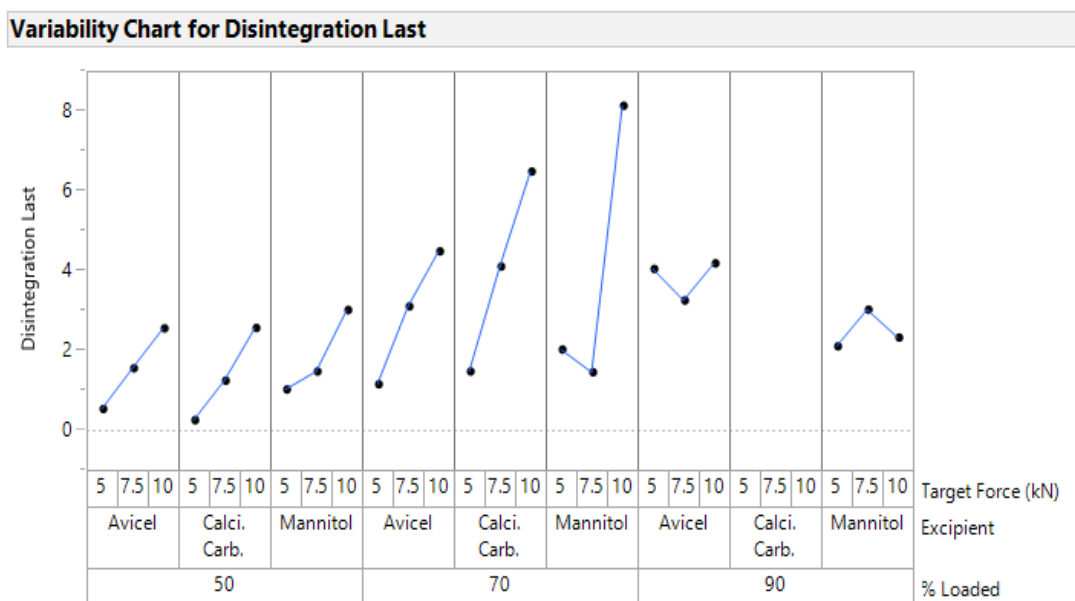


Figure 3.17 Variability chart for Av. Tensile strength (MPa)

Figure 3.18 shows a relatively random pattern for friability data. It should be noted that in order to model the data, values of 10 % friability were used where tablets laminated and failed the friability test, as numerical values only can be utilised by the software. The random nature of the data suggest that other factors also influenced the friability of the tablets. As postulated earlier in Section 3.4.2.6, factors such as lubricant or liquid distribution/homogeneity may

result in 'weak spots' resulting in tablet lamination and failure during testing. Other factors yet to be identified may contribute.

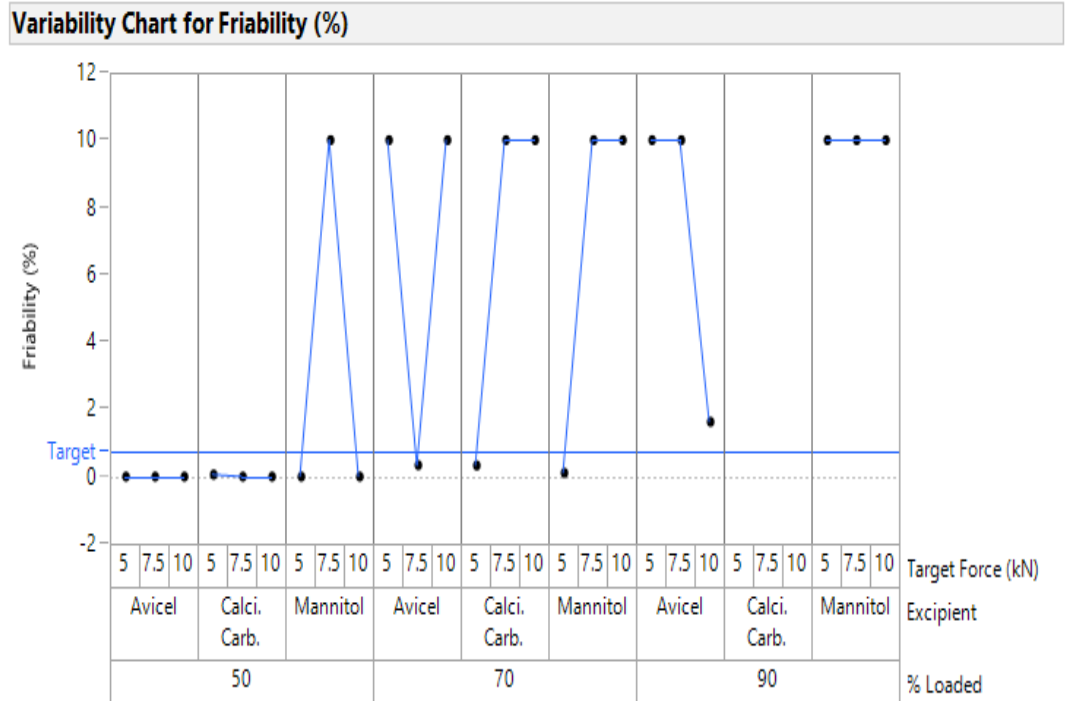


Figure 3.18 Variability chart for Friability (%)

A step wise regression was used to model the tensile strength and the disintegration data; to establish single and two factor interactions. Regression analysis models the relationships between a response variable and one or more predictor variables/input factors (Frost, 2020). The data for friability was not included due to its random nature and its unsuitability for modelling.

A predicted plot of tensile strength was generated as detailed in Figure 3.19. The statistically significant terms in the model ( $P < 0.05$ ) are detailed in Figure 3.20 (the effect summary), the model showed that the most significant input factor was that of % loading, which is not surprising. The second most significant input factor is the two-factor term of % loading and compression force followed finally by the influence of excipient selection.

The data show that for formulation design, the most significant consideration for the formulator is likely to be the selection of loading level as this factor drives the tensile strength of the tablet. Whilst excipient selection was shown to be a significant factor, the influence of excipient selection on tensile strength was less than that of loading. However, it should be considered that these studies only evaluated extra-granular excipient inclusion at 10 % w/w in the blend formulations. It is hypothesised that should this % w/w increase then the influence of excipient addition would increase; as effectively the concentration of liquid in the formulation would be reduced. However, a formulator must be mindful of the target drug load and therefore find the appropriate balance between tablet characteristics and the drug load.

The R-squared value for the model (0.90) shows that the model explains 90 % of the data, with contribution from other factors resulting in the additional 10 % variability in the data.

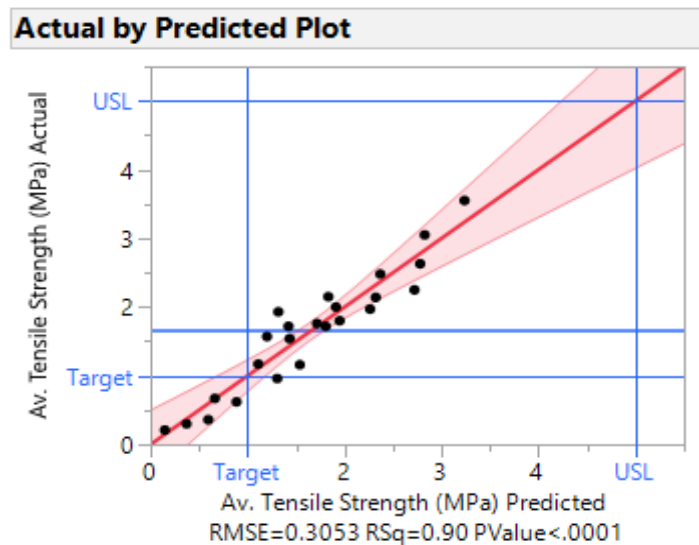


Figure 3.19 Predicted plot for tensile strength (MPa)

Effect Summary			
Source	LogWorth		PValue
% Loaded	8.933		0.00000
% Loaded*Target Force (kN)	2.577		0.00265
Excipient	2.233		0.00585
Target Force (kN)	1.290		0.05129 ^

Figure 3.20 Identified statistically significant input factors for tensile strength prediction

Using the JMP 14.0 software it was possible to derive a model equation to estimate tensile strength of the tablets. The model equation is detailed in Figure 3.21. The model equation could be used to estimate the tensile strength of tablets produced by varying the values of the input factors (% loading, excipient and target force). The benefit of the model is that predictions of tablet characteristics (tensile strength) can be made for tablets containing SPc loadings between those actually produced i.e. between the range 50 % and 90 % loading. This ability would allow a formulator to be able to optimise the % loading to achieve target drug loading and desired tablet characteristics, without the need for trial and error and therefore a reduced amount of practical activities.

Prediction Expression									
4.357492284									
+ -0.047314815 • % Loaded									
+ Match(Excipient)	<table border="0"> <tr> <td>"Avicel"</td> <td>⇒ 0.3086419753</td> </tr> <tr> <td>"Calci. Carb."</td> <td>⇒ -0.101728395</td> </tr> <tr> <td>"Mannitol"</td> <td>⇒ -0.20691358</td> </tr> <tr> <td>else</td> <td>⇒ .</td> </tr> </table>	"Avicel"	⇒ 0.3086419753	"Calci. Carb."	⇒ -0.101728395	"Mannitol"	⇒ -0.20691358	else	⇒ .
"Avicel"	⇒ 0.3086419753								
"Calci. Carb."	⇒ -0.101728395								
"Mannitol"	⇒ -0.20691358								
else	⇒ .								
+ 0.06375 • Target Force (kN)									
+ ( % Loaded - 67.5 ) • ( ( Target Force (kN) - 7.5 ) • -0.006812821 )									

Figure 3.21 Model equation for the determination of tensile strength for SPC loaded Neusilin® US2 and selected extra-granular excipients.

Figure 3.22 shows the prediction model for tensile strength with 95 % confidence limits. The blue zone represented on the Figure, indicates the confidence interval limits. The figure (3.22) provides an example of how the model can be used to predict tensile strength. When used 'live' the software allows a cursor to be used scan across specific input factor values. which automatically adjusts the other input factors values to show the adjustment in associated tensile strength. In Figure 3.22 when 88.46 % SPc loading is selected (vertical dotted red lines indicate selection) with MCC (Avicel) added extra-granularly and a compression force of 5 kN is applied the resultant tensile strength value is predicted to be 1.15 MPa.

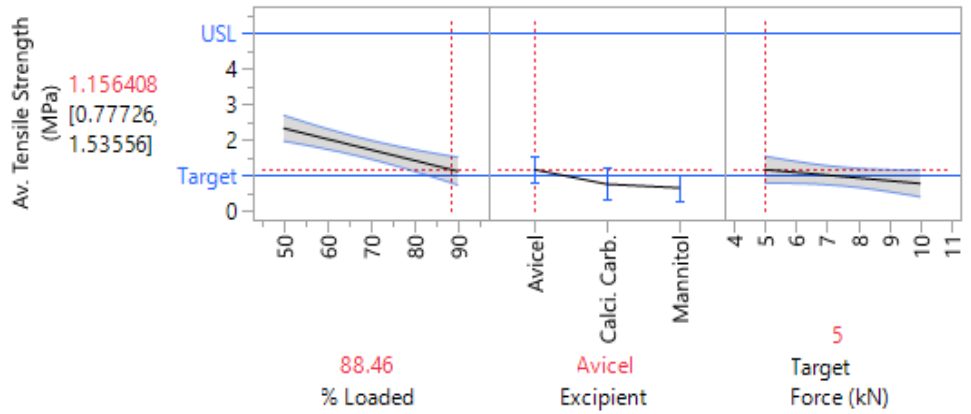


Figure 3.22 Prediction model for tensile strength

Figure 3.23 details a predicted plot for disintegration rate. The statistically significant terms in the model ( $P < 0.05$ ) are detailed in Figure 3.24 (the effect summary), the model showed that the most significant term identified was that of target force. It can be seen that these data points are not linear, the R-squared value is only 0.51 and therefore the ability of the model to accurately predict disintegration rate is limited. Other factors not measured (or yet identified but postulated earlier) are likely to influence the disintegration rate. Identification of other factors and their quantification would be required to be added to the model to improve accuracy.

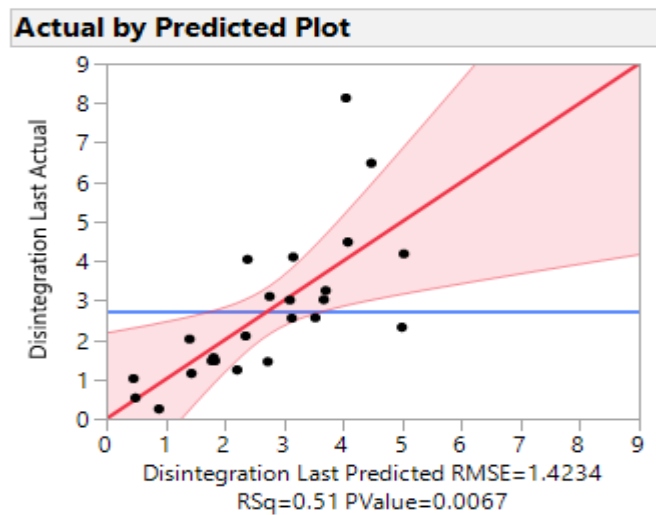


Figure 3.23 Predicted plot for disintegration rate (min)

### Effect Summary

Source	LogWorth		PValue
Target Force (kN)	2.829		0.00148
% Loaded	1.611		0.02447
Excipient	0.076		0.83934

Figure 3.24 Identified statistically significant input factors for disintegration rate prediction

### 3.6 Further Discussion and Conclusions

The primary aim of this chapter was to evaluate the influence of loading a type III lipid formulation on to Neusilin® US2, upon the characteristics of tablets produced. These findings would then determine the requirements for extra-granular excipient addition in attempts to produce robust tablets.

The data showed that increasing the concentration of SPc in the granules (higher loading levels) reduced the true density of the 'liquid granules'. Whilst not initially obvious, because both the tapped and bulk density were reported to increase; it can be concluded that the true density of the loaded Neusilin® US2 decreases as the liquid phase predominates and the pore volume decreases. In simple terms the liquid is less dense than that of solid (non-porous) Neusilin® US2. On a weight by weight basis as liquid concentration in a sample increases the true density therefore decreases as the relative concentration of porous material reduces.

The compressibility of the Neusilin® US2 was reduced with increased loading as expected. For future studies it may be interesting to determine tableting behaviour compared to that of other powdered binary mixtures. Sun (2016) established the tableting classification system (TCS) for binary mixtures, by compressing blends at fixed compression forces and determining the tensile strength of the tablets produced, to profile the various blends. Sun's study allowed the classification of binary blends to be considered for use with API's with known compression mechanisms, for the purposes of expediting formulation development studies. For formulators in the future it would be useful to understand how different lipid-based systems compared when loaded onto Neusilin® US2 at specific compression forces.

The tablets produced from the SPc loaded Neusilin®US2 (without additional compression aids), were not suitably robust (relatively low tensile strength, low friability and extended disintegration). At the highest loading level (90 %) tablets could not be produced at the

shortest dwell time (15 ms). Above 50 % loading levels, the 'liquid granules' exhibited strain rate sensitivity. Therefore, the addition of compression aid was warranted. When compared to LLW loading alone (Chapter 2), where tablets could be produced at higher loading levels; the data suggest that manufacturability/tabletability of a liquisolid formulation is likely to be influenced by the substrate to be loaded.

The addition of the 'extra-granular' excipients was found to improve tablet robustness (tensile strength and disintegration); however, friability was not improved at higher SPc loading levels as many tablets were found to fail (cap/laminate during testing). The poor friability is of concern and would limit the ability to scale up a formulation. It is important to understand the cause of friability, which has not yet been established. Not all tablets were affected in a batch and those that remained intact after testing did not show signs of chipping or abrasion (indicative of low tensile strength). The findings suggest that weak spots in tablets may be present and be due to more random factors, such as inhomogeneous distribution of materials during compression (such as liquid or lubricant rich 'pockets' within the tablet structure), air entrapment (Zavaliangos et al., 2017) or possibly due to structural damage to the tablet during ejection (Wu et al., 2008). The presence of LLW within the SPc could be considered as a potential reason, but since the concentration is relatively low at only 12% it is unlikely in this case and further investigation is necessary to understand the factor(s) behind poor friability.

Previous studies performed by Bejugam et al (2009), Reynolds et al (2017), Schmidtke et al (2017) and Vranikova et al (2016) used experimental design and multiple linear regression analysis to establish relationships between formulation components, compression parameters and the tablet characteristics successfully to aid formulation design. Nilesh and Kishor (2019) used JMP software to guide the formulation development and evaluation of a gastro retentive floating tablet. The use of JMP software to analyse and model the data allowed the identification of two key findings; firstly, the analysis showed that Avicel 200 LM was the most suitable compression aid for increasing tablet mechanical strength with increasing SPc loading. Secondly, the prediction profiler (Figure 3.22) showed that to achieve the maximum theoretical API loading within a tablet (highest % SPc loading), the lowest compression force was required. Compared to standard powder compression properties this phenomenon would not be expected. Increasing tensile strength with increasing force applied would be expected for a typical powder blend (Sun, 2016).

The data in Table 3.4 showed that without extra-granular excipient addition, viable tablets (tensile strength > 1 MPa, disintegration with 15 min and friability < 1.0) could not be produced from Neusilin loaded with SPc alone. Table 3.7 compares the formulations compressed containing the various SPc loading levels. The importance of maximising the loading level can be seen from the API content. An increase in relative API concentration (43 %) would be achieved if viable tablets could be achieved using 90 % loaded SPc compared to 50 % loaded SPc. The values in Table 3.7 assume 10 % w/w API loading in the SMEDDS preconcentrate formulation.

Table 3.7 Comparison of API content across loaded tablet formulations (target tablet weight 250 mg)

Component	50 % Loaded		70 % Loaded		90 % Loaded	
	mg/tablet	% w/w	mg/tablet	% w/w	mg/tablet	% w/w
API	7.0	2.8	8.7	3.5	10.0	4.0
SMEDDS Pc	63.0	25.2	77.8	31.1	89.5	35.8
Neusilin® US2	140.0	56.0	123.5	49.4	110.5	44.2
Compression aid	25.0	10.0	25.0	10.0	25.0	10.0
Super disintegrant	12.5	5.0	12.5	5.0	12.5	5.0
Lubricant	2.5	1.0	2.5	1.0	2.5	1.0

This investigation has shown that tablet disintegration problems associated with compression of SPc loaded Neusilin®US2 can be overcome using croscarmellose sodium at approximately 5 % w/w. At relatively low SPc loading levels < 70 % w/w suitable tablet friability (< 1 %) can be achieved at reduced tablet speeds (60 ms dwell time). However, ≥ 70 % SPc loading, tablet tensile strength and friability requires further improvement.

Whilst further dilution of the loaded ‘liquid granules’ with extra-granular excipient/compression aids would be an obvious step to improve tablet characteristics, dilution limits the API loading potential for this formulation type. Further understanding of several factors, including the influence of liquid distribution throughout the powder bed, the influence of dwell time, the influence of lubricant concentration and distribution upon tablet characteristics would all aid fundamental understanding further. Such characterisation studies as performed by Perez et al (2006) and Sune-Negre et al (2014) to develop expert systems (SeDeM diagrams) to fully characterise the properties of materials to assess compressibility potential/ranking would be useful. For liquid formulations however, such systems may prove limiting, not only due to the potential for variation in API properties and selected excipient variances in compaction mechanism, but to the potential combinations of excipients and concentrations that could be

considered when developing a SMEDDS formulation and their potential to influence tablet characteristics.

## Chapter 4.

### **An investigation into the distribution of SMEDDS preconcentrate in Lquisolid tablets using Raman Spectroscopy.**

#### **4.1 Introduction and aims**

The investigations reported in Chapter 3 found that liquisolid tablet characteristics (tensile strength and disintegration rate) could be improved through the inclusion of extra-granular excipients. However, friability was not improved at higher SMEDDS pre-concentrate (SPc) loading levels as many tablets were found to fail (cap/laminate) during testing (Section 3.5.2).

The cause of poor friability is not obvious, as not all tablets were affected in a batch and those that remained intact after testing did not show signs of chipping or abrasion (indicative of low tensile strength). As friability problems are likely to limit the potential for scale up, this investigation aimed to determine if inhomogeneous distribution of materials, namely the liquid SPc component occurred during compression.

The aim of this study was to understand the influence of compression force upon the distribution of the SPc adsorbed onto the carrier Neusilin®US2, during tablet formation. In simple terms, did the pressure applied, force the liquid out of the pores of the adsorbent to the surface (or specific sites within a tablet) or produce concentration gradients (variable density) throughout a tablet? If this phenomenon was shown, could it be determined that this factor influences tablet friability?

Previous studies have evaluated tablet density distributions using various analytical techniques. Physical methods such as indentation have been used to map variations in density across tablet surfaces and cross sections (Sinha, et al 2010). May et al (2013) evaluated the potential for Terahertz Pulsed Imaging (TPI) to be used for on-line tablet hardness determination, by correlation with tablet density. Djemami and Sinha (2006) evaluated the use of nuclear magnetic resonance imaging to map tablets impregnated with a liquid, to evaluate the influence of die wall friction and punch design upon density distribution within tablets. Ellison et al (2008) evaluated the use of near infra-red (NIR) imaging to produce density profiles for compacts of lactose monohydrate with differing amounts of lubricant; to identify the optimal concentration of lubricant within the formulation.

#### 4.1.1 Applications of Raman spectroscopy for tablet characterisation

In addition to the aforementioned techniques, Raman spectroscopy has also been used to characterise tablet homogeneity and map drug and excipient distribution (Scoutaris et al., 2014).

Zhu et al's review (2014) explains that Raman spectroscopy is based on the inelastic scattering of radiation by a sample, which can be a solid, liquid, or gas. In practice, two types of light scattering (elastic and inelastic) exist when an incident monochromatic light interacts with a molecule. During elastic scattering (Rayleigh scattering), there is no change in the frequency of the photon. The remainder is inelastic scattering (Raman scattering), which is accompanied by a shift in the photon frequency. The frequency difference between the scattered photons and incident photons is the Raman shift ( $\text{cm}^{-1}$ ), which includes vibrational information related to the molecules. Long (2002) described the detailed theory of Raman scattering stating that vibrational information is specific to chemical bonds, the atomic mass in the bond, the electronic environment, and the symmetry of molecules, so Raman spectroscopy provides a "fingerprint" that allows the qualitative analysis of individual compounds. Compared to Rayleigh scattering, Raman scattering is extremely weak; that is, the ratio of the Raman scattered intensity to that of Rayleigh scattering is typically  $10^{-6}$  for pure liquids, whereas for micrometer-sized particles in powder samples it may be as low as  $10^{-12}$ .

Paudel et al (2015) reported that spectral analysis of pharmaceuticals using Raman-based techniques presented some additional benefits over mid- or near-infrared (IR) spectroscopy. Because Raman spectroscopy is a scattering technique, there is no need for a reference light path (as needed for IR/NIR); therefore, it is amenable to fibre optics and allows for remote sampling. Higher lateral spatial and depth resolution is attainable by (confocal) Raman microscopy than by IR microscopy. In many ways, it is possible to characterize samples better than with Fourier-transform IR (FT-IR) spectroscopy. However, any possible fluorescence from the sample should be taken into consideration. A single scan of a typical Raman measurement can collect spectral data in the range of  $4000\text{--}40\text{ cm}^{-1}$ . In addition to the fingerprint region between  $4000$  and  $400\text{ cm}^{-1}$ , the low frequency or far IR region ( $400\text{--}40\text{ cm}^{-1}$ ) of Raman spectra covers some of the important vibration modes that are relevant for the identification of different solid-state forms. Johansson et al (2005), reported that Raman signal (intensity) was not impeded with increasing

compression force and therefore may be a suitable technique to evaluate distribution of SPc within liquid compact.

Raman Spectrophotometers generally consist of: (Renishaw, 2018)

- one or more single coloured light sources (lasers)
- lenses (both to focus the light onto the sample and to collect the scattered light)
- filters (to purify the reflected and scattered light so that only the Raman light is collected)
- a means of splitting the light into its constituent colours (normally a diffraction grating or prism)
- a very sensitive detector (to detect the weak light)
- a device such as a computer to control the whole system, display the spectrum and enable this information to be analysed

The aim of these studies was to investigate the distribution of SPc throughout loaded granules and tablets, to determine if compression force influenced distribution. Raman spectroscopy was used to determine:

- How uniformly the SPc had been distributed throughout the carrier in powder form.
- Whether the distribution of the SPc changed following compression of the powder into a tablet.
- Whether compression force influences SPc distribution within tablets.

## **4.2 Materials**

In addition to those materials detailed in Chapter 3 (Section 3.2), Dipyrindamole (>98 %) 2-[[2-[bis(2-hydroxyethyl)amino]-4,8-di(piperidin-1-yl)pyrimido[5,4-d]pyrimidin-6-yl]-(2-hydroxyethyl)amino]ethanol), batch number BCB14693, was purchased from Sigma Aldrich (UK). Dipyrindamole was added to the SPc formulation as a model drug, to evaluate the distribution of the API in both the granules and tablets characterised.

## **4.3 Methods**

### **4.3.1 SMEDDS preconcentrate preparation**

Samples were prepared as per Section 3.3.1

#### 4.3.2 Carrier loading (SPc)

Neusilin®US2 was loaded with SPc as per Section 3.3.2

#### 4.3.3 Dipyridamole SMEDDS preconcentrate (DSPc) preparation

Dipyridamole was added to the SPc formulation at a concentration of 30 mg per g originally used by Guo et al (2011), see Table 4.1. Dipyridamole was dissolved in IPA using a spatula. LLW and Solutol HS15 were dispensed into a glass beaker and heated at 65°C on a hotplate for 15 min with occasional stirring, until a homogenous liquid formed. Oleic acid [was added to the mixture, the liquid stirred using an overhead stirrer (IKA Eurostar 20, Germany) and 3 blade propeller to mix until visibly homogenous. The mixture was left to cool with occasional stirring until < 30°C. The dipyridamole/IPA mixture was then added to the liquid and mixed for 10 min at 700 rpm.

Table 4.1 Dipyridamole SMEDDS Preconcentrate formulation

Material	% w/w
Dipyridamole	2.91
Labrafac Lipophile WL1349	11.65
Solutol (Kolliphor) HS	40.78
Oleic Acid	17.48
Isopropyl Alcohol	27.18

#### 4.3.4 Carrier loading of DSPc

Carrier loading of DSPc was performed as per section Chapter 3 section 3.3.2.

#### 4.3.5 Compaction

Tablets were produced using the Stylcam® 100R simulator (Medelpharm, France), see Chapter 1 section 1.3. The simulator was fitted with 11.0 mm flat faced tooling and using the 'direct cam' rotary press profile. The die was filled manually prior to compression. A range of compaction forces from 1 (kN) to 20 (kN) were applied. The target tablet weight was 250 mg. A press speed of 5 TPM (60 ms dwell time) was used.

#### 4.3.6 Raman Analysis of Samples

Raman analysis was performed on selected powder and tablet samples, using a RA802 Pharmaceutical Analyser (Renishaw, UK). Prior to use the machine was calibrated. Firstly, calibration of the spectrophotometer was performed using in internal neon lamp standard at 12047.72cm<sup>-1</sup>, 10961.35cm<sup>-1</sup> to calibrate the

wavelength positions. Secondly, a silicon target was used on the sample stage to test the intensity and width vs. target ranges; to check system throughput and resolution were within the expected ranges. The position of the silicon band (default value 520.4  $\text{cm}^{-1}$ ) is used to calibrate the Raman shift (effectively determining the absolute wavelength of the Raman laser to establish the Raman shift value).

Powder samples were spread across a polished steel well slide and tablet samples were mounted in polished steel tablet holders for analysis. For all samples the laser wavelength used was 785 nm.

Raman mapping collects a spectral hypercube (a Raman spectrum from each position on the sample in a single file), rather than a simple intensity image. The hypercube is analysed to produce Raman images (Renishaw, 2018). Raman images (sometimes referred to as maps) depict a variation in spectral information from different points on a sample. A Raman spectrum is a plot of the intensity of Raman scattered radiation as a function of its frequency difference from the incident radiation (usually in units of wavenumbers,  $\text{cm}^{-1}$ ). This difference is called the Raman shift. Note that, because it is a difference value, the Raman shift is independent of the frequency of the incident radiation ([www.kosi.com](http://www.kosi.com), 2020).

Focus tracking was performed using the automated 'LiveTrack' system of the machine, which maintains focus automatically in real time during data collection (Renishaw, 2018). The objective was set at 50xL, the mapped area, step size and total spectra captured were subject to the sample under analysis. Data were collected and images produced using 'Streamline imaging' specific to the RA802 analyser, which uses line illumination for rapid, 2D mapping of samples. The laser illuminates a line on the sample, rather than a spot. 'Streamline imaging' allows the simultaneous collection of spectra from multiple positions on a sample. It allows the use of higher laser powers without damaging the sample (Renishaw, 2018).

## 4.4 Results and Discussion

### 4.4.1 Raman Analysis of Neusilin®US2 loaded with SPc.

To evaluate the distribution of SPc in Neusillin® US2 powder post loading, samples were analysed using the RA802 pharmaceutical analyser. Figure 4.1 shows a sample *in-situ* prior to analysis and the area selected to be analysed.

Due to limited access to the system minimising the number of samples that could be evaluated, the sample was run using ‘empty modelling component analysis’ (EMCA). EMCA reveals systematic variations between the Raman spectra, and highlights the distribution of these variations across the sample as an image. This is achieved without the need for prior knowledge of what is present within the sample (Renishaw, 2018). Comparison of the materials identified in the sample was performed against the library (Renishaw’s archive) of previously characterised materials. Renishaw’s archive is a database of materials previously analysed to allow comparison of spectra to be performed.

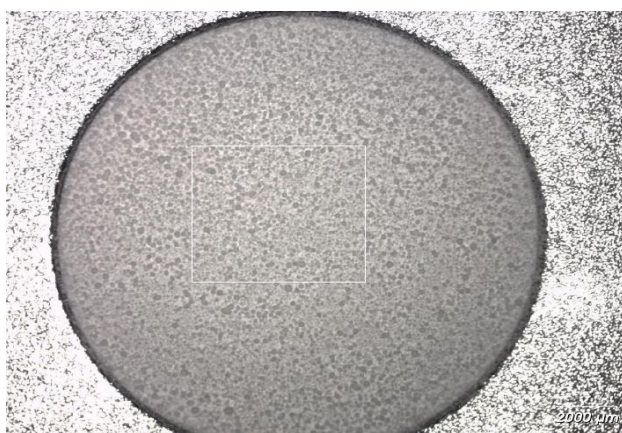


*Figure 4.1 Macro white light view showing 70% w/w loaded Neusilin®US2 powder in a well slide, with analysed area highlighted in white*

Figure 4.2 shows the Raman spectra generated for a sample of 70 % SPc loaded Neusilin® US2. The red line corresponds to the ‘empty modelling component’ which describes the majority of the mapped dataset. All other spectra shown and detailed in Figure 4.2, are library materials with similar spectra. The mapped area (area of sample analysed) was 5.8 mm x 5.0 mm, the step size 15 μm (spacing between acquisition points on the sample) and total spectra captured (number of acquisition points taken across the sample) was approximately 130,000.

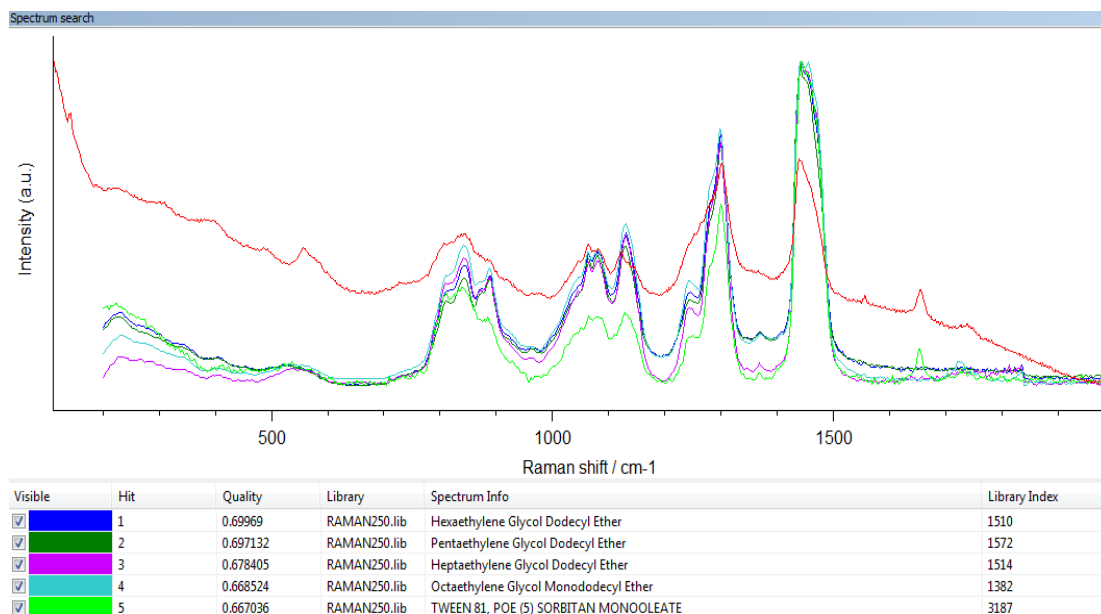


Figure 4.2 Raman spectra for 70 % SPC loaded Neusilin®US2 using empty modelling component analysis. Red indicates the SPC. All other lines relate to library components.

A Raman image of 70 % SPC loaded Neusilin®US2 is shown in Figure 4.3.

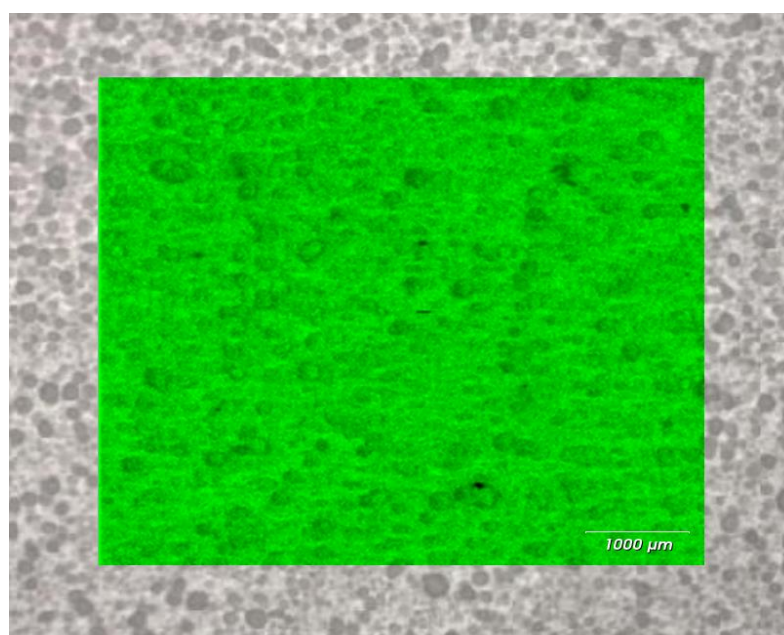


Figure 4.3 Raman image of 70 % SPC loaded Neusilin®US2

Both Figures 4.2 and 4.3 only show one component visible in the Raman spectra and Raman image respectively which appears to be evenly distributed in the sample. The change in colour density in Figure 4.3 correspond to changes to topography rather than another component. It would be expected that at least 2

spectra would be produced from the samples, relating primarily to the carrier (Neusilin® US2) and secondary to the SPc or constituents of the SPc (see Table 3.1, Chapter 3). The similarities in spectrum to the library materials (hexaethylene glycol dodecyl ether to octaethylene glycol ether) is likely attributable to the LLW in the SPc formulation; the LLW essentially comprising of medium chain triglycerides (C<sub>6</sub> to C<sub>12</sub>).

It appeared that Neusilin® US2 gave little response (effectively little vibrational change resulting in little light scattering following excitation) resulting in no specific spectrum detected. Scoutaris et al (2014) reported that Neusilin® US2 displays a characteristic although poorly responsive band at 474 cm<sup>-1</sup> but otherwise no response/bands were detected; this supports the likelihood that the spectrum produced in Figures 4.2 and 4.3 was attributable to the SPc component.

#### 4.4.2 Raman Analysis of the surface(s) of tablets consisting of Neusilin®US2 loaded with SPc.

The surface of tablets were analysed to determine if a gradient of SPc could be determined following compression. Figure 4.4 shows a tablet loaded with 50 % SPc *in-situ* prior to analysis and the area selected to be analysed.



Figure 4.4 Macro white light view showing analysed area of tablet containing 50 % loaded SPc.

Figure 4.5 shows the Raman spectra generated for the 50 % SPc loaded tablet. The empty modelling component analysis was again utilised, and two separate spectra were generated. The top section corresponds to SPc (black) and a library spectrum Pentaethylene glycol dodecyl ether (green). The bottom spectra (blue) matches closely to the library spectra for lactose (red) and suggested that the

sample was contaminated. The source of the contamination is unknown; however, samples were prepared in an open laboratory where lactose was being used in other studies. Airborne cross contamination could not be ruled out. The mapped area was 3.37 mm x 3.5 mm, the step size 5  $\mu\text{m}$  and total spectra captured was approximately 472,000.

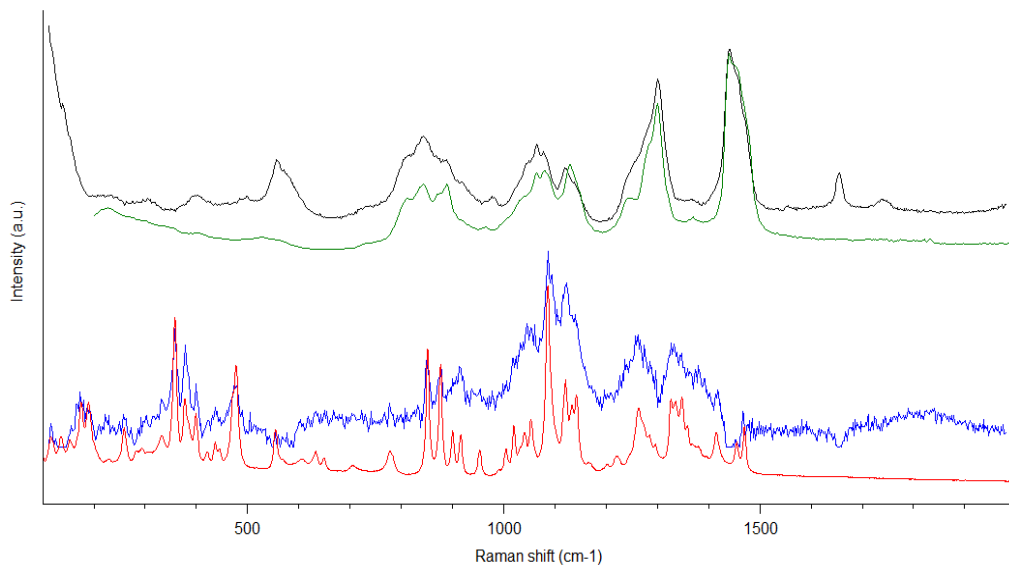


Figure 4.5 Raman spectra for 50 % SPC loaded Neusilin®US2 using empty modelling component analysis compressed at 1 kN applied force. SPC (black), Pentaethylene glycol dodecyl ether (green), contaminant (blue) and lactose (red)

Figure 4.6 shows the Raman images of the two components on the surface of a tablet containing 70 % SPC loaded Neusilin® US2. The SPC (green) is shown on the image on the left and the suspected contaminant lactose (red) on the image on the right.

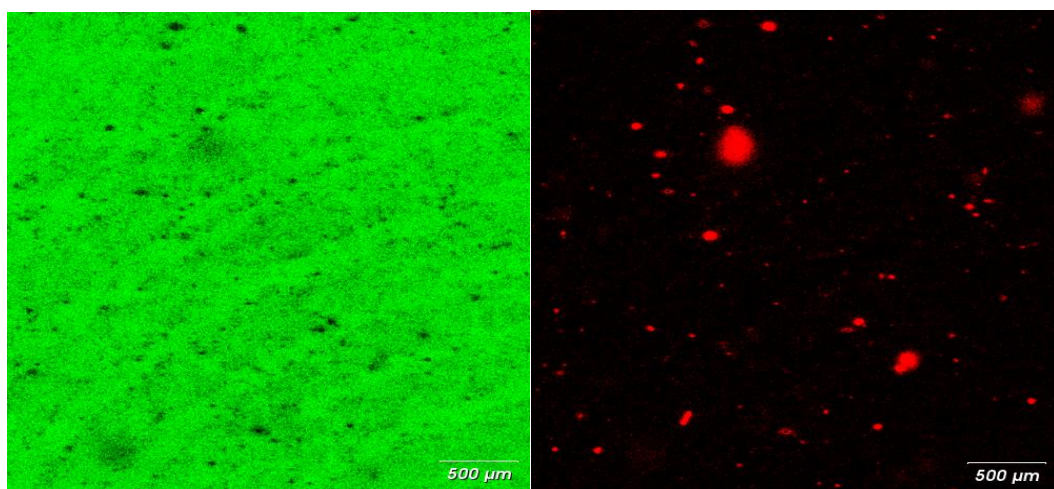
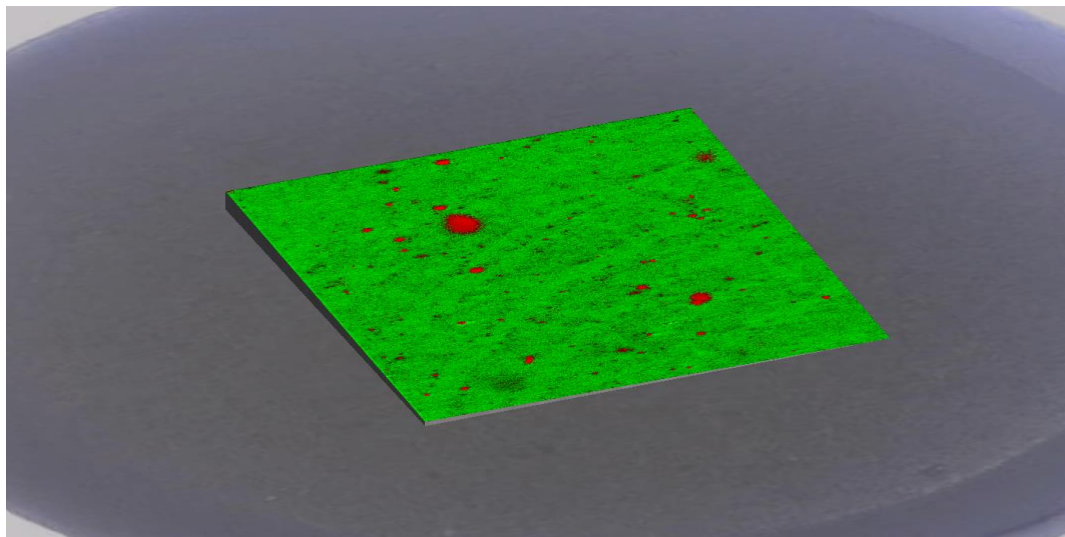


Figure 4.6 Raman image of 70 % SPC loaded Neusilin®US2, left distribution of SPC, right distribution of lactose/contaminant.

Figure 4.7 shows the distribution of the two components on the surface of the tablet.



*Figure 4.7 Overlaid 3D Raman image of Empty Modelling components SPc (green) and 4 (lactose/contaminant, red) at tablet surface (exterior).*

Figures 4.6 and 4.7 show the presence of spatial variations in SPc distribution in terms of colour intensity which indicate striations of variable density are present.

The same process was repeated but analysing the inside surface of the 1 kN tablet. The inside surface of the tablet was prepared using a micro-plane to finely cut the tablet. The mapped area was 4.68 mm x 51.7 mm, the step size 10  $\mu\text{m}$  and total spectra captured was approximately 212,000. Figure 4.8 shows the distribution of the two components on the inner surface of the tablet.

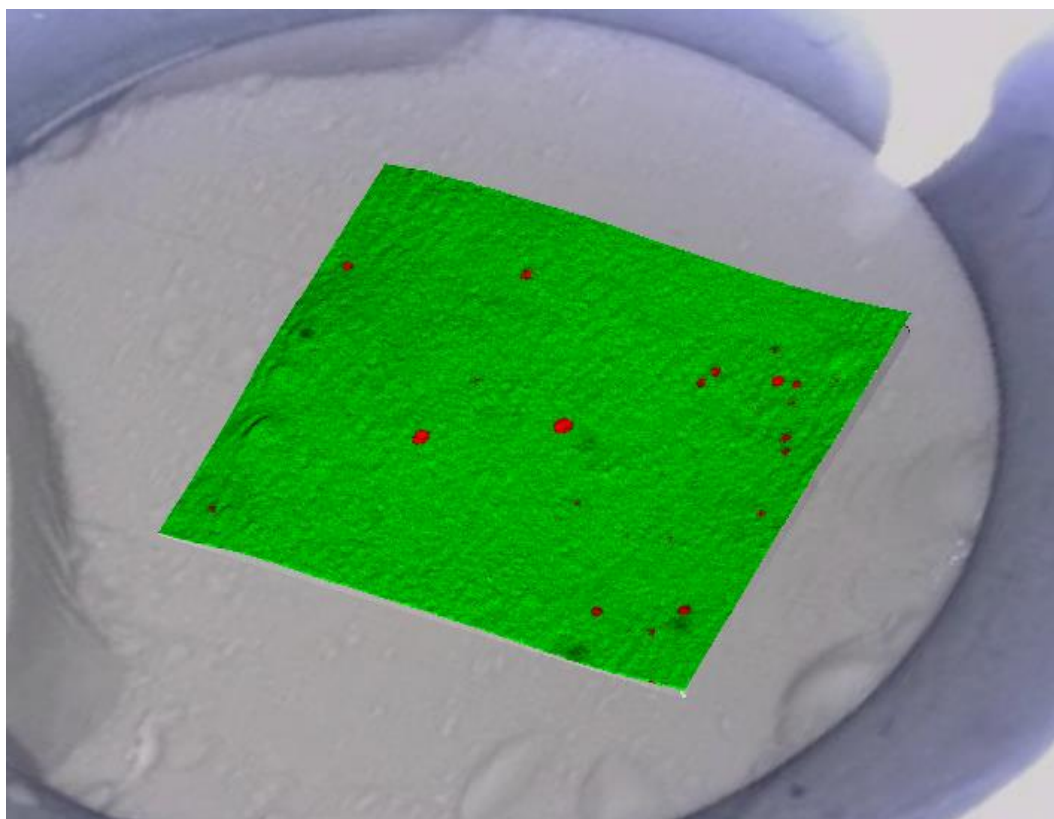


*Figure 4.8 Overlaid 3D Raman image of Empty Modelling components SPc (green) and 4 (lactose/contaminant, red) at tablet surface (inner).*

Unlike Figures 4.6 and 4.7, Figure 4.8 does not exhibit spatial variation which suggests a more uniform distribution of SPc within the tablet compared to the surface, although it should be considered that micro-planing of the tablet may result in a modified surface effect which influences the apparent distribution.

These early evaluations showed that extraction of a Raman spectrum from the Neusilin®US2 powder was difficult as it did not give a strong Raman response. Samples containing 50% and 70% pre-concentrate showed a uniform distribution of SPc in 'granules'. The analysis of the outer surface and inner surface of the 50 % loaded tablet showed that there appeared to be a difference in spatial distribution (density of SPc) at the surface compared the centre of the tablet which appeared to be more uniform, (although this may be a function of the surface preparation). Due to the relatively high concentration of SPc in the samples and the poor response from Neusilin® US2 which failed to provide a contrast against which the SPc distribution could be compared, it was decided to add an additional component to the SPc formulation (the API dipridamole) to enhance the potential for material detection and to evaluate distribution.

#### 4.4.3 Raman Analysis of 'granules' consisting of Neusilin®US2 loaded with DSPc.

Dipyridamole was chosen as an API known to provide a Raman response, (Arnold et al, 2011) and was included at a relatively low concentration relative to the other components within the formulation, to show clear concentration gradients in the event of variable density regions within the tablets.

Figure 4.9 shows 'granular samples' of Neusilin®US2 loaded with 50 % and 90 % DSPc respectively, prior to analysis. The mapped areas were approximately 2.5 mm x 2.0 mm, the step size 10 µm and total spectra captured was approximately 51,000.

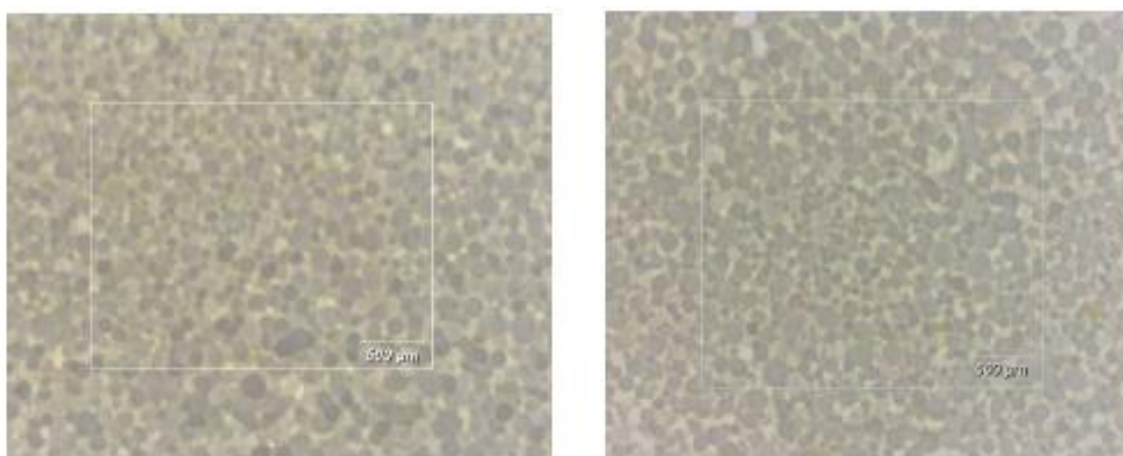


Figure 4.9 Macro white light views showing 50% w/w DSPc loaded Neusilin®US2 powder (left) and 90 % loaded powder (right), with analysed areas highlighted in white.

Figure 4.10 shows Raman images of 'granular samples' of Neusilin®US2 loaded with 50 % and 90 % DSPc respectively. It was not possible to quantify the concentration of dipyridamole in a specific area; however, the colour scale is representative of concentration. In both samples, distinct areas of 'high concentration' of dipyridamole were present. The relative overall concentration of dipyridamole is higher in the 90 % loaded samples as would be expected as 1.8 times the quantity of dipyridamole was added due to the increased loading level (90 % loaded versus 50 % loaded on weight by weight basis).

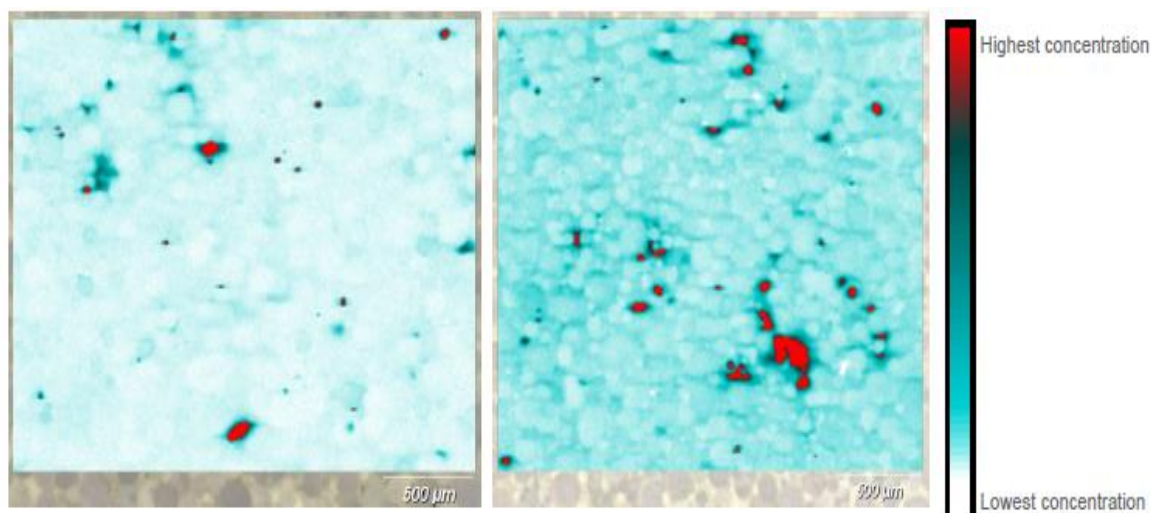


Figure 4.10 Raman image(s) of 50% w/w DSPc loaded Neusilin®US2 powder (left) and 90 % loaded powder (right) concentration of Dipyridamole indicated from white to red.

The observation that areas of high concentration of dipyridamole are present in the powders is interesting and useful to understand. This observation may be attributable to two factors. Firstly, areas of high concentration may be attributable to the simple loading method used to produce the ‘granules’. Whilst it was not obvious that inhomogeneous samples had been produced, (samples were free flowing, granules passed through a 1 mm sieve with ease and no residues found on the mesh post transfer), the loading method may require improvement to ensure granule homogeneity. Secondly, the increased concentration may be attributable to crystallisation of dipyridamole from the SPc formulation. It was not possible to further evaluate the samples using alternative methods such as differential scanning calorimetry (DSC) or X-ray powder diffraction (XRPD) to determine the crystallinity of the dipyridamole present. However, for future studies both these factors should be considered as part of the loading strategy.

#### 4.4.4 Raman Analysis of the surface(s) of tablets consisting of Neusilin®US2 loaded with DSPc.

Tablet samples (both outer surfaces and cross section) were analysed for dipyridamole. Cross sections were prepared by collecting tablets following breaking force determination. Figure 4.11 shows images of a tablet containing 50 % DSPc prior to measurement of an outer surface (left) and a cross section (right).

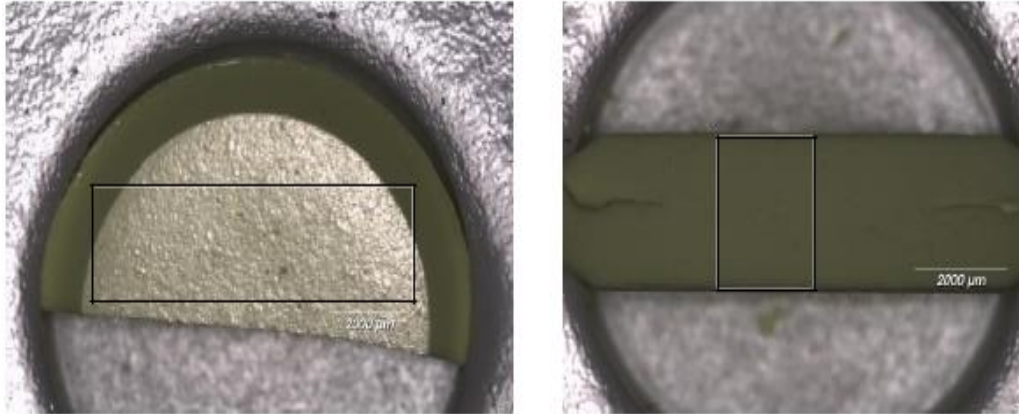


Figure 4.11 Macro white light view showing analysed area of tablet containing 50 % loaded DSPc outer surface (left) and cross section (right)

Figures 4.12 and 4.13 show Raman images of an outer surface and a cross section of tablet containing 50 % DSPc respectively. The images appear very similar in terms of distribution of dipyridamole and whilst ‘pockets’ of high concentration can be seen, there is no obvious increase in number of pockets or distribution of pockets whether at the surface or at the cross section of the tablet.

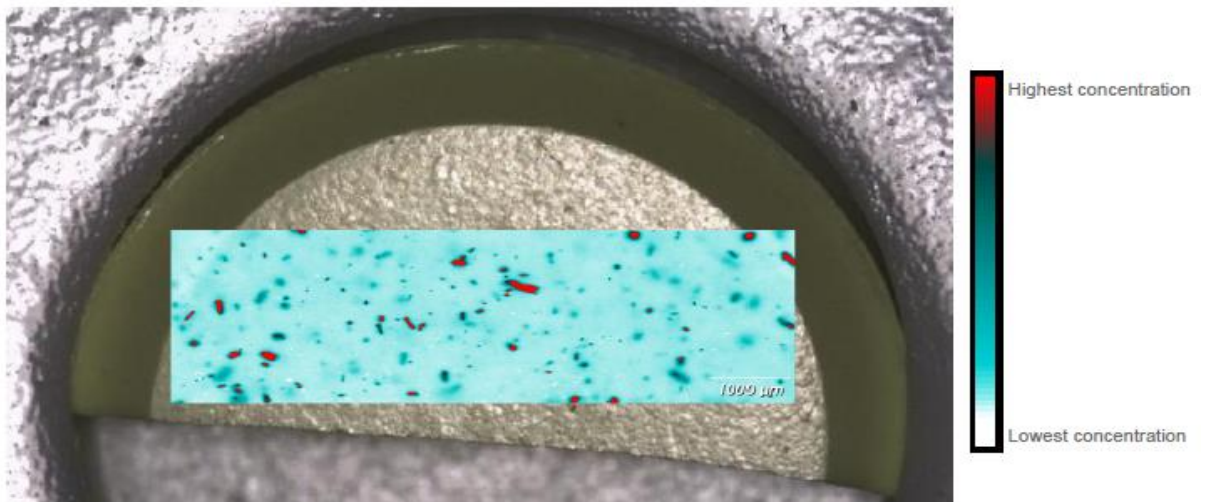


Figure 4.12 Raman image of outer surface 50% w/w DSPc loaded Neusilin®US2 tablet, concentration of Dipyridamole indicated from white to red.

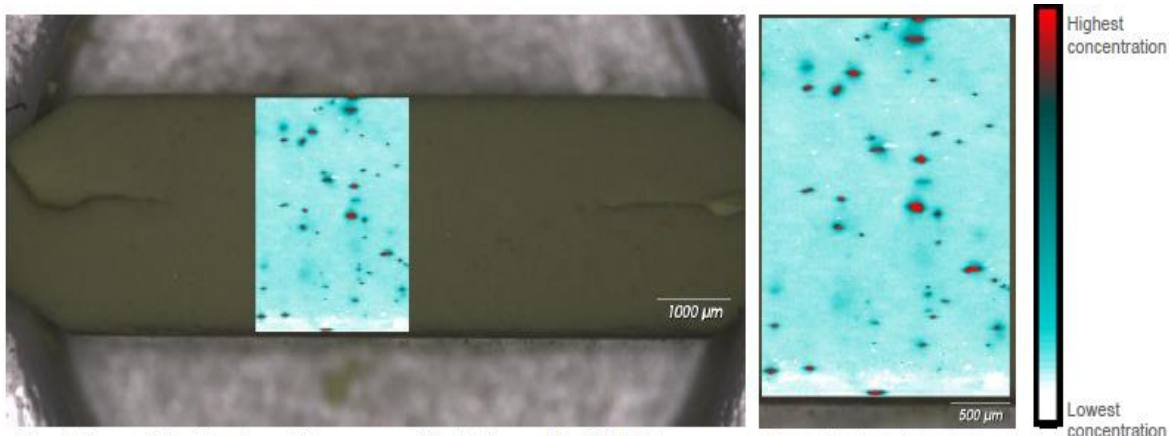


Figure 4.13 Raman image of cross section of 50% w/w DSPc loaded Neusilin®US2 tablet, concentration of Dipyridamole indicated from white to red

Figures 4.14 and 4.15 show Raman images of an outer surface and a cross section of tablet containing 90 % DSPc respectively. Like Figures 4.12 and 4.13 the images appear very similar in terms of distribution of dipyridamole and whilst 'pockets' of high concentration can be seen, there is no obvious increase in number of pockets or distribution of pockets whether at the surface or at the cross section of the tablet.

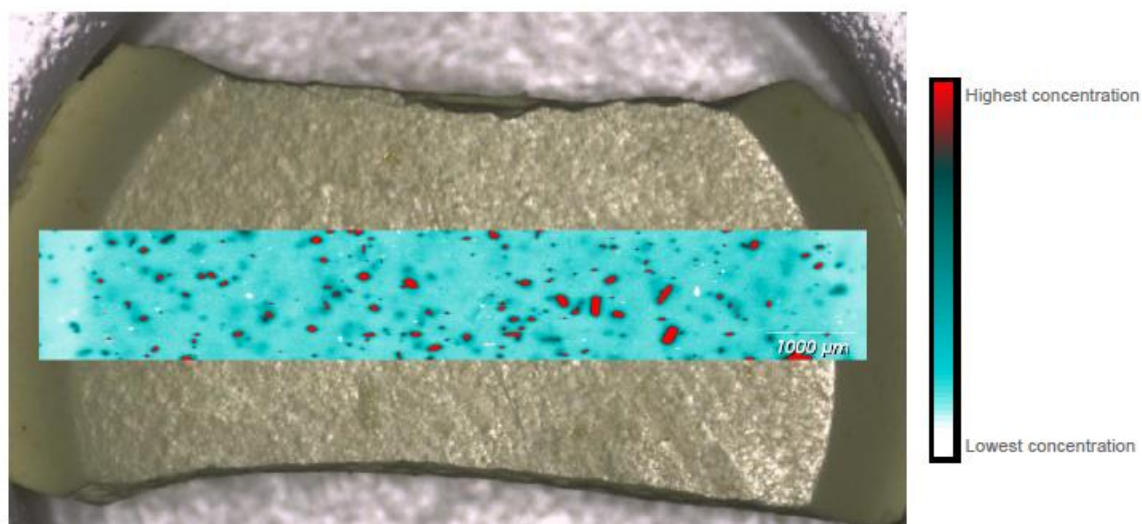


Figure 4.14 Raman image of outer surface 90% w/w DSPc loaded Neusilin®US2 tablet, concentration of Dipyridamole indicated from white to red.

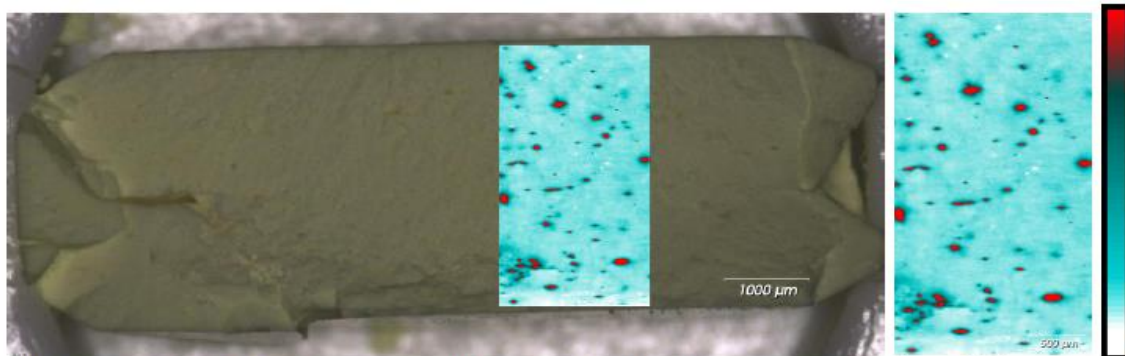


Figure 4.15 Raman image of cross section of 90% w/w DSPc loaded Neusilin®US2 tablet, concentration of Dipyridamole indicated from white to red. Magnification of blue area detailed o cross section is shown on the right.

Figures 4.16 and 4.17 show comparisons of outer surface images and cross-sectional images for the 50 % and 90 % DSPc loaded tablets respectively. When compared, the distribution of dipyridamole is not homogenous in both tablets, neither at the surfaces nor across the sections. However, the inhomogeneity appears to be consistent between both loaded samples (50 % loaded and 90 % loaded respectively). The relative size of the ‘pockets’ of concentrated dipyridamole between the loaded samples is similar, up to 500 micron length in both samples; this finding does not suggest a ‘mass movement’ of liquid during compression or partitioning effect of the liquid and powder during compression, the liquid does not appear to move to the outer surface (or specific areas) of the tablet. These observations suggest that the concentration gradients (pockets) captured in the images at the surface/cross section are a result of the starting material rather than the compression process.

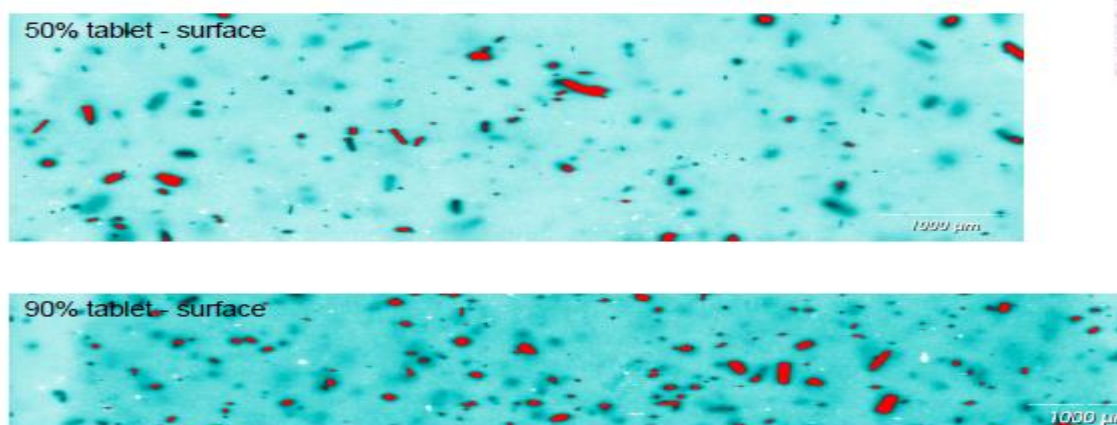


Figure 4.16 Raman image of outer surface 50% w/w DSPc loaded Neusilin®US2 tablet (top), outer surface 90% w/w DSPc loaded Neusilin®US2 tablet (bottom) concentration of Dipyridamole indicated from white to red.

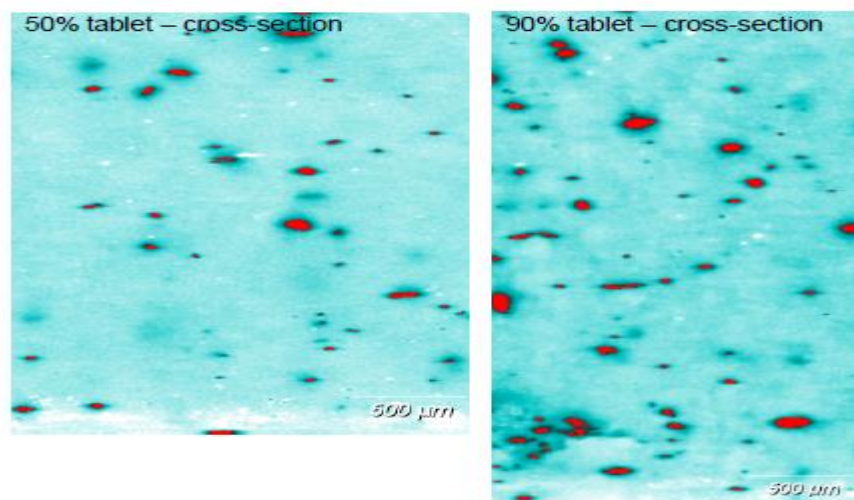


Figure 4.17 Raman image of outer surface 50% w/w DSPc loaded Neusilin®US2 tablet (top), outer surface 90% w/w DSPc loaded Neusilin®US2 tablet (bottom) concentration of Dipyridamole indicated from white to red.

Figures 4.18 and 4.19 show comparisons of outer surface images and cross-sectional images 90 % DSPc loaded tablets, compressed with increasing applied force. As per Figures 4.14 and 4.15, no obvious difference in concentration or increase in 'pocket' size can be seen at either the surface or across the cross section of the tablets, according to the force applied.

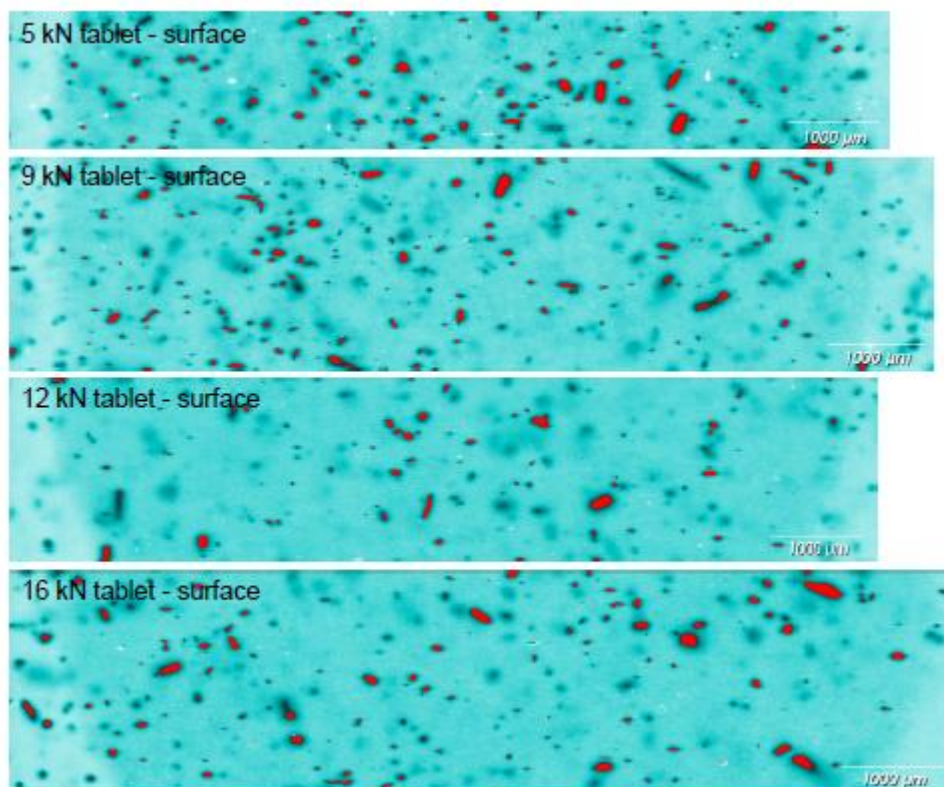


Figure 4.18 Raman image of outer surfaces of 90% w/w DSPc loaded Neusilin®US2 tablets compressed at 5 kN, 9 kN, 12 kN and 16 kN compression force (as indicated from top to bottom of figure), concentration of Dipyridamole indicated from white to red.

A 'vein' can be seen in Figure 4.19, which is attributable to the topography of the surface when split to reveal the cross section.

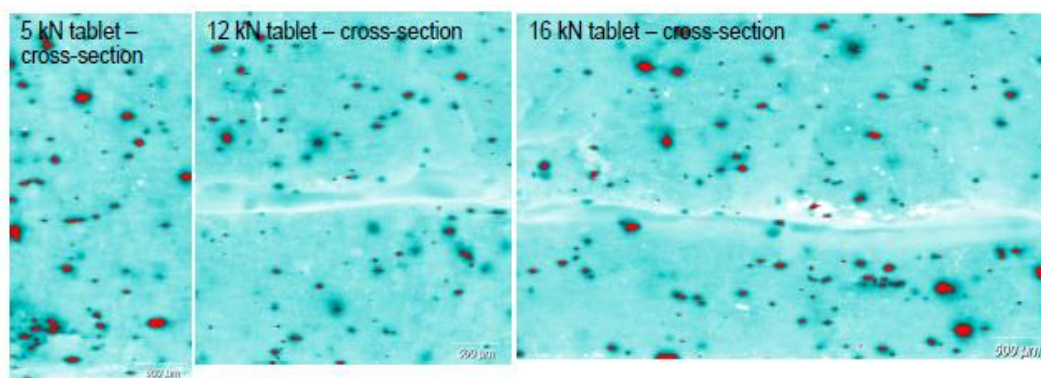


Figure 4.19 Raman image of outer surfaces 90% w/w DSPc loaded Neusilin®US2 tablets compressed at various compression forces (as indicated), concentration of Dipyridamole indicated from white to red.

#### 4.5 Further Discussion and Conclusions

The RA802 Pharmaceutical Analyser was used to assess a range of samples loaded with SMEDDS preconcentrate (SPc and DSPc) including loaded granules and tablets compressed over a range of applied forces.

The adsorbent Neusilin® US2 did not generate a suitable Raman spectrum and therefore could not be analysed effectively. Previous studies performed by Scoutaris et al (2014) reported a similar finding. The SPc formulation could be detected and was shown to be evenly distributed throughout tablet samples, however it was difficult to determine quantifiable differences in concentration across the samples due to the high concentration of preconcentrate in the sample and the lack of contrast against the undetectable Neusilin® US2.

The inclusion of dipyridamole at a relatively low concentration allowed a qualitative assessment of dipyridamole distribution within the loaded granules. Characterisation of the granules at both loading levels (50 % and 90 %) showed a lack of dipyridamole homogeneity. This inhomogeneity may be attributable to crystallisation of the API out of the pre-concentrate solution during loading or to poor distribution of the DSPc during loading resulting in areas (pockets) of high concentration of liquid containing dipyridamole. Visual comparison of size distribution of the pockets was similar irrespective of loading level. However, the quantity of pockets increased proportionally with DSPc loading. These observations suggest that the loaded granules prior to compression were inhomogeneous and of variable density, whether due to pockets of liquid or crystalline dipyridamole. The Raman technique therefore appears to be useful for characterisation of the starting granules prior to compression to determine sample homogeneity.

The findings suggest that improvements to the method of loading may be necessary to improve granule homogeneity. Such improvements could be made through a reduction in sieve size (< 1 mm) to reduce granule size, or an increase in loading temperature to reduce SPc viscosity and to increase spreading potential, or by spraying the SPc onto the carrier with a reduced droplet size. Raman spectroscopy could be a technique to quantify distribution of known constituent(s) in a granule/blend; where quantification could be done through the construction of a calibration curve(s).

Analysis of the tablet samples showed similar findings to that of the granule analysis in terms of 'pocket' distribution and size, which was proportional to the loading level. There were no apparent changes in dipyridamole distribution which would be indicative of liquid mass movement during compression, with increased loading level or increased applied

compression force, compared to that of the starting granules. The concentration of 'pockets' within the samples increases with increasing SPc loading. In 3D terms this phenomenon is likely to increase tablet matrix tortuosity, which in turn results in lack of ordered structure and reduced potential for bond formation in the tablet, leading to reduced tensile strength and friability with increased loading level.

The aim of this study was to understand the influence of compression force upon the distribution of the SPc adsorbed onto the carrier Neusilin® US2, during tablet formation. It was considered that variable density was likely to be a factor in tablet friability, as reported in Chapter 3. Whilst this study was not been able to show density gradients in the tablets tested as a result of the compression process (increasing applied force) as has been shown using other analysis techniques (Ellison et al., 2008; Sinha et al., 2004), it has shown inhomogeneity within the granules prior to compression which had not previously been obvious.

For future studies, Raman spectroscopy could be a valuable tool for granule characterisation and process optimisation. Where the influence of parameter changes to the loading method could be quantified in terms of homogeneity (% w/w) within a specific sample size and specific spatial measurements could be used to determine 'pocket size' to quantify improvements in uniformity. Such measurements could be obtained by other techniques such as assay and particle size analysis, however as a non-destructive simple technique Raman could be a useful tool for the formulator in terms of speed of result and minimal preparation requirements. In addition, the use as thermal techniques such as DSC Demetzos, C. (2008) or XRPD, Siddiqui et al (2015) should be considered to characterise the form of API present within the granule. Changes in API form, particularly during stability may influence *in vitro* release rate from the drug product (formulated tablet) therefore is critical to establish and monitor.

## Chapter 5.

### “Evaluation of sorbent properties post-loading with Gelucire®44/14 and Vitamin E TPGS”

#### 5.1 Introduction and aims

The investigations reported in Chapter 3 found that tablet tensile strength and disintegration rate could be improved through the inclusion of extra-granular excipients. However, friability was not improved at higher SPc loading levels as many tablets were found to cap/laminate during testing. As friability problems are likely to limit the potential for scale up, this investigation aimed to determine if alternative excipients would confer improved compressibility and generate tablets with reduced friability.

To evaluate the influence of alternative excipients upon sorbent properties, post loading, and the characteristics of tablets produced; Gelucire® 44/14 (GEL) and Vitamin E TPGS (TPGS) were selected. As previously mentioned in Section 1.1.4, GEL and TPGS have been used in many lipid-based formulations for bioavailability enhancement in both Type III lipid formulations but also have the potential to be used as standalone excipients for Type IV lipid formulations (Pouton, 2007).

Gelucire® 44/14 (lauroyl polyoxyl-32 glycerides; GEL) is an inert semi-solid waxy material with a melting point of 44 °C and an HLB value of 14. It comprises of short-, medium-, and long-chain fatty acid esters and forms an exceptionally stable, fine dispersion when in contact with the GI fluids at body temperature (Shin, 2019). Various investigations have evaluated the employment of GEL to improve the dissolution rate and bioavailability of numerous water-insoluble drugs, such as Valsartan (Shin et al., 2019), Carbamazepine (Antunes et al., 2013), Phenytoin (Massik et al., 2003) and Panigrahi’s review of Gelucire for modified release drug delivery systems (2018) provides further specific examples. Antunes et al (2013) reported problems with API release from tablet and monolithic forms of Gelucire® 44/14.

Vitamin E d-alpha tocopheryl polyethylene glycol succinate (Vitamin E TPGS) is a non-ionic surfactant, waxy solid with a low-melting point (37°C). Synthesized by esterification of vitamin E succinate with polyethylene glycol (PEG) 1000, it is a water-soluble derivative of natural vitamin E. It has an amphiphilic structure comprising a hydrophilic polar head portion and lipophilic alkyl tail (Yang et al, 2018). TPGS presents the possibility of tableting challenges especially when incorporated in the formulation at a high concentration

(Pandey et al, 2012). Jin and Tatavarti (2010) demonstrated the feasibility of developing tablet dosage forms with TPGS wet granulation formulations. However, the TPGS levels in these formulations were only 10 % w/w and the results indicated that the level of TPGS was the most significant formulation variable.

In addition to evaluating these excipients to improve tablet characteristics, the *in vitro* release rate of dipyridamole as a model drug from the tablets produced was also assessed. Studies by Speybroeck et al (2012) and Williams et al (2014) reported that adsorbing lipid formulations to high-surface area adsorbents such as Neusilin® US2 may result in decreased performance when compared with equivalent liquid formulations. Williams et al (2014) found though that by increasing the hydrophilicity and quantity of surfactant in a formulation provided a means to enhance desorption from Neusilin® US2, although desorption was incomplete in all cases.

Dipyridamole was selected as the model drug following on from the investigations reported in Chapter 3 and the distribution studies reported in Chapter 4. Dipyridamole is a weak base with a pKa value 6.4. Its water solubility is strongly dependent on the pH of different digestive fluids (Guo et al., 2012). Dipyridamole dissolves readily in the stomach but poorly in the intestine, solubility decreases with increasing pH as would be expected for a weak base.

The aim of these studies was therefore to evaluate:

- The influence of Dipyridamole GEL (D-GEL) and Dipyridamole TPGS (D-TPGS) mixtures when loaded, upon the characteristics of Neusilin® US2.
- The influence of D-GEL and D-TPGS upon the compression characteristics of Neusilin® US2 and physical properties of the tablets produced.
- The in-vitro release rate of dipyridamole from tablets produced and the influence of compression force upon release rate.

## 5.2 Materials

In addition to those materials detailed in earlier Chapters, Gelucire® 44/14 (lauroyl polyoxyl-32 glycerides) batch number 164108, was provided free of charge from Gattefosse, France. Vitamin E TPGS 100 (Vitamin E d-alpha tocopheryl polyethylene glycol succinate), batch number 01100092, was purchased from Isochem, UK.

## **5.3 Methods**

### **5.3.1 Dipyridamole/Molten carrier preparation**

The method of preparation was the same using either GEL or TPGS. The dispersions were prepared at a concentration of 30 mg of dipyridamole per 1g of molten carrier, as previously described in Section 4.3.3.

GEL/TPGS were heated at 60 °C overnight in an oven (Genlab, UK). Dipyridamole was dispersed into the molten carrier using a homogeniser (Silverson SL2T, UK) set at 9,000 rpm for 20 min, whilst maintaining the temperature of the mixture at 60 °C using a hotplate (Stuart US, Cole Palmer, UK.).

### **5.3.2 Carrier loading of Neusilin®US2**

Neusilin® US2 was heated in an oven details to 50 °C then added to a jacketed glass vessel details attached to a re-circulating water bath (Haake W19, UK) set at 60 °C. The Neusilin®US2 powder was stirred using a 3-blade paddle and overhead stirrer (IKA Eurostar 20, Germany) at 400 rpm. The molten mixture (Section 5.3.1) was added dropwise via a syringe (over 2 min). Following complete addition of the lipid the mass was mixed for a further 1 min at 600 rpm, prior to sieving via both 2 mm and 1 mm screens (Endecotts, UK). A weight of 50 % relative to the dry adsorbent weight was used as the starting point for loading of the molten mixture to the adsorbent. Thereafter, additions were made at 20 % increments relative to the dry adsorbent weight up to a maximum of 90 %.

### **5.3.3 Tapped and bulk density determination**

As detailed in Section 2.3.1. Samples were tested in triplicate.

### **5.3.4 True density determination**

As detailed in Section 2.4.3. Samples were tested in triplicate.

### **5.3.5 Flow through an orifice**

As detailed in Section 2.4.4. Samples were tested in triplicate.

### **5.3.6. Blend preparation**

Blends were prepared by adding the loaded granules to a 500 mL HDPE (Duma, Germany) followed by the super disintegrant. The container was sealed and

inverted end over end 100 times. The lubricant was sieved (through a 250 µm screen), then added to the granule mixture. The container was sealed and inverted end over end a further 50 times.

### **5.3.7 Compaction**

Tablets were produced using a Stylcam® 100R simulator (Medelpharm, France) fitted with 11.0 mm flat faced tooling and using the 'direct cam' rotary press profile. The die was filled manually prior to compression, target fill weight 250 mg. A range of compaction forces starting from approximately 1 kN increasing to up to 20 kN in approximately 1 kN intervals were targeted to be applied. Tablets were produced to generate manufacturability, tableability, compressability and compactability profiles. Press speeds of 5 tablets per minute (TPM) and 20 TPM (respective dwell times of 60 ms and 15 ms) were used to determine the influence of press speed upon tablet characteristics.

To produce samples for physical characterisation testing, tablets were produced at selected forces (5, 7.5 and 10 kN) at two speeds (dwell times 60 ms and 15 ms).

### **5.3.8 Tablet Characterisation**

Tablets were characterised as per Chapter 3 section 3.3.8.

### **5.3.9 *In vitro* dissolution – Sample analysis**

A HPLC method was adapted to test both blends and off-line samples taken during *in vitro* dissolution assessment. The method was adapted from an existing Quay Pharma method for the assay of dipryidamole. The method parameters are detailed in Table 5.1. Analysis was performed using a Waters Acquity uHPLC system (Waters, Milford, USA) with Empower 3.0 (Waters, Milford, USA) the controlling data system and an Acquity UPLC BEH C18, 100 x 2.1 mm, 1.7 µm column (Waters, Milford, USA). A calibration curve was constructed to establish the working range of the method from 0.05 to 6.7 µg/mL, the R<sup>2</sup> value for the curve produced was 0.9998, indicating suitably for use as detailed in Figure 5.1. Specificity of the method against GEL and TPGS was determined by injecting samples containing GEL and TPGS to check for any interference with the API main peak prior to analysis.

Table 5.1 HPLC Assay method parameters

Parameter	Value				
Column	Acquity UPLC BEH C18, 100 x 2.1 mm, 1.7 µm				
Column Temperature	60 °C (± 3 °C)				
Sample Manager Temperature	5 °C (± 3 °C)				
Mobile Phase A	Water + 0.1 % trifluoroacetic acid (TFA)				
Mobile Phase B	Methanol + 0.1 % TFA				
Mobile Phase C	50:50 % v/v 2-Propanol: Acetonitrile				
Mobile Phase Composition	Time (min)	Flow Rate (mL/min)	A	B	C
	0.00	0.2	50	50	0
	3.00	0.2	10	90	0
	3.10	0.3	5	0	95
	7.00	0.3	5	0	95
	7.10	0.2	50	50	0
12.00	0.2	50	50	0	
Run time	12 minutes				
Wavelength	285 nm				
Injection volume	Auto Addition with HPLC Water		Standard/Sample Solution		
	48 µL		2 µL		
3D data range	190 to 400 nm (if required)				
Sampling rate	5 pts/sec				
Sample manager wash/purge	50:50 water: acetonitrile				

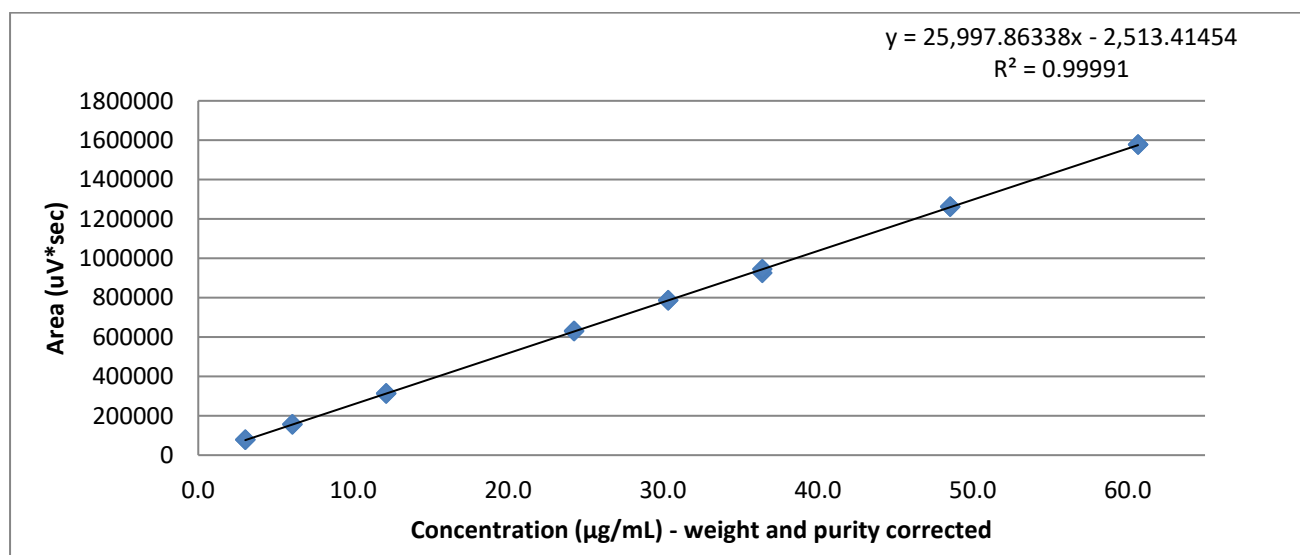


Figure 5.1 Calibration curve for Assay of dipyrindamole

### 5.3.10 *In vitro* dissolution parameters

A USP Type II apparatus was used (Copley, UK) with manual sampling. *In vitro* method conditions are detailed in Table 5.2. pH 3.4 was selected as the medium for dissolution due to solution stability concerns with dipyrindamole at lower pH.

Tablet samples were tested in triplicate against a single blend sample. The blend sample was introduced to the vessel by pouring the pre-weighed sample from a weighing boat through the sample entry port in the lid of the dissolution vessel. It was noted that the blend rapidly wet out and dispersed within the dissolution medium.

Table 5.2 In-vitro dissolution method parameters

Parameter	Value
Apparatus	Paddles (USP apparatus II)
Paddle speed	50 rpm, 200 rpm infinity spin
Dissolution media	pH 3.4 buffer
Media volume	1000 mL
Dissolution bath temperature	37 ± 0.5 °C
Sampling filters	0.2 µm PVDF syringe filters (13 mm diameter) No cannula filters
Sampling time points	5, 10, 15, 30, 45 and 60 minutes at 50 rpm, 90 minutes (after the 60 minutes time point spin set at 200 rpm)

## 5.4 Results and Discussion

### 5.4.1 Characteristics of Neusilin®US2 loaded with D-GEL and D-TPGS.

Table 5.3 details the characteristics of Neusilin® US2 loaded with increasing concentrations of D-GEL and D-TPGS respectively. For the D-GEL loaded granules, the tapped and bulk density values did not show an increasing trend with increased loading, which may be due to either the homogeneity of the starting material or the distribution of D-GEL during loading, resulting in variable particle size distribution and thus, variable consolidation during measurement. Each 'batch' was determined to flow freely which was confirmed by the relatively low Carr's Index and Hausner ratio values. In a similar fashion to the data reported in Chapter 3, the true density of the batches decreased with increasing loading. This data support the previous finding (Section 3.4.1) that when the porosity of the Neusilin® US2 is reduced by a material with a lower density ( $\text{g}/\text{cm}^3$ ), as the concentration of the substrate loaded increases, the true density of the combined material decreases.

For the D-TPGS samples, similar variable density data were generated. Again the loaded granules flowed freely and the true density decreased with increased loading. Note: the true density of the 90 % sample was not determined due to an accident with the sample.

The variable density data reported for both GEL and TPGS samples, may suggest a lack of homogeneity during batch preparation. As per the findings of Chapter 4, further work is necessary to ensure and quantify the homogenous distribution of substrate when loading Neusilin® US2.

Table 5.3 The effect of loading with D-GEL and D-TPGS on the characteristics of Neusilin®US2 (mean  $\pm$  SD, n=3)

Material	% Loading relative to dry sorbent	Tapped Density (g/cm <sup>3</sup> )	Bulk Density (g/cm <sup>3</sup> )	Carr's Index <sup>1</sup> (%)	Hausner Ratio <sup>1</sup>	Flow (g/s <sup>-1</sup> )	True Density (g/cm <sup>3</sup> )
Neusilin® US2 loaded with D-GEL.	50 %	0.30 $\pm$ 0.01	0.26 $\pm$ 0.00	15.2	1.18	3.06 $\pm$ 0.05	1.65 $\pm$ 0.09
	70 %	0.29 $\pm$ 0.04	0.25 $\pm$ 0.02	15.7	1.19	3.66 $\pm$ 0.12	1.56 $\pm$ 0.06
	90 %	0.37 $\pm$ 0.02	0.32 $\pm$ 0.02	14.2	1.17	4.33 $\pm$ 0.06	1.48 $\pm$ 0.05
Neusilin® US2 loaded with D-TPGS	50 %	0.29 $\pm$ 0.00	0.25 $\pm$ 0.00	14.8	1.17	2.97 $\pm$ 0.05	1.79 $\pm$ 0.11
	70 %	0.37 $\pm$ 0.02	0.31 $\pm$ 0.03	16.2	1.19	3.69 $\pm$ 0.03	1.68 $\pm$ 0.06
	90 %	0.34 $\pm$ 0.25	0.29 $\pm$ 0.22	15.3	1.08	4.25 $\pm$ 0.15	ND

#### 5.4.2 Compression of Neusilin® US2 loaded with D-GEL

The loaded granules containing D-GEL were compressed without the addition of further excipient, to determine the compression characteristics of the granules alone.

##### 5.4.2.1 Manufacturability

Figures 5.2 and 5.3 detail manufacturability profiles of the D-GEL loaded granules compressed at dwell times of 60 ms and 15 ms respectively.

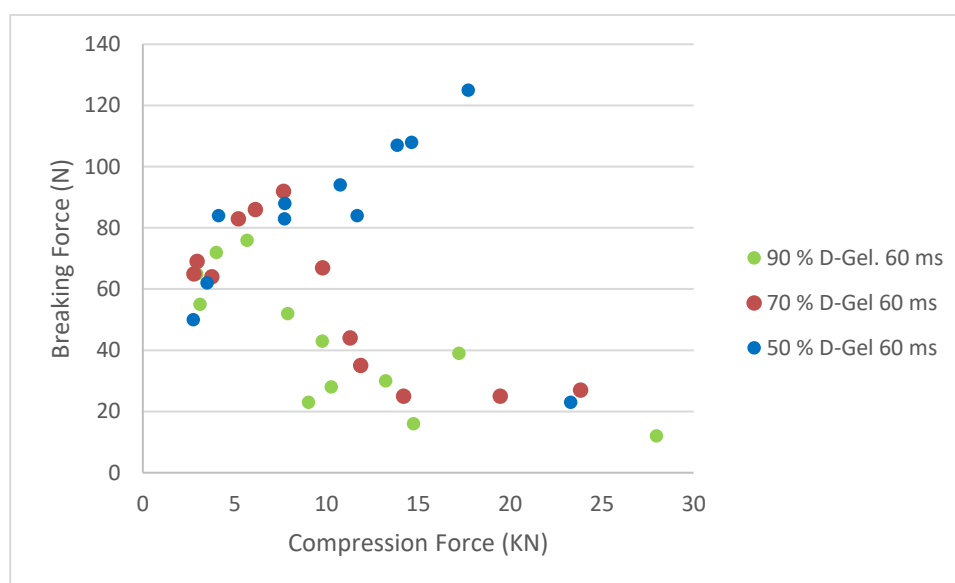


Figure 5.2. Manufacturability profile of Neusilin® US2 loaded with 50, 70 and 90 % D-GEL (dwell time 60 ms)

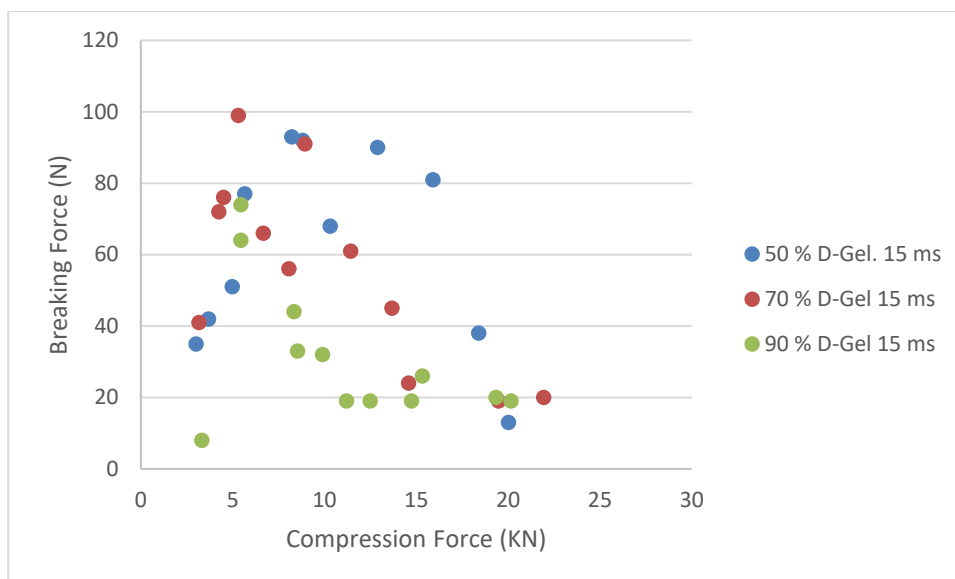


Figure 5.3. Manufacturability profile of Neusilin® US2 loaded with 50, 70 and 90 % D-GEL (dwell time 15 ms)

Figures 5.2 and 5.3 show that loaded D-GEL granules exhibited a reduction in breaking force with increased D-GEL concentration and with increased compression force. This finding was also exhibited when other liquid formulations were loaded on to Neusilin® US2 (see Chapters 2 and 3). For samples containing 50 % loaded D-GEL an obvious strain rate sensitivity is apparent, as with reduced dwell time a reduction in tablet hardness is reported with increasing compression force up to an applied force of 20 kN. This strain rate sensitivity is not obvious with the 70 % and 90 % loaded granules.

#### 5.4.2.2 Tableability

Figures 5.4 and 5.5 show tableability profiles of the D-GEL loaded granules compressed at dwell times of 60 ms and 15 ms respectively. Note: The line bisecting the Y-axis at 1 MPa, allows easy identification of those points which lie above this value and are indicative of suitable tablet tensile strength (Amidon et al., 2009).

Figure 5.3 shows that above 30 MPa applied pressure, all tablets irrespective of D-GEL concentration produced tablets with tensile strength values > 1 MPa until a maximum applied pressure was reached, unique to each loading level of D-GEL. For 50 % D-GEL the tensile strength of loaded granules increased in a linear trend up to approximately 190 MPa. As the concentration of D-GEL increased, the range over which tensile strength increased with applied

pressure decreased. For 70 % D-GEL loaded granules the tensile strength dropped rapidly above 100 MPa and for 90 % D-GEL loaded samples tensile strength was reduced > 55 MPa applied pressure. When compared to 90 % SPc loaded granules (Section 3.4.2) a significant increase in tensile strength is reported for those tablets produced from 90 % loaded D-GEL granules. Tablets > 1 MPa tensile strength (dwell time 60 ms) containing 90 % SPc could not be produced (see Figure 5.4).

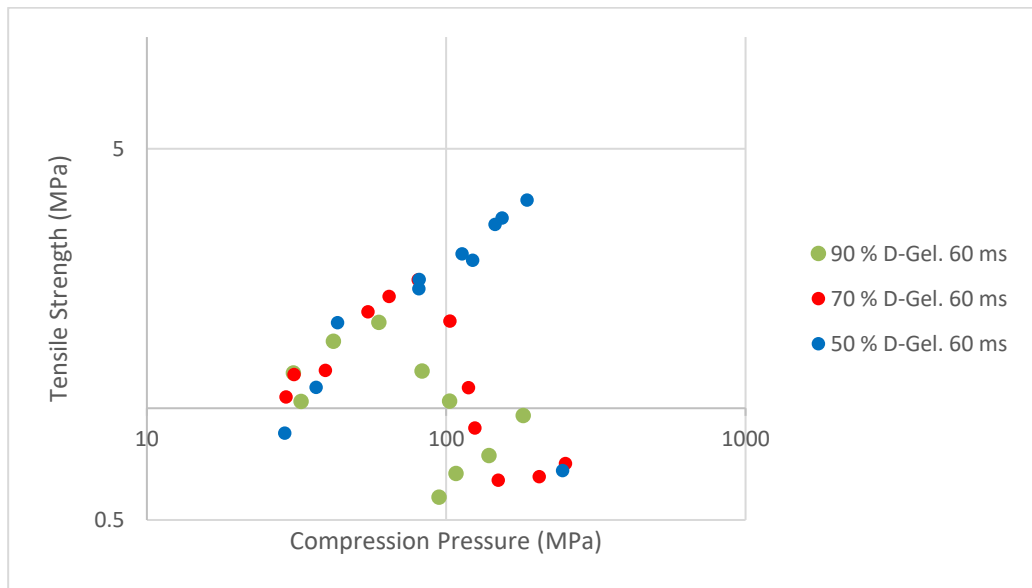


Figure 5.4 Tableability profiles of Neusilin® US2 loaded with 50, 70 and 90 % D-GEL (dwell time 60 ms)

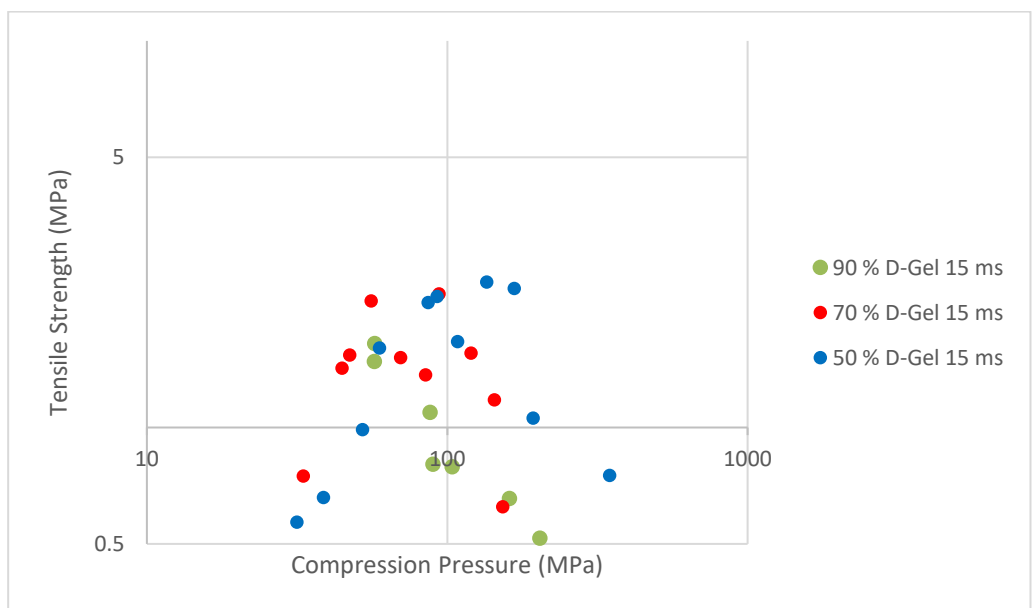


Figure 5.5 Tableability profiles of Neusilin® US2 loaded with 50, 70 and 90 % D-GEL (dwell time 15 ms)

Figure 5.5 shows that with a reduced dwell time (15 ms compared to 60 ms), greater variability in data and a reduced range of increased tensile strength with increased compression pressure was reported for each D-GEL loading level. The compression pressure at which tablets met the target tensile strength of 1 MPa was increased to approximately 40 MPa from approximately 30 MPa at 60 ms. From approximately 100 MPa compression pressure, a reduction in tensile strength was apparent for 50 % D-GEL loaded granules, whereas 70 % D-GEL loaded granules exhibited a reduction from approximately 70 MPa compression pressure. The 90 % D-GEL loaded granules exhibited a negative slope in tensile strength with increased compression pressure. The data suggest that all concentrations exhibit a degree of strain rate sensitivity due to the reduction in range, of force that can be applied, before which tablets failed to meet the desired 1 MPa tensile strength.

Materials which exhibit strain rate sensitivity tend to deform plastically, such as microcrystalline cellulose. It may be assumed that the 'waxy' nature of Gelucire® 44/14 imparts a plastic-like characteristic to the Neusilin® US2. However, a similar 'wax like' material, glyceryl dibehenate, (Compritol® 888 ATO) a hydrophobic fatty acid ester of glycerol with a melting point of ~70°C (Roberts et al, 2012); was investigated by Mužíková et al (2015) and they found that with increased glyceryl dibehenate concentration (relative to the compression aid in the formulation) plasticity values were similar at comparable applied forces. Plasticity values derived from force displacement measurements (Mužíková et al., 2015) were reduced with increased compression force and the reduction in plasticity was attributed to the decreasing number of pores in the compact as higher forces were applied. Variability in tensile strength values were reported subject to concentration of glyceryl dibehenate and applied force. The difference in melting point between Gelucire® 44/14 and Glyceryl behenate (44 °C and ~70 °C respectively) may be a significant factor in the different outcomes observed in the present study. Materials with higher melting points are less likely to flow, at ambient temperatures and to be less viscous and more glass like compared to lower melting point materials.

#### **5.4.2.3 Compressibility**

Figures 5.6 and 5.7 detail manufacturability profiles of the D-GEL loaded granules compressed at 60 ms and 15 ms respectively. The figures show that

as lipid loading increases, porosity is reduced as would be expected. Solid fraction values begin to plateau earlier (lower compression pressure) for granules with the highest concentration of D-GEL. It was hypothesised in Chapter 3 that liquid would be expelled from granule pores during compression until an equilibrium (inter-intra granular liquid movement) is reached. As D-GEL is in a solid state when in the granule form (post cooling), reduced inter-intragranular movement of the D-GEL is likely compared to the liquid formulations, although multidirectional flow of the D-GEL is probable. The point at which the curves plateau in Figures 5.6 and 5.7 (> 100 MPa) are at higher compression pressures compared to Figures 3.7 and 3.8 (< 100 MPa). Therefore, this comparison supports the hypothesis for reduced movement in the D-GEL granules between phases (semi-solid lipid versus solid Neusilin® US2) as increased pressure is required to reduce porosity. Higher solid fraction values are achieved with the D-GEL granules (approximately 0.8) compared to the SPc granules in Chapter 3 (approximately 0.7). As it has been possible to extend the compression range over which viable tablets have been produced it is found that the solid fraction is increased. The D-GEL loaded granules exhibited improved compressibility, compared to the SPc loaded granules.

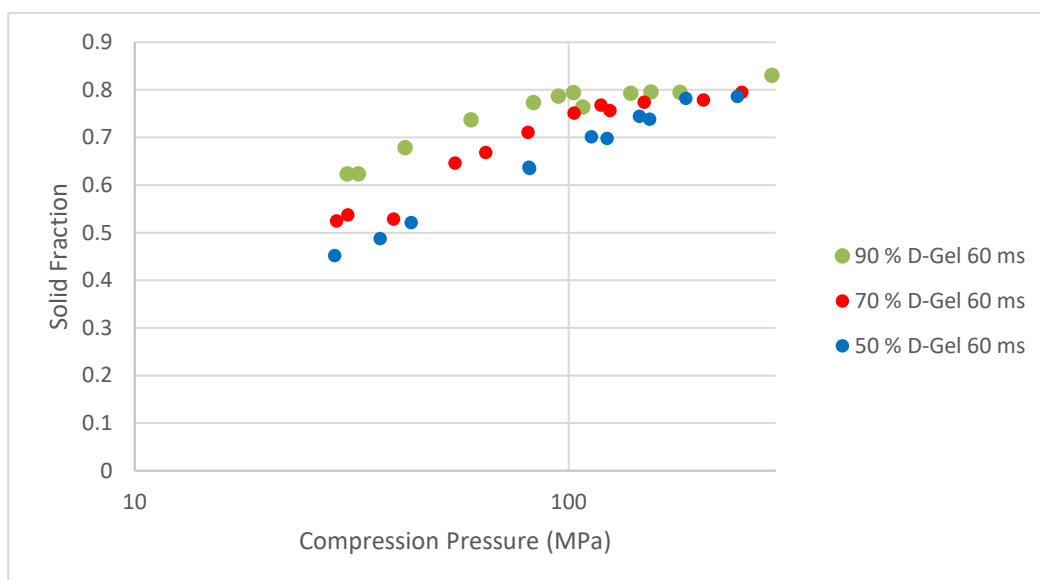


Figure 5.6 Compressibility profiles of Neusilin® US2 loaded with 50, 70 and 90 % D-GEL (dwell time 60 ms)

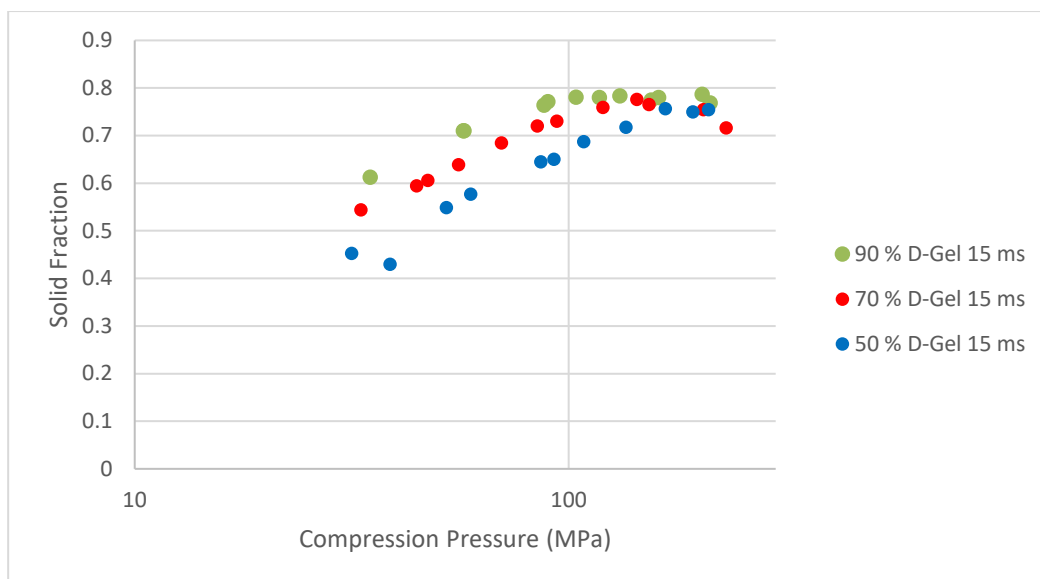


Figure 5.7 Compressibility profiles of Neusilin® US2 loaded with 50, 70 and 90 % D-GEL (dwell time 15 ms)

The data suggest that compression speed does not influence solid fraction values as similar profiles are obtained for each loading level of SPc irrespective of dwell time.

#### 5.4.2.3 Compactibility

Figures 5.8 and 5.9 detail the compactibility profiles of the D-GEL loaded granules compressed at dwell times of 60 ms and 15 ms respectively. The figures show that for each of the materials a critical solid fraction is reached, after which tensile strength begins to decrease, with the exception of 50 % loaded D-GEL granules compressed at 60 ms. When considering the compressibility profile in conjunction with the compactibility profiles, it is likely that the reduction in tensile strength is linked to D-GEL becoming the predominant phase between particles, reducing the formation of inter-particulate bonds between the Neusilin® US2 particles as new surfaces are formed due to particle shear during compression.

A decrease in tensile strength in accordance with increasing press speed (decrease in dwell time) may be expected if the rate of D-GEL flow is faster than that required for bond formation during compression. Additional influencing factors upon tensile strength could be tablet ejection force/speed but these were not evaluated as part of this study.

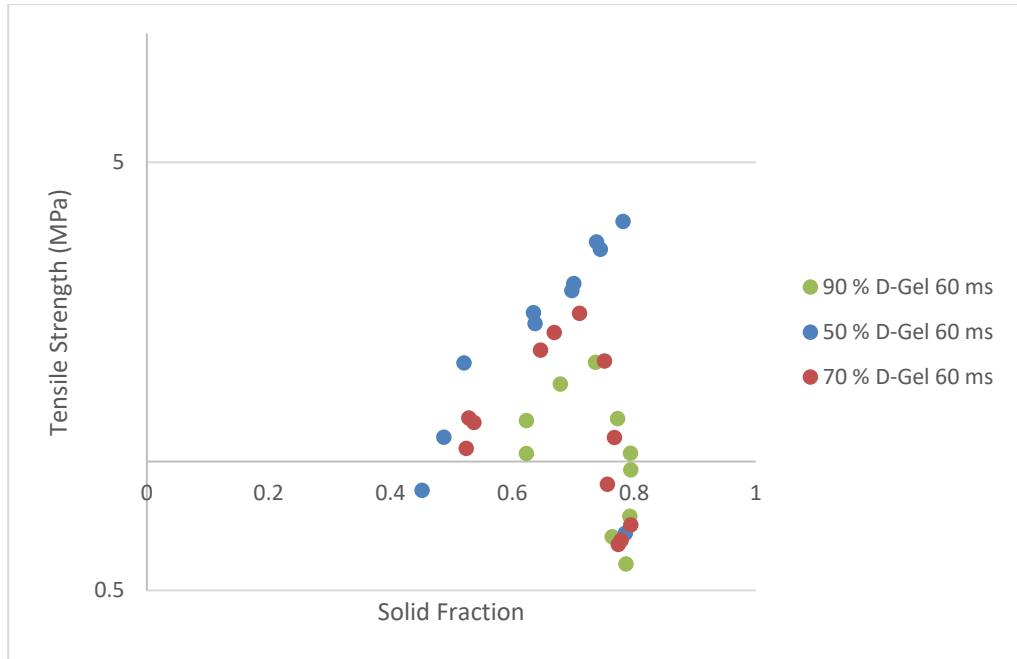


Figure 5.8 Compactibility profiles of Neusilin® US2 loaded with 50, 70 and 90 % D-GEL (dwell time 60 ms)

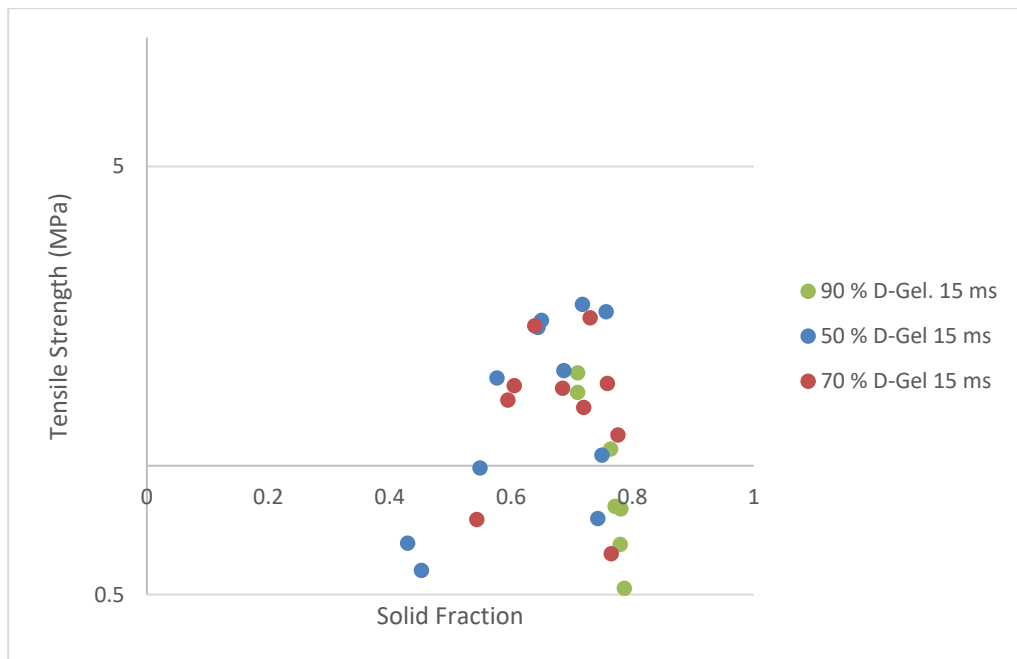


Figure 5.9 Compactibility profiles of Neusilin® US2 loaded with 50, 70 and 90 % D-GEL (dwell time 15 ms)

## 5.4.4 Compression of Neusilin® US2 loaded with D-TPGS

### 5.4.4.1 Manufacturability

Figures 5.10 and 5.11 detail manufacturability profiles of the D-TPGS loaded granules compressed with dwell times of 60 ms and 15 ms respectively.

Figure 5.10 shows that granules loaded with 50 % D-TPGS exhibited a relatively narrow range of increased breaking force with increased compression force, up to approximately 5 kN applied force but above 6 kN, breaking force decreased with increased compression force. This finding contrasts with the 50 % loaded D-GEL samples whereby, breaking force increased with increased compression force up to approximately 20 kN applied force (Figure 5.2). For granules loaded with 70 % and 90 % D-TPGS, the range (of increased breaking force) was reduced further to approximately 4.5 kN applied force, from which breaking force reduced with increased force applied. It should be noted that from above 10 kN applied force, the breaking force of the 70 % loaded samples was unexpectedly lower than that of the 90 % samples. It was noted during hardness testing that tablets were observed to deform slightly prior to a measurement being recorded on the hardness tester. This observation suggested a degree of tablet softening/plasticity which may impact on the breaking force results generated. Further discussion on this observation is provided in Section 5.5.

Figure 5.11 shows similar profiles to that of Figure 5.10 where granules were compressed at a reduced dwell time (15 ms compared to 60 ms). However, breaking force decreased in accordance with increased loading levels as previously found with all other loaded materials.

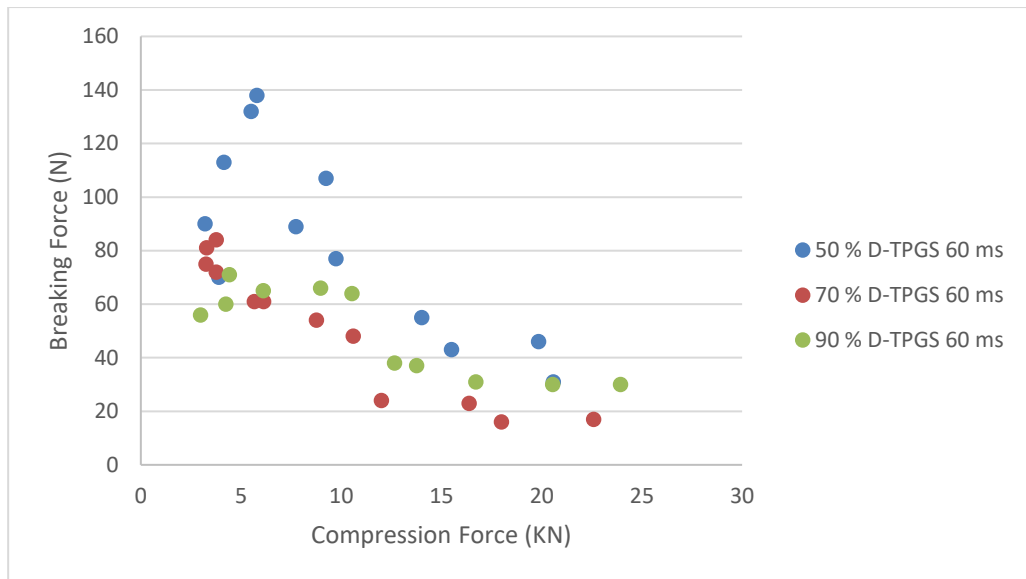


Figure 5.10. Manufacturability profile of Neusilin® US2 loaded with 50, 70 and 90 % D-TPGS (dwell time 60 ms)

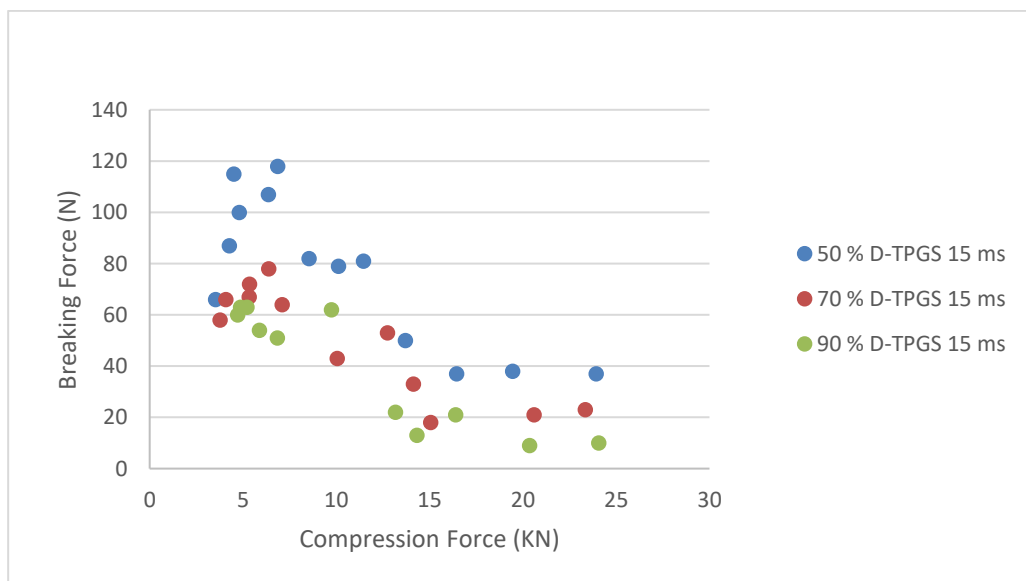


Figure 5.11. Manufacturability profile of Neusilin® US2 loaded with 50, 70 and 90 % D-TPGS (dwell time 15 ms)

#### 5.4.4.2 Tableability

Figures 5.12 and 5.13 detail tableability profiles of the D-TPGS loaded granules compressed at dwell times of 60 ms and 15 ms respectively. Note, the line bisecting the y-axis shows the target strength of 1 MPa. Figure 5.12 shows that granules loaded with 50 % D-TPGS all possessed a tensile strength > 1 MPa indicating relatively robust tablets. For tablets containing 70 % and

90 % D-TPGS granules, > 110 MPa applied pressure caused a reduction in tensile strength below the target 1 MPa signifying weak tablets produced.

Figure 5.13 shows that when compressed with a dwell time of 15 ms granules loaded with 50 % D-TPGS failed to meet the target tensile strength value (> 1 MPa) as the applied compression increased above 135 MPa. For tablets containing 70 % D-TPGS granules, > 130 MPa applied pressure caused a reduction in tensile strength below the target 1 MPa and for 90 % loaded granules > 105 MPa applied force. Strain rate sensitivity of the loaded granules was not obvious.

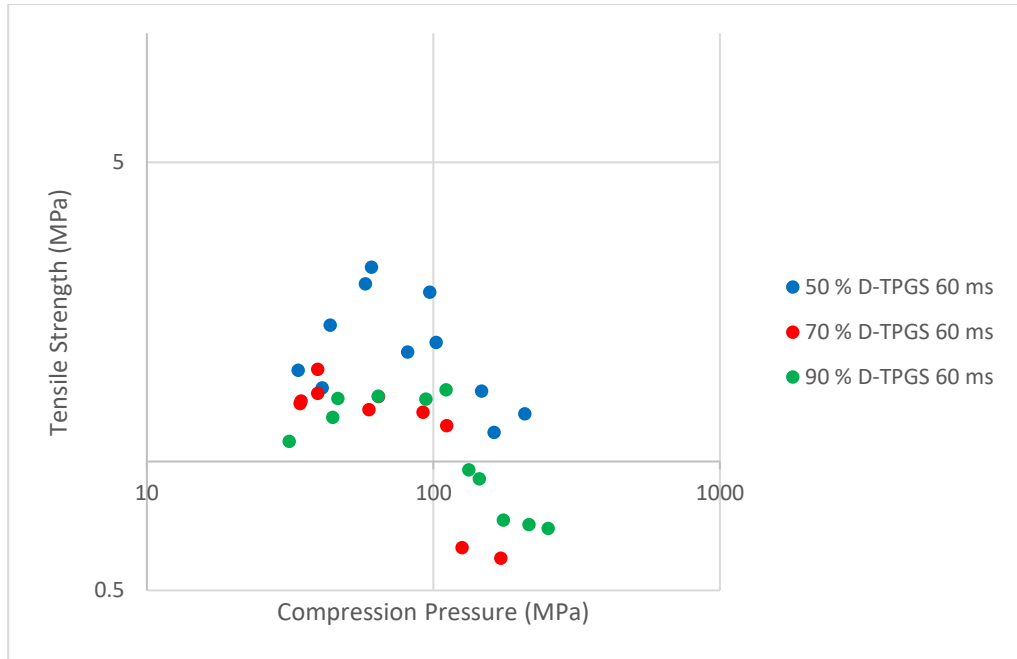


Figure 5.12. Tableability profiles of Neusilin® US2 loaded with 50, 70 and 90 % D-TPGS (dwell time 60 ms)

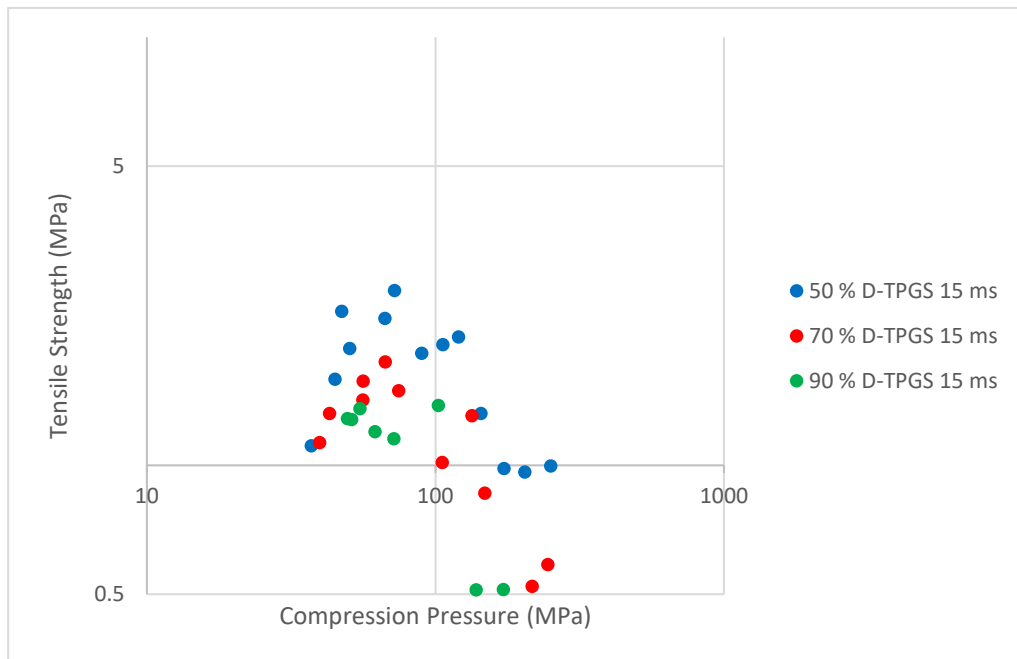


Figure 5.13 Tableability profiles of Neusilin® US2 loaded with 50, 70 and 90 % D-TPGS (dwell time 15 ms)

#### 5.4.4.3 Compressibility

Figures 5.14 and 5.15 detail compressibility profiles of the D-TPGS loaded granules compressed at dwell times of 60 ms and 15 ms respectively. The figures show that the solid fractions achieved were lower than that of the D-

GEL granules (approximately 0.75 versus 0.78 respectively). Note; data are not reported for the 90 % loaded granules as true density was not determined.

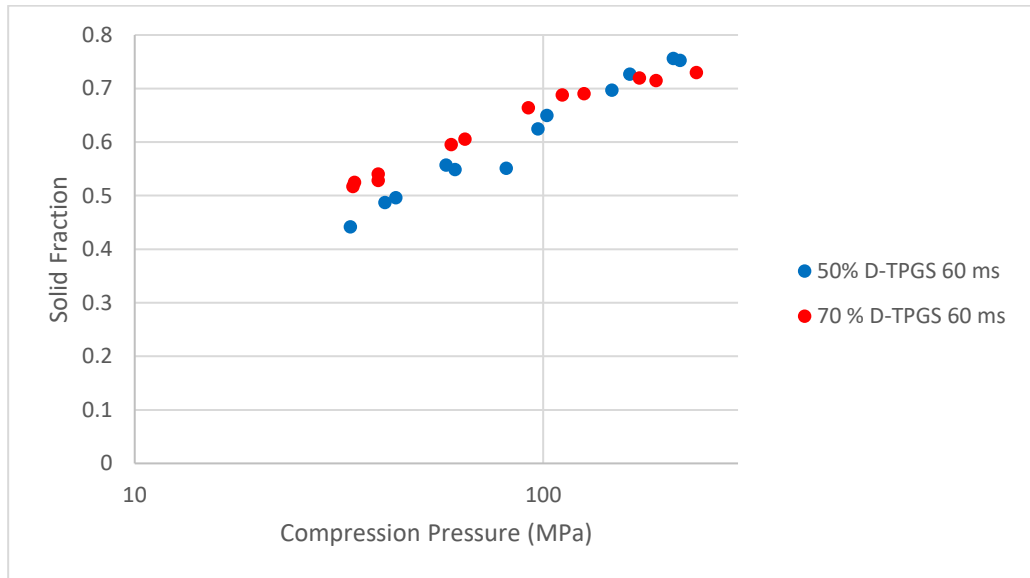


Figure 5.14 Compressibility profiles of Neusilin® US2 loaded with 50 and 70 % D-TPGS (dwelt time 60 ms)

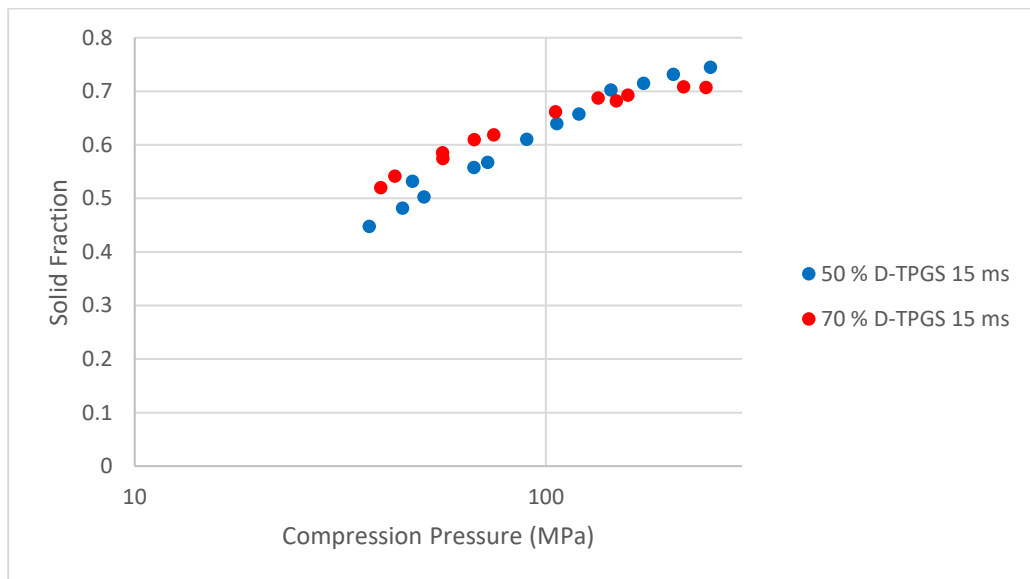


Figure 5.15. Compressibility profiles of Neusilin® US2 loaded with 50 and 70 % D-TPGS (dwelt time 15 ms)

As per the D-GEL granules and SPc granules reported in Chapter 3, the D-TPGS granules did not reach the optimum solid fraction value of 0.85 for tablet formulations as reported by Pitt et al (2015).

#### 5.4.4.4 Compactibility

Figures 5.16 and 5.17 detail compactability profiles of the D-TPGS loaded granules compressed at dwell times of 60 ms and 15 ms respectively. The

figures show that for each of the materials, a critical solid fraction is reached following which tensile strength begins to decrease (> 0.55). As per the D-GEL granules (Figures 5.8 and 5.9) the reduction in tensile strength was linked to D-TPGS becoming the predominant phase between particles, preventing/reducing the formation of inter-particulate bonds or bond formation between new surfaces formed due to particle shear during compression.

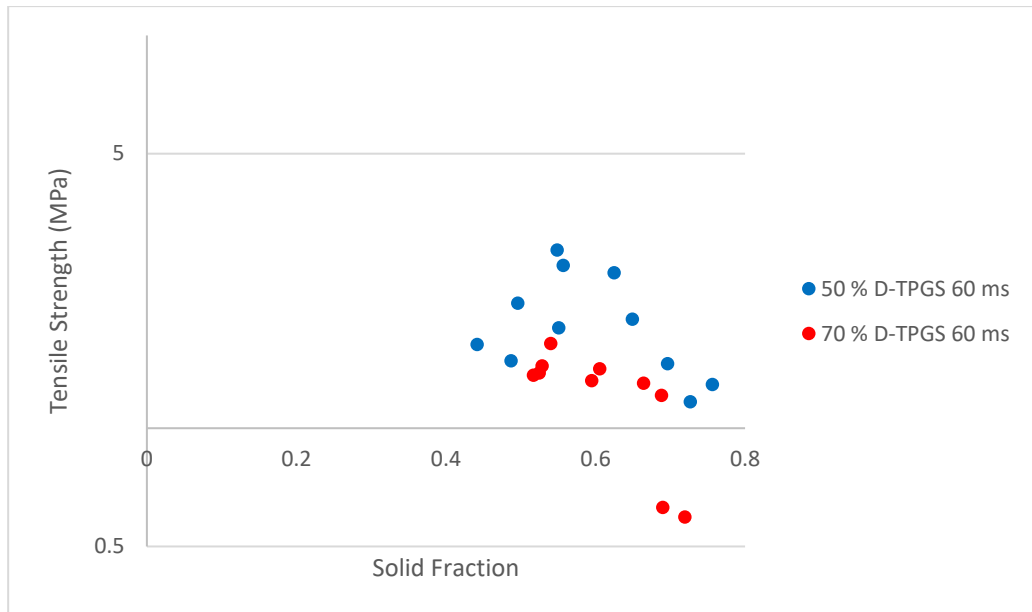


Figure 5.16 Compactibility profiles of Neusilin® US2 loaded with 50 and 70 % D-TPGS (dwell time 60 ms)

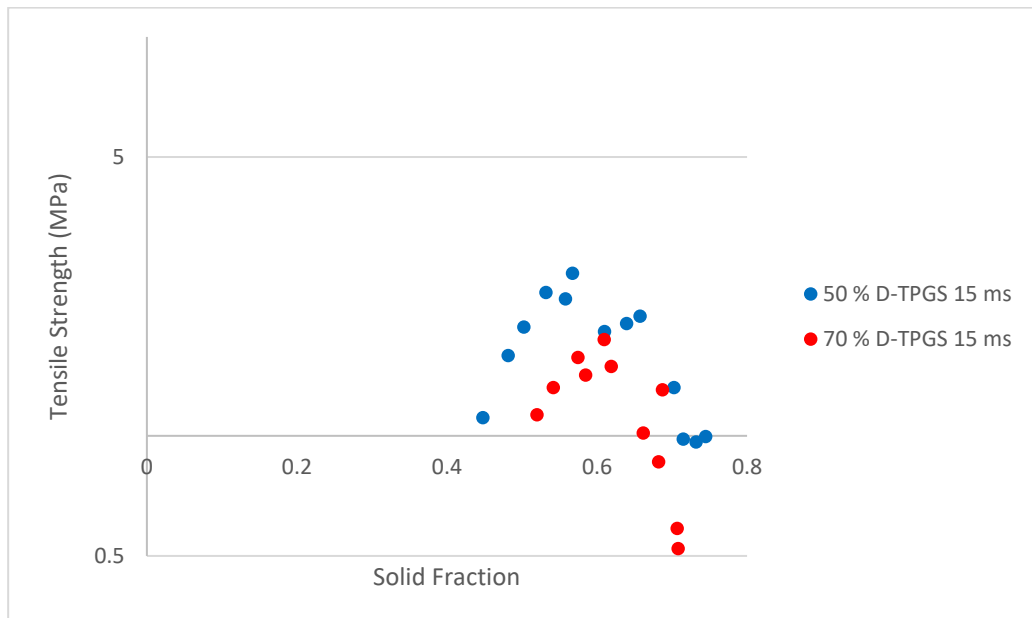


Figure 5.17 Compactibility profiles of Neusilin® US2 loaded with 50 and 70 % D-TPGS (dwell time 15 ms)

#### 5.4.4 Compression of loaded granule blends

Following the positive data produced from compression of the granules alone (tensile strength values > 1 MPa) over a relatively wide range of applied pressure and at both simulated press speeds; blends were formulated without the addition of extra-granular compression aids. As per the blends prepared containing SPc granules in Chapter 3, croscarmellose Na (super disintegrant) and sodium stearyl fumarate (lubricant) were added to the granules to enhance tablet characteristics and aid processing respectively. Table 5.4 details the blends produced.

*Table 5.4 Blend Formulations produced containing D-GEL and TPGS loaded granules with extra granular excipient Croscarmellose Na and sodium stearyl fumarate. Values listed are composition as % w/w.*

Blend Reference	% w/w					
	50 % D-GEL	70 % D-GEL	90 % D-GEL	50 % D-TPGS	70 % D-TPGS	90 % D-TPGS
<b>Material</b>						
Gelucire® 44/14	30.4	37.6	43.2	-	-	-
Vitamin E TPGS	-	-	-	30.4	37.6	43.2
Dipyridamole	0.9	1.2	1.3	0.9	1.2	1.3
Neusilin® US2	62.7	55.3	49.4	62.7	55.3	49.4
Croscarmellose Na	5.0	5.0	5.0	5.0	5.0	5.0
Sodium Stearyl fumarate	1.0	1.0	1.0	1.0	1.0	1.0

#### 5.4.5 Tablet Characteristics

The blends were compressed at three target compression forces (5 kN, 7.5 kN and 10 kN) at a single press speed (dwell time 60 ms). Characterisation data for the tablets containing D-GEL granules is detailed in Table 5.5. Characterisation data for the tablets containing D-TPGS granules is detailed in Table 5.6.

Table 5.5 Characteristics of tablets containing Neusilin®US2 loaded with D-GEL compressed at selected forces (dwell time 60 ms). (n=5 for hardness and tensile strength ± SD)

% Loading	Target Force Applied (kN)	Friability (%)	Av. Thickness (mm)	Av. Hardness (N)	Av. Tensile Strength (MPa)	Disintegration (mm:ss)
50	5	0.00	2.93	124.54 ± 2.65	2.46 ± 0.06	04:39
50	7.5	0.00	2.45	110.34 ± 8.61	2.61 ± 0.25	05:22
50	10	0.33	2.36	114.72 ± 9.05	2.81 ± 0.21	06:19
70	5	0.00	2.70	96.92 ± 4.11	2.08 ± 0.09	05:22
70	7.5	0.07	2.40	85.46 ± 5.47	2.06 ± 0.14	07:10
70	10	0.20	2.27	61.00 ± 4.60	1.56 ± 0.12	07:21
90	5	0.00	2.63	86.08 ± 1.52	1.90 ± 0.03	07:10
90	7.5	0.19	2.43	55.74 ± 11.29	1.33 ± 0.27	07:10
90	10	0.00	2.32	48.48 ± 16.00	1.21 ± 0.39	06:48

Table 5.6 Characteristics of tablets containing Neusilin®US2 loaded with D-TPGS compressed at selected forces (dwell time 60 ms) (n=5 for hardness and tensile strength ± SD)

% Loading	Target Force Applied (kN)	Friability (%)	Av. Thickness (mm)	Av. Hardness (N)	Av. Tensile Strength (MPa)	Disintegration (mm:ss)
50	5	0.00	2.32	119.64 ± 10.68	2.99 ± 0.21	03:07
50	7.5	0.07	2.32	150.64 ± 8.14	3.76 ± 0.20	04:22
50	10	0.00	2.32	147.10 ± 16.66	3.67 ± 0.40	05:32
70	5	0.00	2.32	95.02 ± 7.99	2.37 ± 0.17	05:52
70	7.5	0.00	2.32	73.98 ± 6.98	1.85 ± 0.17	07:05
70	10	0.26	2.32	48.88 ± 7.26	1.22 ± 0.18	07:17
90	5	0.06	2.32	82.70 ± 4.63	2.06 ± 0.10	08:49
90	7.5	0.00	2.32	59.30 ± 11.60	1.48 ± 0.28	09:20
90	10	0.13	2.32	46.92 ± 9.23	1.17 ± 0.23	09:58

Figures 5.21, 5.22, 5.23 detail variability charts (as discussed in Chapter 3, section 3.3.9) relating to tablet tensile strength, friability and disintegration rate respectively.

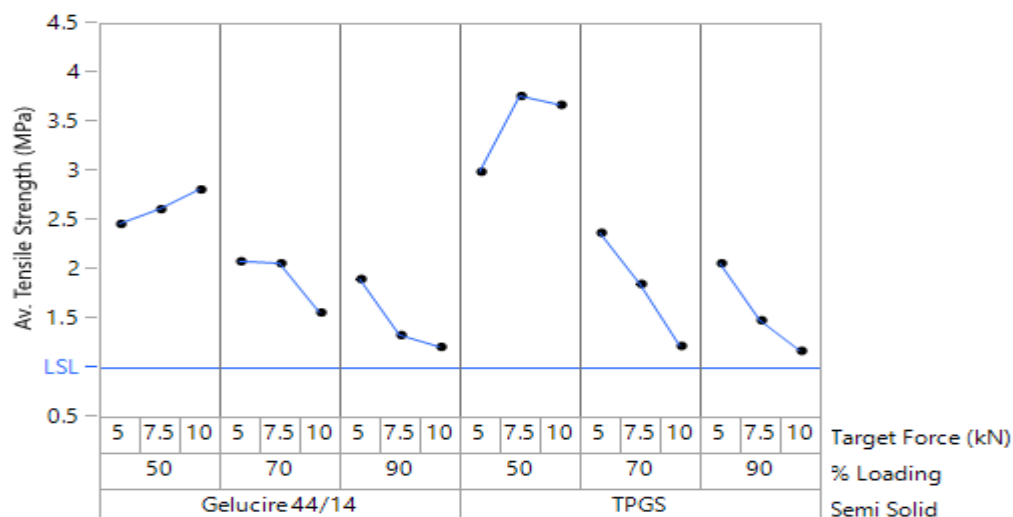


Figure 5.21 Variability chart showing the effect of semi-solid type, loading level and compression force on mean tablet Tensile strength. (Note: LSL indicates lower spec limit of 1 Mpa).

Figure 5.21 shows that all tablets produced irrespective of loading material or concentration of material loaded were > 1 MPa tensile strength. For D-GEL containing tablets only the 50 % loaded tablets increased in tensile strength with increased applied force, which was expected as per Figure 5.2. For the remaining D-GEL subsets a decreasing trend was reported with increased loading level and increased applied force.

For those tablets containing 50 % loaded D-TPGS granules, higher tensile strength values were reported than all other tablets produced. A high degree of overlap in tensile strength values (across the range of applied force) between those tablets containing 70 % and 90 % loaded granules is noted. This data is significant in terms of maximising the achievable dose to be delivered for a formulation.

Compared to the data presented in Figure 3.16 for SPc formulations containing 10 % w/w extra-granular excipients, it can be seen (Figure 5.21) that a much higher loading (90 %) of both D-GEL and D-TPGS can be achieved in order to produce viable tablets with > 1 MPa tensile strength.

Figure 5.22 shows that all tablets produced, irrespective of loading material or concentration of material loaded exhibited low friability (< 0.4 %). The data did not show any specific trends but suggests that all tablets were robust and would

be suitable for scale up and subsequent processing (coating or packaging). This is in stark contrast to formulations containing SPc loaded granules (see Figure 3.18 in Chapter 3) where even formulations containing 50 % loaded granules were reported to fail friability. Tablets containing D-GEL and D-TPGS appear to demonstrate superior physical characteristics.

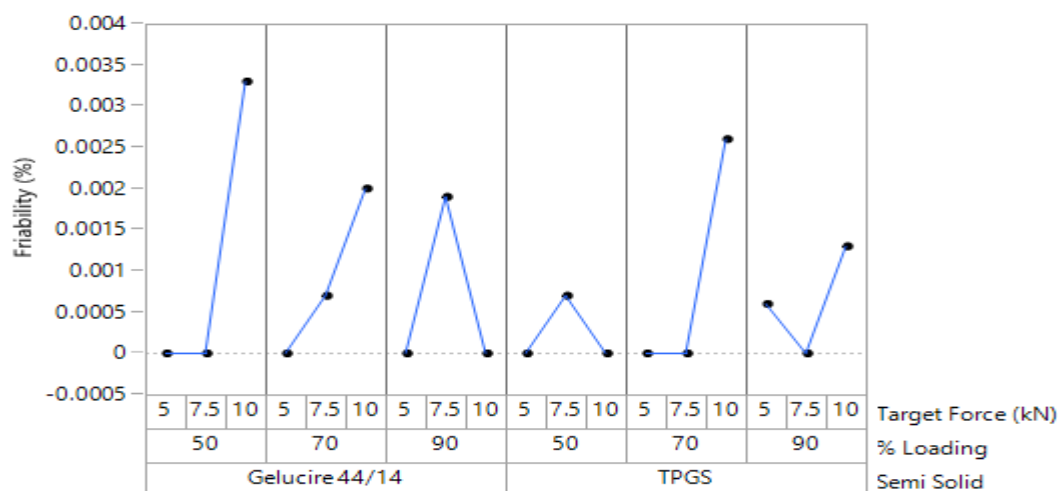


Figure 5.22 Variability chart showing the effect of semi-solid type, loading level and compression force on tablet friability.

Figure 5.23 shows that all tablets produced, irrespective of loading material or concentration of material, disintegrated in < 10 min. For those tablets containing D-GEL an increasing trend in disintegration time is apparent with increasing D-GEL loading and compression force until a plateau is reached at about 7 min. These data suggest that for tablets containing  $\geq 70\%$  D-GEL compressed above 5 kN, the disintegration rate was driven by a predominant factor, which is likely to be the Gelucire® 44/14 dissolution/dispersion rate as increased compression force did not result in extended disintegration times.

The disintegration time of tablets containing D-TPGS exhibited an increase with increased loading and increased compression force. This data indicated that the rate-limiting factor for disintegration is likely to be the rate of dispersion/dissolution of Vitamin E TPGS.

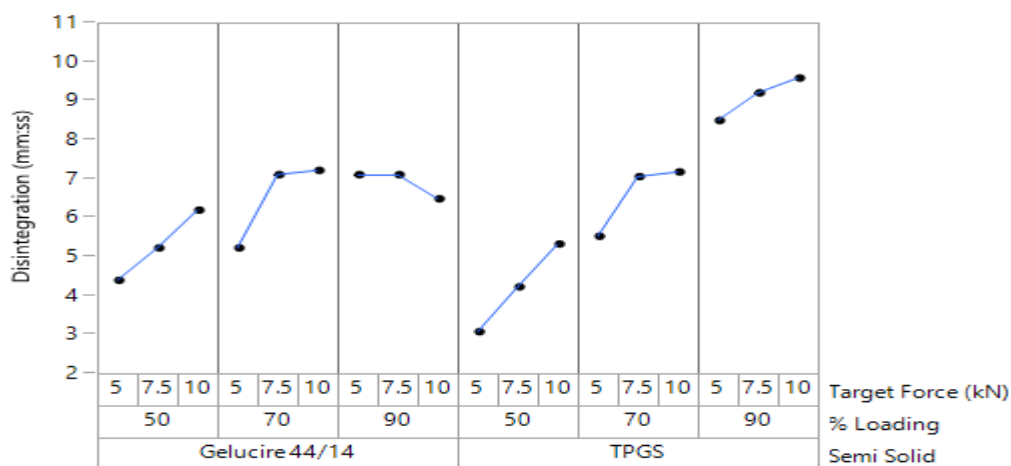
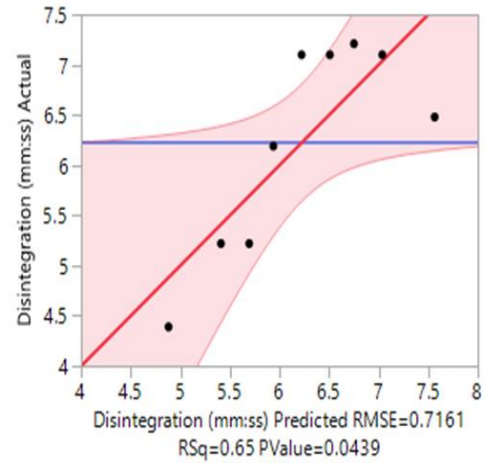
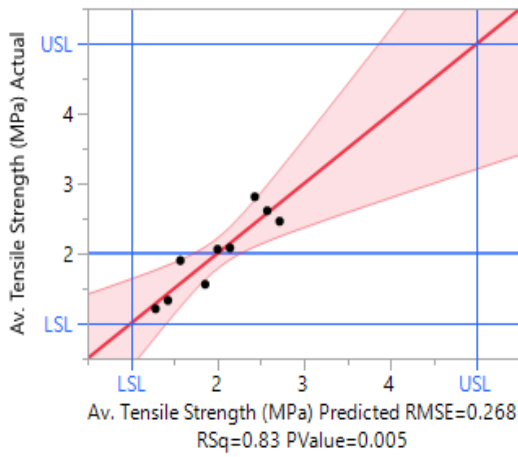


Figure 5.23 Variability chart showing the effect of semi-solid type, loading level and compression force on tablet disintegration time.

A step wise regression model was used to generate predicted plots (as discussed in Chapter 3 section 3.3.9) for each of the semi solid formulations using single factor and two factor interactions. Figure 5.24 details the predicted plots for tensile strength, disintegration and friability for the D-GEL formulations. For tensile strength and disintegration, the most significant term ( $P < 0.05$ ) was that of % loading although the  $R^2$  values were not particularly high and indicative of data point variation from the models applied (0.83 and 0.65 respectively). For friability the most significant term was also ' % loading '. However, the  $P$  value was  $> 0.05$ , indicating that this model is not particularly accurate and that another, not yet measured factor may be contributing. However, due to the relatively low friability values produced across all subsets of tablets produced, this poor correlation is not necessarily a concern for future studies.

Figure 5.25 details the predicted plots for tensile strength, disintegration and friability for the D-TPGS formulations. For tensile strength, the most significant term ( $P < 0.05$ ) was % loading although the  $R^2$  value was not particularly high (0.78), however for disintegration the  $R^2$  value was 0.98 with % loading as the most significant term. This model implies that other factors are insignificant in influencing disintegration time compared to the concentration of vitamin E TPGS in the formulation. Similarly, to Figure 5.24 the model for friability is not accurate, but again due to the low values produced, this finding is not a concern for future studies.

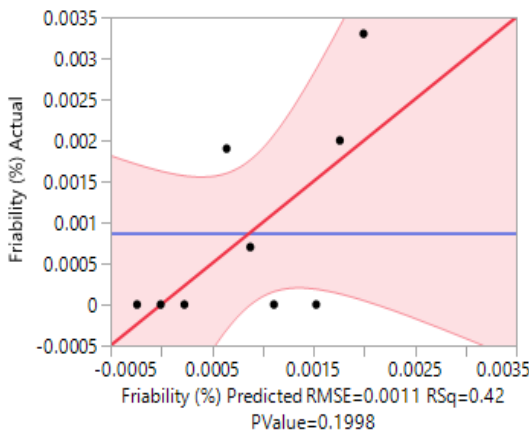


**Parameter Estimates**

Term	Estimate	Std Error	t Ratio	Prob> t
Intercept	4.4388889	0.512136	8.67	0.0001*
% Loading	-0.028667	0.00547	-5.24	0.0019*
Target Force (kN)	-0.057333	0.043758	-1.31	0.2380

**Parameter Estimates**

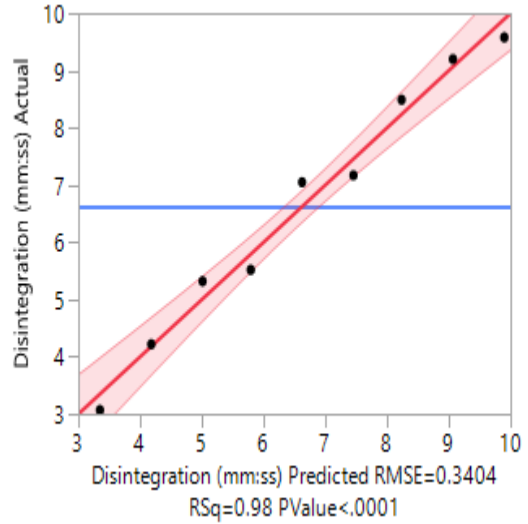
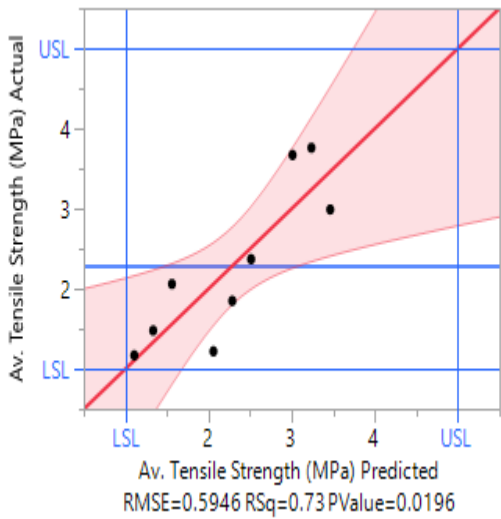
Term	Estimate	Std Error	t Ratio	Prob> t
Intercept	1.7916667	1.36861	1.31	0.2384
% Loading	0.0406667	0.014617	2.78	0.0319*
Target Force (kN)	0.2113333	0.116937	1.81	0.1207



**Parameter Estimates**

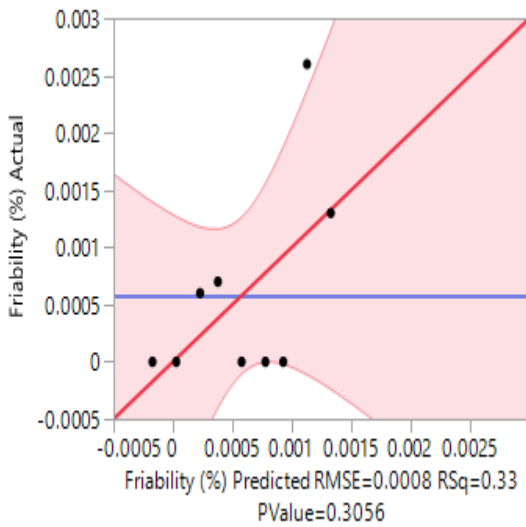
Term	Estimate	Std Error	t Ratio	Prob> t
Intercept	-0.000956	0.002071	-0.46	0.6608
% Loading	-1.167e-5	2.212e-5	-0.53	0.6169
Target Force (kN)	0.0003533	0.000177	2.00	0.0929

Figure 5.24 Predicted plots and Identified statistically significant input factors for tablets containing D-GEL granules, for prediction of tensile strength (top left), disintegration (top right) and friability (bottom left).



Parameter Estimates				
Term	Estimate	Std Error	t Ratio	Prob> t
Intercept	6.2963889	1.136372	5.54	0.0015*
% Loading	-0.047583	0.012137	-3.92	0.0078*
Target Force (kN)	-0.090667	0.097094	-0.93	0.3864

Parameter Estimates				
Term	Estimate	Std Error	t Ratio	Prob> t
Intercept	-4.422222	0.65063	-6.80	0.0005*
% Loading	0.1221667	0.006949	17.58	<.0001*
Target Force (kN)	0.3326667	0.055591	5.98	0.0010*



Parameter Estimates				
Term	Estimate	Std Error	t Ratio	Prob> t
Intercept	-0.001772	0.001607	-1.10	0.3123
% Loading	0.00001	1.716e-5	0.58	0.5813
Target Force (kN)	0.00022	0.000137	1.60	0.1602

Figure 5.25 Predicted plots and Identified statistically significant input factors for tablets containing D-TPGS granules, for prediction of tensile strength (top left), disintegration (top right) and friability (bottom left).

#### 5.4.5 *In vitro* dissolution assessment

Figures 5.26 a) and b) and 5.27 show *in vitro* dissolution profiles for tablets containing D-GEL loaded granules (50 %, 70 % and 90 % respectively). Each profile details the mean of three replicates with range bars showing the maximum and minimum result at each timepoint. Each blend was compressed at three selected compression forces (5 kN, 7.5 kN and 10 kN) as per the data presented in Table 5.5. Each figure also details a single profile (n=1) for the uncompressed blend for comparison purposes. It should be noted that following sampling at the 60 min time point the paddle speed was increased from 50 rpm to 200 rpm to maximise the hydrodynamic potential in the dissolution pots, in the event that the full extent of API release had not been achieved.

The uncompressed blend sample for each loaded granule, (which were included for comparison against the corresponding tablets in Figures 5.26 and 5.27) exhibited 100 % nominal release within 5 min.

In Figure 5.26 a) (50 % D-GEL containing tablets), all tablets irrespective of compression force achieve > 90 % at the 10-minute time point. No obvious trend in reduction of % dipyridamole dissolved at the 5-minute time point was noted with increased compression force (7.5 kN and 10 kN tablet overlay). Tablets containing 70 % D-GEL loaded granules are detailed in Figure 5.26 b), a trend in reduced % dissolved is reported, with increased applied force. However, all samples achieved > 95 % dissolved at the 15 min time point. A more profound retardation in dissolution with increased D-GEL loading (90 %) and increased compression force is reported in Figure 5.27. A delay in release at the 5 min time point is apparent for all tablets at each compression force, an increased variation between replicates (n=3 per compression force) can be seen with the length of the error bars at this time point compared to Figures 5.26 a) and b). These findings suggest that D-Gel loading above 70 % may impact on dissolution rate and therefore should be considered during formulation development activities. The data for the tablets containing D-GEL loaded granules show a trend of reduced dipyridamole release with increased D-GEL loading which appears to influence release rate more than increased compression force. The full extent of release was achieved with all tablets without the need to increase the hydrodynamic force within the vessels (to 200 rpm), and all tablets achieved near complete release within 30 mins.

Figures 5.28 a) and b) and 5.29 show *in vitro* dissolution profiles for tablets containing D-TPGS loaded granules (50 %, 70 % and 90 % respectively). Compression conditions and replicate details were as Figures 5.26 to 5.27.

The blend sample for each loaded granule (Figures 5.28 to 5.29) exhibited > 95 % release within 10 min. Compared to the D-GEL blends, there was a slight retardation in release rate with those granules containing 70 % and 90 % D-TPGS. These data suggest that the Vitamin E TPGS dissolves at a slower rate to the Gelucire® 44/14.

Figure 5.28 a) shows the *in vitro* release rate for 50 % D-TPGS loaded tablets compressed at 5, 7.5 and 10 kN respectively. A clear retardation of dipyrindamole release rate can be seen with increasing compression force. At the 30 min timepoint all tablets achieve 100 % nominal release. This release is markedly lower than the corresponding D-GEL tablets (Figure 5.26 a)) where all tablets were found to fully dissolve within 15 minutes.

Figure 5.28 b) shows the *in vitro* release for 70 % D-TPGS loaded tablets. Whilst all tablets achieved 100 % nominal release at the 30 min time point, the profiles show an initial lag at the early time points (5 and 10 min) compared to the 50 % D-TPGS tablets compressed at the same force (Figure 5.28 a), which therefore shows a reduction in initial release with increased vitamin E TPGS concentration.

As D-TPGS concentration increases further (90 % loaded granules) Figure 5.29 shows a marked reduction in dissolution for those tablets compressed at 7.5 and 10 kN where the full extent of dissolution was not achieved until the increased paddle speed was applied after 60 min. The profile for those tablets containing 90 % D-TPGS and compressed with an applied force of 5 kN, did however, achieve the full extent of release at 30 min with a relatively narrow inter tablet variation (see Figure 5.29 associated range bars). This finding suggests that it is both the combination of increased loading level and compression force that causes the retardation. This finding is important to recognise for future studies when arriving at excipient selection for a formulation and setting compression parameters.

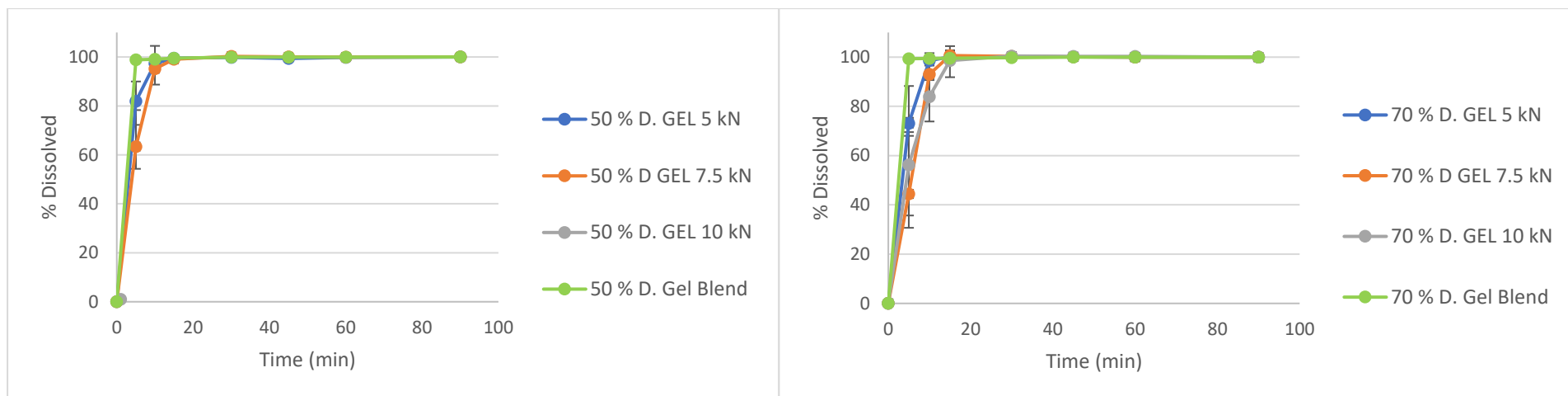


Figure 5.26 a) In-vitro dissolution profile for tablets containing 50 % loaded D-Gel granules (mean values  $n=3 \pm$  min-max range). b) In-vitro dissolution profile for tablets containing 70 % loaded D-Gel granules (mean values  $n=3 \pm$  min-max range).and compressed at 5, 7.5 or 10kN

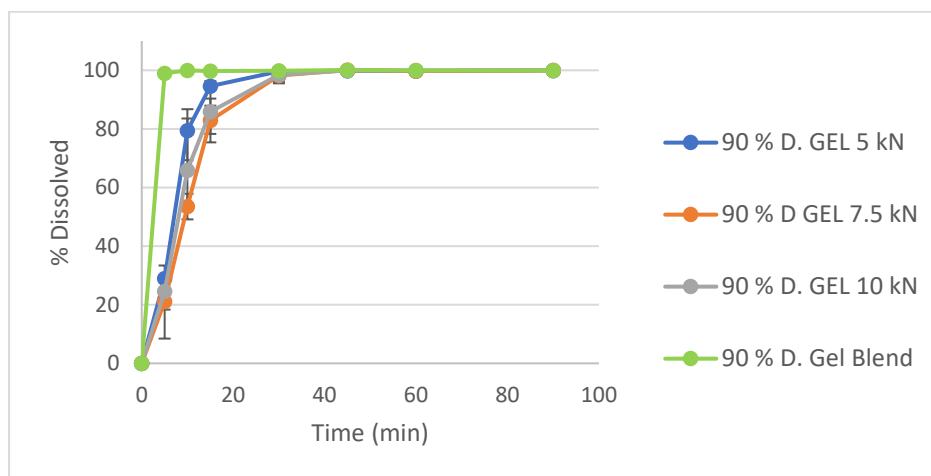


Figure 5.27 In-vitro dissolution profile for tablets containing 90 % loaded D-Gel granules (mean values  $n=3 \pm$  min-max range). and compressed at 5, 7.5 or 10kN

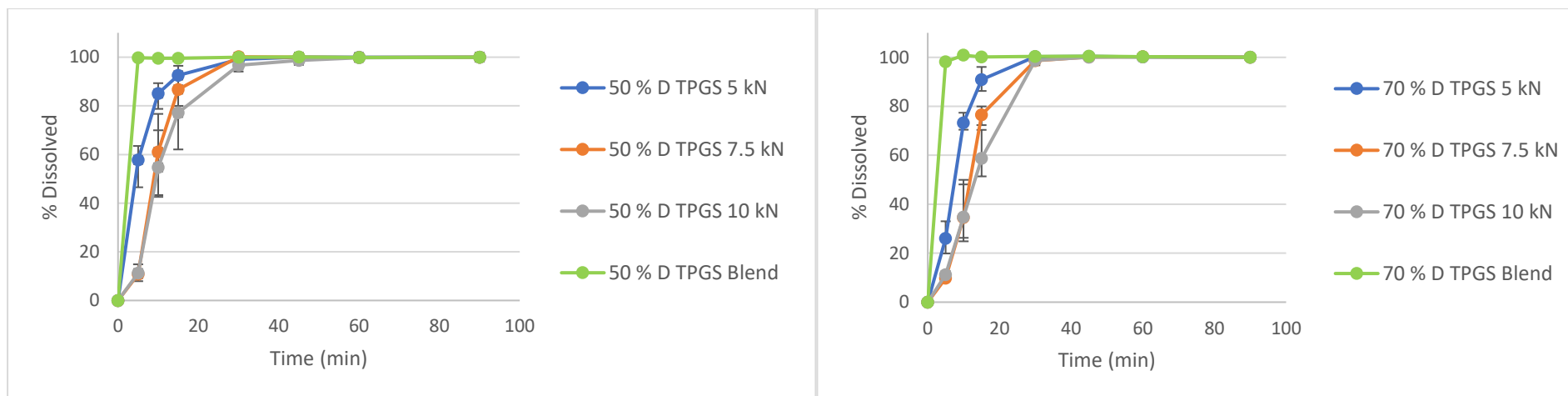


Figure 5.28 a) In-vitro dissolution profile for tablets containing 50 % loaded D-TPGS granules, (mean values  $n=3 \pm$  min-max range). b) In-vitro dissolution profile for tablets containing 70 % loaded D-TPGS granules, (mean values  $n=3 \pm$  min-max range). and compressed at 5, 7.5 or 10kN

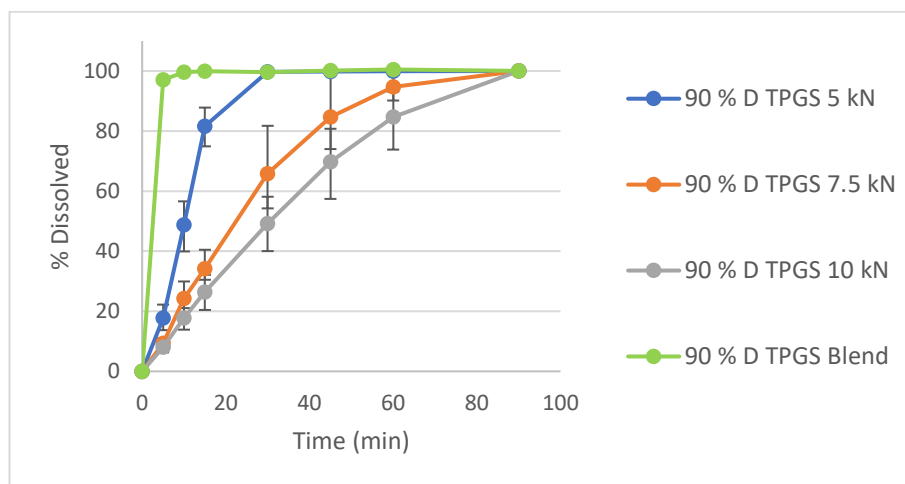


Figure 5.29 In-vitro dissolution profile for tablets containing 90 % loaded D-TPGS granules(mean values  $n=3 \pm$  min-max range) and compressed at 5, 7.5 or 10kN

## 5.5 Further Discussion and Conclusions

One of the primary aims of the investigation was to evaluate the influence of loading Gelucire®44/14 and Vitamin E TPGS on to Neuslin® US2, upon the characteristics of granules produced. The data showed that increasing the concentration of either of the excipients in the granules (higher loading levels) reduced the true density of the granules. The true density of the loaded Neulin®US2 decreased as the liquid phase increased reducing the pore volume. The flowability of all loaded granules was good. These findings suggested that the method of loading of the molten excipients was appropriate and resulted in a suitable distribution of both the GEL and TPGS. For future studies it would be interesting to evaluate the influence of loading temperature and loading parameters such as mixing speed and rate of molten excipient addition rate upon the distribution of GEL or TPGS and any API (dissolved or suspended) in these excipients.

Of the two excipients added, Gelucire® 44/14 was found to be the most compressible. Figure 5.2 shows that 50 % loaded granules exhibited an increase in breaking force and tensile strength up to 180 MPa applied pressure, whereas for vitamin E TPGS at the same loading, breaking force and tensile strength only increased up to approximately 90 MPa (see Figure 5.12, approximately half the applied force range. The studies reported in this Chapter show that the granules containing either D-GEL or D-TPGS produced robust tablets without the need for additional compression aids and the tablets were not friable. The potential for robust tablet production without the dilution of loaded granules with extra-granular compression aids, offers significant benefits for the formulator when trying to maximise drug loading in a formulation. Compared to liquid lipid formulations, semi-solid Type IV formulations may be considered superior in terms of tablet loading potential.

Blends produced contained super disintegrant and lubricant at (5 % w/w and 1 % w/w respectively). All tablets characterised exhibited low friability and tensile strength values > 1 MPa. It was noted however, with some of the higher loaded tablets that during breaking force testing, indentation of the tablets was apparent prior to the tablet fracture. Whilst this phenomenon might affect the validity of the data when considering the requirements of USP 40, <1217>, 2020 for tablet breaking force determination. The deformation prior to breaking may result in variable data generation. Due to the low friability values produced, the findings suggested that breaking force testing may be of reduced value for certain liquisolid tablet formulations. One of the main purposes of determining tablet hardness is to ensure that tablets are sufficiently robust to handle further processing stages such as coating and packaging without damage. Typically, high

friability values are also indicative of low tablet robustness. Further studies are necessary to evaluate the relevance of breaking force determination when developing lipid-based tablets.

The disintegration time for the tablets produced was under 10 mins (irrespective of the excipient loaded). For those tablets containing vitamin E TPGS it could be seen that disintegration rate was reduced with both increased loading and increased compression force. Predictive modelling of the tablet characteristics showed that the main influencing factor for both disintegration and tensile strength for tablets containing either material was the loading level. The underlying factor driving friability though could not be modelled accurately. This may have been due to low variation in friability results, irrespective of loading or compression force applied. It does not appear in the literature that modelling has been applied previously to the loading of lipid-based tablet formulations and the resulting tablet characteristics; probably due to the focus of studies on establishing a formulation to enhance bioavailability rather than establishing critical process parameters for scale up. However, it is believed that such modelling methods combined with design of experiment studies as used by Bejigam et al (2009) to determine formulation factors upon tablet characteristics, and by Vranikova et al (2016), to determine the effects of super disintegrant upon liquisolid tablet characteristics, could be applied during future studies to reduce development times and the number of iterations involved during early formulation studies.

It was noted prior to commencement of these studies, that *in vitro* dissolution from lipid based formulations loaded on to Neuslin® US2 may fail to release the full extent of the API under selected conditions (Speybroeck et al., 2012 and Williams et al., 2014) or the lipid formulation may negatively impact the digestion process (selection of non-digestible surfactants) during lipolysis testing (Vithani et al, 2017 and Jannin et al, 2015). Gelucire® 44/14 was determined to be digestible whereas Vitamin E TPGS is non-digestible (Vithani et al, 2017). The data presented in section 5.4.5 show that the D-GEL formulations result in complete release of the API irrespective of loading level within 30 min. Atunes et al (2013) were also able to develop tablets containing Gelucure® 44/14 for carbamazine delivery with complete API release within 10 min. However, the formulation required the inclusion of an effervescent mixture of citric acid and sodium bicarbonate to enhance *in vitro* dissolution rate. For the D-TPGS formulations only the 90 % loaded tablets compressed at 10 kN failed to release the full extent of API. However, the release rate was impaired in comparison to the release rate of formulations containing Gelucire®44/14.

Whilst it was not the aim of this study to optimise a formulation for the delivery of dipyridamole, for future studies any formulation considered appropriate for a selected API would require additional screening to evaluate the lipid encapsulation efficiency of the formulation such as lipolysis or transfer model testing as evaluated by McCarthy and co-workers (2017) to assess the potential of *in vivo* success in bioavailability enhancement.

This study has shown that the semi-solid materials Gelucire®44/14 and vitamin E TPGS when loaded on Neusilin® US2 at loading levels of up to 90 % (relative to adsorbent weight) can be used to produce tablets > 1MPa tensile with low friability (< 0.4 %) and rapid disintegration (< 10 min). The tablet formulations did not require the addition of extra granular compression aids, only 5 % w/w superdisintegrant (croscarmellose Na) and 1 % w/w lubricant (sodium stearyl fumarate) were necessary. Previously formulations investigated and reported in Chapters 2 and 3 found that liquid formulations did not produce tablets that were as robust at equivalent loading levels. If appropriate for selection, Gelucire® 44/14 and vitamin E TPGS may therefore offer significant advantages over liquid formulations for the formulation of lipid-based tablets.

## Chapter 6.

### General Discussion and Conclusions

#### 6.1 Background and Summary of the Research Project

The aim of these studies was to investigate the compression properties of lipid-based tablet formulations. The purpose was to establish the potential, or conversely; limitations of liquisolid tablet dosage forms; to support a formulator during dosage form design of new formulations.

Whilst the concept of liquisolid tablet dosage forms is not new, the focus of most studies appears to be on the development of a tablet formulation using a model drug to enhance bioavailability; without consideration for scale up and establishment of both specifications (in compliance with pharmacopeial monographs) and quality critical process parameters. Deliberately the current studies described in this thesis did not focus upon the biological considerations of the formulations prepared through extensive *in vitro/in vivo* characterisation studies; rather the focus was on:

- The physical characterisation of the granules and tablets produced.
- Understanding the influence of processing parameters upon the characteristics of the tablets produced.
- Understanding how formulations could be optimised for compliance with compendial monographs (for immediate release tablets).

For a formulation to be truly beneficial it must be sufficiently robust to be scaled, evaluated in clinical studies and the process validated for commercialisation. These studies begin to bridge the gap to be able understand whether a lipid-based formulation could be converted to a liquisolid tablet formulation with the potential for scale up.

An overview of the studies performed is detailed in Figure 6.1.

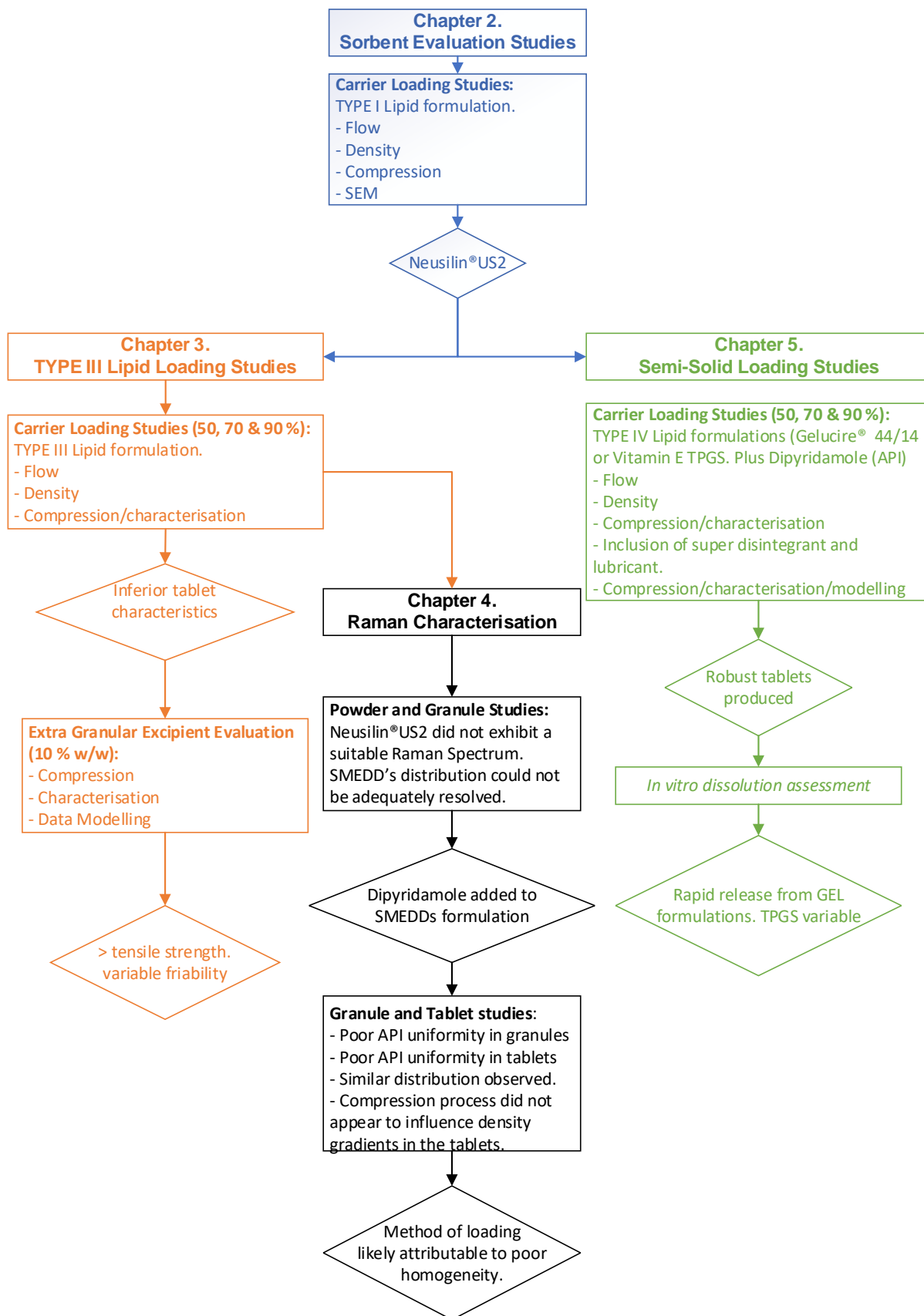


Figure 6.1 Overview of studies performed

### 6.1.1 Sorbent Evaluation Studies

Characterisation of a wide range of sorbents pre- and post-loading with Labrafac Lipophile WL1349® LLW (Type I lipid formulation), was performed to identify the most preferable sorbent for further studies. Sorbent selection was based upon loading potential (density and flow characteristics) and compression characteristics (manufacturability potential) post loading. The magnesium aluminometasilicates (Neusilin® grades) were the only sorbents to exhibit suitable compression properties with relatively low strain rate sensitivity values (< 3 %). The sorbent of choice (selected on compression characteristics) was Neusilin® US2. Loadings up to 170 % LLW produced free flowing powders; however, tablets could only be successfully produced at up to 110 % loading (of LLW). Tablet press speed (dwell time) was found to influence the tensile strengths of the tablets.

The selection of Neusilin® US2 as the adsorbent of choice was supported by work performed by Mura et al (2012) and Gumaste et al (2013) who both compared a range of adsorbents for characteristics post loading with different SMEDDS formulations. The work by Mura et al (2012) did not investigate the influence of compression parameters upon tablet characteristics. However, the work of Gumaste et al (2013) investigated tableability of loaded adsorbents (containing 1:1 ratio of adsorbent to liquid, effectively 100 % loaded); their study concluded that only Neusilin® US2 could be compressed successfully without the need for extra granular excipients. Hentzschel et al (2012), evaluated Neusilin® US2 as an adsorbent and were able to produce tablets at > 1 MPa tensile strength when loaded at 150 %. However, compression was performed on a single station press at a speed of 16 strokes/min. The associated dwell time therefore is likely to be > 60 ms and could be a significant factor in the ability to produce viable tablets.

Studies performed Sander and Holm (2009), Cirri et al (2016), Veranikova et al (2016) and Seljak et al (2018), all utilised Neusilin® US2 as the adsorbent for the production of liquisolid tablets. However, those studies were not focussed upon the compression characteristics of the formulations produced but, confirm the interest in Neusilin® US2 for lipid delivery.

The data presented in Chapter 2 provides a more extensive indication of the limitations for Neusilin® US2 use in liquisolid tablet formulations, when compared to other work reported. It was found that above 110 % loading viable tablets could not be produced (> 1 MPa tensile strength) and that loaded granules were found to

exhibit strain rate sensitive behaviour. Such knowledge is important for a formulator when embarking upon a liquid-solid tablet development exercise when considering the ability to scale the formulation.

### **6.1.2 Type III Lipid Loading Studies**

Studies detailed in Chapter 3 evaluated a model Type III (lipid formulation) SMEDDS preconcentrate (SPc) formulation, containing Labrafac Lipophile WL1349. Neusilin® US2 was loaded at 50 %, 70 % and 90 % relative to the dry adsorbent. The loading levels (50 – 90 %) were selected following the data generated in Chapter 2, whereby viable tablets could be produced at up to 110 % loading (subject to dwell time). These loading levels bracket that suggested by Tan (2013) in their review of solid carriers for lipid-based formulations which suggested 40 % w/w (approximately 67 % loaded relative to the dry adsorbent) optimum loading for dry emulsions. Characterisation of the loaded granules showed that increasing the concentration of SPc in the granules (higher loading levels) reduced the true density of the 'liquid granules'. It was concluded that the true density of the loaded Neusilin® US2 decreases as the liquid phase predominates and the pore volume of the Neusilin®US2 decreases. This finding did not correlate with corresponding increases in bulk and tapped density values but can be explained by the reduction in intergranular porosity.

The compressibility of the Neusilin® US2 was reduced with increased SPc loading. The tablets produced from the SPc loaded Neusilin® US2 granules (without additional compression aids), were not suitably robust (relatively low tensile strength, low friability and extended disintegration). The compression range over which viable tablets are formed is limited for all granules at each loading level. This finding does not comply with general rules for powder compression as outlined in USP 40 Chapter <1062> (2020) for tabletability, compressibility and compactability. For all granules, a critical force is reached at which the liquid phase appears to dominate and tablet tensile strength then begins to reduce with increasing force. Rather than a 'yield point' at which certain materials permanently deform; the granules appear to reach a 'liquid point' at which the liquid dominates the tablet characteristics with increasing force/pressure applied. The understanding of this 'liquid point' will be essential for formulation optimisation and process parameter selection. This point is not believed to have been discussed in the literature previously. Gumaste et al (2013) reported that tabletability of loaded Neusilin® US2

was reduced when increased to 200 % or 300 % loading. However, stepwise incremental studies to establish maximum loading levels were not reported.

At the highest loading level (90 %) tablets could not be produced at the shortest dwell time (15 ms), confirming the strain rate sensitivity of the SPc loaded granules at high loading levels (as reported in Chapter 3, section 3.4.2). Studies reported by Gumaste (2013), showed that viable tablets (> 1 MPa tensile strength) could be produced containing 100 % lipid loaded granules. However, the influence of dwell time was not reported. Gumaste et al (2013) did report that applied compression pressure > 135 MPa was detrimental to tablet tensile strength which correlates with the trends reported in Chapter 3.

As studies in Chapter 3 showed that above 50 % loading levels, the 'liquid granules' exhibited strain rate sensitivity, the addition of extra granular compression aids was investigated to improve tablet characteristics. Several studies report the inclusion of extra-granular excipients in liquid solid tablet formulations, including Seljak et al (2018 – 10 % w/w Avicel® PH 102), Vranikova et al (2015 – approximately 50 % w/w Lactose) and Cirri et al (2016 – approximately 25 % w/w Kollidon CL). Whilst the studies performed by both Vranikova et al and Cirri et al focus on improving tablet disintegration rate, the addition of such high % w/w of excipient(s) in the formulations are likely to influence the compression properties of the formulations and resultant tablet characteristics. Such high % w/w of excipients will impact upon the maximum drug loading that could be achieved by these formulations. Neither study investigated the influence of the selected excipients at the concentrations included in the formulations upon the compression properties of the formulations.

The addition of the 'extra-granular' excipients to the SPc granules was found to improve tablet robustness (tensile strength and disintegration) however friability was not improved at higher SPc loading levels as many tablets were found to cap/laminate during testing. However, not all tablets were affected in a batch and those that remained intact after testing did not show signs of chipping or abrasion (indicative of low tensile strength). These observations suggested that another factor (in addition to tensile strength) such as distribution of the liquid substrate in the tablet may have contributed to the variable friability.

Statistical analysis software (JMP) was used to analyse the tablet characterisation data, which identified that Avicel 200 LM was the most suitable compression aid for

increasing tablet mechanical strength with increasing SPc loading. The prediction profiler functionality of the software showed that to achieve the maximum theoretical API loading within a tablet (highest % SPc loading), the lowest compression force was required. This finding is in direct contrast to standard conventional theory (USP 40, <1062>, 2020) for powder compression and supports the 'liquid point' theory.

Tablets containing SPc at all loading levels evaluated were found to disintegrate rapidly with the inclusion of 5 % w/w croscarmellose sodium and 1 % w/w sodium stearyl fumarate as lubricant. At relatively low SPc loading levels (< 70 % w/w) suitable tablet friability (< 1 %) can be achieved at reduced compression speeds (60 ms dwell time). However,  $\geq 70$  % SPc loading, tablet tensile strength and friability requires further improvement.

### **6.1.3 SMEDDS distribution studies**

To understand the cause of variable tablet friability, Raman spectroscopy was used to analyse loaded granules and tablets. The aim was to evaluate the hypothesis that, concentration gradients formed in the tablets during compression caused by liquid movement. Thus, causing 'weak spots' resulting in capping/lamination. Neusilin® US2 did not generate a suitable Raman spectrum and therefore could not be analysed effectively. The SPc formulation could be detected and was shown to be evenly distributed throughout tablet samples. However, it was difficult to determine quantifiable differences in concentration across the samples due to the high concentration of pre-concentrate in the sample and the lack of contrast against the undetectable Neusilin® US2. The API-dipyridamole was included in the SPc formulation at a relatively low concentration which allowed a qualitative assessment of dipyridamole distribution within the loaded granules and tablets. Characterisation of both the granules and tablets showed poor dipyridamole homogeneity. This inhomogeneity may be attributable to crystallisation of the API out of the pre-concentrate solution during loading or to poor distribution of the DSPc during loading resulting in areas (pockets) of high concentration of liquid containing dipyridamole. The size distribution (visual determination) of the pockets was similar irrespective of loading level. However, the quantity of pockets increased proportionally with DSPc loading. These observations suggest that the loaded granules prior to compression were inhomogeneous and of variable density. The findings suggest that improvements to the method of loading may be necessary to improve granule homogeneity, which may in turn improve tablet robustness and reduce friability. Studies performed by Gumaste et al (2013) and Seljak et al (2018)

evaluated the distribution of loading material onto Neusilin® US2 using scanning electron microscopy. The studies concluded that the lipids loaded were predominantly adsorbed into the porous structure of the Neusilin® US2 granules. However, it could be seen for granules loaded  $\geq 200\%$ , that lipid was present at the granule surface. For future studies, loaded granule characterisation using a combination of both SEM and Raman imaging maybe useful for optimisation of the loading process to understand the influence of loading process parameters on lipid distribution at both the micro (individual granule – using SEM) and macro (samples containing multiple granules - Raman) scale.

### **6.1.5 Semi-solid loading studies**

The liquid studies highlighted limitations of loading Type I and Type III lipid formulations on to Neusilin® US2, in terms of the influence of increasing loading level on the reduction in favourable tablet characteristics (tensile strength and friability) and the requirement for extra granular compression aids to be included within a formulation ( $> 50\%$  loading) which ultimately reduces the potential to achieve high drug loading. Alternative Type IV lipid formulations consisting of semi-solid excipients, Gelucire® 44/14 and Vitamin E TPGS with the inclusion of dipyridamole were therefore evaluated to determine if such excipients could infer improved tablet characteristics.

When either Gelucire® 44/14 or Vitamin E TPGS were loaded onto Neusilin® US2, the true density of the granules was reduced, as had previously been found when loading SPc. The flowability of all loaded granules was good. Of the two excipients added, Gelucire® 44/14 was found to be the most compressible; neither dipyridamole-Gelucire (D-GEL) nor dipyridamole-Vitamin E TPGS (D-TPGS) granules required additional compression aids to produce robust tablets. All tablets characterised were found to exhibit low friability and tensile strength values  $> 1$  MPa. It was noted however, that with some of the higher loaded tablets that during breaking force testing, indentation of the tablets was apparent prior to tablet fracture. The findings suggested that breaking force testing may be of reduced value for certain formulations, assuming that tablet friability was not of concern. The disintegration time for the tablets produced was under 10 mins (irrespective of the excipient loaded). A relationship in increased disintegration time with increased compression force and increased loading level was exhibited for those tablets containing vitamin E TPGS. Predictive modelling of the tablet characteristics showed that the main influencing factor for both disintegration rate and tensile

strength of tablets containing either material was the loading level. The underlying factor(s) influencing friability though could not be modelled accurately. This may have been due to low variation in friability results, irrespective of loading or compression force applied. Antunes et al (2013) investigated methods of tablet production using Gelucire® 44/14 as carrier for Carbamazepine. These studies evaluated melt granulation and spray drying approaches to produce excipient loaded granules prior to compression. The excipients used were not those typically classed as adsorbents (microcrystalline cellulose and pregelatinised starch for melt granulation studies). The compression properties of the loaded granules were not established and it was found that disintegration times and in-vitro release rate was relatively slow from the tablets produced, unless an effervescent disintegration system was employed in the formulation.

*In vitro* dissolution testing was performed upon the various D-GEL and D-TPGS tablet formulations. The data showed that the D-GEL formulations achieved complete release of the API irrespective of loading level with 30 min. However, for the D-TPGS formulations exhibited a retarded release rate in comparison, the 90 % loaded tablets compressed at 10 kN failed to release the full extent of API under the test conditions. Williams (2014), reported that API's dissolved in Type III lipid formulations (SEDD's) are loaded onto Neusilin®, it is difficult to recover the complete extent of API during in-vitro desorption assessment. However, they report that desorption can be increased by increasing the hydrophilicity of the loading formulation. Due to the complete extent of dipyridamole recovery reported in Chapter 5, where applicable, Gelcucire® 44/14 may offer an alternative option as a Type IV lipid formulation for loading on to Neusilin® US2 to improve the extent of API released.

The rate of API dissolution from the D-GEL formulations was much greater than that reported by Antunes et al (2013) even when 10 % super-disintegrant was included. The use of Neusilin® US2 as an adsorbent may offer significant advantages for GEL loading compared to those methods and excipients selected by Antunes et al (2013). Adsorption of the GEL into the pores of Neusilin® US2 may reduce the potential for GEL to become the continuous phase in a tablet, thus driving disintegration rate by erosion as appears to be the case reported by Antunes et al (2013). The low porosity excipients microcrystalline cellulose and pregelatinised starch were likely to be encapsulated by GEL during granulation which becomes the predominant phase in the tablet driving tablet disintegration rate.

The studies in Chapter 5 showed that the semi-solid materials Gelucire®44/14 and vitamin E TPGS when loaded on Neusilin®US2 at loading levels of up to 90 % (relative to adsorbent weight) produced tablets > 1 MPa tensile with low friability (< 0.4 %) and rapid disintegration (< 10 min). The tablet formulations did not require the addition of extra granular compression aids, only 5 % w/w super-disintegrant (croscarmellose Na) and 1 % w/w lubricant (sodium stearyl fumarate) were necessary. Formulations containing Type I or Type III formulations did not produce tablets that were as robust at equivalent loading levels. If appropriate for selection, Gelucire® /14 and vitamin E TPGS may therefore offer significant advantages over liquid formulations for the formulation of lipid-based tablets. Presently, Gelucire® 44/14 and vitamin E TPGS are commonly used as Type IV lipid carriers and filled directly into hard gelatin or hydroxypropylmethyl cellulose (HPMC) capsules, tablet formulations are not commonly considered as an option within industry and therefore a tablet approach could add significant value to the “toolkit” available to formulators when developing new products.

## **6.2 Conclusion**

The aims of this research project have been met by establishing an understanding and expanding the knowledge of the compression behaviour of liquisolid formulations. A key outcome is the development of the novel investigational plan outlined in Figure 6.2. The plan proposes a theoretical outline for the development of liquisolid tablet formulations based upon the findings of these studies, to aid a formulator when embarking on such a development exercise, highlighting considerations against which formulations could be designed and characterised.

A number of critical characteristics are advised to be determined, which have been detailed as the ‘liquid points’. These ‘liquid points’ are believed to be critical to be understood, it is these values for compression force/pressure and solid fraction that indicate the point at which the ‘liquid phase’ predominates the compression process and is likely to limit tablet robustness. These values therefore drive compression parameters and guide product scale-up.

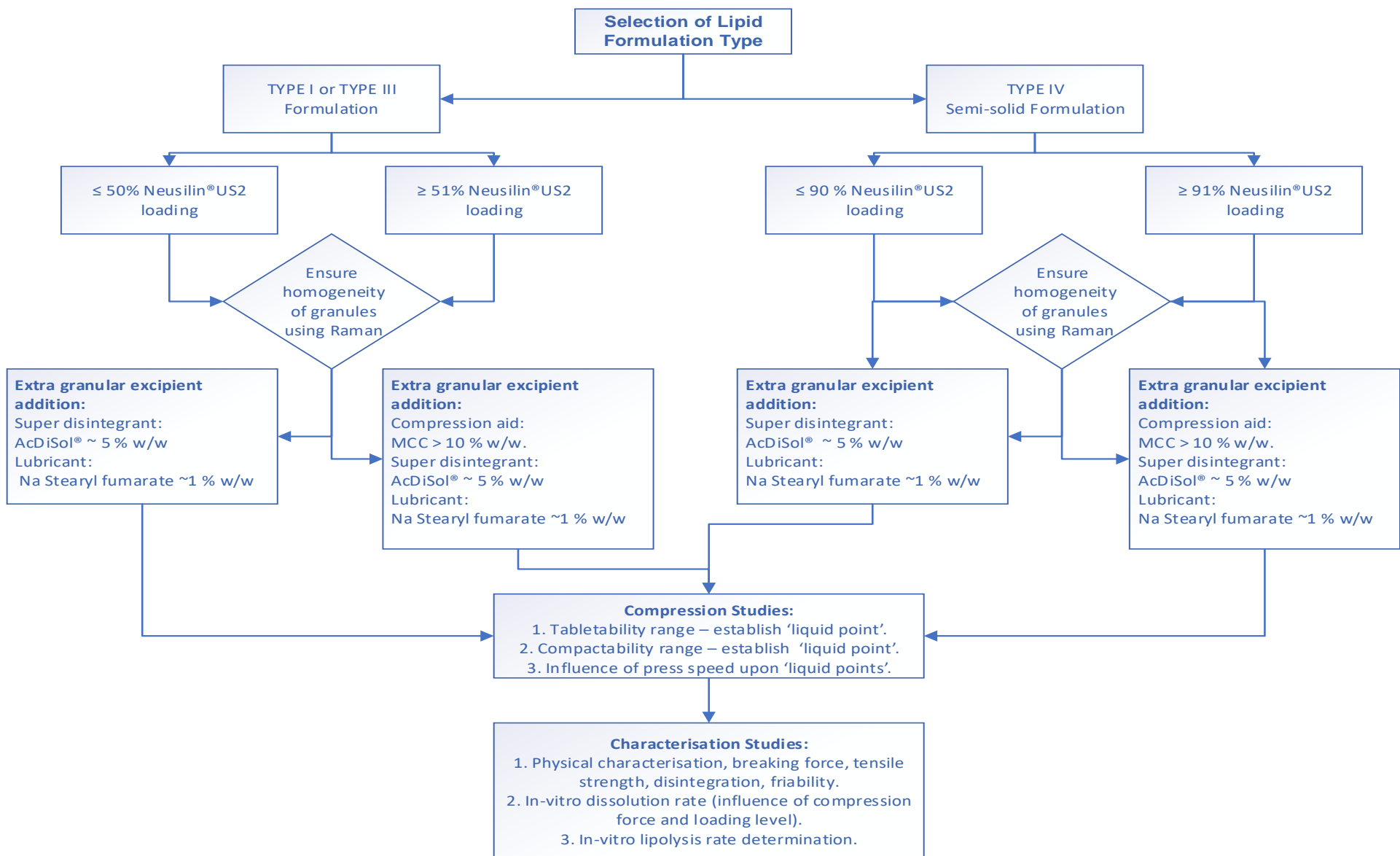


Figure 6.2 Proposed investigational plan for the development of liquid-solid tablet formulations.

### 6.3 Potential Future Work

Several studies may form a continuation of this work, including:

- i. Investigations into the influence of lipid loading upon ejection force, and whether capping or lamination as reported in Chapter 3 is attributable/influenced by high ejection force.
- ii. Investigations to evaluate the influence of pre-compression force upon tablet characteristics.
- iii. Investigations into the relevance of breaking force determination and tensile strength values, for tablets containing high concentrations of lipids, where deformation of a tablet is apparent prior to breaking.
- iv. Formulation stability and the influence of primary packaging selection upon the physical characteristics of liquid-solid tablets according to time and storage conditions (temperature and humidity).
- v. The influence of API and API concentration and loading level of a semi-solid formulation upon tablet characteristics, where the API is either dissolved or suspended in the molten carrier.
- vi. Whether there is a relationship between true density and compressibility/compactability and tableability. If a relationship can be established, whether true density can be used as an indicator for tablet tensile strength. This indicator may be more representative for liquid-solid tablets than solid fraction.
- vii. Whether liquid-solid tablet formulations can be coated readily with both aesthetic and functional coats.
- viii. Whether the process can be scaled to 100,000 unit batch size. To determine to ability to commercialise such a process.
- ix. Finally, it would be interesting to evaluate the potential to develop a co-processed excipient containing Neusilin® US2 and selected lipid/surfactants. To use with BCS class II molecules for use in PK studies or early clinical evaluation (safety studies) to reduce inter and intra patient variability. Such an excipient may allow rapid development of prototypes to reduce time to clinic.

## References:

- Allgeier, M.C. Piper, J.L. Hinds, J. Yates, M.H. Kolodsick, K.J. Meury, R. Shaw, B. Kulkarni, M.R. Remick, D.M (2016). Isolation and Physical Property Optimization of an Amorphous Drug Substance Utilizing a High Surface Area Magnesium Aluminometasilicate (Neusilin® US2). *Journal of Pharmaceutical Sciences*; 105, 3105-3114.
- Amidon, G. L, Lennernas, H. Shah, V.P, Crison, J.R. (1995) A theoretical basis for a Biopharmaceutic drug classification: The correlation of in vitro drug product dissolution and in-vivo bioavailability. *Pharmaceutical Research*, Vol 12, 3.
- Amidon, G. and Sun, C.C. (2014) Proposed new USP general information chapter "Tablet Compression Characterization <1062>" Article *in Pharmacopeial Forum* - January. 42(5) In-Process Revision: <1062> Tablet Compression Characterization
- Amidon, G. E, Secreast, P. J. Mudie, D. (2009). Chapter 8 – Particle, powder and compact characterisation. In: Qui, Y, Chen, Y, Zhang, G. Z. Z. editors. *Developing solid oral dosage forms*. San Diego: Academic; p 163-86.
- Antunes, A.F. De Geest, B.G. Vervaet, C. Remon, J.P. (2013). Gelucire® 44/14 based immediate release formulations for poorly water-soluble drugs. *Drug Development and Industrial Pharmacy*; 39 (5): 791–798.
- Arnolda, Y.E. Imanidisa, G. Kuentza, M.T. (2011). Advancing in-vitro drug precipitation testing: new process monitoring tools and a kinetic nucleation and growth model *Journal of Pharmacy and Pharmacology*; 63: 333–341.
- Aulton. M.E. (2018) Chapter 12. Powder Flow. *Aulton's Pharmaceutics. The design and manufacture of medicines*. 5<sup>th</sup> Edition.
- Beers, M.H. Berkow, R. (1999) *The Merck Manual of Diagnosis and Therapy*, 17<sup>th</sup> edition, Merck & Co., Inc., New Jersey.
- Bejugam, N.K. Parish, H.J. Shankar, G.N. (2009) Influence of Formulation Factors on Tablet Formulations with Liquid Permeation Enhancer Using Factorial Design *AAPS Pharmaceutcal Science and Technology*. Vol. 10, No. 4.

Butler, J. M, Dressman, J. B. J. (2010) The developability classification system: Application of biopharmaceutics concepts to formulation development. *Journal of Pharmaceutical Sciences*. 99. 4943. 2010.

Chan, L.M. Lowes, S. Hirst, B.H. (2004). The ABC's of drug transport in intestine and liver: efflux proteins limiting drug absorption and bioavailability. *European Journal of Pharmaceutical Sciences* 21, 25-51.

Chavan, R.B. Modi, S.R. Bansal, A.K. (2015). Role of solid carriers in pharmaceutical performance of solid supersaturable SEDDs of celecoxib. *International Journal of Pharmaceutics*. 495, 374-384.

Cheng, R.K, Shajeel, A.H. (2004) Effect of a lipoidic excipient on the absorption profile of compound UK 81252 in dogs after oral administration. *Journal of Pharmacy and Pharmaceutical Sciences*. 7 (1), 8-12.

Cirri, M. Roghi, A. Valleri, M. (2016). Development and characterisation of fast-dissolving tablet formulations of glyburide based on solid self-microemulsifying systems. *European Journal of Pharmaceutics and Biopharmaceutics*; 104, 19-29.

Djemai, A. Sinka, I.C. (2006). NMR imaging of density distributions in tablets. *International Journal of Pharmaceutics*; 319, 55 – 62.

Demetzos, C. (2008) Differential Scanning Calorimetry (DSC): A Tool to Study the Thermal Behavior of Lipid Bilayers and Liposomal Stability, *Journal of Liposome Research*, 18:3, 159-173.

Denny, P.J. (2002). Compaction equations: a comparison of the Heckel and Kawakita equations / *Powder Technology*; 127,162–17

El-Kattan, A. and Varma, M. (2012). Oral Absorption, Intestinal Metabolism and Human Oral Bioavailability, *Topics on Drug Metabolism*, Dr. James Paxton (Ed.), ISBN: 978-953-51-0099-7, InTech.

El Massik, M.A. Abdallah, O.Y. Galal, S. Daabis, N.A. (2003). Semisolid Matrix Filled Capsules: An Approach to Improve Dissolution Stability of Phenytoin Sodium Formulation. *Drug Development and Industrial Pharmacy*; 29, 5, 531–543.

Ellison, C.D. Ennisb, B.J. Hamada, M.L. Lyon, R.C. (2008). Measuring the distribution of density and tableting force in pharmaceutical tablets by chemical imaging. *Journal of Pharmaceutical and Biomedical Analysis*; 48,1–7.

FDA. Guidance for Industry Q8(R2) Pharmaceutical Development. (2009). U.S. Department of Health and Human Services. Food and Drug Administration. Center for Drug Evaluation and Research (CDER). Center for Biologics Evaluation and Research (CBER).

Fell, J. Newton, M.J. (1970). Determination of tablets strength by the diametral compression test. *Journal of Pharmaceutical Sciences*; 59:688-91.

Fulper, D. Downey, D. Wang, H. (2009) Evaluation of capsule cracking with hygroscopic fills: An alternative view. *Tablets & Capsules*. 1. September.

Grote, S. Kleinebudde, P. (2018) Impact of functionalized particle structure on roll compaction/dry granulation and tableting of calcium carbonate. *International Journal of Pharmaceutics*; 544, 235–241

Gumaste, S.G. Dalrymple, D.M. Serajuddin, A.T.M. (2013). Development of Solid SEDDS, V: Compaction and drug release properties of tablets prepared by adsorbing lipid-based formulations onto Neusilin® US2. *Pharmaceutical resolutions*; 30:12:3186-3199

Gumaste, S.G. Pawlak, S.A. Dalrymple, D.M. Nider, C.J. Trombetta, L.D. Serajuddin, A.T.M. (2013). Development of solid SEDDS IV: Effect of adsorbed lipid and surfactant on tableting properties and surface structures of different silicates; 30:12:3170-3185

Guo, F. Zhong, H. He, J. Xie, B. Liu, F. Xu, H. Liu, M. Xu, C. (2011). Self microemulsifying drug delivery system for improved oral bioavailability of dipyridamole: preparation and evaluation. *Archives of Pharmaceutical Research*. 34 (7), 113-23.

Gurjar, R. Chan, C. Y. S. Curley, P. Sharp, J. Chiong, J. Rannard, S. Siccardi, M. Owen, A. (2018) Inhibitory effects of commonly used excipients on P-glycoprotein in Vitro. *Mol. Pharmaceutics*, 15, 4835-4862.

Heckel R.W. (1961). An analysis of powder compaction phenomena. *Transactions of the Metallurgical Society of AIME*; 221:1001–8.

Hentzschel, C.M. Alnaief, M. Smirnova, I. Sakmann, A. Leopold, C.S. (2012) Enhancement of Griseofulvin release from Liquisolid compacts. *European Journal of Pharmaceutics and Biopharmaceutics*; 80:1:130-135.

Ingvild, K. (2011) *Compression Analysis of Pharmaceutical Powders: Assessment of Mechanical Properties and Tablet Manufacturability Prediction*. Thesis. University of Tromsø

Ito, Y. Kusawake, T. Ishida, M. Tawa, R. Shibata, N. Takada, K. (2005). Oral solid gentamicin preparation using emulsifier and adsorbent. *Journal of controlled release*; 105, 23-31

Jannin, V. Musakhanian, J. Marchaud, D. (2008) Approaches for the development of solid and semi-solid lipid-based formulations. *Advanced drug delivery reviews* 60. 734 – 746.

Jannin, V. Chevrier, S. Michenaud, M. Dumont, C. Belotti, S. Chavant, Y. Demarne, F. (2015). Development of self-emulsifying lipid formulations of BCS class II drugs with low to medium lipophilicity. *International Journal of Pharmaceutics* 495, 385 – 392.

Jin, F and Tatavarti, A. (2010). Tableability assessment of conventional formulations containing Vitamin E tocopheryl polyethylene glycol succinate. *International Journal of Pharmaceutics*; 389, 58–65.

Johansson, J. Pettersson, S. Folestad, S. (2005). Characterization of different laser irradiation methods for quantitative Raman tablet assessment. *Journal of Pharmaceutical and Biomedical Analysis*; 15;39(3-4):510-6

JRS Pharma. PRUV®. Sodium stearyl fumarate, Ph. Eur., NF, JPE. Product literature *Beyond Tablet Lubrication*. (Downloaded from JRS website; Mar 2020).

Kawabata, Y. Wada. K. Nakatani, M. Yamada, S. Onoue, S. (2011) Formulation design for poorly water-soluble drugs based on biopharmaceutics classification system: Basic approaches and practical applications. *International Journal of Pharmaceutics*, 420 1-10

Kawakita, K. Ludde, H. (1970). Some considerations on powder compression equations. *Powder Technology*; 4, 61.

Kohli, K., Chopra, S., Dhar, D., Arora, S., Khar, R.K., (2010) Self-emulsifying drug delivery systems: an approach to enhance oral bioavailability. *Drug discovery today*. Vol 15, 21/22.

Larhrib, H. Wells, J.I. Rubinstein, M.H. (1997) Compressing polyethylene glycols: the effect of compression pressure and speed *International Journal of Pharmaceutics*; 147, 199 – 205

Li, P. Hynes, S.R. Haefele, T.F. Pudipeddi, M. Royce, A.E. Serajuddin, A.T. (2009) Development of clinical dosage forms for a poorly water-soluble drug II: formulation and characterisation of a novel solid microemulsion pre-concentrate system for oral delivery of a poorly water-soluble drug. *Journal of Pharmaceutical Sciences*. Vol 98, 5.

Lixia, C. Farber, L. Zhang, D. Li, F. Farabaugh, J. (2013). A new methodology for high drug loading wet granulation formulation development, *International Journal of Pharmaceutics*; 441 790–800.

Long, D.A. (2002) *The Raman Effect: A Unified Treatment of the Theory of Raman Scattering by Molecules*. John Wiley & Sons: Chichester, UK.

May, R.K. Su, K. Han, L. Zhong, S. Elliot, J.A. Gladden, L.F. Evans, M. Shen, Y. Zeitler, J.A. (2013). Hardness and density distributions of pharmaceutical tablets measured by Terahertz pulsed imaging. *Journal of Pharmaceutical Sciences*. Vol. 102. No. 7.

McCarthy, C.A. Faisal, W. O'Shea, J.P. Murphy, C. Ahern, R.J. Ryan, K.B. Griffin, B.T. Crean, A.M. (2017). In vitro dissolution models for the prediction of in vivo performance of an oral mesoporous silica formulation. *Journal of Controlled Release*; 250, 86–95.

Michaut. F. Busignies, V. Fouquereau, C. Huet de Barochez, B. Leclerc, B. Tchrelloff, P. (2010). Evaluation of a Rotary Tablet Press Simulator as a Tool for the Characterization of Compaction Properties of Pharmaceutical Products. *Journal of Pharmaceutical Sciences*; 99, 6.

Mura, P. Valleri, M. Cirri, M. Mennini, N. (2012) New solid selfmicroemulsifying systems to enhance dissolution rate of poorly water soluble drugs. *Pharmaceutical Development and Technology*;17(3):277–284.

Mužiková, J. Muchová, S. Komersova, A. Ločař, V. (2015). Compressibility of tableting materials and properties of tablets with glyceryl behenate. *Acta Pharmaceutica*; 65, 91–98.

Osamura, T. Takeuchi, Y. Onodera, R. Kitamura, M. Takahashi, Y. Tahara, K. Takeuchi, H. (2016) Characterisation of tableting properties measured with a multi-functional compaction instrument for several pharmaceutical excipients. *Journal of Pharmaceutics*. 20;510(1):195-202

Natoli, D. Levin, M. Tsygan, L. Liu, L. (2017). Chapter 33 - Development, Optimization, and Scale-Up of Process Parameters: Tablet Compression. *Developing Solid Oral Dosage Forms (Second Edition)*. *Pharmaceutical Theory and Practice*; Pages 917-951

Nilesh, P. Kishor, S. Formulation Development and Evaluation of Gastro Retentive Floating Tablet of Atorvastatin using Statistical Design (JMP Software) *Journal of Drug Delivery & Therapeutics*. 2019; 9(4-A):19-25

Pandey, P. Sinko, P.D. Bindra, D.S. Hamey, R. Gour, S. Vema-Varapu, C. (2013). Processing challenges with solid dosage formulations containing vitamin E TPGS. *Pharmaceutical Development and Technology*; 18, (1), 296–304.

Panigrahi, K.C, Patra, Ch. N, Jena, G.K, Ghose, D. Jena, J. Panda, S. K. Sahu, M. Gelcucire: (2018) A versatile polymer for modified release drug delivery system. *Future journal of Pharmaceutical sciences*. 4, 102 – 108.

Patel, S. Kaushal, A. M. Bansal. K. (2006) Compression Physics in the Formulation Development of Tablets. *Critical Reviews in Therapeutic Drug Carrier Systems*, 23(1):1–65.

Paudel, A. Rajjada, D. Rantanen, J. (2015). Raman spectroscopy in pharmaceutical product design. *Advanced Drug Delivery Reviews*; 89, 3–20.

Pe´rez, P. Suñé-Negre, J.M. Miñarro, Roig, M. Fuster, R. Garcıa-Montoya, E. Hernandez, C. Ruhi, R, Tico, J.R. (2006). A new expert system (SeDeM Diagram) for

control batch powder formulation and preformulation drug products. *European Journal of Pharmaceutics and Biopharmaceutics*; 64, 351–359

Pitt, K.G. Heasley, G.M. (2013) Determination of the tensile strength of elongated tablets, *Powder Technology*; 238, 169–175

Pitt, K.G. Webber, R. Dey, D. Gamlen, M. (2015). Compression prediction accuracy from small scale compaction studies to production presses. *Powder Technology*; 270, 490–493

Ponikva, M (2008) Chapter 12, Exposure of Humans to Fluorine and Its Assessment. *Fluorine and Health. Molecular Imaging, Biomedical Materials and Pharmaceuticals.*

Porter, C.J. Trevaskis, N.L. Charman, W.N. (2007) Lipids and lipid-based formulations: optimising the oral delivery of lipophilic drugs. *Nature Reviews*. Vol 6. 231- 245.

Pouton, C.W. (2000) Lipid formulation for oral administration of drugs: non-emulsifying, self-emulsifying and 'self-microemulsifying' drug delivery systems. *European Journal of Pharmaceutical Sciences*. 11, 2, 593 – 598.

Pouton, C.W. (2006) Formulation of poorly water-soluble drugs for oral administration: Physicochemical and physiological issues and the lipid formulation classification system. *European Journal of Pharmaceutical Sciences*; 2, 9, 278–287.

Pouton, C.W and Porter C.J.H. (2008) Formulation of lipid-based delivery systems for oral administration: Materials, methods and strategies. *Advanced drug delivery reviews*. 60. 625-637.

Qian, K. Bogner, R. (2012) Application of mesoporous silicon dioxide and silicate in oral amorphous drug delivery systems. *Journal of Pharmaceutical Sciences*. 101, 2, 444-63.

Raval, C. Joshi, N. Patel, J. Upadhyay, U.M. (2012). Enhanced oral bioavailability of olmesartan by using novel solid self-emulsifying drug delivery system. *International Journal of Advances in Pharmaceutical Sciences*; 2:82-92

Reddy, M.S. Reddy, N.S. Reddy, M. (2014). Solubility Enhancement of poorly water-soluble drug Efavirenz by solid self-emulsifying drug delivery systems. *International journal of pharma research and review*; 3, 4, 20-28.

Renishaw Technical Datasheet: (2018). Raman spectroscopy explained L9836-9033-01-D.

Reynolds, G.K. Campbell, J.I. Roberts, R.J. (2017). A compressibility-based model for predicting the tensile strength of directly compressed pharmaceutical powder mixtures. *International Journal of Pharmaceutics*; 531, 215–224.

Roberts, M. Vellucci, D. Mostafa, S. Miolane, C. Marchaud, D. (2012). Development and evaluation of sustained-release Compritol® 888 ATO matrix mini-tablets, *Drug Development and Industrial Pharmacy*; 38, 1068–1076.

Roberts, R. J. Rowe, R.C. (1985) The effect of punch velocity on the compaction of a variety of materials. *Journal of Pharmacy and Pharmacology*; 37:377–84.

Sander, C and Holm, P. (2009). Porous Magnesium Aluminometasilicate tablets as carrier of a cyclosporine self-emulsifying formulation. *AAPS. Pharmaceutical Science and Technology*; Vol.10. no 4.

Saxena, S. Singh, H, N. Agrawal, V, K. Chaturvedi, S. (2013) Lipid Excipients in Self Emulsifying Drug Delivery Systems. *Asian Journal of Biomedical and Pharmaceutical Sciences*; 3 (22), 16-22.

Schmidtke, R. Schröder, D. Mentha, J. Staaba, A. Brauna, M. Wagner, K.J. (2017) Prediction of solid fraction from powder mixtures based on single component compression analysis. *International Journal of Pharmaceutics*; 523, 366–375.

Scoutaris, N. Vithani, K. Slipper, I. Chowdhry, B. Douroumis, D. (2014). SEM/EDX and confocal Raman microscopy as complementary tools for the characterization of pharmaceutical tablets. *International Journal of Pharmaceutics*; 470, 88–98.

Seljak, K. B. Ilic, I.G. Gasperlin, M. Pobrick (2018). Self-microemulsifying tablets prepared by direct compression for improved resveratrol delivery. *International Journal of Pharmaceutics*; 548, 263-275.

Sheskey, P.J. Cook, W. G. Cable, C.G. (2017) *Handbook of Pharmaceutical Excipients* 8<sup>th</sup> Edition. Pharmaceutical Press.

Shin, D.J. Chae, B.R. Goo, Y. T. Yoon, H.Y. Kim, C.H. Sohn, S. Oh, D. Lee, A. Song, S.H. Choi, Y.W. (2019) Improved Dissolution and Oral Bioavailability of Valsartan

Using a Solidified Supersaturable Self-Microemulsifying Drug Delivery System Containing Gelucire® 44/14. *Pharmaceutics*; 11, 58.

Shubhajit, P.I. Sun, C.C. (2017). Gaining insight into tablet capping tendency from compaction simulation *International Journal of Pharmaceutics*. Volume 524, Issues 1–2, Pages 111-120.

Shukla, T. Pandey, S. Upmanyu, N. Chandel, H.S. Sudheesh, M.S. (2016) Journey of tablet industry: Compressed to modified release tablet. *Pharma Times - Vol. 48 - No. 11 – November*.

Siddiqui, A. Rahman, Z. Korang-Yeboah, M. Khan, M.A. (2015) Development and validation of X-ray diffraction method for quantitative determination of crystallinity in warfarin sodium products. *International Journal of Pharmaceutics*, 493, 1–6

Sinha, T. Bharadwaj, R. Curtis, J.S. Hancock, B.C. Wassgren, C. (2010). Finite element analysis of pharmaceutical tablet compaction using a density dependent material plasticity model. *Powder Technology*; 202, 46–54

Soh, J.L.P. Grachet, M. Whitlock, M. Lukas, T (2013). Characterization, optimisation and process robustness of a co-processed mannitol for the development of orally disintegrating tablets, *Pharmaceutical Development and Technology*; 18, 172–185.

Sovány, T. Kása, P. Pintye-Hódi, K. (2009) Comparison of the Halving of Tablets Prepared with Eccentric and Rotary Tablet Presses *AAPS Pharmaceutical Science and Technology*; Vol. 10, No. 2.

Speybroeck, M.V. Williams, H.D. Nguyen, T.H. Anby, M.U. Porter, C.J.H. Augustijns, P. (2012). Incomplete Desorption of Liquid Excipients Reduces the in Vitro and in Vivo Performance of Self-Emulsifying Drug Delivery Systems Solidified by Adsorption onto an Inorganic Mesoporous Carrier. *Molecular Pharmaceutics*; 9, 9, 2750-2760.

Spireas, S. and Srinivas, S. (1998). Enhancement of prednisolone dissolution properties using liquisolid compacts. *International Journal of Pharmaceutics*; 166: 177 – 188.

Sun, C.C. (2016). Review: A classification system for tableting behaviours of binary powder mixtures *Asian journal of pharmaceutical sciences*; 11, 486–491

Sun, D. Wei, X. Xue, X. Fang, Z. Ren, M. Lou, H. Zhang, H. (2014) Enhanced oral absorption and therapeutic effect of acetylpuerarin based on D- $\alpha$ -tocopheryl polyethylene glycol 1000 succinate nanoemulsions. *International Journal of Nanomedicine*; 9 3413–3423.

Suñé-Negre, J.M. Roig, M. Fuster, R. Hernández, C. Ruhí, R. García-Montoya, E. Pérez-Lozano, P. Miñarro, M. Ticó, J.R. (2014). New classification of directly compressible (DC) excipients in function of the SeDeM Diagram Expert System. *International Journal of Pharmaceutics*; 470, 15–27.

Tan, A. Rao, S. Prestidge, C.A. (2013). Transforming Lipid-Based Oral Drug Delivery Systems into Solid Dosage Forms: An Overview of Solid Carriers, Physicochemical Properties, and Biopharmaceutical Performance. *Pharmaceutical Research*; 30:2993-3017

Tarliera, N. Soulairola, I. Sanchez-Ballester, N. Baylaca, G. Auberta, A. Lefevreb, P. Bataillea, B. Sharkawia, T. (2018). Deformation behavior of crystallized mannitol during compression using a rotary tablet press simulator. *International Journal of Pharmaceutics*; 547, 142–149

The chemist and druggist [electronic resource], 162, 3888. August 28, 1954.

The European Pharmacopoeia (Ph Eur) (2017) 9.0. EDQM.

The specialty excipient Neusilin® Fuji Chemical Industry Co. Ltd. 2009.

Thomas, N. Holm, R, Rades, T. Müllertz, A. (2012) Characterising lipid lipolysis and its implication in lipid-based formulation development. *The AAPS journal*. 14. 4. 860 – 871.

Thoorens, G. Krier, F. Leclercq, B. Carlin, B. Evrard. B. (2014). Microcrystalline cellulose, a direct compression binder in a quality by design environment—A review. *International Journal of Pharmaceutics*; 473, 64–72

USP general Chapter <1062> (2017). Tablet Compression Characterization USP40-NF35.

USP general Chapter <846> (2017). Specific Surface Area. USP40-NF35.

Viana, M. Jouannin, P. Pontier, C and Chulia, D. (2002). About pycnometric density measurements. *Talanta*; 57, 583- 593.

Vithani, K. Hawley, A. Jannin, V. Pouton, C. Boyd, B.J. (2017) Inclusion of Digestible Surfactants in Solid SMEDDS Formulation Removes Lag Time and Influences the Formation of Structured Particles During Digestion. *The AAPS Journal*, Vol. 19, No. 3

Vraníková, B. Gajdziok, J. Doležel, P. (2017) The effect of superdisintegrants on the properties and dissolution profiles of liquisolid tablets containing rosuvastatin. *Pharmaceutical Development and Technology*; Mar; 22 (2) :138-147.

Vranikova, B. Gajdziok, J. Vetchy, D. (2015) Determination of flowable liquid retention potential of aluminometasilicate carrier for liquisolid systems preparation. *Pharmaceutical Development and Technology*; 20:7:839-844

Vranikova, B. Pavlokova, S. Gajdziok, J. (2016) Experimental design for determination of effects of superdisintegrant combinations on liquisolid system properties. *Journal of Pharmaceutical Sciences*.1-9.

Wang, J.J. Guillot, M.A. Bateman, S.D. Morris, K.R. (2004). Modelling of adhesion in tablet compression. II. compaction studies using a compaction simulator and an instrumented tablet press, *Journal of Pharmaceutical Sciences*; 93, 407–417.

Whalley, I.E. (1981). The compression of liquids. *Physics and Chemistry of the Earth*. Volumes 13–14, 273-294.

Williams, H.D. Speybroeck, M.V. Augustijns, P. Porter, C.J.H. (2014). Lipid-Based Formulations Solidified Via Adsorption onto the Mesoporous Carrier Neusilin®US2: Effect of Drug Type and Formulation Composition on *In Vitro* Pharmaceutical Performance. *Journal of Pharmaceutical Sciences*; 103, 1734–1746.

Wu, C.Y. Hancock, B.C. Mills, A. Bentham, A.C. Best, S.M. Elliott, J.A. (2008). Numerical and experimental investigation of capping mechanisms during pharmaceutical tablet compaction. Powder Technology. 181, 121–129.

Yang, C. Wu, T. Qi, Y. Zhang, Z. (2018) Recent Advances in the Application of Vitamin E TPGS for Drug Delivery. Theranostics; 8(2): 464-485.

Zavaliangos. A. Katz, J.M. Daurio. D. Johnson, M. Pirjanian, A. Nunez, F.A. (2017) Prediction of Air Entrapment in Tableting: An Approximate Solution. Journal of Pharmaceutical Sciences; Volume 106, Issue 12, Pages 3604-3612.

Zheng, Y. Zheng, M. Ma, Z. Xin, B. Gio, R. Xu, X. (2015) Polar Lipids, Biology, Chemistry, and Technology, Sugar fatty acid ester, Chapter 8, Pages 215-243 edited by Moghis U. Ahmad, Xuebing Xu

Zhu, X. Xu, T. Lin, Q. Duan, Y. (2014). Technical Development of Raman Spectroscopy: From Instrumental to Advanced Combined Technologies. Applied Spectroscopy Reviews. 49, 1.

<https://www.jmp.com/support/help/en/15.1/index.shtml#page/jmp/variability-chart.shtml>

<https://www.accessdata.fda.gov/scripts/cder/iig/index.cfm> accessed 25th October 2019.

<https://www.medicines.org.uk/emc/print-document?documentId=30359> 01/10/2015  
Summary of product characteristics, Lynparza 50 mg Hard Capsules.

Neusilin®. The extraordinary excipient for solid oral dosage forms. (2007) Technical newsletter.

[http://www.fujichemical.co.jp/english/newsletter/newsletter\\_pharma\\_0710.html](http://www.fujichemical.co.jp/english/newsletter/newsletter_pharma_0710.html)

<https://statisticsbyjim.com/glossary/regression-analysis/> (accessed 01 May 2020).

[https://www.kosi.com/na\\_en/products/raman-spectroscopy/raman-technical-resources/raman-tutorial.php#](https://www.kosi.com/na_en/products/raman-spectroscopy/raman-technical-resources/raman-tutorial.php#) (accessed 01 May 2020).

<https://products-re.evonik.com/www2/uploads/productfinder/AEROSIL-300-Pharma-EN.pdf>

<https://products-re.evonik.com/www2/uploads/productfinder/AEROSIL-200-VV-Pharma-EN.pdf>

[https://www.saphw.ch/sites/default/files/attachments/pharmalunch\\_nov2015\\_presentation\\_monsuur.pdf](https://www.saphw.ch/sites/default/files/attachments/pharmalunch_nov2015_presentation_monsuur.pdf)

## **Appendix: Conference List**

**Attendance:** AAPS Biotechnology Conference May 2012 (San Diego). May 2012

**Presentation:** Phase I formulation studies – selecting the appropriate oral dosage form in early stage development: Orphan Drug World Congress, (Brussels) September 2014.

**Poster Presentation:** The influence of oily vehicle loading upon the flow and compaction properties of a range of pharmaceutically acceptable adsorbents. Faculty postgraduate research seminar and poster day. June 2014.

**Presentation:** Phase I formulation studies- considerations for FIM. Inform Europe 2015 – Barcelona – November 2015.

**Presentation:** Oral Drug Delivery of Live Biotherapeutics for First In Human Studies. 6<sup>th</sup> American Drug Delivery and Formulation Summit, (Boston). August 2017.

**Presentation:** Direct Compression of Liquisolid Dosage forms. Merck/Medel Pharm: Future of Solid Dosage Forms Seminar (Lyon). September 2017.

**Presentation:** Oral Drug Delivery of Live Biotherapeutics for First In Human Studies. Microbiome Drug Development Europe (Paris): January 2018

**Attendee.** Next Gen Immunology (Israel) February 2018.

**Presentation:** Drug Product Development: Considerations for FiM Studies. Bionow (Northern Oncology) Alderley Park. February 2018.

**Presentation:** Oral Drug Delivery of Live Biotherapeutics for First In Human Studies. Formulation & Drug Delivery USA Congress (San Diego). March 2018.

**Presentation:** Oral Drug Delivery of Live Biotherapeutics for First In Human Studies. 5<sup>th</sup> Microbiome R&D Collaboration forum (Rotterdam). March 2018.

**Presentation:** Oral Drug Delivery of Live Biotherapeutics for First In Human Studies. 4<sup>th</sup> Annual Formulation & Drug Delivery Congress (London). May 2018

**Presentation:** Oral Drug Delivery of Live Biotherapeutics for First In Human Studies. 19<sup>th</sup> Annual Drug Discovery Summit/2<sup>nd</sup> Annual Microbiome Discovery and Development Congress (Berlin). June 2018